Copyright is owned by the Author of the thesis. Permission is given for a copy to be downloaded by an individual for the purpose of research and private study only. The thesis may not be reproduced elsewhere without the permission of the Author.

Characterization of ACC Oxidase from the Leaves of *Malus domestica* Borkh. (Apple)

A thesis presented in partial fulfilment of the requirements
for the degree of

Doctor of Philosophy
in
Plant Biochemistry and Molecular Biology

Institute of Molecular BioSciences
Massey University,
Palmerston North
New Zealand

Jan E. Binnie

2007

ABSTRACT

The expression, accumulation and kinetic properties of 1-aminocyclopropane-1-carboxylic acid (ACC) oxidase (ACO), the enzyme which catalyses the final step in the ACC-dependent pathway of ethylene biosynthesis in plants, is examined.

The investigation is divided into three sections: (i) identification of two ACO genes in apple leaf tissue, designated *MD-ACO2* and *MD-ACO3*, (ii) kinetic analyses of each of the three isoforms of ACO in apple (MD-ACO1, MD-ACO2 and MD-ACO3) expressed in *E. coli*, and (iii) temporal and developmental expression *in vivo* of each of the ACO genes and accumulation of the corresponding gene products in leaf and fruit tissue.

The coding regions of putative ACO gene transcripts were generated from leaf tissue using RT-PCR. Sequence alignments and interrogation of the expressed sequence tags (ESTs) database indicated that the entire open reading frame (ORF) sequences were encoded by two distinct genes, and these are designated *MD-ACO2* and *MD-ACO3*. A third *ACO* gene had been identified in apple by other research workers previously, and designated *MD-ACO1*. Differences are obvious in the number of base-pairs (bp) constituting the entire ORF of *MD-ACO1* (942 bp), *MD-ACO2* (990 bp) and *MD-ACO3* (966 bp). *MD-ACO1* and *MD-ACO2* share a close nucleotide sequence identity of 93.9 % in the ORF but diverge in the 3′ untranslated regions (3′-UTR) (69.5 %). In contrast, *MD-ACO3* shares a lower sequence identity with both *MD-ACO1* (78.5 %) and *MD-ACO2* (77.8 %) in the ORF, and in the 3′-UTR (*MD-ACO1*, 68.4 %; *MD-ACO2*, 71 %). A comparison of the gene structures show that the endonuclease restriction sites are unique to each individual *MD-ACO* sequence. Genomic Southern analysis, using probes spanning the 3′-UTR and the 3′-end of the coding region confirmed that *MD-ACO3* is encoded by a distinct gene. However, while the distinction between *MD-ACO1* and *MD-ACO2* is not as definitive, different gene expression patterns adds credence to their distinctiveness. Each of the three deduced amino acid sequences contain all of the residues hitherto reported to be necessary for maximal ACO activity.

Expression of *MD-ACO1*, *MD-ACO2* and *MD-ACO3* as fusion proteins in *E. coli* was induced using isopropyl-β-$_D$-thiogalactopyranoside (IPTG), the recombinant proteins purified by nickel-nitrilotriacetic acid (NiNTA) affinity chromatography and the products had predicted masses determined from the nucleotide sequences, including the His-tag of 38.53 kDa (MD-ACO1), 40.39 kDa (MD-ACO2) and 39.3 kDa (MD-ACO3). Polyclonal antibodies were raised against the *MD-ACO3* fusion in rabbit for western blot analysis. Antibodies had been raised previously

against recombinant MD-ACO1, and while it was considered likely the MD-ACO2 would be recognized by the MD-ACO1 antibodies, MD-ACO2 does not appear to be recognized *in vivo* by the antibody.

Analyses of the kinetic properties of the three apple ACOs was undertaken. Apparent Michaelis constants (K_m) of 89.39 μM (MD-ACO1), 401.03 μM (MD-ACO2) and 244.5 μM (MD-ACO3) have been determined which suggests differences in the affinity of each enzyme for the substrate ACC. Maximum velocity (V_{max}) was determined for MD-ACO1 (15.15 nmol), MD-ACO2 (12.94 nmol) and MD-ACO3 (18.94 nmol). The catalytic constant (K_{cat}) was determined for MD-ACO1 (6.6×10^{-2}), MD-ACO2 (3.44×10^{-2}) and for MD-ACO3 (9.14×10^{-2}), with K_{cat}/K_m ($\mu M\ s^{-1}$) values of 7.38×10^{-4} $\mu M\ s^{-1}$ (MD-ACO1), 0.86×10^{-4} $M\ s^{-1}$ (MD-ACO2) and 3.8×10^{-4} $\mu M\ s^{-1}$ (MD-ACO3). The optimal pH for MD-ACO1 was 7.0 - 7.5, MD-ACO2 7.5 - 8.0 and MD-ACO3 7.0 - 8.0. All three isoforms exhibited absolute requirements for the co-substrate ascorbate *in vitro* with optimal activity at 30 mM. Similarly, ferrous iron ($FeSO_4.7H_20$; of 15 – 25 μM) and sodium bicarbonate ($NaHCO_3$; of 30 mM) were required for optimal activity, and were the same for all isoforms. No significant difference in thermostability was found in this study between the MD-ACO isoforms at the P = 0.05 level. However, the activities of the enzyme differed significantly between temperatures over time.

In vivo expression of each of the ACO genes in leaf tissue determined using RT-PCR and cDNA Southern analysis reveal that both *MD-ACO2* and *MD-ACO3* are expressed in young leaf tissue and in mature leaf tissue. While *MD-ACO3* is expressed predominantly in young leaf tissue, *MD-ACO2* (in common with *MD-ACO1*) is expressed predominantly in mature fruit tissue. None of the *MD-ACO*s were observed to be senescence associated genes (SAG). MD-ACO3 protein accumulated predominantly in young leaf tissue and less intensely in both mature leaf tissue and young fruit tissue, while MD-ACO1 accumulated only in mature fruit tissue. For the developmental studies, samples were collected at approximately 11 am in this study. *MD-ACO2* and *MD-ACO3* were also expressed in leaf tissue collected over a 24 h period in the spring and also in the autumn. For both genes transcripts accumulated in the presence of fruit but tended to disappear in the absence of fruit.

These results show that *MD-ACO1*, *MD-ACO2* and *MD-ACO3* are differentially expressed, and that MD-ACO3 is encoded by a gene distinct from MD-ACO1 and MD-ACO2. MD-ACO1 and MD-ACO2 are either allelic forms of the same gene or closely clustered. Although there is some variation in kinetic properties which may reflect different physiological environments, they do not vary greatly.

ACKNOWLEDGEMENTS

I would like to express my sincere gratitude to my supervisor Professor Michael T. McManus for guiding me through this work with enthusiasm, humour, encouragement and patience. Such an experienced and trusted advisor is a privilege to interact with; thank you for your time Michael, and consideration, I feel I cannot say enough.

I wish to acknowledge my three consecutive second supervisors at HortResearch, Dr Dennis Greer, Dr Dr Jens Wünsche and Dr Stuart Tustin. I am particularly grateful to Dennis Greer, now at the Charles Sturt University in Australia, for securing funding from HortResearch for an Enterprise Scholarship with the New Zealand Foundation for Research Science and Technology. To Jens Wünsche, now back in Germany, at Stuttgart University, thank you for your expertise and advice in the orchard at Crosses Road, Havelock North Research Centre, particularly for your assistance with the portable photosynthetic system. Thanks also to my final supervisor Stuart Tustin.

This is also a good opportunity to thank the great team at HortResearch in the Hawkes Bay, including Jens, Stuart, Dr Steven McArtney, and many others for answering the numerous questions I threw at them, Paul Brookfield for help with the GC, the orchard harvesting manager (Armann) for organizing the fruit to be picked when I wanted the trees to be stripped of fruit, to the security guards who held back the dogs as I collected samples in the middle of the night, and to the many others who I asked for assistance during my research. I would also like to thank HortResearch for providing the gala apple trees specifically for my use during this project. Dr Robert Simpson at HortResearch in Palmerston North for assistance with the EST database searches and Dr Andy Allen at HortResearch in Auckland for providing the virtual northern data.

I gratefully acknowledge the assistance of Michael's post-doc Richard Scott, research assistances Anya Lambert and Susanna Leung for assistance with the cloning, as well as technicians Cait Inglis (especially when shifting labs) and Lena Ling. Also the other members of Michael's crew who were in the lab when I arrived, Simone, Vikki, the mad Greg, Trish, Ning and Balance. To the masters students for their breath of fresh air, Fiona, tall Mathew and the taller Mathew. Elizabeth, I've really enjoyed your friendship and fun, as well as the discussions about our respective research. To the newer ones Marissa, Jolla, Ludivine and Aluh, I wish you all the best with your studies, and to Michael's new post-doc Sarah-Jane Dorling for being enthusiastic about everything.

My appreciation also goes to many members of the Institute of Molecular Biosciences; in the Allan Wilson Centre, Trish McLenachen for her help with the bioinformatics, Associate Professor Peter Lockhart, Dr Lesley Collins and Richard Carter for assistance with the construction of the phylogenetic tree, Lorraine Berry for sequencing, and many others; Gill Norris's lab, particularly the legendary Trevor Loo; to the IMBS post-docs generally for their suggestions and encouragement, and importantly to the technical support particularly Chris Burrows and Carol Flyger, and also Paul Hocquard; and to the many others who for one reason or another have been asked for assistance, thank you all. Also thanks to the Institute of Fundamental Science people, particularly Peter Lewis and the workshop guys.

I would like to thank the New Zealand Foundation for Research, Science and Technology (FRST) together with the Horticulture and Food Research Institute of New Zealand Ltd (HortResearch) for a Bright Future Enterprise Scholarship.

I am also grateful to the New Zealand Society of Biochemistry and Molecular Biology, the New Zealand Society of Plant Physiologists (now Biologists) and the Institute of Molecular Biosciences for providing generous travel assistance grants for me to attend conferences including the 7th International Symposium on the Plant Hormone Ethylene, in Pisa, Italy.

My final and very special thanks must go to my partner John for the support and encouragement he has given me throughout the project, and for making life fun despite the PhD.

TABLE OF CONTENTS

ABSTRACT ..... **ii**
ACKNOWLEDGEMENTS ..... **iv**
TABLE OF CONTENTS ..... **vi**
LIST OF FIGURES ..... **xii**
LIST OF TABLES ..... **xv**
LIST OF ABBREVIATIONS ..... **xvii**
ABBREVIATIONS FOR AMINO ACIDS ..... **xxi**

Chapter One: INTRODUCTION **1**
1.1 ETHYLENE IN PLANT DEVELOPMENT **1**
1.2 ETHYLENE PERCEPTION AND SIGNAL TRANSDUCTION **2**
1.2.1 Ethylene Perception **2**
1.2.2 Ethylene Signal Transduction **4**
1.3 ETHYLENE BIOSYNTHESIS IN HIGHER PLANTS **6**
1.3.1 SAM Synthetase **8**
1.3.2 ACC Synthase (ACS) **10**
1.3.3 Conjugation of ACC **14**
1.4 ACC OXIDASE (ACO) **15**
1.4.1 The Ethylene-Forming Enzyme (EFE) **15**
1.4.2 Catalytic Mechanism of ACC Oxidase **17**
1.4.3 ACC Oxidase Gene Expression in Higher Plants **22**
1.5 CIRCADIAN REGULATON AND BIOLOGICAL CLOCKS **26**
1.6 *MALUS DOMESTICA* L. BORKH. (APPLE) **28**
1.6.1 ACC Oxidase in *Malus domestica* **29**
1.6.1.1 Expression of ACC Oxidase in Apple **29**
1.6.1.2 Purification, Characterization and Kinetic Properties of ACC Oxidase in apple **30**
1.6.1.3 Requirement of Apple ACC Oxidase for Co-substrate and Co-factors **32**
1.6.1.4 Localization of ACC Oxidase in Apple **36**
1.6.1.5 The Focus of Apple Studies **37**
1.7 OBJECTIVE AND AIMS OF THE THESIS **39**

Chapter Two: MATERIALS AND METHODS 40

2.1 PLANT MATERIAL 40

2.1.1 Harvesting of Plant Material 40

2.1.2 Chlorophyll Quantification 43

2.1.2.1 Statistical Analysis 43

2.1.3 Leaf Carbon Assimilation Measurements 44

2.1.4 Protein Extraction from Apple Tissue 44

2.2 MOLECULAR METHODS 44

2.2.1 Growth and Storage of *E. coli* 44

2.2.1.1 Luria-Bertani (LB) Media and LB Ampicillin^{100} Plates 44

2.2.1.2 Preparation of Competent Cells 45

2.2.2 Isolation of Ribonucleic Acid (RNA) 46

2.2.2.1 Extraction of Total RNA 46

2.2.2.2 Quantification of RNA in Solution 49

2.2.3 Reverse Transcriptase Polymerase Chain Reaction (RT-PCR) 49

2.2.3.1 Generation of cDNA using Reverse Transcriptase 50

2.2.3.2 Amplification of cDNA by Polymerase Chain Reaction 50

2.2.3.3 Primers Used for In-Frame Cloning 54

2.2.3.4 Relative Quantitative RT-PCR using Quantum RNA™ 18S Internal Standards 57

2.2.4 Cloning of PCR Products into Plasmid Vectors 58

2.2.4.1 Ethanol Precipitation of DNA or RNA 58

2.2.4.2 Quantification of DNA 59

2.2.4.3 Agarose Gel Electrophoresis of DNA 59

2.2.4.4 DNA Recovery from Agarose Gels 60

2.2.4.5 DNA Ligation 61

2.2.4.6 Transformation of *E. coli* using the Heat Shock Method 63

2.2.5 Characterizaton and Sequencing of Cloned DNA in *E. coli* 64

2.2.5.1 Isolation of Plasmids from *E. coli* by the Alkaline Lysis Method 64

2.2.5.2 Plasmid Isolation from *E. coli* by the Rapid Boiling Method 65

2.2.5.3 Digestion of DNA with Endonuclease Restriction Enzymes 65

2.2.5.4 Purification of Plasmid DNA for Sequencing 66

2.2.5.5 Purification of PCR Products 67

2.2.5.6 Preparation for Automated Sequencing of DNA 68
2.2.6 DNA Sequencing Analysis 69
2.2.6.1 Sequence Alignment 69
2.2.6.2 Sequence Phylogeny 69
2.2.7 Southern Analysis 70
2.2.7.1 Isolation of Genomic DNA 70
2.2.7.2 Digestion of Genomic DNA 71
2.2.7.3 Southern Blotting of Genomic DNA 72
2.2.7.4 Southern Blotting of cDNA Fragments 73
2.2.7.5 Labelling DNA for Southern Analysis with [α-^{32}P] -dATP 74
2.2.7.6 Hybridisation and Washing of DNA Blots 74
2.2.7.7 Stripping Southern Blots 75
2.3 EXPRESSION, PURIFICATION, ANALYSIS OF ENZYME ACTIVITY AND PROTEIN ACCUMULATION 75
2.3.1 Preliminary Induction of Recombinant Proteins 76
2.3.2 Large Scale Induction of Recombinant Proteins 76
2.3.3 Isolation of Glutathione-S-Transferase (GST) Fusion Proteins 77
2.3.4 Purification of His-Tagged Proteins by Metal Chelate Affinity Chromatography 79
2.3.4.1 Cleaning of Nickel Nitrilotriacetic Acid (Ni-NTA) Resin 79
2.3.4.2 Cleavage of the Histidine Tag (His-Tag) from the Fusion Protein Using Tobacco Etch Virus (TEV) Protease 80
2.3.4.3 Acetone Precipitation of Recombinant Proteins 81
2.3.5 Sephadex G-25 Gel Filtration Chromatography 81
2.3.6 Fast Protein Liquid Chromatography (FPLC) 82
2.3.6.1 Anion Exchange Chromatography 83
2.3.6.2 Column Cleaning 83
2.3.7 The Bradford Protein Assay 84
2.3.8 ACC Oxidase Assay 84
2.3.8.1 Determination of pH Optimum 85
2.3.8.2 Optimal Requirements for Co-Substrate and Co-Factors 86
2.3.8.3 Determination of K_m, V_{max} and K_{cat} 86
2.3.8.4 Determination of Thermal Stability 86
2.3.9 Ethylene Analysis 87

2.3.9.1 Measurement of Ethylene using Gas Chromatography....87
2.3.9.2 Measurement of Ethylene Production in Plant Tissues....87
2.3.9.3 Ethylene Calculations....87
2.3.10 Sodium Dodecyl Sulphate-Polyacrylamide Gel Electrophoresis (SDS-PAGE)....88
2.3.10.1 Preparing and Running Linear (12 %) SDS-PAGE....88
2.3.10.2 Preparing and Running Gradient (10 % to 20 %) SDS-PAGE....90
2.3.10.3 Coomassie Brilliant Blue (CBB) Staining....90
2.3.11 Western Analysis....91
2.3.11.1 Production of Primary Polyclonal Antibodies....91
2.3.11.2 Electrophoretical Transfer of Proteins from Gel to PVDF Membrane....91
2.3.11.3 Immunodetection of Proteins on PVDF Membrane....93
2.3.11.4 Amino Acid Sequencing of N-Terminal Peptide Sequences....94

Chapter Three: RESULTS....95
3.1 ACC OXIDASE GENES IN *MALUS DOMESTICA* BORKH. (APPLE)...95
3.1.1 Molecular Cloning of Protein-Coding Regions of ACC Oxidase Genes in *Malus domestica* (cultivar: Gala)....95
3.1.2 Confirmation of Putative ACC Oxidase cDNAs....97
3.1.3 Expressed Sequence Tag (EST) Searches at HortResearch....104
3.1.4 Summary of Gene Nomenclature....107
3.1.5 Genomic Structure of the *Malus domestica* ACC Oxidase Genes....108
3.1.6 Sequence Analysis of ACC Oxidase from *Malus domestica*....111
3.1.6.1 Nucleotide Sequence Identities Amongst the ORF of MD-ACO1, MD-ACO2 and MD-ACO3....111
3.1.6.2 NCBI Nucleotide Database BLAST Analysis of the Entire ORF for Each of the ACC Oxidase Sequences....111
3.1.6.3 Analysis of the Deduced Translational Sequences of Each of the ACC Oxidase Proteins....115
3.1.7 Confirmation by Southern Analysis that *MD-ACO3* is Encoded by a Gene Distinct from *MD-ACO1* and *MD-ACO2*....117
3.1.8 Evidence that Three Members of the *MD-ACO* Multi-gene Family are Differentially Expressed *In Vivo*....122

3.2 EXPRESSION AND CHARACTERIZATION OF MD-ACO1, MD-ACO2 AND MD-ACO3 AS RECOMBINANT PROTEINS 130

3.2.1 Protein Expression of MD-ACO1, MD-ACO2 and MD-ACO3 130

3.2.1.1 Expression of Recombinant Protein in *E. coli* 130

3.2.1.2 Purification of His-Tagged Fusion Proteins 133

3.2.2 Characterization of Polyclonal Antibodies Raised Against MD-ACO Fusion Proteins 139

3.2.2.1 Protein Accumulation of MD-ACO1/MD-ACO2 and MD-ACO3 in Apple Tissue 143

3.2.2.2 Protein Analysis: Removal of the His-Tag 143

3.2.3 Kinetic Properties of MD-ACO1, MD-ACO2 and MD-ACO3 146

3.2.3.1 Optimal Substrate and Co-factor Requirements for MD-ACO Activity 146

3.2.3.2 The Michaelis-Constant (K_m) and Maximum Velocity (V_{max}) of the MD-ACO Isoforms for ACC 148

3.2.3.3 Assessment of some Kinetic Parameters using the Same ACC Oxidase Isoform Generated in Two Different Expression Vector Systems 152

3.2.3.3 Thermostability of MD-ACO1, MD-ACO2 and MD-ACO3 154

3.3 ACC OXIDASE GENE EXPRESSION IN THE BOURSE SHOOT LEAVES OF APPLE 157

3.3.1 Physiological Measurements, MD-ACO Protein Accumulation and Gene Expression During Leaf Development 157

3.3.1.1 Change in Chlorophyll Concentration 157

3.3.1.2 Photosynthesis Measurements 159

3.3.1.3 Protein Accumulation and Gene Expression 163

3.3.2 ACC Oxidase Gene Expresson and Protein Accumulation in the Leaves of Apple Over a 24 h Period 170

Chapter Four: DISCUSSION 176

4.1 OVERVIEW 176

4.2 ACC OXIDASE GENES IN *MALUS DOMESTICA* 176

4.2.1 Evidence of a Multi-Gene Family in Apple by Genomic Southern Analysis 176

4.2.2 Gene Structure of *MD-ACO1*, *MD-ACO2* and *MD-ACO3*; Comparison of Exons and Introns 178
4.2.3 Translated Products of MD-ACO Genes 180
4.2.4 Confirmation of *MD-ACO* Differential Gene Expression *In Vivo* 181
4.3 EXPRESSION AND CHARACTERIZATION OF MD-ACO1, MD-ACO2 AND MD-ACO3 AS RECOMBINANT PROTEINS 187
4.3.1 Kinetic Properties of the MD-ACO Isoforms 187
4.3.2 Thermostability of MD-ACO1, MD-ACO2 and MD-ACO3 195
4.3.3 Physiological Significance of the Kinetic Properties of MD-ACOs 197
4.3.4 Some Possible Limitations of Expressing MD-ACOs in *E. coli* 200
4.4 ACC OXIDASE ACCUMULATION AND GENE EXPRESSION IN THE BOURSE SHOOT LEAVES OF *MALUS DOMESTICA* 202
4.4.1 MD-ACO Accumulation and Gene Expression During Leaf Development 203
4.4.2 MD-ACO Accumulation and Gene Expression in Leaves Over a 24 h Period 206
4.5 Summary 210
4.6 Future Directions 211

APPENDIX 1A 212
APPENDIX 1B 213
BIBLIOGRAPHY 215

LIST OF FIGURES

Figure 1.1 Ethylene biosyntheis and the Yang (Methionine) Cycle 7

Figure 1.2 The stoichiometry of the reaction catalyzed by ACC oxidase 17

Figure 2.1 The bourse shoot leaves o f Apple 42

Figure 2.1 Sequence of the primers used in RT-PCR to amplify putative ACC oxidase sequences 51

Figure 2.3 The map and schematic diagram of the pGEX-GP-3 Vector and the vector multiple cloning site 55

Figure 2.4 The map and schematic diagram of the pProEX-1 Vector and the vector multiple cloning site 56

Figure 2.5 pGEM® -T Easy Vector circle map and sequence reference points 62

Figure 2.6 Sequence of the promoter and multiple cloning site of the pGEM®-T Easy Vector 63

Figure 2.7 Arrangement of the apparatus used to transfer DNA samples to Hybond™ -N^+ Membranes 73

Figure 2.8 Western blotting apparatus: assembly of the electrophoretic transfer of proteins from an acrylamide gel to PVDF membrane 92

Figure 2.9 BioRad semi-dry trans-blot cell 92

Figure 3.1 PCR amplification of a putative ACC oxidase cDNA using RT-generated cDNA templates from total RNA isolated from newly initiated green leaves, mature green leaves and senescing leaves 96

Figure 3.2 Cloning of putative cDNAs encoding ACC oxidase in newly initiated green leaves, mature green leaves and senescing leaves of *Malus domestica* generated using RT-PCR 98

Figure 3.3 Comparison between the translated sequences of the partial cDNAs JEB:α and JEB:β with corresponding ACC oxidase sequences as indicated 104

Figure 3.4 Comparison of the deduced amino acid sequences of JEB:α (*MD-ACO2*) with Genbank accession number AF015787 and EST 120223 and EST 153710 106

Figure 3.5 Comparisons of the deduced amino acid sequences of JEB:β (*MD-ACO3*) with EST 179706 and EST 192136 108

Figure 3.6 Gene structure of *MD-ACO1* and *MD-ACO2* with a putative structure determined for *MD-ACO3* 109

Figure 3.7 Comparison of the deduced amino acid sequences of the open reading frames of MD-ACO1, MD-ACO2 and MD-ACO3 116

Figure 3.8 Phylogenetic analysis of the three ACC oxidase amino acid sequences from *Malus domestica* with other ACC oxidase genes in the Genbank database 118

Figure 3.9 Specificity of *MD-ACO1*, *MD-ACO2* and *MD-ACO3* as probes in blotting analysis 119

Figure 3.10 Southern analysis of *Malus domestica* genomic DNA 121

Figure 3.11 Virtual northern 122

Figure 3.12 Evidence that *MD-ACO1*, *MD-ACO2* and *MD-ACO3* are expressed differentially *in vivo* 124

Figure 3.13 The position of the forward intron spanning primers of *MD-ACO1*, *MD- ACO2* and *MD-ACO3*, the forward position of the probe primers,and the reverse 3′-UTR primers used for both fragments and probes 126

Figure 3.14 Relative quantitative RT-PCR analysis of *MD-ACO1*, *MD-ACO2* and *MD-ACO3* expression *in vivo* 127

Figure 3.15 Confirmation that *MD-ACO1*, *MD-ACO2* and *MD-ACO3* are differentially expressed *in vivo* using cDNA Southern analysis 129

Figure 3.16 MD-ACO1, (putative) MD-ACO2 and (putative) MD-ACO3 expressed in *E. coli* (strain BL-21) using the pGEX expression vector 131

Figure 3.17 Specific activities of recombinant MD-ACO1, MD-ACO2 and MD-ACO3 expressed in the pGEX Vector 134

Figure 3.18 Comparison of the molecular mass of recombinant MD-ACO3 expressed using the pGEX Vector with MD-ACO3 expressed using the pProEX-1 vector, after separation on a 10 to 20 % SDS-PAGE gradient gel 135

Figure 3.19 SDS-PAGE of MD-ACO1, MD-ACO2 and MD-ACO3 following Metal Chelate Chromatography 136

Figure 3.20 Separation of active recombinant MD-ACO using a Mono Q Anion Exchange column 138

Figure 3.21 Recombinant His-tagged proteins after purification by metal Chelate Affinity Chromatography, Sephadex G-25 and Anion Exchange Chromatography 140

Figure 3.22 Detection of ACC oxidase in apple fruit and apple leaves using antibody raised against MD-ACO1 on western blot 141

Figure 3.23 Detection, using western analysis, of ACC oxidase in apple fruit and apple leaves by an antibody raised against MD-ACO3 142

Figure 3.24 Accumulation of MD-ACO1/MD-ACO2 and MD-ACO3 in various tissues of apple 144

Figure 3.25 Cleavage of the histidine tag from recombinant MD-ACO2 and MD-ACO3 using tobacco etch virus (TEV) protease, and subsequent evaluation of enzymatic activity 145

Figure 3.26 Effect of MD-ACO concentration on the V_{max} of MD-ACO1, MD-ACO2 and MD-ACO3 147

Figure 3.27 Activity assays of MD-ACO1, MD-ACO2 and MD-ACO3 without the presence of sodium bicarbonate ($NaHCO_3$) in the reaction mixture 150

Figure 3.28 Recombinant MD-ACO1, MD-ACO2 and MD-ACO3 activity as a function of ACC concentration 151

Figure 3.29 Recombinant MD-ACO2 activity as a function of ACC concentration, expressed in the pGEX vector 153

Figure 3.30 Thermal stability of *Malus domestica* ACC oxidase at incubation temperatures of 25 °C, 35 °C and 45 °C 155

Figure 3.31 Changes in chlorophyll concentration as an indicator of leaf maturation in *Malus domestica* 158

Figure 3.32 Changes in chlorophyll concentration as an indicator of leaf senescence in *Malus domestica* 160

Figure 3.33 Chlorophyll concentration as an indicator of leaf senescence in *Malus domestica* 161

Figure 3.34 Leaf carbon assimilation in *Malus domestica* as an indicator of leaf senescence 162

Figure 3.35 ACC oxidase accumulation in the leaves of *Malus domestica*, from early to mid-season, using antibodies raised against MD-ACO1 164

Figure 3.36 ACC oxidase accumulation in the leaves of *Malus domestica*, from early to mid-season, using antibodies raised against MD-ACO3 165

Figure 3.37 Changes in ACC oxidase protein accumulation in leaf tissue from mid-season through to senescence (2003) in *Malus domestica* 166

Figure 3.38 RT-PCR analysis and cDNA Southern blot analysis of ACC oxidase gene expression (2003) 168

Figure 3.39 Gene expression and protein accumulation of ACC oxidase from mid-season through to senescence 169

Figure 3.40 Circadian rhythm of ACC oxidase gene expression over 24 h in the leaves of *Malus domestica* (November, 2003) 171

Figure 3.41 Circadian rhythm of ACC oxidase gene expression over 24 h in the leaves of *Malus domestica* (April, 2004) 172

Figure 3.42 Circadian rhythm of ACC oxidase gene expression over 24 h in the leaves of *Malus domestica* (fruit removed from the tree; April, 2005) 174

Figure 3.43 Circadian rhythm of ACC oxidase gene expression over 24 h in the leaves of *Malus domestica* (with fruit; April, 2005) 175

LIST OF TABLES

Table 1.1 Summary of some properties of ACC oxidase purified from apple 33

Table 1.2 Summary of the requirements of apple ACC oxidase for co-substrate and co- factors 35

Table 2.1 Names and addresses of the manufacturers of reagents and specialized equipment 41

Table 2.2 Primers used in this study 52

Table 3.1 Distribution of colonies and clones containing ACC oxidase inserts from apple leaf tissue 97

Table 3.2A Results of a nucleotide BLAST search against JEB:α, 819 bp cDNA sequence 99

Table 3.2B Results of a nucleotide BLAST search against JEB:β, 816 bp cDNA sequence 100

Table 3.3A Partial cDNAs of JEB:α and JEB:β aligned with ACC oxidase sequences from the NCBI Genebank database 102

Table 3.3B Nucleotide identity (%) between JEB:α and JEB:β and ACC oxidase sequences from three cultivars of *Malus domestica* 103

Table 3.4 Identity (%) between EST 153710 and the cDNA X61390 (pAP4), JEB:α:AF015787 and JEB:β 105

Table 3.5 Identity (%) between ESTs (192136 and 179706) and the cDNA pAP4, JEB:α and JEB:β sequences 107

Table 3.6 Identity amongst the genomic DNA sequences of *MD-ACO1*, *MD-ACO2* and *MD-ACO3* 110

Table 3.7A Opening reading frame nucleotide sequence identities of *MD-ACO1*, *MD-ACO2* and *MD-ACO3* 112

Table 3.7B Nucleotide sequence identities of the 3′-UTR of *MD-ACO1*, *MD-ACO2* and *MD-ACO3* 112

Table 3.7C Translated amino acid sequence identities of MD-ACO1, MD-ACO2 and MD-ACO3 112

Table 3.8A Results of a nucleotide BLAST search against the *Malus domestica* ACC oxidase (*MD-ACO1*) 942 bp cDNA entire open reading frame sequence 113

Table 3.8B Results of a nucleotide BLAST search against the *Malus domestica* ACC oxidase (*MD-ACO2*) 990 bp cDNA entire open reading frame sequence 114

Table 3.8C Results of a nucleotide BLAST search against the *Malus domestica* ACC oxidase (*MD-ACO3*) 966 bp cDNA entire open reading frame sequence 114

Table 3.9 A comparison of MD-ACO1, (putative) MD-ACO2 and (putative) MD-ACO3 132

Table 3.10 NaCl concentration at which MD-ACO1, MD-ACO2 and MD-ACO3 elute from the Mono Q column at pH 7.5, compared with the estimated pI of each of the proteins 139

Table 3.11 Summary of substrate and co-factor requirements for MD-ACO1, MD-ACO2 and MD-ACO3 for optimal activity 149

Table 3.12 Summary of kinetic properties of MD-ACO1, MD-ACO2 and MD-ACO3. 152

Table 3.13 Some kinetic properties using the pGEX and pProEX-1 expression vectors 153

Table 3.14 Summary of thermal stability of *Malus domestica* ACC oxidases at incubation temperatures of 25 °C, 35 °C and 45 °C 156

Table 4.1 Comparison of the kinetic properties of recombinant and purified ACOs from apple and other species 189

Table 4.2 Summary of the specific activities of ACOs 191

LIST OF ABBREVIATIONS

A_{595}	Absorbance at 595 λ nm
ACC	1-aminocyclopropane-1-carboxylic acid
ACO	ACC Oxidase
ACS	ACC Synthase
AEC	1-amino-2-ethyl-cyclopropane-1-carboxylic acid
AdoMet	S-adenosyl-L-methionine
AEC	1-amino-2-ethyl-cyclopropane-1-carboxylic acid
Amp^{100}	Ampicillin (100 mg mL^{-1})
amu	Atomic mass unit
ANS	Anthocyanidin synthase
APS	Ammonium persulphate
BCIP	5-bromo-4-chloro-3-indoyl phosphate
BLAST	Basic Logical Alignment Search Tool
Borax	di-Sodium tetraborate decahydrate
bp	Base-pair
BSA	Bovine serum albumin
°C	Degrees Celsius
ca.	*circa* (approximately)
CAPS	3-(Cyclohexylamino)propanesulfonic acid
CBB	Coomassie Brilliant Blue
cv.	Cultivar
Ci	1 Curie = 3.7×10^{10} disintegrations per second
CTAB	Hexadecyltrimethylammonium bromide
DAFB	Days after full bloom
cDNA	DNA complimentary to a RNA, synthesized from RNA by reverse transcription *in vitro*
dATP	2'-deoxyadenosine 5'-triphosphate
dCTP	2'-deoxycytidine 5'-triphosphate
dGTP	2'-deoxyguanosine 5'-triphosphate
DAOCS	Deacetoxycephalosporin C synthase
DEAE	Diethylaminoethyl
DEPC	Diethyl pyrocarbonate
DMF	N,N-dimethyl formamide
DMSO	Dimethyl sulphoxide
DNA	Deoxyribonucleic acid

DNase	Deoxyribonuclease
DSBH	Double stranded beta helix (jellyroll)
dNTP	2'-deoxynucleotide 5'-triphosphate
DTT	Dithiothreitol
dTTP	2'-deoxythymidine 5'-triphosphate
DW	Dry weight
E. coli	*Escherichia coli*
EDTA	Ethylenediaminetetra acetic acid
EFE	Ethylene forming enzyme
EIN	Ethylene insensitive
EST	Expressed Sequenced Tag
ExPASy	Expert protein analysis system: proteomics server of the Swiss Institute of Bioinformatics (SIB)
FID	Flame ionization detector
FPLC	Fast protein liquid chromatography
FW	Fresh weight
GACC	1-(gamma-L-glutamylamino)cyclopropane-1-carboxylic acid
g	Acceleration due to gravity (9.8 m/s^2)
g	Gram
GC	Gas Chromatography
GCG	Gene Computer Group
GST	Glutathione S-Transferase
GUS	*E. coli* β-glucuronidase
h	Hour
His-tag	Histidine tagged
IgG	Immunoglobulin G
IEC	Internal ethylene concentration
IPTG	Isopropyl-β-$_D$-thiogalactopyranoside ($C_9H_{18}O_5S$)
IPNS	Isopenicillin N synthase
Kb	Kilo base-pairs
kDa	Kilo Daltons
K_i	Inhibition constant
K_m	The Michaelis constant (substrate needed to occupy 50 % of the active sites)
L	Litre
LB	Luria-Bertani (media or broth)
Log	Logarithm
M	Molar (moles per litre)

MACC	1-(malonylamino) cyclopropane-1-carboxylic acid
MCS	Multiple cloning site
MD-ACO	*Malus domestic* ACC Oxidase
mol	mole (amount of a substance, Avogadro's number)
μmol	Micromole
mg	Milligram
μg	Microgram
mL	Millilitre
μL	Microlitre
Milli-Q water	Water purified by a Milli-Q ion exchange column
min	Minute
MOPS	Sodium [3-(*N*-Morpholino)]propanesulphonate
Mr	Relative molecular mass (g mol^{-1})
n	Number of replicate
NBT	*p*-nitro blue tetrazolium chloride
NCBI	National Center for Biotechnology Information
ng	Nanograms
Ni-NTA	Nickel-nitrilotriacetic acid
nL	Nanolitres
nmol	Nanomole
2-ODD	2-oxogluturate dependent dioxygenase
OD_{595}	Optical Density at 595 λ nm
ORF	Open reading frame
PA	1,10-phenanthroline
PAGE	Polyacrylamide gel electrophoresis
PBS	Phosphate buffered saline (50 mM sodium phosphate, pH 7.4 containing 250 mM NaCl)
PBS-T	Phosphate buffered saline containing 0.5 % (v/v) Tween-20
PCR	Polymerase chain reaction
Pers. Comm.	Personal communication
pH	-Log (H^+)
pI	Isoelectric point
pmol	Picomole
pn	Net photosynthesis (carbon assimilation measurements)
ppm	Parts per million
PVDF	Polyvinylidine difluoride
PVP-40	Polyvinyl pyrrolidone
PVPP	Polyvinyl polypyrrolidone

3´RACE	Three prime-rapid amplification of cDNA ends
RNA	Ribonucleic acid
RNase	Ribonuclease
RO	Reverse osmosis
RT-PCR	Reverse Transcriptase-polymerase chain reaction
s	Second
SAM	S-adenosyl-$_L$-methionine
SAP	Shrimp alkaline phosphatase
SDS	Sodium dodecyl sulphate
SEM	Standard error of the mean
SSPE	Saline, sodium phosphate, and EDTA buffer
TEMED	*N*, *N*, *N*', *N*'-tetramethylethylenediamine
T_m	Melting temperature (in molecular biology: the temperature at which DNA strands separate in preparation for annealing)
TEV	Tobacco etch virus
Tris	Tris (hydroxymethyl) aminomethane
Triton X-100	Octylphenoxy polyethoxyethanol
Tween-20	Polyoxyethylenesorbitan monolaurate
U	Unit (commercial enzymes are in U μL^{-1}, where unit is based on enzyme activity)
UTR	Untranslated region
UV	Ultra violet light
V	Volt (m^2 kg $s^{-3}A^{-1}$)
V_{max}	Maximum velocity
v/v	Volume per volume
w/v	Weight per volume
w/w	Weight per weight
X-Gal	5-Bromo-4-chloro-3-indolyl β-$_D$-galactopyranoside

AMINO ACID ABBREVIATIONS

Amino Acid (AA)	Three-letter abbreviation	One-letter abbreviation
Alanine	Ala	A
Arginine	Arg	R
Asparagine	Asn	N
Aspartic acid	Asp	D
Cysteine	Cys	C
Glutamine	Gln	Q
Glutamic acid	Glu	E
Glycine	Gly	G
Histidine	His	H
Isoleucine	Ile	I
Leucine	Leu	L
Lysine	Lys	K
Methionine	Met	M
Phenylalanine	Phe	F
Proline	Pro	P
Serine	Ser	S
Threonine	Thr	T
Tryptophan	Trp	W
Tyrosine	Tyr	Y
Valine	Val	V

Chapter One INTRODUCTION

1.1 Ethylene in Plant Development

Ethylene (C_2H_4), the simplest unsaturated hydrocarbon, was identified as the active component in illuminating/coal gas which caused abnormal horizontal growth in pea seedlings by Neljubov 1901 (cited in Abeles, 1973), while working in St. Petersburg. He demonstrated the "triple response" by exposing etiolated pea seedlings to different concentrations of the gas, which resulted in arrested elongational growth (at 0.1 $\mu L\ L^{-1}$), lateral swelling of elongating parts (at 1.0 $\mu L\ L^{-1}$) and loss of normal gravitropic responses (at 10 $\mu L\ L^{-1}$) (Osborne, 1989a). Proof that plants produce ethylene was eventually provided using chemical absorptive techniques to trap and analyse the gases released from ripening apples (Gane, 1934). Following the application of gas chromatography to ethylene analysis (Burg and Stolwijk, 1959; Huelin and Kennett, 1959), the phytohormone was found to play an important role in regulating many plant processes (Abeles, 1973; 1992; Kende and Zeevart, 1997).

Ethylene is produced in all higher plants (Osborne, 1989a), with the exception of *Potamogeton pectinatus* which is unable to produce ethylene and yet survives successfully in the environment (Summers *et al.*, 1996). In climacteric fruit, ethylene is necessary for the coordination and completion of ripening as illustrated by the slowing or inhibition of ripening in ethylene-suppressed transgenic plants (Oeller *et al.*, 1991; Picton *et al.*, 1993; Theologis *et al.*, 1993; Bleecker and Kende, 2000; Giovannoni, 2000; Alexander and Grierson, 2002), and *via* analysis of inhibitors of ethylene biosynthesis and perception (Yang, 1985; Giovannoni, 2001). It may also be important for non-climacteric fruit ripening (Chervin *et al.*, 2004), long considered and ethylene-independent process (Lelievre *et al.*, 1997). Ethylene is involved in the abscission of apple and peach fruitlets (Cin *et al.*, 2005; Bonghi *et al.*, 2000), and regulates the timing of abscission (Osborne, 1989b; 1991; Henderson *et al.*, 2001). Also the biosynthesis of fruit pigments, textures, flavours and the volatile esters associated with aroma in climacteric fruits are ethylene-dependent (Lelievre *et al.*, 1997; Defilippi *et al*, 2005; Park *et al.*, 2006). The hormone can modify programmed leaf senescence by upregulating senescence-associated genes (SAG) and down regulating photosynthetic-associated genes (PAG) (Bleecker *et al.*, 1988; Grbić and Bleecker, 1995; Miller *et al.*, 1999; Hunter *et al.*, 1999; Huang *et al.*, 2001; Gepstein *et al.*, 2003; Gribić, 2003; Jing *et al.*, 2005), and promoting floral tissue senescence (Sisler *et al.*, 1996; Sisler and Serek, 1997; Hunter *et al.*, 2002). Other processes range from seed germination, including breaking seed dormancy, and seedling emergence (Harpham *et al.*, 1991; Kepczynski and Kepczynska, 1997; Matilla, 2000; Petruzzelli *et al.*, 2000); shoot elongation and the regulation of epinastic growth responses (Sanders *et al.*, 1990; Petruzzelli *et*

al., 1994; Woeste et al., 1999); root production and growth, and root growth initiation (Sarquis *et al*., 1992; Zacarias and Reid, 1992; Finlayson *et al*., 1996; Dolan, 1997). This gaseous hormone can affect plant tissues some distance from its site of biosynthesis (Tieman and Klee, 1999), and a stressed plants chances of survival are decreased without the ability to initiate ethylene-related responses (see review by Grichko and Glick, 2001). With such a wide range of effects in higher plants, the regulation of ethylene biosynthesis, perception and signal transduction is complex (Johnson and Ecker, 1998), and these aspects of the hormone biology will be introduced below.

1.2 Ethylene Perception and Signal Transduction

1.2.1 Ethylene Perception

Studies using radiolabelled ethylene demonstrated that plants had ethylene binding sites (Sisler, 1991), but the inability to purify the binding component(s) and to identify the pathway components by biochemical approaches proved recalcitrant (Jiang and Fu, 2000). To date ethylene receptors, pathway intermediatories and transcription factors have been elucidated by screening mutants with an altered triple response, predominantly of *Arabidopsis* and *Lycopersicon esculentum*, but also in other species such as *Medicago truncatula*, peach, rice and melon (see review by Bleecker and Kende, 2000; Stepanova and Ecker, 2000; Ciardi and Klee, 2001; Alexander and Grierson, 2002; Guo and Ecker, 2004).

In *Arabidopsis* the ethylene triple response (etr) and ethylene insensitive (ein) mutants were first isolated (Bleecker *et al*., 1988; Guzman and Ecker, 1990), and have led to the identification of the ethylene receptor genes ETR1 (Chang *et al*., 1993), ETR2 (Sakai *et al*., 1998), the ethylene response sensors (ERS1 and ERS2) and EIN4 (Hua *et al*., 1995; 1998). When the ETR1 protein was over-expressed in yeast, and the cells treated with [C^{14}]-ethylene, evidence was gathered that the transformants could bind ethylene (Schaller and Bleecker, 1995). Indeed all five ethylene receptors in *Arabidopsis* have been shown to bind ethylene (Schaller and Bleecker, 1995; Hall *et al*., 2000), and the apparent half-life for dissociation of ethylene from ETRI is at least 12.5 h (Schaller and Bleecker, 1995). High affinity binding of ethylene is mediated by a copper (Cu^{+}) cofactor which acts as a transition metal. The copper ion is chelated by a conserved cysteine at position 65 (C^{65}), and a conserved histidine at position 69 (H^{69}), located in the second transmembrane domain of the ETR1 protein (Rodriguez *et al*., 1999). A copper transporting ATPase, (RAN1) in *Arabidopsis*, is thought to deliver copper for the assembly of functional ethylene receptors (Schaller and Kieber, 2002). ETR1 contains three membrane spanning regions at the N-terminal end of the protein, forms homodimers via disulphide bridges (Schaller *et al*., 1995) and is localized to the endoplasmic reticulum (Chen *et al*., 2002). The

ETR1 receptor shares homology with the prokaryotic family of two-component histidine kinase receptors in bacteria (Wurgler-Murphy and Saito, 1997; Pirrung, 1999; Schaller, 2000; Urao *et al.*, 2000). Two-component regulators are typically composed of a sensor protein with an input domain that receives signals and a catalytic transmitter domain that autophosphorylates an internal histidine residue. The second component, a response regulator protein, is composed of a receiver domain that receives phosphate from the transmitter on a conserved aspartate residue and an output domain that mediates the response depending on the phosphorylation state of the receiver (Chang and Meyerowitz, 1995; Stock *et al.*, 2000). Histidine kinase activity of ETR1 has been biochemically confirmed (Gamble *et al.*, 1998). For some of the ethylene receptors the receiver domain is the carboxyl-terminal domain (Chang and Stadler, 2003). Subfamily-1 receptors comprising ETR1 and ERS1 (also localized to the endoplasmic reticulum in melon; Ma *et al.*, 2006), have three hydrophobic subdomains at the N terminus, where ethylene binding occurs, and contain all five of the functionally defined histidine kinase sequence motifs. In contrast subfamily-2, which includes ETR2, ERS2 and EIN4, have an additional hydrophobic extension at the N-terminus, and contain only one or two of the histidine kinase sequence motifs (see review by Wang *et al.*, 2002). The crystal structure of the ETR1 receiver domain indicates that they form dimers (Muller-Dieckmann *et al.*, 1999). One member of each subfamily (ERS1 and ERS2) lack receiver domains (Chang and Bleecker, 2004). Interestingly, members of the photoreceptor family, the phytochromes, have a histidine kinase domain related to two-component systems but exhibit serine/threonine kinase activity (Fankhauser *et al.*, 1999), which supports the notion that the ETR2 class of receptors may function not as histidine kinases but possibly as serine/threonine kinases. For example, autophosphorylation of a tobacco subfamily-2 ethylene receptor has been demonstrated on serine and threonines *in vitro* (Zhang *et al.*, 2004a), and all five receptor proteins from *Arabidopsis* have been shown to display autophosphorylation *in vitro*. Autophosphorylation is predominantly on serine residues (Moussatche and Klee, 2004), and mutation of the histidine residues conserved in two-component systems does not abolish this serine autophosphorylation function (Moussatche and Klee, 2004).

The five *Arabidopsis* ethylene receptors are functionally active and differentially regulated (Schaller and Bleecker, 1995; Hua and Meyerowitz, 1998). Although the elimination of ethylene receptors activates ethylene responses (Hua and Meyerowitz, 1998; Schaller and Kieber, 2002), and an increase in the number of receptors is thought to desensitize the pathway (Ciardi *et al.*, 2000), the absence of ethylene results in the inactivation of ethylene responses (Bleecker *et al.*, 1999). Binder *et al.* (2004a; 2004b) propose a model in which clustered receptors act cooperatively during growth recovery after ethylene withdrawal.

In tomato, six ETR like genes have been isolated and designated as LeETR1, LeETR2 and LeETR3, historically the *never-ripe* gene, denoted as NR (Wilkinson *et al.*, 1995; Payton *et al.*, 1996; Zhou *et al.*, 1996; Tieman and Klee, 1999; Ciardi and Klee, 2001), LeETR4, LeETR5 and LeETR6 (Lashbrook *et al.*, 1998; Tieman *et al.*, 2000, Moussatche and Klee, 2004). LeETR1 and LeETR2 are similar to ETR1 in *Arabidopsis*, and LeETR3, like ERS1 and ERS2, is not associated with a receiver domain, while LeETR4 is an ETR2 class member with a receiver domain (Wang *et al.*, 2002). Interestingly, peach ETR1 mRNA undergoes unusual alternative splicing that potentially results in three different mature transcripts (Bassett *et al.*, 2002; Rasori *et al*, 2002).

Two studies describe the identification of a new class of protein in *Arabidopsis* (Resnick *et al.*, 2006) and in tomato (Barry and Giovannoni, 2006) that interacts with ethylene receptors to negatively regulate ethylene responses. In *Arabidopsis* the protein restores activity to the dominant ethylene insensitive *etr1* mutant and is thus designated REVERSION-TO-ETHYLENE SENSITIVITY1 (RTE1) (Resnick *et al.*, 2006). In tomato, a Green-ripe mutant (*Gr*), identified as having a 5′ deletion, caused ectopic expression of Green-ripe (GR) in all tissues. Although the reduced ethylene responsiveness occurred predominantly in fruit tissues, resulting in the inhibition of fruit ripening (never ripe), a subset of ethylene responses associated with floral senescence, abscission and root elongation are also impacted in mutant plants, but to a lesser extent (Barry and Giovannoni, 2006), suggesting tissue-specific modulation of ethylene responses. These results are consistent with a previous study by Barry *et al.* (2005) in which tomato fruit do not respond to ethylene whereas seedlings show a normal response in the presence of the *Gr* mutant. GR is a member of the same family as RTE1, both are integral membrane proteins and modify the action of two-component regulators (receptors) in all eukaryotes (excluding fungi) (Klee, 2006).

1.2.2 Ethylene Signal Transduction

Through screening T-DNA insertion lines of *Arabidopsis*, one phenotype was identified that displayed the triple response without ethylene treatment, and therefore the "constitutive triple response" (ctr1) mutant was identified (Kieber, 1993). Epistatic studies revealed that the CTR1 gene product acts downstream of the ethylene receptors (Kieber *et al.*, 1993; Hua *et al.*, 1995; Roman *et al.*, 1995; 1998; Sakai *et al.*, 1998). The comparison with bacterial two component systems suggests a phospho-relay may pass the signal downstream. The presence of ethylene has been shown transiently to increase polypeptide phosphorylation *in vivo* (Raz and Fluhr, 1993). The carboxyl half of the CTR1 protein contains a kinase domain with similarity to the Raf family of serine/threonine kinases that function in mitogen-activated kinase (MAPK)

cascades in animals (Kieber, 1993; Huang *et al.*, 2003), they also show some tyrosine kinase activity, and may autophosphorylate on both threonine and tyrosine (Wu *et al.*, 1991; for a review of MAP kinases in plants refer to Morris, 2001). Based on this similarity, CTR1 may function as a mitogen-activated protein kinase kinase kinase (MAP3K) in analogous fashion to Raf, and initiate signalling through a MAPK cascade. Ethylene has been shown to stimulate MAPK like activity in *Arabidopsis* (Novikova *et al.*, 2000; Ouaked *et al.*, 2003), which suggests that both negative and positive transductions may be mediated through MAP kinase cascades (Novikova *et al.*, 2000; Ouaked *et al.*, 2003). The N-terminus of CTR1 was found capable of directly interacting with both the histidine kinase and receiver domains of ETR1, and the histidine kinase domain of ERS1 (Clark *et al.*, 1998). The current model of hormonal action suggests that in the absence of ethylene the CTR1 interacts with the receptor (Schaller and Kieber, 2002; Huang *et al.*, 2003), possibly in response to the phosphorylation state and / or conformational changes in the receptor, or CTR1 could be complexed with receptors but regulated through intermediatories (Schaller and Kieber, 2002) and the response pathway is blocked. Binding of ethylene by the receptors releases the negative CTR1 regulation allowing ethylene responses to occur (Bleecker *et al.*, 1999). Association of the CTR1 protein with the endoplasmic reticulum has been observed using immunoblot assays (Gao *et al.*, 2003), which co-location with the ETR1 receptor and supports the view that CTRI interacts directly with the receptor.

Two tomato sequences showing significant sequence homology with *Arabidopsis* CTR1 have been reported by a group in England (TCTR2; Lin *et al.*, 1998; Alexander and Grierson, 2002), and a group in France (ER50; Zegzouti *et al.*, 1999). Leclercq *et al.* (2002) expressed ER50, designated LeCTR1, in the *Arabidopsis* ctr1 mutant under the direction of the 35S promoter which restored normal ethylene signalling. In contrast to the constitutive expression of the *CTR1* gene in *Arabidopsis* (Kieber *et al.*, 1993), in tomato the *CTR1* gene is expressed differentially (Leclercq *et al.*, 2002).

EIN2 acts downstream of CTR1 and encodes an integral membrane protein of 1294 amino acids (Alonso *et al.*, 1999), predicted to be located at the nuclear membrane (Chang and Shockey, 1999). EIN2 contains 12 predicted transmembrane domains in the N- terminal third of the polypeptide, a region that exhibits significant similarity to the Nramp family of cation transporters. However, experiments to detect metal transporting activity in EIN2 have failed (Thomine *et al.*, 2000). By contrast the carboxyl-terminal hydrophilic region contains a coiled-coil structure, which has a role in protein-protein interactions, but generally does not show homology to any known protein (Schaller and Kieber, 2002; Shibuya *et al.*, 2004). EIN2 is a single-copy gene and is the only gene known in which loss-of-function mutations result in

complete loss of ethylene responsiveness (Chen and Bleecker, 1995; Roman *et al.*, 1995). EIN2 has been found to be a positive component in ethylene signalling in rice (Jun *et al.*, 2004). Expression of EIN2 mRNA is spatially and temporally regulated in *Petunia hybrida* during plant development (Shibuya *et al.*, 2004), indicating the central role of EIN2 in ethylene signal transduction. Genetic evidence has shown the EIN2 acts downstream of CTR1 and upstream of EIN3 (Wang *et al.*, 2002).

The cloning of EIN3 provided direct evidence for nuclear regulation in the ethylene transduction pathway (Chao *et al.*, 1997). EIN3 is a plant specific DNA binding protein (Guo and Ecker, 2003), and is the founding member of a family that contains at least five additional EIN3-like proteins (EILs) (Chao *et al.*, 1997; Wang *et al.*, 2002). EIN3 contains acidic proline rich and glutamine rich domains consistent with transcriptional activation domains. Direct evidence EIN3 and EILs function as transcription factors comes from the finding that they bind to a promoter element (the primary ethylene response element; PERE) in the ethylene response factor 1 (ERF1) gene (Solano *et al.*, 1998). In *Arabidopsis* EIN3 protein levels increase rapidly in response to ethylene, on condition that receptors (ETRI and EIN4), CTRI, EIN2 (and the cytosolic proteins EIN5 and EIN6) are functional. Conversely, in the absence of ethylene, EIN3 is quickly degraded *via* a ubiquitin protease pathway, mediated by F-box proteins (EBF1 and EBF2) (Guo and Ecker, 2003). ERFs (also referred to as ethylene response element binding proteins; EREBPs) are a family of transcription factor proteins (Fujimoto *et al.*, 2000; Nakano *et al.*, 2006) which have been found to bind to a GCC-box, and while some members such as ERF1 function as transcriptional activators other members function as repressors (Fujimoto *et al.*, 2000). Some ERFs contain GCC-boxes in their promoters, suggesting the existence of transcriptional cascades that involves EIN3/EILs and the ERFs (Solano *et al.*, 1998; Binder *et al.*, 2004b).

1.3 Ethylene Biosynthesis in Higher Plants

In higher plants, ethylene biosynthesis follows the pathway from methionine to S-adenosyl-methionine (SAM), to 1-aminocyclopropane-1-carboxylic acid (ACC) to ethylene (Adams and Yang, 1979) (refer Figure 1.1).

Direct evidence that ethylene was derived from carbon 3 and carbon 4 (C-3 and C-4) of methionine *in vivo* was provided by feeding labelled methionine to apple fruit tissue (Lieberman *et al.*, 1966). In similar experiments where labelled methionine was fed to apple fruit tissue, the formation of 5'-methylthioadenosine (MTA) and 5-methylthioribose (MTR) in parallel with ethylene production, confirmed that SAM was a substrate in the biosynthesis of ethylene

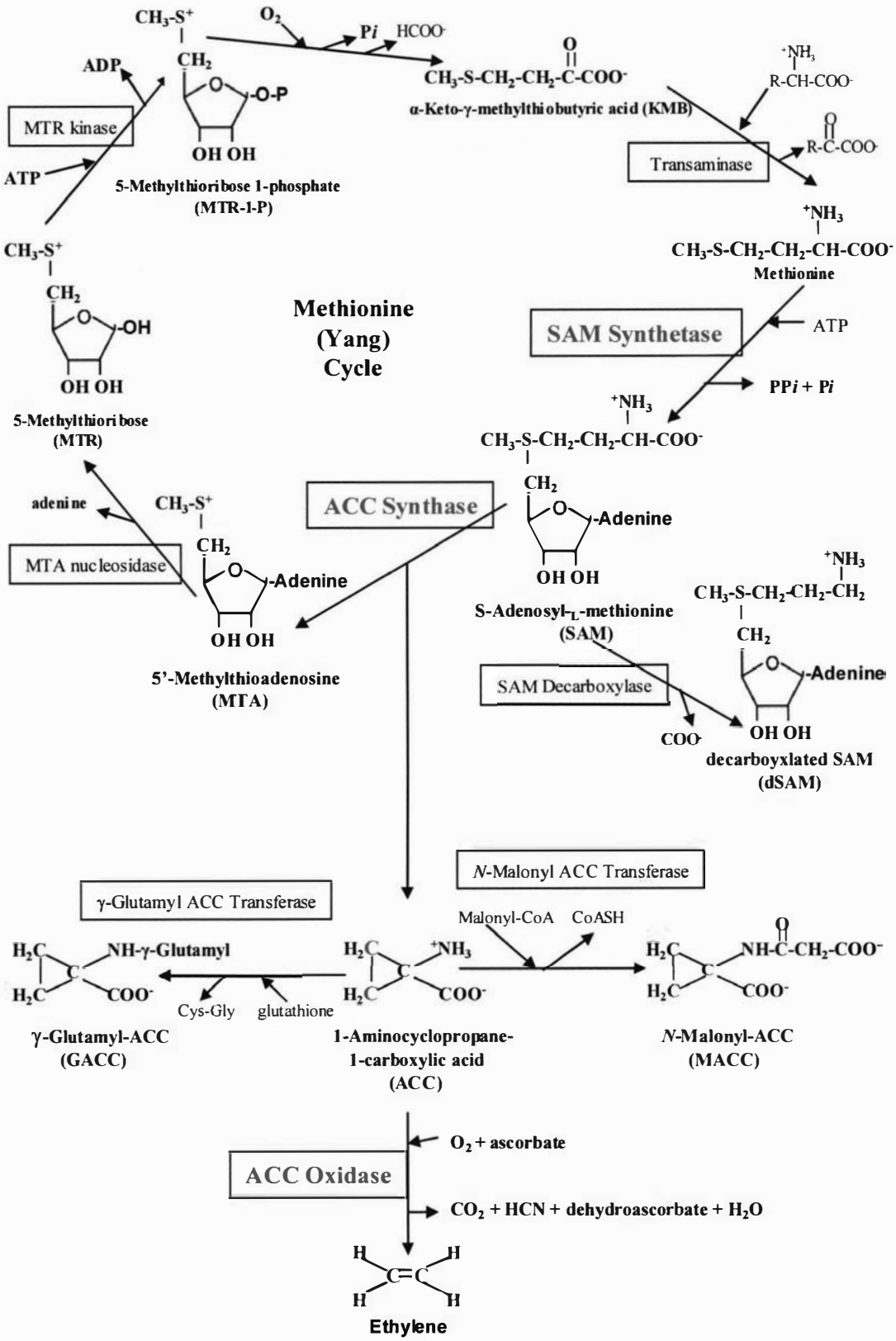


Figure 1.1: Ethylene Biosynthesis and the Yang (Methionine) Cycle
(modified from Miyazaki and Yang, 1987)

(Adams and Yang, 1977). Interestingly, unripe apple was found to be incapable of producing MTA, MTR or ethylene from administered methionine. Advantage was taken of the well known fact that a nitrogen atmosphere causes a cessation in ethylene production by pears and apples and the subsequent re-exposure to air results in a surge of ethylene production. Again using labelled methionine fed to apple tissue, MTR and a compound later identified as ACC (Lizada and Yang, 1979) were formed on exposure to a nitrogen atmosphere without the concomitant production of ethylene (Adams and Yang, 1979). These experiments showed that the conversion of ACC to ethylene in apple tissue was oxygen-dependent. Later, the carboxyl carbon of ACC (C-1 of methionine) was found to be liberated as CO_2 (Peiser *et al.*, 1984) and the production of cyanide (C-2 and N-1 of methionine) was confirmed (Pirrung, 1985). Cyanide in plants is rapidly converted to β-cyanoalanine and can further be converted into asparagine. The observed discrepancy between the amount of methionine available to produce ethylene with the actual amount of ethylene produced by apples (Baur and Yang, 1972) lead to investigations using labelled MTR (^{3}H on the methyl group and ^{14}C on the ribose moiety) showed that both radioisotopes were incorporated equally into methionine in apple tissue, and provided evidence for sulphur recycling in plants (Yung *et al.*, 1982). The methionine salvage pathway (known as the Yang or methionine cycle) is closely coupled to the ethylene biosynthetic pathway (Figure 1.1).

There are three enzymes in the ethylene biosynthetic pathway (each of which will be discussed later), SAM synthetase which converts methionine to SAM, ACC synthase which converts SAM to ACC, and ACC oxidase (ACO) which converts ACC to ethylene (Figure 1.1). Ethylene can regulate the activity of ACO (Liu *et al.*, 1985a), ACC synthase (Bufler, 1984) as well as ACC-malonyl-transferase (Liu *et al.*, 1985a; 1985b). ACC synthase is considered to be the major control point in the ethylene biosynthetic pathway, exhibiting the classic rate-limiting properties of rapid induction and rapid degradation. More recently, evidence for the notion that ACO is regulated is supported by the existence of small multigene families which have been observed to be both developmentally and environmentally responsive, exhibiting clear differential expression, rather than the widely held view that the activity of ACO is always constitutive.

1.3.1 SAM Synthetase

S-adenosyl-methionine (SAM; also known as AdoMet) is synthesized by the transfer of an adenosyl group from ATP to the sulphur atom of methionine in a reaction catalyzed by SAM synthetase. SAM synthetase is found in both prokaryotic and eukaryotic organisms (Tabor and Tabor, 1984) and two isoforms have been found to be differentially expressed in

Saccharomyces cerevisiae (Thomas and Surdin-Kerjan, 1991). SAM is not only used for ethylene biosynthesis (Yang and Hoffman, 1984; Kende, 1993), but is also decarboxylated and used for the biosynthesis of polyamines (Miyazaki and Yang, 1987) (Figure 1.1). The major forms of polyamines are putrescine, spermine and spermidine and they are found in every plant cell (Pandey et al., 2000). SAM, as the major donor of methyl groups, is used ubiquitously for the methylation of proteins, carbohydrates, lipids and nucleic acids, and not surprisingly SAM synthetase has been classified by Fluhr and Mattoo (1996) as a housekeeping enzyme. However, only a minor portion of SAM is thought to be utilised for ACC production, and so it has been suggested that SAM levels are not rate limiting for ethylene biosynthesis (Yu and Yang, 1979; Pelman *et al*, 1989). The application of polyamines has been shown to inhibit ethylene production in some plants (Pandey *et al*., 2000). For example, in carnation flowers the application of spermine delayed flower senescence, reduced ethylene production, ACC content, and activity and transcript levels of both ACS and ACO (Lee *et al*., 1997). However, reduction in ethylene production and ACC levels could be a result of the upregulation of SAM decarboxylase, rather than anything to do with SAM synthetase, since the downregulation of SAM synthetase would necessarily reduce polyamine biosynthesis and disrupt transmethylation reactions throughout the plant. Interestingly, Huan *et al*., (2001) report the enhanced expression of the SAM decarboxylase gene during sweet potato leaf senescence. In contrast, SAM synthetase genes have been shown to increase in response to drought stress (Mayne *et al*., 1996), salt stress (Espartero *et al*., 1994), fungal and bacterial elicitors (Kawalleck *et al*., 1992; Arimura et al., 2002), mechanical stimuli (Kim *et al*., 1994), exposure to ozone (Tuomainen *et al*., 1997) and during climacteric fruit ripening (Whittaker *et al*., 1997), indicating that SAM synthetase is induced during periods of enhanced ethylene synthesis (Boerjan *et al*., (1994).

SAM synthetase is encoded by a small multigene family in plants which is differentially expressed in response to developmental and environmental stimuli (Peleman *et al*., 1989; Schroder *et al*., 1997). For example, differential expression has been observed during senescence in carnation flowers (Woodson *et al*., 1992), in response to treatment of pea ovaries with indole-3-acetic acid (IAA) (Gomez-Gomez and Carrasco, 1998), and in fruit of *Actinidia chinensis* SAM synthetase transcripts were shown to be induced by exposure to exogenous ethylene (Whittaker *et al*., 1997). However, as vital as SAM synthetase is for the biosynthesis of ethylene, its many other biochemical commitments cannot be overlooked when assessing its regulatory role in this pathway.

1.3.2 ACC Synthase (ACS)

ACS (SAM methylthioadenosine-lyase) is a pyridoxal-5'-phosphate (PLP) requiring enzyme, which is present in the cytosolic fractions, and catalyzes the reaction which converts SAM into ACC and MTA (Adams and Yang 1977; 1979; Yang and Hoffman, 1984)(Figure 1.1). In common with other PLP-dependent enzymes, ACS is competitively inhibited by aminoethoxyvinylglycine (AVG) and aminoethoxyacetic acid (AOA) (Imaseki, 1999). Also, during the catalysis of SAM to ACC and MTA small amounts of the highly reactive intermediatory, vinylglycine (the aminobutyl portion of SAM) is produced (in a 1:30,000 ratio with ACC) which covalently binds to the active site of ACS resulting in irreversible inhibition of enzyme activity (Satoh and Yang, 1988; 1989a; 1989b), so that at high substrate concentrations ACS activity is reduced (Boller *et al.*, 1979) and the inhibition is time dependent (Boller, 1985; Satoh and Esashi, 1986). In the biosynthesis of ethylene, an obvious competitor of ACS for substrate is SAM decarboxylase (amongst many others, as SAM is a ubiquitous molecule in nature and the major donor of methyl groups), which is important as the decarboxylation of SAM commits the molecule to the formation of polyamines (Miyazaki and Yang, 1987) (Figure 1.1), essential for plant growth and development (Pandey *et al.*, 2000). The physiological functions of ethylene and the polyamines are distinct and at times antagonistic, particularly during leaf and flower senescence and during fruit ripening (Pandey *et al.*, 2000), and so the regulation of ACC synthase and SAM decarboxylase is tightly coupled.

ACS was first identified in homogenates of ripening tomato pericarp tissue (Boller *et al.*, 1979; Yu *et al.*, 1979), and subsequently purified, after a wounding pre-treatment, from which two monoclonal antibodies recognising different epitopes of the protein were raised and used to develop a sensitive ELISA for ACS (Bleecker *et al.*, 1986; 1988). The purified protein was found to be active as a monomer with a molecular mass of 50 kDa by SDS-PAGE, but translational products yielded a protein of 56 kDa (Bleecker *et al.*, 1986; 1988), suggesting that ACS undergoes post-translational processing *in vivo*. Consistent with these findings, the molecular mass of ACS from winter squash also varied from 50 kDa *in vivo* to 58 kDa for the translated products (Nakajima *et al.*, 1988). While an active ACS purified from zucchini was found to have a molecular mass of 86 kDa by gel filtration, that of the denatured enzyme 46 kDa, indicating that this ACS isoform in zucchini fruit is active as a homodimer (Sato *et al.*, 1991). More recently it has been shown that, at least eight *Arabidopsis* ACS isozymes function as homodimers (Yamagami *et al.*, 2003; Ecker, 2004), and may also form functional heterodimers (Tsuchisaka and Theologis, 2004a). Although there was no indication of proteolytic modification for an ACS purified from apple fruit, found to be active as a monomer, with a molecular weight of 52 ± 4 kDa (Yip *et al.*, 1991; Dong *et al.*, 1991), the

characterisation of the apple enzyme expressed in *Escherichia coli* (*E. coli*)(White *et al.*, 1994) and preliminary X-ray analysis of the apple ACS crystal structure (Hohenester *et al.*, 1994) suggest that ACS is dimeric in nature. ACS from tomato and apple have been observed to be dimeric, in the crystal structure (Capitani *et al.*, 1999; Huai *et al.*, 2001), and by mutant complementation studies for tomato ACS (Tarun *et al.*, 1998; Tarun and Theologis, 1998), where the sharing of an active site by two monomers within a dimeric unit was observed. Consistent with other PLP-dependent aminotransferases the catalytic mechanism of LE-ACS2 involves two intermediate aldimine linkages, of PLP and SAM, with lysine at position 278 (K^{278}), other essential amino acids (P^{26}, Y^{27}, F^{28}, A^{54}, Y^{152}, P^{153}, R^{157}, Y^{240}, K^{278} and R^{412}), and then substrate conversion followed by transaldimination to release the product (Huai *et al.*, 2001). In a previous study, the active site of ACS had been identified in apple and tomato fruits by radioactive labelling of SAM and PLP (Yip *et al.*, 1990), in which it was found that the lysine residue that binds PLP via an aldimine linkage was also alkylated with vinylglycine leading to irreversible inactivation of the enzyme.

ACS has a high affinity for SAM, with apparent K_m^{SAM} values ranging from 12 μM for an apple ACS expressed in *E. coli* (White *et al.*, 1994) to 60 μM for a partially purified enzyme from zucchini fruit (Nakajima and Imaseki, 1986). The apparent K_m^{SAM} for the *Arabidopsis* isoforms ranges from 8.3 to 45 μM (Yamagami *et al.*, 2003), with the K_{cat} values varying from 0.19 to 4.82 s^{-1} per monomer. ACSs have pH optimum in the alkaline region, with an optimum of pH 8.0 for an enzyme partially purified from mung bean fruit (Tsai *et al*, 1988; 1991), pH 9.5 for an enzyme from zucchini fruit (Sato *et al.*, 1991) and pH values ranging between 7.3 and 8.2 for all of the *Arabidopsis* isozymes (Yamagami *et al.*, 2003). Both the length and primary sequence of the C-terminal region of various ACS are hypervariable (Theologis, 1992), which has been found to affect its enzymatic function as well as dimerisation (Fluhr and Mattoo, 1996). Therefore, despite a high degree of similarity in the rest of the protein (Theologis, 1992), the overall amino acid sequence identities of ACS vary widely from 48 % to 97 % (Spanu *et al.*, 1994). ACS is generally considered to be the major rate-limiting enzyme in the ethylene biosynthetic pathway. This is due to the low abundance of the enzyme, [< 0.0001 % of total soluble protein in the pericarp of ripening tomato fruit; (Bleecker, 1986), and ~1.5 ng of LE-ACS6 in every 100 μg of total protein extract; (Liu and Zhang, 2004)], to the rapid induction, instability of the enzyme (Bleecker *et al.*, 1988), and because the rate of ethylene production appears to correlate well with the enzymatic activity (Rottman *et al.*, 1991; Kende, 1993; Yang and Dong, 1993). The half life (t½) of ACS, as determined by the rapid decay of enzyme activity after treatment of tissues with cycloheximide, varied from 58 min in wounded tomato fruit (Kim and Yang, 1992), 25 min in mung bean hypocotyls (Yoshii and Imaseki, 1982) to 20 min in tomato leaves (Spanu *et al.*, 1990).

It is well established that protein phosphorylation and dephosphorylation are important regulators of enzymatic activity. As ACS is a major control point in the regulation of ethylene biosynthesis, studies are underway to unravel the post-translational modifications responsible for the rapid induction and the rapid inhibition of ACS. For example, in general the basal level activity of ACS is very low in tissues that do not produce a significant amount of ethylene, and stress induced ethylene production is associated with a rapid increase in cellular ACS activity. Recently, Liu and Zhang, (2004) have demonstrated that the mitogen activated protein kinase (MAPK; designated MPK6) is induced by stress to phosphorylate *Arabidopsis* AT-ACS2 and AT-ACS6 at conserved serine residues (S^{480} S^{483} and S^{488}) of the carboxyl terminus. Evidence that MPK6 is required for the induction of AT-ACS2 and AT-ACS6 is also provided by genetic studies (Liu and Zhang, 2004). As the levels of phosphorylation were proportional to the number of phosphorylation sites, this linearity shows that each phosphorylation site is independent of the other phosphorylation sites. Given that the stability of these proteins is positively correlated with the amount of phosphorylation, and evidence from preliminary studies using proteasome inhibitors indicates that the ubiquitin-proteasome pathway is involved in the degradation of AT-ACS6, it is likely that phosphorylation prevents or slows down this process. As a consequence of phosphorylation of AT-ACS2 and AT-ASC6 by MPK6, these proteins accumulate leading to increased activity and ethylene production. Interestingly, AT-ASC2 and AT-ASC6 have been observed to act synergistically. This stress-induced activation of MPK6 has been observed to occur within one to several minutes, which represents one of the earliest responses in plants under stress (Liu and Zhang, 2004). Also, kinetic analysis for phosphorylated AT-ACS6 displays a similar V_{max} (390 μmol h^{-1} mg^{-1}) and K_m (49 μM) for its substrate SAM to the unphosphorylated AT-ACS6 (V_{max} 332 μmol h^{-1} mg^{-1}; K_m, 42 μM) suggesting that phosphorylation of AT-ACS6 by MPK6 does not alter the enzymatic activity of AT-ACS6 (Liu and Zhang et al., 2004). Since AT-ACS2 and more importantly AT-ACS6 have been identified as the substrates for MPK6, this links the MAPK cascade directly to the induction of ethylene biosynthesis in plants under stress.

Tomato LE-ACS2 from pericarp tissue has been shown to be phosphorylated by an unidentified wound induced calcium-dependent protein kinase (CDPK) at S^{460} (Tatsuki and Mori, 2001), which is conserved in the C-terminus of many ACS isozymes (Yamagami *et al.*, 2003), including AT-ACS2 and AT-ACS6. This indicates that AT-ACS2 and AT-ACS6 may be regulated by two different kinase pathways. Further, the observation that wounding induces a long-lasting ethylene induction in tomato pericarp tissue but only a transient induction of ethylene in leaf tissue has suggested the presence of tissue-specific pathways (Tatsuki and Mori, 1999), and/or maybe the induction of different LE-ACS isoforms. Also, pulse-chase experiments with phosphatase/kinase inhibitors have shown that the t½ of phosphorylated LE-

ACS2 was longer than the non-phosphorylated form (Mori *et al.*, 2006), which supports the hypothesis that phosphorylation of ACS explains the rapid increase in ethylene production in response to wounding, and for the burst of ethylene produced during climacteric fruit ripening (Tatsuki and Mori, 2001).

The regulation of ACS is further highlighted with the ongoing characterization of the function of the ETO1 protein of *Arabidopsis*. For example, over expression of ETO1 inhibits the induction of ethylene production (Vogel *et al.*, 1998) and promotes AT-ACS5 degradation (Chae et al., 2003; Wang *et al.*, 2004). Conversely, the *eto* mutants of *Arabidopsis* over-produce ethylene and display the triple response (Wang *et al.*, 2004) whilst enhancing the stability of AT-ACS5 and AT-ACS9 (Yamagami *et al.*, 2003). The C-terminal end AT-ACS5 has been observed to target the protein for rapid proteolysis by the 26S proteosome (Chae *et al.*, 2006), and this rapid degradation requires the ETO1 protein, which acts as a substrate-specific adaptor protein to promote ubiquitination of AT-ACS5. ETO1 has been shown not to interact with AT-ACS6 and AT-ACS2 (*pers comm.* Wang and Ecker, cited in Ecker, 2004). It should be noted that AT-ACS1 is enzymatically inactive and AT-ACS3 is a pseudogene, AT-ACS10 and AT-ACS12 encode aminotransferases, leaving eight authentic AT-ACS genes (Yamagami *et al.*, 2003). It remains to be determined whether AT-ACS7 is also post-transcriptionally regulated because the regulatory C-domain is missing (Yamagami *et al.*, 2003).

The gene encoding ACS was first cloned from zucchini (Sato and Theologis, 1989), and many have been cloned since (see review by Grichko and Glick, 2001) and are developmentally regulated or differentially expressed in response to various internal and external inducers (Lanahan *et al.*, 1994; Theologis, 1992; Yi *et al.*, 1999; Bekman *et al.*, 2000). For example, in *Arabidopsis* thirteen ACS genes have been isolated (Schaller and Kieber, 2002) and show both distinct and overlapping patterns of expression (Tsuchisaka and Theologis, 2004b). In seedlings of *Arabidopsis*, it was shown very early that each *ACS* family gene had a specific response to wounding, anaerobiosis, and treatment with lithium chloride and auxin (Liang *et al.*, 1992). Further, in leaf development of *Arabidopsis*, *AT-ACS1* expression is highest at leaf emergence and decreases sharply in rapidly expanding leaves (Smalle *et al.*, 1999), while *AT-ACS6* expression is induced in senescent leaves during ozone exposure (Miller *et al.*, 1999). At least eight *LE-ACS* genes have been isolated (Van Der Straeten *et al.*, 1990; Rottman *et al.*, 1991; Johnson and Ecker, 1998; Alexander and Grierson, 2002). In apple *MD-ACS1*, there is allelic variation in the level of transcript during fruit ripening (Sunako *et al.*, 1999).

1.3.3 Conjugation of ACC

ACC is not only converted to ethylene in plants, but can also be conjugated with malonyl in a malonyl CoA-dependent reaction into *N*-malonylamino-1-cycloproprane-1-carboxylic acid (*N*-malonyl-ACC / MACC), a reaction catalysed by *N*-malonyltransferase (Amrhein *et al.*, 1981; Hoffman *et al.*, 1982; 1983; Peiser and Yang, 1998). Alternatively, ACC can be conjugated to glutamic acid in a glutathione-dependent reaction to form 1-(gamma-$_L$-glutamylamino) ACC (GACC) catalysed by glutamyl ACC transferase (Martin *et al.*, 1995; Peiser and Yang, 1998). Although ACC is known to be metabolized to α-ketobutyrate and ammonia in some microorganisms (Honma and Shimomura, 1978), there is no evidence of such a deamination reaction in plant tissue (Amrhein *et al.*, 1981). The amount of ACC in higher plants therefore must be regulated by at least four enzymes, ACS, ACO, *N*-malonyltransferase and glutamyl ACC transferase (Figure 1.1).

MACC is found throughout the plant, including vegetative tissue, seeds and in ripening fruit (Satoh and Esashi, 1984; Yang and Dong, 1993; Peiser and Yang, 1998; Lara and Vendrell, 2000; Tan and Bangerth, 2000). N-malonyltransferase has been partially purified from mung bean (Guo *et al.*, 1992; Benichou *et al.*, 1995) and tomato (Martin and Saftner, 1995). Two isoforms have been identified in mung bean that have different molecular masses (35 and 55 kDa) and kinetic parameters (Benichou *et al.*, 1995). MACC has been thought to be a stable conjugate in germinating peanut seeds and wheat leaves, unable to be hydrolyzed to release free ACC *in vivo* (Hoffman *et al.*, 1983) and studies with *Acer pseudoplatanus* cells indicated that MACC is synthesized in the cytosol and stored in the vacuole (Bouzayen *et al.*, 1988). However, the observation in cotton cotyledonary tissue of fluctuations in MACC suggested that MACC is metabolized (Jasoni *et al.*, 2002), possibly to ACC or transported to another location. This observation concurs with earlier studies which demonstrated that when radioactive MACC was applied to tobacco and watercress, radioactive ACC and ethylene were formed (Jiao *et al.*, 1986). Also, *N*-malonyltransferase activity has been shown to have developmental and tissue-specific patterns of expression in tomato (Martin and Saftner, 1995; Peiser and Yang, 1998), and MACC accumulates differentially in the pulp and peel during apple fruit development (Lara and Vendrell, 2000; Tan and Bangerth, 2000), although MACC levels increased and remained high during the apple climacteric.

Conjugation of ACC into GACC using *in vivo* feeding of radiolabelled ACC to tomato tissue discs, was found in mature-green fruit in amounts about 10 % of that of MACC, but was not detected in fruits at other ripening stages, although GACC was formed *in vitro* in extracts from fruit of all ripening stages (Peiser and Yang, 1998). In contrast, Martin *et al.* (1995) found

GACC in both preclimacteric and climacteric tomato fruit, using protein extracts in assays initiated with radiolabelled ACC, and report higher levels of GACC than the amounts found for MACC. Peiser and Yang (1998) did not support the proposal that GACC formation could be more important than MACC formation in tomato fruit, and concluded that MACC is the major, if not the sole, conjugate of ACC in plant tissues. Interestingly, glutathione is a tripeptide synthesized from cysteine, glycine and glutamic acid, and is involved in scavenging hydrogen peroxide and other reactive oxygen species, as well as serving as an amino acid transporter.

1.4 ACC Oxidase (ACO)

1.4.1 The Ethylene-Forming Enzyme (EFE)

Identification of the ethylene forming enzyme (EFE) has lagged behind ACC synthase because although ethylene could be produced by the administration of ACC to a wide variety of plant tissue *in vivo* (Cameron *et al.*, 1979), the ability to produce ethylene was not retained *in vitro*, following homogenisation and the administration of ACC. Many enzymes were assessed as the ethylene forming enzymes, including peroxidase, an IAA-oxidase, a carnation microsomal enzyme, a pea microsomal enzyme and an enzyme from a pea seedling, but ethylene production *in vivo* did not correspond to the ethylene production *in vitro* (Yang and Hoffman, 1984). For example, the reported K_m for ACC (K_m^{ACC}) for the pea microsomal enzyme in a cell-free homogenate ranged between 15 mM to 400 mM, values that were much higher than the K_m^{ACC} of 66 μM reported for the enzyme *in vivo* from pea epicotyls (McKeon and Yang, 1984).

As the ACC molecule possesses reflective symmetry but lacks geometric (rotational) symmetry, the two methylene groups of ACC could be distinguished by an enzyme which stereodifferentiates. Ethyl substitution of each of the four methylene hydrogens of ACC results in four stereoisomers of 1-amino-2-ethyl-cyclopropane-1-carboxylic acid (AEC), whose absolute configurations are (1R, 2R), (1S, 2S), (1R, 2S), and (1S, 2R). Therefore, when each of the four stereoisomers of AEC was administered to post climacteric apple and (1R, 2S)-AEC was preferentially converted to 1-butene (Hoffman *et al.*, 1982), this observation demonstrated that the enzyme converting ACC to ethylene exhibited stereospecificity towards the 2-ethyl-ACC stereoisomer (1R, 2S)-AEC *in vivo*, and could also be used to validate the authenticity of EFE activity *in vitro*. This is important as ACC can be converted to ethylene non-enzymatically by oxidants (Boller *et al.* 1979; Lizada and Yang, 1979) including oxidative free radicals (Legge *et al.*, 1982), such as in the Fenton reaction (Fe^{2+} and H_2O_2) and in the presence of xanthine and xanthine oxidase (McRae *et al.*, 1983). In some plant tissues under light, in the presence of Cu^{2+}, non physiological evolution of ethylene may be derived from lipid peroxidation (Sandmann and Boger, 1980).

Slater *et al.* (1985) first identified the ethylene forming enzyme (EFE) as the translation product of an mRNA isolated from tomato fruits. They identified nineteen non-homologous groups of tomato ripening-related clones. One of these clones, designated pTOM13 (now *LE-ACO1*) was shown to be homologous to an mRNA, which accumulated prior to the wounding-induced ethylene peak in unripe fruit and leaf tissue of tomato (Smith *et al.*, 1986). Subsequently, *pTOM13* was shown to be induced by ethylene in mature green tomato fruit (Maunders *et al.*, 1987). Following the observation of greatly reduced ethylene production by tomato plants transformed with *pTOM13* in the antisense orientation, Hamilton *et al.* (1990) suggested that the gene encoded an enzyme involved in ethylene biosyntheis. It appeared that from a comparison of the molecular mass of partially purified ACC synthase from zucchini fruit (53 kDa; Sato *et al.*, 1991) with the translation product of pTOM13 (35 kDa; Smith *et al.*, 1986), the coded protein was too small to be an ACC synthase (Hamilton *et al.*, 1990). To further confirm whether *pTOM13* could encode EFE, an activity assay *in vivo* was performed on leaf discs from both wild type and plants transformed with *pTOM13* in the antisense orientation, and it was shown that the ethylene forming ability was reduced in the antisense plants in a gene dosage-dependent manner (Hamilton *et al.*, 1990). In addition, Hamilton *et al.* (1991) then reported that a full-length clone of *pTOM13* (designated *pRC13*) was found to confer EFE activity when the cDNA was expressed heterologously in yeast.

The deduced amino acid sequence of *pTOM13* was found to have 33 % identity and 58 % similarity with flavonone 3-hydroxylase from *Antirrhinum majus* which is a member of the 2-oxoglutarate-dependent dioxygenases (2-ODDs) (Prescott, 1993; Prescott and John, 1996; Iturriagagoitia-Bueno *et al.*, 1996). This enzyme is known to be a non-haem iron-containing protein requiring anaerobic conditions during extraction and Fe^{2+} and a reducing agent (ascorbate) for maximal activity *in vitro* (Britsch and Grisebach, 1986). By incorporating these components into the reaction mixture *in vitro*, Ververidis and John (1991) were the first to demonstrate authentic EFE activity *in vitro* from the soluble fraction of melon fruit, and the failure of previous attempts to assay enzymatic activity was now attributed to the loss of these cofactors during protein extraction from plant tissue.

Confirmation for both EFE activities *in vitro* and *in vivo* was achieved by finding a parallel increase in preclimacteric apple fruits treated with ethylene (Fernándcz-Maculct and Yang, 1992), and by the stereospecificity of the reaction (Ververidis and John, 1991; Kuai and Dilley, 1992; Fernández-Maculet and Yang, 1992; Dong *et al.*, 1992b). The stoichiometry of the EFE reaction *in vitro* was then determined (Dong *et al.*, 1992b) and as a consequence of this, EFE was renamed 1-aminocyclopropane-1-carboxylic acid (ACC) oxidase (ACO) (EC.1.4.3), and is now classed as a 2-oxoacid dependent dioxygenase (2-ODD)(Prescott and John, 1996).

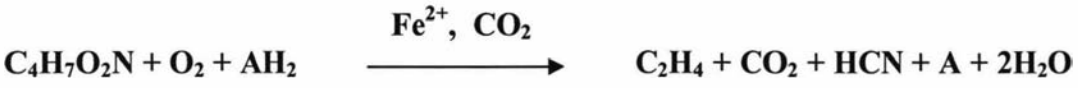


Figure 1.2: The Stoichiometry of the Reaction Catalyzed by ACC Oxidase
In this reaction ACC oxidase catalyses the oxidation of ACC and ascorbate in the presence of dioxygen to ethylene, carbon dioxide, cyanide, dehydroascorbate and water. AH_2 and A stand for ascorbate and dehydroascorbate, respectively. Ferrous iron and carbon dioxide are co-factors.

Once ACC oxidase (ACO) activity, *in vitro*, was fully recovered from crude protein extracts using appropriate cofactors (ascorbate and Fe^{2+}), purification and characterization of the enzyme from many plant species progressed quickly. For example, in pear (Vioque and Castellano, 1994; 1998; Fonseca *et al.*, 2004), avocado (McGarvey and Christofferson, 1992), banana (Moya-Leon and John, 1995), breadfruit (Williams and Golden, 2002), tomato (Smith *et al.*, 1994; Zhang *et al.*, 1995; Barlow *et al.*, 1997) and kiwifruit (Xu *et al.*, 1998). Partially purified and crude enzyme extract from carnation flowers (Nijenhuis-De Vries *et al.*, 1994; Kosugi *et al.*, 1997). Kinetic analyses of ACO activity demonstrate that the enzyme exists as more than one isoform in *Trifolium repens* (Gong and McManus, 2000) and in tomato (Bidonde *et al.*, 1998). (for the Purification, Characterization and kinetic properties of ACO in apple, refer section 1.6.1.2)

1.4.2 Catalytic Mechanism of ACC Oxidase

Most 2-oxoglutarate-dependent dioxygenases (ODDs) have an absolute requirement for 2-oxoglutarate as a co-substrate, and a reductant (Prescott and John, 1996), whereas ACO is not stimulated by 2-oxoglutarate and is inhibited *in vitro* by the molecule (Dupille and Zacarias, 1996; Iturriagagoitia-Bueno *et al.*, 1996; Vioque and Castellano, 1998) at concentrations of ~ 1mM (Vioque and Castellano, 1998). The suggestion that ACO originated by an alteration in substrate specificity from 2-oxoglutarate to ACC (John, 1997) is in keeping with these inhibition studies. Another atypical ODD is isopenicillin *N* synthase (IPNS) which also does not use 2-oxoglutarate, and has been extensively used as a model to predict the secondary structure and to elucidate the catalytic mechanism of ACO (Shaw *et al.*, 1996; Kadyrzhanova *et al.*, 1997; 1999; Dilley *et al.*, 2004; Seo *et al.*, 2004; Iturriagagoitia-Bueno *et al.*, 1996; Lay *et al.*, 1996; Zhang *et al.*, 1997) as the crystal structure was available (Roach *et al.*, 1995) prior to the solving of the crystal structure of ACO from *Petunia hybrida* (Zhang *et al.*, 2004b).

Ferrous iron (Fe^{2+}) is now confirmed to be an essential co-factor for ACO (Bouzayen *et al.*, 1991), and the observation that neither 2-methyl-1,2-dipyridyl-1-propane nor phenylhydrazine inhibit the activity of ACO (purified from apple) demonstrated that ACO is not a haem iron protein, but a non-haem iron(II) dependent protein (a dioxygenase) (Dupille *et al.*, 1993). At the active site of avocado recombinant ACO expressed in *E. coli*, Fe^{2+} is oxidized to ferric iron (Fe^{3+}) during a single turnover reaction (Rocklin *et al*, 2004), determined using electron paramagnetic resonance (EPR) spectroscopy. In a nice study, the inactivation of recombinant LE-ACO (*pTOM13* expressed in *E. coli*), by diethylpyrocarbonate (DEPC) provided evidence that two or three His residues were rapidly *N*-carboxyethylated (Zhang *et al.*, 1995), and although tomato (LE-ACO1) contains approximately nine His residues, the modifications are most likely to occur at the active site. Further, when Fe^{2+} together with ACC, ascorbate and DEPC were added to the reaction mixture, the enzyme activity was protected by 60 to 80 %, while in the absence of Fe^{2+} the enzyme activity was observed to decrease to 20 % (Zhang *et al.*, 1995), which indicates that Fe^{2+} is binding to at least one His residue at the active site of ACO. Spectroscopic studies using the electron nuclear double resonance (ENDOR) technique, identified two His residues in the Fe^{2+} coordination sphere of avocado ACO expressed in *E. coli* (Tierney *et al.*, 2005).

There is now convincing evidence from site-directed mutagenesis studies on the iron binding site of apple ACO expressed in *E. coli* (Shaw *et al.*, 1996; Kadyrzhanova *et al.*, 1997; 1999) and from mutagenesis and metal-catalyzed oxidation of tomato ACO expressed in *E. coli* (Zhang *et al.*, 1997; Tayeh *et al.*, 1999) that H^{177}, D^{179} and H^{234} bind Fe^{2+} during catalytic activity. Other conserved residues (H^{39}, H^{56}, H^{94} and H^{211}) are important for catalytic activity (Zhang *et al.*, 1997; Tayeh *et al.*, 1999; Zhang *et al.*, 2004b), but have not been consigned roles. Analysis of the recently resolved crystal structure of ACO confirm that the active site contains a single Fe^{2+} ligated by three residues H^{177}, D^{179} and H^{234} (Zhang *et al.*, 2004b), which have equivalent residues in IPNS and other ODDs (Kadyrzhonova *et al.*, 1997; 1999; Rocklin *et al.*, 2001). This "2-His-1-carboxylate facial triad" which holds the Fe^{2+} centre in the active site, thereby leaves three sites available for exogenous ligand binding (Rocklin *et al.*, 1999; Zhou *et al.*, 2001).

An iron catalytic centre is extremely versatile as it can dynamically coordinate multiple exogenous ligands and promote interactions between them. With such a wide range of possible interactions, together with the multiple transition states involved in converting O_2 and ACC to ethylene, CO_2 and HCN, the mechanism of the two-electron oxidation of ACC to ethylene remains largely unclear, and investigations using site-directed mutagenesis, spectroscopy and crystallography are often difficult to interpret. For example, although ACO requires the

presence of ascorbate and CO_2/HCO_3^-, the roles played by these reagents, the order of substrate addition, and the mechanism of oxygen activation remain controversial. The proposed mechanism that both ascorbate and O_2 bind to the Fe^{2+} which initiates the O_2 activation process (Zhang *et al.*, 1997; Pirrung *et al.*, 1998) differ from the more recent proposals of Rocklin *et al.* (1999), Zhou *et al.* (2001) and Tierney *et al.* (2005) that ACC and O_2 bind Fe^{2+} simultaneously thereby allowing the correct orientation to promote electron transfer between them and initiate catalysis. The two-electron oxidation of ACC requires Fe^{2+}, O_2, ascorbate and CO_2 *in vitro* (Veriveridis and John, 1991; Dong *et al.*, 1992; Peiser *et al.*, 1984; Adams and Yang, 1979), and seems to proceed *via* two successive one-electron transfer processes (Pirrung *et al.*, 1998). Spectroscropic and crystallographic studies have revealed that the mechanisms of ACO, like other 2-ODDs (IPNS, Roach *et al.*, 1995; deacetoxycephalosporin C synthase, DAOCS; Valegård *et al.*, 1998, and anthocyanidin synthase, ANS, Wilmouth *et al.*, 2002), involve binding of dioxygen to a five-coordinate Fe^{2+} in the enzyme-substrate complex (Costas *et al.*, 2004; Rocklin *et al.*, 1999; Zhou *et al.*, 2002; Zhang *et al.*, 2004b).

Spectroscopic evidence that both the α-amino and α-carboxylate groups of ACC bind directly to iron complexed to ACO (from avocado expressed in *E. coli*) was provided by Rocklin *et al.* (1999), as studied with a readily formed ACO.Fe^{2+}.NO.ACC ternary complex which does not undergo reaction turnover (NO is alanine, the structural analog of ACC, labelled with ^{15}N and ^{17}O). However, mutagenesis studies using apple ACO expressed in *E. coli* concluded that R^{244}, S^{246} and T^{157} are binding sites for the ACC carboxyl group (Kadyrzhanova *et al.*, 1999; Dilley *et al.*, 2003), based on steady-state kinetics of the mutants $R^{244}K$, $S^{246}A$ and $T^{157}A$ as single double and triple mutants of the three residues. The K_m for ACC (K_m^{ACC}) of the triple mutant was increased while the V_{max} was decreased. This is consistent with the ACC carboxyl group interacting with the R^{244} guanidinium group and the hydroxyl group of S^{246} and T^{157}. In the crystal structure of petunia ACO, although R^{244} is directed away from the active site, a conformational change could bring the side chain into the active site, and perhaps indirectly bind to Fe^{2+} *via* a water molecule (Zhang *et al.*, 2004b), and could bind HCO_3^-. Interestingly, R^{244} and S^{246} form the tripeptide motif (RXS; X denotes any residue) which is a typical phosphorylation site. A further proposal from spectroscopic analysis of recombinant avocado ACO is that R^{244} and R^{175} do bind $NaHCO_3$, which in turn binds an iron bound O_2 derived intermediate to enable correct proton and electron transfer (Rocklin *et al.*, 1999). Chemical modification has shown that apple recombinant ACO does not catalyze by the hydroxylation of the amino terminal of ACC (Charng *et al.*, 2001). Of the three conserved cysteine residues observed (C^{28}, C^{133} and C^{165}) only the C^{28} residue is important for catalysis in apple ACO (Kadyrzhanova *et al.*, 1997; 1999).

Covalent modification studies using apple ACO expressed in *E. coli* implicate the lysine residues K^{158}, K^{230} or K^{292} as the most critical for ascorbate activation (Kadyrzhanova *et al.*, 1999; Dilley *et al.*, 2003). This observation is based on pyridoxal-5-phosphate (PLP), which is a potent inhibitor of ACO and can readily form Schiff bases with lysine, competing with ascorbic acid for lysine binding sites. Ascorbic acid binds to proteins *via* salt bridges and H-bonding (Li *et al.*, 2001), but may form a Schiff base with lysine. Of note is that K^{158} is adjacent to T^{157}, the residue proposed to bind the carboxyl group of ACC. Also, in kiwi fruit ACO expressed in *E. coli*, the mutation of K^{158} (to A^{158} and C^{158}) resulted in almost complete loss of enzyme activity (Lay *et al.*, 1996). Analysis of the crystal structure of petunia ACO suggests that K^{158} should be accessible for Schiff base formation with pyridoxal (Zhang *et al.*, 2004b). However, in petunia ACO and other 2-ODDs, a well-defined binding site for ascorbate has not been identified, although electron transfer from ascorbate may be mediated via Y^{289} in the active site of petunia ACO (Zhang *et al.*, 2004b). Mutagenesis studies using recombinant MD-ACO1 from apple suggest the ascorbate interacts with the side chains of R^{244} and S^{246} (Seo *et al.*, 2004). Also as crystallographic evidence suggests that ascorbate does not bind directly to ascorbate peroxidase (Sharp *et al.*, 2003), it may be that ascorbate does not chelate to the non-haem iron of ACO either. *In vitro*, catalytic oxidation of ACC can be coupled to the oxidation of ascorbate (Dong *et al.*, 1992b; Smith *et al.*, 1992; Vioque and Castellano, 1994) although the *in vivo* stoichiometry of the ACO reaction is uncertain. In addition to the proposed role of ascorbate as a reducing agent to complete the reaction turnover (Dilley *et al.*, 2003; Rocklin *et al.*, 2004), possibly at two separate points in catalysis (Rocklin *et al.*, 2004), spectroscopic evidence has been provided by Zhou *et al.* (2001), Rocklin *et al.* (2004) and Tierney *et al.* (2005) that ascorbate has an effector role, which may involve binding at a secondary site far from the active site and causing a conformational change in ACO.

In apple recombinant ACO, the proposal that HCO_3^- (not CO_2) binds directly to R^{175} and thus positions Fe^{2+} into its binding site (H^{177}, D^{179} and H^{234}) has been made by Dilley *et al.* (2003). Although in the crystal structure of petunia ACO R^{175} is on a loop directed away from the active site, a conformational change could bring the side chain into the Fe^{2+} binding site (Zhang *et al.*, 2004b). Mutants of E^{175}, Q^{175}, H^{175}, A^{175} and G^{175} were unable to interact with HCO_3^-, whereas the addition of carbonic anhydrase stimulated the activity of the wild type R^{175}. As for the proposed role of CO_2 (Zhou *et al.*, 2001), the presence of HCO_3^- may allow the continuous turnover of the reaction and prevent the inactivation of ACO (Dilley *et al.*, 2003). The addition of $NaHCO_3^-$ (as CO_2) to ACO incubations has been observed to both increase K_{cat} and protect ACO from oxidative deactivation (Rocklin *et al.*, 2004; Zhang *et al.*, 2004b). Activity *in vitro* of purified ACO from apple fruit is completely abolished in a CO_2-free atmosphere, but can be reversed (Dong *et al.*, 1992b). ACO is unusual in that it requires $NaHCO_3$ *in vitro* as an

activator (Dong *et al.*, 1992b; McRae *et al.*, 1983; Smith and John, 1993), although CO_2 itself and (not HCO_3^-) has been identified as the active species for ACO purified to near homogeneity (Fernández-Maculet *et al.*, 1993) and partially purified (Poneleit and Dilley, 1993) from apple fruit tissue.

The mechanism by which carbon dioxide activates apple recombinant ACO has been examined by site-directed mutagenesis (Kadyyrzhanova *et al.*, 1997; 1999; Charng *et al.*, 1997). The mechanism was proposed to be similar to the CO_2 activation of RUBISCO which is through the formation of carbamate at a lysine residue. Of eight complctely conserved lysine residues (K^{72}, K^{144}, K^{158}, K^{172}, K^{199}, K^{230}, K^{292} and K^{296}) all mutant forms were activated by CO_2 indicating that none of these lysine residues were the carbamylation target for CO_2 activation. For kiwi fruit ACO, Lay *et al.* (1996) suggests that the carbamate is formed at R^{300}. For apple ACO, residues in the C-terminus E^{297}, R^{299} and E^{301} are important for enzyme activity particularly R^{299} which may be involved in the mechanism of CO_2 activation (Kadyrzhanova *et al.*, 1999). Further, both K^{296} and R^{296} have been suggested to play important roles in enzyme activity due to their positive charges (Yoo *et al.*, 2006). The ACO motif K^{296} to E^{301} is conserved over 24 species, including apple (Yoo et al., 2006). Interestingly, truncation of the tomato *pTOM13* ACO C-terminus after M^{304} generated mutants with <5 % the activity of wild type, and truncation from E^{302} led to almost complete (<1 %) loss of activity, although activity was stimulated by bicarbonate (*pers. comm.* Zhang and Schofield, cited in Zhang *et al.*, 2004b). Oddly, in the crystal structure of petunia, the C terminus of each ACO monomer interlocks with the C terminus of an adjacent molecule to form a tetramer. Both hydrophobic and electrostatic interactions appear to be involved at this interface involving the following residues E^{222} to K^{297}, K^{279} to M^{304} *via* a water molecule; L^{288} to F^{294}; F^{294} to F^{294}; and R^{300} to D^{219} and Y^{285} (Zhang *et al.*, 2004b), but may be an artefact due to the constraints of the crystalline lattice, which only shows the dimeric and tetrameric forms of petunia ACO.

A three-dimensional structure of apple recombinant ACO was determined using mutagenesis and comparative modelling methods (Seo *et al.*, 2004) and as for the crystal structure of petunia ACO (Zhang et al., 2004b), the main chain of ACO contains a distorted double-stranded β-helix (DSBH or jelly-roll) core. The active site is located at the end of the DSBH near to the C-terminus and is well defined as a wide cleft (Seo *et al.*, 2004; Zhang *et al.*, 2004b), which appears to be open compared to those for IPNS and other 2-ODDs. On the inner surface of the active site the residues are mostly hydrophobic and well conserved when compared with those of IPNS and other 2-ODDs. The DSBH is stabilized by hydrophobic interactions that involve residues including F^{33}, I^{184}, L^{186}, Q^{188}, F^{187}, L^{195}, L^{197}, V^{206}, V^{214}, V^{215}, V^{236} and F^{250}. Also an extended helix is stabilized by residues L^{68}, A^{79}, M^{84} and electrostatic interactions between R^{64}

and D^{85}, and Y^{57} and W^{86}. The stabilization of the secondary structure is important to allow the tertiary structure adjustments necessary for the correct orientation of the active site.

If the proposal that electrons are transferred from one avocado recombinant ACO monomer to another (Rocklin *et al.*, 2004), the observation that a loop projects into the active site of another monomer in the crystal structure of petunia may be relevant (Zhang *et al.*, 2004b), and the residues which may be important if intramolecular electron transfer involving a protein residue occurs, are Q^{78}, E^{80}, D^{83}, K^{158}, H^{177}, F^{250}, N^{252}, Y^{285}, Y^{289}.

ACO is unstable during catalysis (Smith *et al.*, 1994; Pirrung *et al.*, 1993; 1998; Iturriagagoitia-Bueno *et al*, 1996; Zhang *et al.*, 1997; Barlow *et al.*, 1997; Zhang *et al.*, 2004b) and several mechanisms for the inactivation of ACO have been observed. 1) Partial unfolding of ACO occurs in the absence of substrates and co-factors with a consequent reduction of the t½ of the enzyme, although the inactivation is relatively slow and does not involve the fragmentation of the protein. 2) Rapid inactivation of ACO occurs in the presence of Fe^{2+} and ascorbate. This inactivation is thought to be caused by oxidative damage due to the generation of hydrogen peroxide from the interaction of Fe^{2+} and ascorbate in aerobic conditions, as the inactivation does not occur in the presence of catalase (a catalase protectable inactivation). 3) ACO also undergoes metal-catalyzed autocleavage which is not catalase protectable. Two cleavage sites have been identified by N-terminal sequencing of ACO, one between L^{186} and F^{187} and the second between V^{214} and V^{215}. Analysis of the crystal structure indicates that these sites are on adjacent strands of the DSBH, which is consistent with ACO cleavage being mediated by leakage of a reactive oxygen species from the iron at the active site. This is also consistent with the observation that no ACO fragmentation occurs when the enzyme is denatured prior to the addition of ascorbate and Fe^{2+}. Additionally, non-haem iron oxygenases have been found to catalyze several types of post-translational modification reactions of their amino acid side chains (Ryle and Hausinger, 2002).

1.4.3 ACC Oxidase Gene Expression in Higher Plants

It is now well established that *ACO* belongs to a small multi-gene family in numerous plant species (e.g. Pogson *et al.*, 1995; Lasserre *et al.*, 1996; Barry *et al.*, 1996; Kim *et al.*, 1998; Hunter *et al.*, 1999; Ruperti *et al.*, 2001; Chen and McManus, 2006). Following identification of the first *ACO* cDNA in *Lycopersicon esculentum* (designated as *pTOM13*) (Slater *et al.*, 1985; Hamilton *et al.*, 1990; 1991; Bouzayen *et al.*, 1993) many *ACO* gene families have now been identified through screening genomic libraries. *ACO* cDNA clones isolated from tomato were designated *LE-ACO1*, *LE-ACO2*, *LE-ACO3* and *LE-ACO4* (Bouzayen *et al.*, 1993; Barry

et al., 1996; Nakatsuka *et al.*, 1998), with a sequence identity of 88-94 % between *LE-ACO1*, *LE-ACO2* and *LE-ACO3* (Lasserre *et al.*, 1996), and a fifth putative *LE-ACO5* (Sell and Hahl, 2005). *LE-ACO1* shares a high sequence identity with apple *ACO* (*AP4-ACO*: 74 %) and with the predicted peptide sequence an identity of 88 % (Holdsworth *et al.*, 1987). In peach, two distinct *ACO* genes share a coding sequence identity of 77.7 % (Ruperti *et al.*, 2001). *PP-ACO1* is organized as 4 exons interrupted by 3 introns, whereas *PP-ACO2* has only 2 of the 3 introns present in *PP-ACO1*, and lacks the second intron. The introns and 5′ and 3′ untranslated regions of *PP-ACO1* and *PP-ACO2* show degrees of homology ranging between 44 % and 50.4 %. *PP-ACO1* and *PP-ACO2* have the highest sequence identity with apple *ACO* (*AP4-ACO*: 85.4 %) and petunia (*PH-ACO3*: 84.1 %) (Ruperti *et al.*, 2001). In the melon family *CM-ACO1* has a coding region interrupted by three introns, but the other two genes (*CM-ACO2* and *CM-ACO3*) have only two introns (Lasserre *et al.*, 1996). Similarly, in the petunia family, *PH-ACO1* has four exons while *PH-ACO2, PH-ACO3* and *PH-ACO4* have three exons (Tang *et al.*, 1993). An ACO from avocado (*pAVOe3*) shares a high sequence identity with apple *ACO* (*AP4-ACO*: 72 %) and with the predicted peptide sequence an identity of 84 % (McGarvey *et al.*, 1990). Using cDNA screening, three members in sunflower seedlings (Liu *et al.*, 1997), two in banana fruit (Huang *et al.*, 1997; Huang and Do, 1998), two in potato (Nie *et al.*, 2002; Zanetti *et al.*, 2002), three in tobacco (Kim *et al.*, 1998), one in apricot (Mbéguié-A-Mbéguié *et al.*, 1999) and one in pear (Gao *et al.*, 2002) have been identified. Sequence comparison from more than thirty *ACO* genes indicated a high nucleotide sequence identity (70-80 %) both within the same family and between families from different plant species (Lasserre *et al.*, 1996).

Many *ACO*s are differentially expressed during plant development (Barry et al., 1996; Lasserre *et al.*, 1996; Blume and Grierson, 1997; Hunter *et al.*, 1999; Rasori *et al.*, 2003; Chen and McManus, 2006) and in response to environmental stimuli (Dong *et al.*, 1992; Ross *et al.*, 1992; Balagué *et al.*, 1993; Fluhr and Mattoo , 1996; Nakajima *et al.*, 2001; Moeder *et al.*, 2002), including *Petunia hybrida PH-ACOs* (Tang *et al.*, 1993) and mung bean *ACO*s (Kim and Yang, 1994). In broccoli for example, *ACC-Ox1* is expressed in senescent and reproductive tissues and *ACC-Ox2* is only expressed in reproductive tissues (Pogson *et al.*, 1995).

In tomato, the expression of *LE-ACO1*, *LE-ACO2*, *LE-ACO3* and *LE-ACO4* was examined using a combination of northern analysis and ribonuclease protection assays (Barry *et al.*, 1996; Nakatsaku *et al.*, 1998). *LE-ACO1* was barely detectable in green leaves but rapidly increased at the onset of senescence (27-fold) and continued to rise, *LE-ACO2* was not detected in leaf tissue, and *LE-ACO3* was present in green leaf tissue, and transiently at the onset of senescence to a level approximately half that of the *LE-ACO1* message. Similarly, in fruit *LE-ACO1* increased rapidly from basal levels at the onset of the climacteric and remained high, *LE-ACO2*

was not detected in fruit (but is present in flower tissue) and *LE-ACO3* appeared transiently at the onset of senescence to a level approximately 13-fold less than *LE-ACO1*. *LE-ACO4* increased from basal levels at the onset of the climacteric and persisted through ripening, but to a much lower level than *LE-ACO1*. *LE-ACO5*, has recently been observed to be expressed in response to anaerobiosis mainly in the fruits but also in the leaves (Sell and Hahl, 2005). Expression was also examined with the β-glucuronidase (GUS) reporter gene fused to the promoter region of *LE-ACO1* and transformed into tomato (Blume and Grierson, 1997). The *LE-ACO1* promoter was induced in a similar way to that of the endogenous *LE-ACO1* gene, with major increases during leaf senescence and fruit ripening, but *LE-ACO1* expression was lower in ripening fruit relative to the amount induced during leaf senescence, in contrast to endogenous mRNA which is more abundant in ripening fruit. It is suggested that the known high stability of the GUS protein may contribute to the differences between the endogenous LE-ACO activity when compared with the LE-ACO1-GUS activity (Blume and Grierson, 1997). *LE-ACO1* is induced by ethylene, methyl jasmonate, powdery mildew, wounding (Blume and Grierson, 1997) and ozone (Nakajima *et al.*, 2001; Moeder *et al.*, 2002). *LE-ACO1* (and perhaps *LE-ACO4*) is clearly a senescence-associated-gene (SAG), while *LE-ACO3* may be a photosynthetic-associated-gene (PAG).

In peach (*Prunus persica*), northern analysis using total RNA with probes to the 3'-UTR were used to examine the differential expression of *PP-ACO1* and *PP-ACO2*. *PP-ACO1* increased dramatically during fruit ripening and leaf senescence (a senescence-associated gene; SAG), and transcript was present in abscission zones, and flower and root tissues, as well as being wound and ethylene inducible. *PP-ACO2* transcript was detected only in peach fruitlets, roots and hypocotyls (Ruperti *et al.*, 2001). Expression was also examined with the GUS reporter gene fused to the promoter region of *PP-ACO1* and *PP-ACO2* and transformed into tomato (Rasori *et al.*, 2003). The *PP-ACO1* promoter induced in transgenic tomato plants corroborated the expression pattern in peach, whereas the *PP-ACO2* promoter induced expression in immature and ripe fruit, senescent leaf and abscission zones. However, the suggestion that *PP-ACO2* may be more stable in the transgenic plant (Rasori *et al.*, 2003) awaits further analysis. Different lengths of the *PP-ACO1* promoter region fused to the GUS reporter gene transformed into tomato demonstrated the presence of tissue-specific regions (Moon and Callahan, 2004), and investigations using 5′-deletion assays in combination with transient expression assays in peach fruit tissue identified an ethylene responsive element (ERE) and two auxin-responsive elements (Rasori *et al.*, 2003).

In melon (*Cucumis melo*), the expression levels of *CM-ACO*s were monitored by RT-PCR analysis using specific primers. Under these conditions *CM-ACO1* is expressed predominantly

in ripe fruit, with detectable transcripts in leaves and etiolated hypocotyls, while wound and ethylene treatment induced significant amounts in the leaves. *CM-ACO2* expression was limited to low levels in etiolated hypocotyls, and *CM-ACO3* is expressed predominantly in flower tissue with very little in leaves and hypocotyls, and no expression in the fruit. When the PCRs were run for 30 cycles basal levels were detected for all three genes in all conditions (Lasserre *et al.*, 1996). Expression was examined with the GUS reporter gene fused to the promoter region of *CM-ACO1* and *CM-ACO3* and transformed into tobacco (Lasserre *et al.*, 1997). The *CM-ACO1* gene promoter was induced by ethylene, wounding and copper sulphate treatment (2 ERE, and 7 WUN elements), while expression was low in young leaves then increased sharply at the onset of chlorophyll breakdown (a SAG, similar to *LE-ACO1* in tomato leaves and *PP-ACO1* in peach leaves). In contrast, the *CM-ACO3* gene promoter was induced predominantly in young green leaves and then declined at the onset of senescence, while dense staining was also observed in all floral tissue.

White clover (*Trifolium repens*) *ACO* genes are expression differentially during leaf development (Hunter et al., 1999; Chen and McManus, 2006). For example, the expression of *TR-ACO1* is predominantly in the apical tissues, *TR-ACO2* expression is mainly in the green leaf tissue, with highest expression in newly initiated leaf tissues, and *TR-ACO3* expression is initiated in newly senescent leaf tissues and increases with leaf yellowing (similar to the SAGs of tomato, peach and melon leaves), and then declines at leaf necrosis (Hunter *et al.*, 1999). Studies using *E. coli* β-glucuronidase (GUS) fused to the 5′-UTR and upstream promoter regions of each of the *TR-ACO*s, and introduced into white clover, showed that the *TR-ACO1* promoter directs highest expression in the apical tissues, axillary buds, and leaf petioles in younger tissues and then declines in the ageing tissues, while *TR-ACO2* promoter drives expression in both younger, mature green and in ageing tissue. The *TR-ACO3* and *TR-ACO4* promoters also direct expression in the ontologically older tissues (SAGs), including axillary buds and leaf petioles (Chen and McManus, 2006). The wider distribution of the GUS TR-ACO2 fusion when compared with the endogenous TR-ACO2 may reflect the greater stability of the GUS enzyme.

Leaf senescence is a highly controlled and multifactorial sequence of events comprising the terminal developmental stage (Picton *et al.*, 1993; Smart, 1994; John *et al.*, 1995; Gan and Amasino, 1995; Oh *et al.*, 1996; Buchanan-Wollaston, 1997; Buchanan-Wollaston *et al.*, 2003; Grbić, 2003) at the onset of which many senescence associated genes (SAG) are up-regulated, including *ACO* in many species. For example, in white clover *TR-ACO3* expression increased rapidly at the onset of leaf senescence (Hunter *et al.*, 1999; Chen and McManus, 2006), as did *LE-ACO1* (Barry *et al.*, 1996; Blume and Grierson, 1997; Nakatsaku *et al.*,

1998), *PP-ACO1* (Ruperti *et al.*, 2001; Rasori *et al.*, 2003) and *CM-ACO1* (Lasserre *et al.*, 1996; 1997). In tobacco *NG-ACO1* and *NG-ACO3* are also highly expressed in senescent leaves, while *NG-ACO2* is constitutively expressed in all leaf tissue (Kim *et al.*, 1998). In potato leaves, *ST-ACO1* is expressed predominantly in the senescent leaves, whereas *ST-ACO2* is expressed in young and green leaves only (Nie *et al.*, 2002). In papaya, *CP-ACO1* is induced before fruit maturity and *CP-ACO2* is induced at a late state of fruit ripening and leaf senescence and is wound and ethylene inducible consistent with the WUN and ERE motifs (Chen *et al.*, 2003). Some developmental processes such as fruit ripening and seed development may induce leaf senescence (Noodén and Guiamét, 1989), many genes are up-regulated during senescence (Huang *et al.*, 2002) and rapid leaf senescence was observed when an *Arabidopsis* hexokinase was overexpressed in tomato (Dai *et al.*, 1999) suggesting that high sugar levels may induce senescence (Sheen, 1990).

1.5 Circadian Regulation and Biological Clocks

Plant circadian rhythms in nature are always entrained to 24 h by the day / night cycle and the rhythms are all reset by light and / or temperature (Barak *et al.*, 2000; Fankhauser and Staiger, 2002; Eriksson and Millar, 2003). The photoperiod sensor allows plants to respond to the annual cycle of day length by making flowers, tubers, or frost-tolerant buds at appropriate seasons (Imaizumi *et al.*, 2003; Eriksson and Millar, 2003).

Three families of plant photoreceptors have now been identified; the phototropins, cryptochromes and phytochromes (Cashmore et al., 1999; Casal, 2000; Christie and Briggs, 2001). Upon light perception these photoreceptors initiate signalling cascades, which interact and integrate the signals generated by different photosensory pigments (Casal, 2000; Quail, 2002a; 2002b) and also serve as a resetting cue for the circadian clock (Devlin, 2002). Upon light perception, phytochromes translocate from the cytosol to the nucleus (Nagy and Schaefer, 2000; 2002) and have been found to influence light-responsive promoters by direct contact with transcription factors (Fankhauser and Staiger, 2002). The persistence of circadian rhythms even in the absence of environmental timing cues (Thain *et al.*, 2004; Nováková *et al.*, 2005) indicates that they are driven by a self-sustaining oscillator. Integral to the endogenous clock are proteins that oscillate with a 24 h rhythm, *via* rhythmically transcribed genes and feed back of the clock / oscillator proteins to inhibit transcriptional activity of their own genes after a certain delay (Carpenter *et al.*, 1994; Alabadi *et al.*, 2001; Young and Kay, 2001; Staiger, 2002; Carré and Kim, 2002; Staiger *et al.*, 2003; Tenorio *et al*, 2003). Posttranscriptional regulation of the clock transcripts as well as posttranslational modifications of the clock proteins contribute to the maintenance of the 24 h periodicity (Nimmo, 1998; Edery, 1999; Allada *et*

al., 2001). Thus the phases of clock gene mRNA and clock protein oscillations, including the expression of photoreceptors, are indicators of endogenous time keeping which helps to optimize the plants chances of survival.

For example, cytokinin metabolism is tightly regulated by the circadian clock, and the phytohormones cytokinin, auxin and abscisic acid also exhibit diurnal variation in tobacco leaves, with peak levels 1 h after the middle of the light period (Nováková *et al.*, 2005). Similarly, the production of ethylene peaks approximately 1 h after the subjective midday and troughs in the middle of the subjective night to undetectable levels, in sorghum seedlings (Morgan *et al.*, 1997; Finlayson *et al.*, 1999), in *S. longipes* (Kathiresan *et al.*, 1996), in cotton plants (Jasoni *et al.*, 2002) and *Arabidopsis* seedlings (Thain *et al.*, 2004). The production of ethylene positively correlated with both *ACO* transcript and the ACO activity levels in these studies. In contrast, neither the ACC content (Emery *et al.*, 1997) nor four of the *S. longipes-ACS* transcripts identified (Kathiresan *et al.*, 1998) correlate with ethylene production. However, ethylene production levels are tightly correlated with *Arabidopsis-ACS8* steady-state transcript levels, with an ethylene peak at subjective midday and a trough in the middle of the subjective night (Thain *et al.*, 2004). Further, light controls the expression of *AT-ACS8* by negative feedback regulation through ethylene signalling superimposed on the endogenous circadian regulation. Light was found to regulate the biosynthesis of ethylene directly (Jasoni *et al.*, 2002) in leaf tissue, provided that carbon dioxide is not limiting (Grodzinski *et al.*, 1982; 1983; Kao and Yang, 1982; Yang and Hoffman, 1984; Poneleit and Dilley, 1992). Earlier studies had reported that the conversion of ACC to ethylene was inhibited by light (Gepstein and Thimann, 1980; De Laat *et al.*, 1981; Wright, 1981). However, in these studies the leaf tissues were incubated in enclosed containers under light or dark conditions where the concentrations of carbon dioxide were not maintained and therefore decreased or increased as a result of photosynthetic or respiratory activities. A circadian-type rhythm has been observed in an ACO from the green leaf tissue of white clover (TR-ACO2), where both the accumulation and activity of ACO peak at 12 am and at 12 pm with a trough at 9 pm (Du and McManus, 2006), which suggests the absence of a light regulated mechanism.

Also, rubisco activase mRNA in apple plantlets displays a typical oscillating pattern of expression, with minimum expression observed at midnight (< 15 %) and maximum expression observed 2 h into the light period, and then dropping back to 20 % of the maximum expression 2 h before the beginning of the dark period (Watillon *et al.*, 1993). Also aldose-6-phosphate reductase (A6PR), a key enzyme in the biosynthesis of sorbitol (a sugar alcohol) showed significant diurnal fluctuations in apple leaves, with the highest A6PR activity observed at 10 am under natural light conditions, approximately 30 % higher than the activity determined at

night (Zhou *et al.*, 2001), sorbitol, the major photosynthate in Rosaceae (such as apple, peach and pear; Nii, 1997) also exhibited a strong circadian rhythm in mature leaves of apple in concert with A6PR.

1.6 *Malus domestica* L. Borkh. (Apple)

The genus *Malus* consists of about 15 primary species, including 2 from Europe, 4 from North America, and the rest from Asia (Westwood, 1993), but there is no agreement among taxonomists as to how many species this genus comprises (Gardiner *et al.*, 2007). Most of our domestic varieties derive from *Malus pumila* Mill., the common apple of Europe (Westwood, 1993; Harris *et al.*, 2002). *Malus domestica* belongs to the family Rosaceae, and together with other species forms the subfamily Maloideae (Challice, 1974). The origin of the basic haploid number of 17 for *Malus* and other Pomoideae has been suggested by several studies to have evolved by hybridization between the sub-families Spiraeoideae (haploid 9) and Prunoideae (haploid 8) (Challice and Westwood, 1973; Challice, 1974; Lespinasse *et al.*, 1999; 2000). This resulted in an allopolyploid with a basic haploid number of 17 (Newcomb *et al.*, 2006) and an estimated genome size of 743 to 796 Mb (Arumuganathan and Earle, 1991). Earlier studies suggested a basic haploid number of 7 (also common in other genera of Rosaceae) which doubled, with three of the chromosomes repeated a third time leading to the haploid number of 17 (Darlington and Moffett, 1930), and an autopolyploidy explanation derived from the 9 haploidy of Spiraeoideae (Morgan *et al.*, 1994). Although the majority of the cultivated apples are ancient tetraploids they are functional diploids (2n = 34), some are thought to be complex polyploids (Korban and Chen, 1992). For example, even though apple (*Malus* Mill.) generally has a haploid number of 17, the somatic chromosome number can be 34, 51, 68 or 85. Apple cv Gala has 34 chromosomes (Westwood, 1993). Apple has a long juvenile period (6 to 8 years), a high level of self-incompatibility, and because of their allogamous nature have a high degree of heterozygosity, so that cultivars are propagated vegetatively (Lespinasse *et al.*, 1999) by grafting scions onto rootstock (Jensen *et al.*, 2003). Also dwarfing and some insect resistance traits can be conferred by rootstocks (Ferree and Carlson, 1987).

Apple is a deciduous, rarely evergreen tree or shrub (Westwood, 1993). The three types of apple leaf are designated: spur leaves; bourse shoot leaves and extension shoot leaves. Extension shoot leaves are the most recently classified and these leaves are found on shoots that extend from non-fruiting branches. A spur is a short woody shoot that is the primary fruiting structure for most fruit trees. The spur leaves (generally small leaves) grow in a rosette formation just above the scale scars of the spur on the structure known as the bourse. The bourse shoot then grows from a bud on the bourse structure from early to mid-October and

finish their extension by mid to late January at latitude 39° 28' and longitude 176° 49' (Havelock North, in the Hawkes Bay, New Zealand). The leaves on the bourse shoot are called bourse shoot leaves. Both spur leaves (primary leaves) and bourse leaves (secondary leaves), are therefore closely associated with fruiting. Spur leaves develop very early (often before flowering), and tend to senesce a few months later (generally by the end of petal fall). Bourse leaves, by contrast, develop more slowly and appear later in the season. The leaves grow larger and remain on the tree for a few months after the fruit has dropped off. The mineral content of apple fruit (calcium, magnesium and potassium) can be reduced by the removal of the bourse leaves early in the season (Volz *et al.*, 1996), but the calcium content of apple fruit decreases more in response to spur leaf removal (Volz *et al.*, 1996; Lang and Volz, 1998). [Calcium has been implicated as an important secondary messenger in the ethylene signal transduction pathway (Raz and Fluhr, 1992)]. Other hormones such as abscisic acid have been reported to stimulate climacteric ethylene biosynthesis following abscisic acid treatment of attached Granny Smith apples (Lara and Vendrell, 2000), however, plant hormonal cross-talk in apple is complex and requires further study (Klee, 2003). Malic acid, the predominant organic acid in apple and the main substrate for respiration in apple (*via* malate dehydrogenase or NAD malic enzyme), decreases as the acid is increasingly decarboxylated during the fruit ripening climacteric and thereby reduces the acidity of the fruit (Hulme and Rhodes, 1971).

Public sequence databanks now contain in excess of approximately 200,000 expressed sequence tags (ESTs) from apple, which correspond to approximately 23,000 contiguous sequences (clusters containing more than one EST) (Korban *et al.*, 2004; Newcomb *et al.*, 2006; Park *et al.*, 2006) which can be interrogated to access the full length sequences of identified partial sequences. For a review of gene mapping in apple refer to Gardiner *et al.*, (2007).

1.6.1 ACC Oxidase in *Malus domestica*

1.6.1.1 Expression of ACC Oxidase in Apple

ACO gene expression and its role in fruit ripening has been a major research focus for many years in apple (Ross *et al.*, 1992; Dong *et al.*, 1992 a and b; Dilley *et al.*, 1995; Zhu *et al.*, 1995; Bolitho *et al.*, 1997; Atkinson *et al.*, 1998; Tan and Bangerth, 2000; Costa *et al.*, 2005; Cin *et al.*, 2005; Park *et al.*, 2006) with fewer studies on *ACO* gene expression in other tissues, for example the leaves. There is evidence from Southern hybridization analysis at low stringency (Ross *et al.*, 1992) and *in situ* hybridizations (Zhu *et al.*, 1995) that *ACO* genes may also be present in the apple genome as small families. Apple *pAP4-ACO* may contain heterozygous alleles of different molecular weights and restriction patterns (Castiglione *et al.*, 1999).

An ethylene-related cDNA (clone *pAP4*) from ripening apples was first cloned by Ross *et al.*, (1992) in New Zealand and, simultaneously (in press at the same time), Dong *et al.*, (1992a) isolated an identical ACO cDNA (*pAE12*) from apple fruit, in California. The *pAP4* apple sequence has been found at two loci in the cultivar Prima x Fiesta, one on chromosome 5 and the other on chromosome 10 (Maliepaard *et al.*, 1998). The *pAP4* cDNA has been fused between the galactose inducible promoter and the terminator of the yeast expression vector pYES2, and transformed into *Saccharomyces cerevisiae* strain F808 by Wilson *et al.* (1993), allowing these cells to convert ACC to ethylene.

The apple *pAP4-ACO* gene promoter has been studied through a series of 5′ deletions fused to the GUS reporter gene and then transformed into tomato (Atkinson *et al.*, 1998). Low sequence homology was observed between the apple *pAP4-ACO* 5′ sequence upstream of the coding sequence and the corresponding sequences of tomato (*LE-ACO1*), melon (*CM-ACO1*) and petunia (*PH-ACO1*). Apple *pAP4-ACO* promoter fragments of 1966 bp and 1199 bp conferred ripening-specific expression in transgenic tomato fruit, consistent with the northern analysis data showing that apple *pAP4-ACO* is up-regulated in ripening apple fruit. However, no GUS activity was observed in developing (mature green) fruit or in other tissues, including leaves, wounded leaves, flowers or roots. A lack of GUS activity in the wounded leaves of the transgenic tomato plants is also consistent with the absence of wound-inducible *pAP4-ACO* gene expression in apple leaves. The longer (1966 bp) sequence contains two potential ethylene responsive elements (ERE) and the shorter sequence contains a transcription factor binding site which is involved in floral tissue developmental identity. Interestingly, a shorter promoter sequence of 450 bp induced GUS expression in a basal fruit tissue-specific pattern, but without the ripening developmental pattern. Therefore, the *AP4-ACO* promoter has at least 3 major regions: one related to tissue-specific regulation, one related to ripening specific expression and the third related to ethylene responses (Atkinson *et al.*, 1998). This implies that the regulation of the ripening process, tissue-specificity, and the ethylene response are all directed by different binding factors.

1.6.1.2 Purification, Characterization and Kinetic Properties of ACC Oxidase in Apple

ACO has been isolated in crude extracts, partially purified or purified to homogeneity and characterized in the fruits of apple. ACO activity *in vitro* has been demonstrated in apple fruit (Dong *et al.*, 1992b; Fernández-Maculet and Yang, 1992; Kuai and Dilley, 1992; Dilley *et al.*, 1993; Poneleit and Dilley, 1993; Fernández-Maculet *et al.*, 1993; Dupille *et al.*, 1993; Pirrung *et al.*, 1993; Mizutani *et al.*, 1995). However, the ACO has only been purified to near homogeneity or homogeneity from the fruits of apple by Dong *et al.*, (1992), Fernández-

Maculet *et al.*, (1993), Dupille *et al.*, (1993) and Pirrung *et al.*, (1993) (refer Table 1.1). The degree of enzyme purification may influence the observed kinetic results. For example, in a crude extract there may be more than one isoform, whereas in an extract purified to homogeneity a single isoform is more likely to be present. Also in a crude extract the enzyme concentration may be more difficult to determine so that the amount of enzyme in the ACO assay could be over estimated. The specific activity for the extracts purified to homogeneity (18 nmol mg^{-1} min^{-1}; Pirrung *et al.*, 1993), purified to near homogeneity (20 nmol mg^{-1} min^{-1}; Dong *et al.*, 1992b) and partially purified (20 nmol mg^{-1} min^{-1}; Poneleit and Dilley, 1993) apparently have a similar degree of purity. However, the specific activity for the crude extracts determined by Kuai and Dilley (1992) of 40 to 100 nL mg^{-1} h^{-1} (*ca.* 1.78 to 4.5 nmol mg^{-1} h^{-1}) and by Fernández-Maculet and Yang, (1992) of 60 nL g^{-1} h^{-1} (*ca.* 2.67 nmol g^{-1} h^{-1}) are very low. Authentic ACO activity is determined *in vitro* using two criteria; firstly by comparing *in vitro* ethylene production with *in vivo* ethylene produced, after exogenous ethylene is administered to preclimacteric apple fruit (Fernández-Maculet and Yang, 1992) or correlated with the ethylene produced during the climacteric in apple (Dilley *et al.*, 1993), and secondly, by stereospecificity towards 2-ethyl-ACC (allocoronamic acid) stereoisomers for 1-butene production (Hoffman *et al.*, 1982; Fernández-Maculet and Yang, 1992). To confirm that the purified protein from apple fruit had an amino sequence that corresponded to the deduced amino acid sequence of the apple *ACO* cDNA, clone *pAE12* (Dong *et al.*, 1992a), the protein was cleaved with cyanogan bromide (CNBr) and the fragments matched (Dong *et al.*, 1992b), and also shared a strong identity to the deduced *pTOM13* amino acid sequence (Dupille *et al.*, 1993).

Determination of the molecular mass of purified ACO may give values different from those predicted by the cDNA sequence, as a consequence of possible post translational modifications (Table 1.1). For example, in eukaryotics a specific methionine amino-terminal peptidase (MAP) removes the initiator methionine when the initiator methionine is followed by (a residue with a relatively small side chain) A, S, G, V or P (Kendall and Bradshaw, 1992), and for A, S and G the amino terminus is acetylated (Boissel *et al.*, 1985). However, when the adjacent residue is charged (E, D, K and R) processing does not occur (Rubinstein and Martin, 1983). Such post translational processing would block the N-terminus and could explain why no amino acid sequence was obtained originally from the purified ACO by Edman methods (Dong *et al.*, 1992b). Further, electrospray mass spectrometry (EMS) showed that the molecular mass of an ACO purified from apple fruit (35.332 ± 5 amu) was approximately 50 amu higher than that predicted from the cDNA sequence with the initiator methionine removed, but that acetylation of the N-terminus would explain both the amu discrepancy and the inaccessibility of the N-terminus of ACO to sequencing (Pirrung *et al.*, 1993). There is also the possibility of

glycosylation, but the absence of N-linked substitution at a potential glycosylation site in a sequenced peptide and lack of reactivity towards a mixture of seven different biotinylated lectins (Dupille *et al.*, 1993), suggests the N-linked glycosylation is absent. However, the possibility of an O-glycosidic bond can not be ruled out. As the molecular mass of the native ACO from purified apple fruit is of a similar molecular mass to that of the denatured protein, it was assumed that the enzyme was active as a monomer (Dong *et al*, 1992b; Dupille *et al.*, 1993). The purification, molecular masses, the range of pH optima and the Michaelis constants (K_m; a measure of the affinity an enzyme has for its substrate) for apple ACO at various stages of purification are shown in Table 1.1.

1.6.1.3 Requirement of Apple ACC Oxidase for Co-substrate and Co-factors

ACO extracted from apple fruit tissue has an absolute requirement for ascorbate *in vitro* (Dong *et al.*, 1992b; Fernández-Maculet and Yang, 1992; Dilley *et al.*, 1993), and follows Michaelis-Menton kinetics (Dupille *et al.*, 1993; Dilley *et al.*, 1993; Seo *et al.*, 2004). Ascorbate is stoichiometrically converted to dehydroascorbate, and hence serves as a co-substrate in the conversion of ACC to ethylene by ACO being concurrently oxidized into dehydroascorbate (Dong *et al.*, 1992). Dehydroascorbate, as an ascorbate analog, is slightly inhibitory to ethylene production (K_i of 0.68 mM) (Dilley *et al.*, 1993), while L-ascorbate acid-6-palmitate strongly inhibits ACO competitively (K_i of 20 μM) (Dilley *et al.*, 1993). Ferrous iron ($FeSO_4$) is required in the conversion of ACC to ethylene (Fernández-Maculet and Yang, 1992; Dilley *et al.*, 1993; Dupille *et al.*, 1993) and is an absolute requirement (Dong *et al.*, 1992).

Direct evidence for CO_2 activation on ACO activity *in vitro* first came from Dong *et al.*, (1992b) who found that activity *in vitro* of the purified enzyme from apple fruit was completely abolished in a CO_2-free atmosphere, but that this was reversible. Other studies found that CO_2 was required to make ACO catalytically competent (Poneleit and Dilley, 1993; Pirrung *et al.*, 1993). However, inclusion of sodium bicarbonate ($NaHCO_3$) in the assay buffer offers greater operational simplicity than using the gas (CO_2) and there is also evidence from recombinant apple ACO that HCO_3^- (not CO_2) is the active species (Dilley *et al.*, 1993). The effect of CO_2/HCO_3^- on the kinetics of ACO is not simple. For example, as the CO_2/HCO_3^- concentration is increased *in vitro*, the apparent K_m for ACC,ascorbate, dioxygen and Fe^{2+} have been observed to increase several fold for ACO purified from apple fruit to near homogeneity (Ferández-Maculet *et al.*, 1993), from partially purified apple fruit extracts (Poneleit and Dilley, 1993) and in enzyme from crude apple fruit extracts (Mizutani *et al.*, 1995), concomitant with an increase in the V_{max} by as much as 10 fold (Poneleit and Dilley, 1993; Ferández-Maculet *et al.*, 1993; Mizutani *et al.*, 1995). Similarly, the affinity of ACO for CO_2 has been observed to decrease as

Table 1.1: Summary of some Properties of ACC Oxidase Purified from Apple

Purity (fold)	Purification steps	Molecular mass Native (kDa)	Molecular mass Denatured (kDa)	pI	pH Optimum	K_m for ACC (μM)	Reference
Crude extract	Slurry filtered and Centrifuged	-	-	-	-	17	Fernández-Maculet and Yang (1992)
		-	-	-	[1]7.4 - 6.7	-	Mizutani *et al.* (1995)
Partially purified (10)	Polyethylene glycerol (PEG) fractionation						
	Calcium phosphate gel	-	-	-	[2]7.2 - 7.6	5.8, [3]6.4, 8	Kuai and Dilley (1992)
	Absorption	-	-	-	-	6.0	Dilley *et al.* (1993)
		-	-	-	[4]6.8	[5]2 , 7, 20	Poneleit and Dilley (1993)
Near homogeneity (180)	DEAE Sepharose anion exchange						
	Phenyl Sepharose hydrophobic interaction						
	Sephadex G-150 gel filtration	39	35	-	-	-	Dong *et al.* (1992b) Fernández-Maculet *et al.*, (1993)
		-	-	-	-	[6]28, 121	
Homogeneity (170)	$(NH_4)_2SO_4$ precipitaton Phenyl Sepharose hydrophobic interaction						
	DEAE Memsep 1000 anion exchange						
	Superose 12 gel filtration						
	Mono Q anion exchange	39	40	-	[4]7.4	20	Dupille *et al.* (1993)
Homogeneity (21)	$(NH_4)_2SO_4$ precipitaton						
	Butyl Toyopearl 650 M Hydrophobic interaction						
	DEAE Toyopearl anion exchange						
	Mono P chromatofocusing						
	Superdex 75 gel filtration	[8]35.3	[7]40	-	-	12 ± 4	Pirrung *et al.* (1993) K_{cat} (2.5 ± 0.2) x10^{-3} s^{-1}
In vivo	Apple fruit tissue discs		-	-	-	8.1	Yip *et al.* (1988)
Homogeneity	Recombinant clone pAE12 expressed in *E.coli*; pAE20		-	-	-	230	Charng *et al.* (1997; 2001) K_{cat} 0.07 s^{-1}
	Recombinant *MD-ACO1*		-	-	-	105	Yoo *et al.*(2006);K_{cat} 0.054

[1]CO_2 (ambient, 20 %) in MOPS buffer: [2]pH 7.2 in Tris-HCl buffer, and pH 7.6 in phosphate buffer; [3]K_M^{ACC} 6.4 determined at pH 7.2 in Tris-HCl; [4]pH in Tris-HCl buffer; [5]CO_2 (ambient, 5 % and 20 %); [6]K_m^{ACC} at 0.03 % and 4 % CO_2 respectively; [7]SDS-PAGE denatured; [8] electrospray mass spectrometry (EMS)

the levels of CO_2 increase (Mizutani *et al.*, 1995). Further, the pH required for maximum enzyme activity shifts to the acidic side as the levels of CO_2 increase, even with the pH maintained by using a HCO_3^-/CO_2 buffer. As CO_2 passes very rapidly through membranes where it hydrates and dissociates into H^+ and HCO_3^- thereby lowering the intracellular pH, the physiological implications of this molecule on the activity of ACO are probably multi-dimensional. For example, photosynthesis may lower the endogenous CO_2 levels in the leaves whereas ripening fruit would likely have sufficient CO_2 to sustain ethylene production.

The Michaelis-constant (K_m) for another substrate dioxygen, of the partially purified ACO from apple fruit was found to be 0.4 % (v/v) O_2 in the presence of 1 mM ACC (Kuai and Dilley, 1992). The concentration of internal oxygen which results in half-maximal ethylene production by apple fruit tissue is reported to be 0.2 % (v/v) (Burg, 1973). In addition, ACC concentration in apple fruit was observed to affect the K_m for O_2 with the K_m being 0.3 % (v/v) O_2 determined at 10 mM ACC, but 6.2 % (v/v) O_2 in the absence of ACC (Yip *et al.*, 1988).

The requirements for co-substrate and co-factors are summarized in Table 1.2.

The extreme lability of the apple ACO is consistent with a non-haem iron protein (Pirrung *et al.*, 1993), which has now been confirmed as neither phenylhydaxine nor 2-methyl-1,2-dipyridyl-1-propane inhibit apple ACO activity (Dupille *et al.*, 1993). For example, ACO from the fruit of cv. Golden Delicious loses activity during turnover (Poneleit and Dilley, 1992; Pirrung *et al.*, 1993; Dupille *et al.*, 1993) with a half-life (t½) of approximately 2 h at 23 °C (Pirrung *et al.*, 1993). When the reaction is allowed to proceed *in vitro* without supplemental CO_2 beyond 15 min, ACO is subject to catalytic inactivation (Poneleit and Dilley, 1992). Further, the enzyme is heat sensitive with a optimal temperature range from 23 °C to 30 °C (Pirrung *et al.*, 1993; Dupille *et al.*, 1993; Poneleit and Dilley, 1992; Charng *et al.*, 2001), and decreased activity at 35 °C (Dupille *et al.*, 1993) with complete inactivation at 100 °C for 5 min (Fernández-Maculet and Yang, 1992; Kuai and Dilley, 1992). Even the storage of a crude extract at 2 °C or 4 °C reduces the activity of the enzyme (Fernández-Maculet and Yang, 1992; Kuai and Dilley, 1992; Poneleit and Dilley, 1993). However, the addition of 1,10-phenanthroline (PA) to a purified extract of apple (incubated at 4 °C for 18 h under aerobic conditions) preserved 91.5 % of the initial ACO activity (Dupille *et al.*, 1993), and concurs with the incubation of purified apple extract for 18 h at 4 °C under nitrogen (N_2; anaerobic conditions) where 92 % of ACO activity was preserved. In contrast, the extract under aerobic conditions without the addition of PA and incubated at 4 °C for 18 h was not stabilized and lost 80 % of the initial ACO activity (Dupille *et al.*, 1993). As the instability of ACO was believed to be due to either the aerobic auto-oxidation of ascorbate catalysed by Fe^{3+} and/or the denaturation of the enzyme by Fe^{3+}

generated by oxidation of Fe^{2+} (Dupille *et al.*, 1993), the addition of PA, an inhibitor of metallo-proteases, probably prevents these processes through the chelation of Fe^{2+}.

Table 1.2: Summary of the Requirements of Apple ACC Oxidase for Co-substrate and Co-factors

Purity: Reference	Ascorbate mM	$FeSO_4$ µM	$NaHCO_3$ mM	CO_2 (gas phase) % (v/v)	O_2 (gas phase) % (v/v)
Crude extract					
(Fernández-Maculet &Yang, 1992)	[1]30	[1]50	-	-	-
(Mizutani *et al.*, 1995)	[1]30	[1]50	105	20	-
Partially purified					
(Kuai and Dilley, 1992)	[1]30	[1]100	-	-	[1]0.1-20
(Poneleit and Dilley,1993)	5	[1]100	-	0.03,5,20	-
(Dilley et al., 1993)	5	3	-	-	[1]0.1-20
Near homogeneity					
(Dong *et al.*,1992b)	1	10	10	-	-
(Fernández-Maculet *et al.*, 1993)	1	20	-	4	-
Homogeneity					
(Dupille *et al.*, 1993)	3	10 (20 + [2]PA)	-	-	-
(Pirrung *et al.*, 1993)	[1]10	[1]100	5	-	-
Recombinant clone pAE12 expressed in *E. coli*; pAE20					
(Charng *et al.*, 2001)	[1]20	[1]20	[1]100	-	-
(Yoo *et al.*, 2006)	[1]10	[1]10	-	4.2	-

[1] used in the ACC oxidase assay, without direct evident of optimization
[2] 1,10-phenanthroline

Alpha-aminoisobutyrate (AIB; an analog of ACC) competitively inhibited the conversion of ACC to ethylene by ACO *in vitro* (Fernández-Maculet and Yang, 1992; Charng *et al.*, 1997), with a K_i value of 5.7 mM for a crude extract of ACO (Fernández-Maculet and Yang, 1992), while a recombinant ACO (clone *pAE12*; Dong *et al.*, 1992a) expressed in *E. coli* (strain BL-21), had a K_i for AIB of 14.7 mM (Charng *et al.*, 1997). This indicates that the native enzyme from the crude extract is more sensitive to the inhibitor when compared with the recombinant enzyme (by approximately 2.5 fold). Cobalt ions (Co^{2+}) also inhibit the conversion of ACC to

ethylene (Fernández-Maculet and Yang, 1992; Kuai and Dilley,1992), where Co^{2+} at 50 μM resulted in 70 % inhibition (Fernández-Maculet and Yang, 1992). Even in the absence of ACO, ACC was oxidized to ethylene in the presence of 100 μM of Co^{2+} at pH 7.2, and at higher pH values more ethylene was produced, while at low concentrations of Co^{2+} proportionately less ethylene was produced (2 μM =7 %, 10 μM=46 %, 25 μM =50 %; Kuai and Dilley,1992). Purified ACO is also inhibited by amino acid hydroxmates which may act through both chelating and hydrophobic interactions at the active site (Pirrung *et al.*, 1995). Other chelating agents, such as tropolones, inhibit ACO activity *in vitro* which was recovered in the presence of Fe^{2+} (Mizutani *et al.*, 1995). A cyclobutane ACC analog 1-aminocyclobutane-1-carboxylate (ACBC), strongly inhibited the activity *in vitro* of the partially purified ACO from senescing carnation flowers (Kosugi *et al.*, 1997), and it was suggested that ACBC could bind to the active site of ACO, which is likely also to occur with apple ACO.

Apple is a climacteric fruit, with a clear respiratory climacteric and ethylene peak associated with ripening (Park *et al.*, 2006; Newcomb *et al.*, 2006). Although the control for the onset of autocatalytic ethylene biosynthesis is not yet clear (Lara and Vendrell, 2000), it is well known that internal ethylene increases during fruit maturation (Lay-Yee *et al.*, 1990; Atkinson *et al.*, 1998; Tan and Bangerth, 2000). In preclimacteric fruit *in vivo* and *in vitro* ACO activity was not detected (Dilley *et al.*, 1993), accumulation of the enzyme was not observed (Lara and Vendrell, 2000), and very little ethylene is produced (Dong *et al.*, 1992b; Fernández and Yang, 1992). However, when treated with ethylene a parallel increase in ACO activities and the induction of *ACO* transcript (Dong *et al.*,1992b; Fernández and Yang, 1992), together with the formation of ACC and MACC is observed (Tan and Bangerth, 2000). But, exogenous ethylene did not overcome the inability of prematurely harvested fruit to produce sufficient ACC and ACO activity to trigger autocatalytic ethylene production (Tan and Bangerth, 2000; Lara and Vendrell, 2000). This data indicates that the earlier the preclimacteric fruits are harvested, the weaker the response to exogenous ethylene (Choi *et al.*, 1994; Tan and Bangerth, 2000), so that the fruit is increasingly stimulated by ethylene as development progresses.

1.6.1.4 Localization of ACC Oxidase in Apple

Anderson *et al.* (1979) prepared protoplasts from apple fruit tissue and found that ethylene production was greatly inhibited by Triton X-100 and osmotic shock that caused lysis of the protoplasts. Over 90 % of the total protein in the homogenate was associated with the pellet fraction in the absence of PVPP and then was solubilized in 25 mM MOPS with 0.1 % Triton X-100 (Dong *et al.*, 1992b). Since the detergent rapidly inactivates the enzyme, 30 % (v/v) glycerol was included and following solubilization the detergent was removed by protein

adsorption to a DEAE-sepharose column. Observations that ACO from apple is purified primarily by hydrophobic interactions (Pirrung *et al.*, 1993), suggests that the enzyme can form significant associations with hydrophobic surfaces. Both hydrophobic and electrostatic interactions have been observed using crystallography (Zhang *et al.*, 2004), to be involved in the interlocking of the C-terminus region of adjacent ACO monomers. However, due to the restraints of the crystalline lattice the interaction between adjacent monomers may be artefactual, and may instead be the means by which ACO retains a close association with the lipid bilayer. ACO activity is detected only in intact protoplasts and vacuoles, where the integral membrane structure, and potential, is thought to maintain Fe^{2+} and ascorbate in sufficiently high concentrations (Lieberman, 1979; Fernández Maculet and Yang, 1992; Dong *et al.*, 1992b). Consequently, when these membranes are homogenized ethylene biosynthesis is totally lost. Five percent (w/v) polyvinyl polypyrrolidone (PVPP) greatly improves recovery of the enzyme by binding polyphenols in the apple tissue (Kuai and Dilley, 1992: Fernández Maculet and Yang, 1992) and can be used as an alternative to 0.1 % (v/v) Triton X-100 (Dong *et al.*, 1992b; Fernández Maculet and Yang, 1992). Immunocytolocalization experiments performed by Rombaldi *et al.*, (1994) indicated that ACO is located at the cell wall in the pericarp of climacteric apple. Ramassay *et al.*, (1998) combined cell fractionation and immunocytological methods and found that ACO is mainly associated with the external face of the plasma membrane of apple fruit, a periplasmic location. However, due to lack of motifs such as transmembrane helices in the sequence of ACO to suggest that it is an integral membrane protein and the absence of an N-terminal conserved signal sequence which is considered to be required for targeting (Pirrung *et al.*, 1993), it was proposed that ACO is not secreted *via* the endoplasmic reticulum (ER) pathway (Rombaldi *et al.*, 1994). Chung *et al.*, (2002) observed that the *in vitro* translated apple ACO was not co-processed or imported by the canine pancreatic rough microsomes (CPRM), a system widely used to identify signal peptides for protein translocation across ER, suggesting that apple ACO does not contain a signal peptide for ER transport. However, it is known that not all plasma membrane or secretory proteins contain an N-terminal consensus sequence that is cleaved following translocation across the ER membrane. Recently, Chung *et al.* (2002) re-examined the subcellular localization of ACO in apple fruit by immunogold labelling with a highly specific antibody raised against the recombinant apple enzyme. It was demonstrated that apple ACO was located mainly, if not solely, in the cytosol of climacteric apple fruit mesocarp cells.

1.6.1.5 The Focus of Apple Studies

Many physiological studies have investigated the relationship between the leaves and fruit of apple (Tustin *et al.*, 1997; Greer *et al.*, 1997; Wünsche and Palmer, 1997; Wünsche *et al.*, 2000; Greer *et al.*, 2002) with regards to the contribution of fixed carbon from leaf tissue for

apple fruit development and growth, and for subsequent carbohydrate storage to fuel leaf initiation and floral bud break and development in the spring. Similarly, many studies have examined the roles of ACO and ethylene in apple fruit (Ross *et al.*, 1992; Dong *et al.*, 1992a; 1992b; Fernández-Maculet and Yang, 1992; Dupille *et al.*, 1993; Pirrung *et al.*, 1993; Dilley *et al.*, 1993; 1995; Ramassamy *et al.*, 1998; Atkinson *et al.*, 1998; Tan and Bangerth, 2000; Lara and Vendrell, 2000; Chung *et al.*, 2002; Tartachnyk and Blanke, 2004; Costa *et al.*, 2005). By contrast, ACO has not been examined in the leaves of apple, although the role of ACO in leaf senescence has been undertaken in other species (John *et al.*, 1995; Kim *et al.*, 1998; Hunter *et al.*, 1999; Nie *et al.*, 2002; Chen *et al.*, 2003; Chen and McManus, 2006). Since ACO has also been identified as a senescence associated gene (SAG) in the leaf tissue of many species (Barry *et al.*, 1996; Lassere *et al.*, 1996; Hunter *et al.*, 1999; Nakatsaku *et al.*, 1998; Ruperti *et al.*, 2001; Rasori *et al.*, 2003; Chen and McManus, 2006), which is induced at the onset of senescence, these observations suggest that a SAG may also be present in apple leaf tissue. Based on these observations, a model may be developed in which leaf senescence could be delayed if the SAG ACO in leaf tissue was down-regulated, which in turn could lengthen the photosynthetic capacity of the plant, leading to increased photosynthate and hence carbohydrate storage for the following spring. Therefore, the broad aim of this study is to investigate ACO in the apple leaf tissue of the recently bred Royal Gala cultivar (developed in the 1930/40s and introduced in the 1960/70s from a cross between the Kidd's Orange Red and the Golden Delicious cultivars; Gardiner *et al.*, 2007), to determine if different members of the ACO gene family are expressed during leaf ontogeny, with particular reference to leaf maturation and senescence.

1.7 Objective and Aims of the Thesis

The primary objective of this thesis is to isolate and characterize the expression of ACO genes from leaf tissues of apple (*Malus domestica*) at different developmental stages. The focus is on leaf tissue to act as a point-of-difference from the many studies that have focussed, thus far, on apple fruit tissue.

To achieve the primary objective, the following experimental aims were attempted.

- Isolation of RNA sequences corresponding to *MD-ACO* genes from the leaves of apple;
- Investigation of the differential expression of the *MD-ACO* genes in leaf and in fruit tissue at different developmental stages;
- Raise antibodies to the protein products of the *MD-ACO* genes, and to examine differential protein accumulation in leaf and fruit tissues at different developmental stages;
- Express the *MD-ACO* gene in *E. coli* and to compare the kinetic parameters of each MD-ACO isoform as a recombinant protein; and
- Examine the diurnal expression of MD-ACO genes and accumulation of MD-ACO proteins over a 24 h period.

Chapter Two MATERIALS AND METHODS

Unless otherwise stated, all of the chemicals used were from Sigma Chemical Company or BDH Laboratory Supplies, and of analytical grade or better. All solutions were made using water purified by reverse osmosis (RO), followed by filtration by microfiltration through a system containing ion exchange, solvent exchange, organic and inorganic removal cartridges (Mill-Q, Millipore Corporation). Sterilization by autoclaving at 103 kPa for at least 20 min or by filtering through a sterile 0.22 μm nitrocellulose filter (Millex®-GS sterilizing filter unit, Millipore Corp.). Centrifugations were carried out using an Eppendorf microcentrifuge 5417C (Pierce LabSupply) or a Sorvall® RC-5B centrifuge, using rotor SS-34 or rotor GS3; or a benchtop Sorvall® RT7 (DuPont Instruments, USA) or benchtop Eppendorf Centrifuge 5702R A-4-38. A digital pH meter (Radiometer Copenhagen, France) was used to measure the pH of solutions. An Ultrospec 3000 UV/visible spectrophotometer (Pharmacia Biotech) or a NanoDrop®ND-1000 spectrophotometer (NanoDrop Technologies) were used to measure the optical density values of RNA and DNA. An 8-channel single-beam microplate absorption photometer (Anthos Labtec Instruments) was used to measure the absorbance values of protein. The details of these and the other reagents and specialised equipment are listed in Table 2.1.

2.1 Plant Material

2.1.1 Harvesting of Plant Material

Bourse shoot leaves were harvested at one of the Hawkes Bay Research Centre orchards of HortResearch in Havelock North (latitude 39° 40'; longitude 176° 53') in the Hawkes Bay, New Zealand. Fifteen fully grown and fruiting Royal Gala apple trees (10 years old), grafted onto M9 dwarfing rootstock, were selected for the project and not used for any other experimental purposes. The trees were planted at a spacing of 5 x 2.5 metres and were grown in north-south orientated rows, trained as tender spindles. The bourse shoot leaves are shown in relation to the spur leaves and the fruit as Figure 2.1(A), and the relation of the apical bourse shoot leaves to the basal bourse shoot leaves are shown as Figure 2.1(B). A detailed description of these leaf types is given in section 1.6.

Bourse shoots were tagged prior to the collection of leaf samples in order to randomize the samples, this was particularly important later in the season because the bourse shoot leaves change colour differentially during senescence. However, for sampling early in the season, as the bourse shoots grow from a bud on the bourse structure from early to mid October and finish their extension growth by mid to late January, tagging was typically carried out either on the day of leaf sampling, or a day or so earlier, so that the selection of the bourse shoots was

Company	Full Company Name	Company Address
All Pro Imaging	All Pro Imaging Corp	Hicksville, NY, USA
Ajax	Ajax Chemicals	Auburn, NSW, Australia
Alltech	Alltech Associates Inc.	Deerfield, II, USA
Ambion	Ambion ® The RNA Company	Austin, Texas, USA
Amersham	Amersham Biosciences	Buckinghamshire, UK
Anthos	Anthos Labtech Instruments	Salzberg, Austria
Applied Biosystems	Applied Biosystems	Foster City, CA, USA
Becton Dickenson	Becton Dickenson Medical Pte Ltd	Rutherford, NJ, USA
BDH	British Drug Houses	Poole, Dorset, UK
Bio-Rad	Bio-Rad Laboratories	Hercules, CA, USA
BOC Gases	BOC Gases (NZ) Ltd	PN & Hawkes Bay, NZ
Boehringer Mannheim	Biohringer Mannheim Biochemica	Mannheim, Germany
Constant Systems	Constant Systems Ltd	Northants, UK
DuPont	DuPont Instruments	Wilmington, DE, USA
Difco	Difco Laboratories	Detroit, MI, USA
Eppendorf	Eppendorf AG (Pierce LabSupply)	Hamburg, Germany
Fujifilm	Fuji Photo Film Co Ltd	Tokyo, Japan
Gibco-BRL	Life Technologies (Gibo-BRL)	Gaithersburg, MD, USA
Hewlett Packard	Hewlett Packard Corporation	Berkshire, UK
Hitachi	Hitachi Corporation	Tokyo, Japan
Hybaid	Hybaid Ltd	Middlesex, UK
Invitrogen	Invitrogen™	Carlsbad, CA, USA
Immobilin-P	Millipore Corporation	Bedford, MA, USA
NanoDrop	NanoDrop Technologies	Rockland, DE, USA
Nunc	Nalge Nunc International	Roskilde, Germany
Pall	Pall Gelman Laboratories	Ann Arbor, MI, USA
Perkin Elmer	Perkin Elmer Life Sciences Inc.	Boston, MA, USA
Pharmacia	Pharmacia Biotech	Uppsala, Sweden
PP Systems	Portable Photosynthetic Systems	Haverhill, MA, USA
Promega	Promega	Madison, WI, USA
Qiagen	Qiagen Inc.	Valencia, CA, USA
Reidel-de Haen ag seelze	Reidel-de haen ag seelze	Hannover, Germany
Roche	Roche diagnostics GmBH	Mannheim, Germany
Savant	Savant Instruments	Farmingdale, NY, USA
Serva Feinbiochemica	Serva Feinbiochemica	Heidelberg, Germany
Shimadzu	Shimadzu Corporation	Kyoto, Japan
Sigma	Sigma Chemical Company	St Louis, MO, USA
Tropix	Tropix	Bedford, MA, USA
Univar	Univar	Auburn, NSW, Australia
VirTis	The VirTis Company	Gardiner, NY, USA
Vivaspin	Vivascience Ltd.	Hannover, Germany
Whatman	Whatman International Ltd	Maidstone, UK

Table 2.1: Names and Addresses of the Manufactures of Reagents and Specialised Equipment.

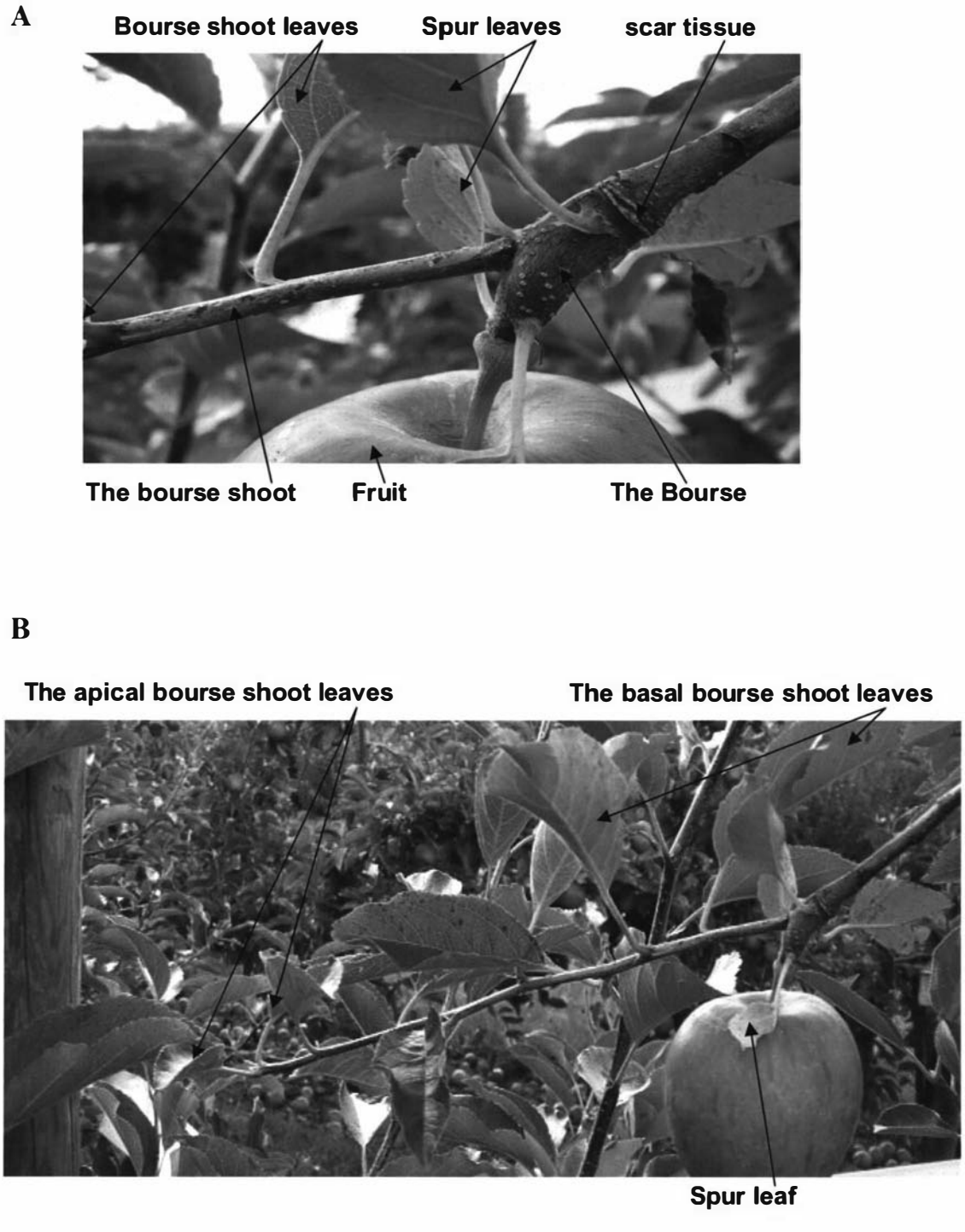


Figure 2.1: The Bourse Shoot Leaves of Apple

The bourse shoot leaves of Gala apple in relation to the fruit (A), and the full length of the bourse shoot from basal leaves to apical leaves (B).

standardized. For example, as the bourse shoot buds begin and finish their extension growth at different times, together with the fact that bourse shoots vary in length and leaf number, during this growth phase it would not have been possible or appropriate to pre-tag earlier. Leaf samples were always collected at 11 am, snap frozen in liquid nitrogen and then stored at -80 °C. Later in the season when the bourse shoot growth had terminated, all of the appropriate bourse shoots were tagged for the duration of the collection period. For example, leaves were typically collected twice prior to fruit removal and then at approximately 10 day intervals until leaf fall or necrosis. Fruiting and non-fruiting bourse shoots at approximately 50 cm in length were selected.

2.1.2 Chlorophyll Quantification

Leaf tissue was excised free from the midrib, frozen in liquid nitrogen, ground to a fine powder under liquid nitrogen, and then 50 to 200 mg transferred to a microcentrifuge tube (in triplicate) where the chlorophyll was extracted with 1 mL of N, N-dimethylformamide (DMF). To do so samples were mixed vigorously by vortexing and left for 24 h at 4° C in the dark (Moran and Porath,1980). Prior to chlorophyll determination the samples were mixed vigorously by vortexing, and the cellular debris pelleted by centrifugation at 20 800 x *g* for 6 min at room temperature. An aliquot (100 μL) of the supernatant was added to DMF (1 mL) in a microcentrifuge tube, mixed well before transferring to a quartz cuvette, and the optical density at both 647 nm and 664.5 nm determined (in triplicate) using an Hitachi UV-Vis spectrophotometer (model U-1100, Hitachi). DMF was used for 100% absorbance at both 647 nm and 664.5 nm. Chlorophyll concentrations were calculated using the formula of Inskeep and Bloom, 1985 (Moran, 1982). From the known weight of leaf tissue μg g^{-1} FW was calculated.

Chlorophyll *a*	=	12.7 $A_{664.5}$	-	2.79 A_{647}	(μg mL^{-1})
Chlorophyll *b*	=	20.7 A_{647}	-	4.62 $A_{664.5}$	(μg mL^{-1})
Total Chlorophyll	=	17.9 A_{647}	+	8.08 $A_{664.5}$	(μg mL^{-1})

2.1.2.1 Statistical Analysis

The existence of significant differences between data was tested using an Analysis of Variance (ANOVA), performed using Microsoft Excel 2000. A difference between means at the 5 % ($P \leq 0.05$; 95 %) was considered significant, with a difference at the 1 % level ($P \leq 0.01$; 99 %) being highly significant.

Calculation of standard errors: the variance between data replicates in this thesis are expressed as standard errors. All of the graphs and data were generated, and the standard errors calculated, using the software programme Microsoft Excel version 2000 (Microsoft, USA). The standard error is calculated by first calculating the standard deviation (SD), using the Microsoft Excel SD function, then dividing the SD by the square root of the number of samples.

2.1.3 Leaf Carbon Assimilation Measurements

Physiological (in the field) measurements were able to be obtained using a Circas-1 portable photosynthetic system (PP Systems, Haverhill, MA, USA) which contains a combined open infra-red gas analysis system. Leaf carbon assimilation was measured as net carbon exchange (NCE), also described as net photosynthesis or pn, with units of μmol. m^2 s^{-1}. The system analyses the internal concentration of CO_2 in the leaf in ppm, and also compares the CO_2 flowing into the leaf with the CO_2 flowing out.

2.1.4 Protein Extraction from Apple Tissue

Reagents:

- Extraction buffer: 0.1 mM Tris-HCl buffer (pH 7.5), containing 30 mM sodium-ascorbate, 10 % (v/v) glycerol, 4 mM DTT, 1.0 % (v/v) Triton

ACO was extracted from apple leaf and fruit tissue by a very simple modified procedure, based on that of Britsch and Grisebach (1986) for the extraction of flavanone-3-hydroxylase and modified by Fernández-Maculet and Yang (1992) for ACO extraction from the fruits of apple.

Leaf tissue (free from the midrib) or apple fruit tissue was ground under liquid nitrogen to a fine power. Extraction buffer was added in a 3:1 (v/w) ratio to the ground frozen powder, and the mixture vortexed vigorously for 2 to 3 min before centrifugation at 20 800 x *g* for 20 min at 4 °C. The supernatant (crude extract) was then transferred to a fresh tube, and the protein concentration determined by the Bradford protein assay (section 2.3.7), prior to separation on SDS-PAGE (section 2.3.10) in preparation for western blot analysis (section 2.3.11)

2.2 Molecular Methods

2.2.1 Growth and Storage of *E. coli*

2.2.1.1 Luria-Bertani (LB) Media and LB Ampicillin^{100} Plates

Reagents:

- Bacto-tryptone (Difco Laboratories)

- Bacto-yeast extract (Difco Laboratories)
- NaCl
- Ampicillin (Sigma)
- Agar (Gibco-BRL)
- Glycerol

Luria-Bertani (LB) broth: 1% (w/v) bacto-tryptone, 0.5% (w/v) bacto-yeast extract, 1% (w/v) NaCl. The components were dissolved in water, the pH adjusted to 7.0 (using NaOH) prior to autoclaving, after which the sterile broth was stored at room temperature.

Solid media was made by adding agar 1.5% (w/v) to the LB broth, and then autoclaving. Prior to pouring the molten media into sterile petri dishes (plates) in a lamina flow cabinet, the liquid was cooled to *ca.* 40 °C, then sterile ampicillin was added to give a final concentration of 100 μg mL^{-1} (Amp^{100}), from a stock solution (100 mg mL^{-1}). The ampicillin had been sterilized using an acrodisc® syringe filter 0.2 μm supor® membrane (Pall Gelman Laboratories) and stored at -20 °C. Each of the LB-Amp^{100} plates was then sealed with parafilm and stored at 4 °C.

E. coli were grown in LB broth and ampicillin (100 μg mL^{-1}) at 37 °C with shaking at ~200 rpm. To store bacteria for a longer time, cultures were preserved as frozen glycerol stocks in cryotubes (Nunc). To do this *E. coli* cells in LB broth (700 μl) were added to glycerol (300 μl of 100% (v/v)), the suspension snap frozen in liquid nitrogen and stored at -80 °C. *E. coli* cultures were revived from the frozen glycerol stocks every few months by plating an aliquot of the frozen stock onto fresh LB-Amp^{100} agar plates. *E. coli* were also grown on LB-Amp^{100} plates typically overnight (~16 h) at 37 °C, and could be stored on LB-Amp^{100} plates at 4 °C for periods of up to three to five months.

2.2.1.2 Preparation of Competent Cells

Reagents:

- $CaCl_2$
- Glycerol
- LB broth (refer section 2.2.1.1)

E. coli cells used for transformation were prepared from *E. coli* strain DH5α (Gibco BRL) and *E. coli* strain BL-21-SI™ (Invitrogen). LB broth (10 mL) was inoculated with a single colony of *E. coli* and incubated overnight at 37 °C at 200 rpm. Fresh LB broth (40 mL) was then

inoculated with 0.4 mL of the overnight culture and incubated at 37 °C until cell growth reached an optical density of 0.4 at 600 nm (A_{600} = 0.4); typically 2 to 3 h. The bacteria were pelleted by centrifugation at 2 500 x *g* for 5 min at 4 °C, and after discarding the supernatant, the bacterial pellet was resuspended in 10 mL of ice-cold $CaCl_2$ (60 mM), a further 10 mL $CaCl_2$ (60 mM) was then added and the cells incubated on ice (30 min). The cell suspension was then centrifuged at 2 500 x *g* for 5 min at 4 °C, the supernatant discarded and the cells resuspended in 4 mL of $CaCl_2$ (60 mM) containing glycerol 15% (v/v). The competent cells were then stored as 300 µl aliquots at -80 °C.

2.2.2 Isolation of Ribonucleic Acid (RNA)

RNA is tolerant of salt, solvent and temperature conditions. It is highly resistant to shear and can be vortex-mixed without detriment (Strommer *et al.*, 1993). The principal concern of working with RNA is the presence of ribonuclease (RNase), both endogenous (released from membrane bound organelles) and in the environment, which can be difficult to eliminate or inactivate.

To prevent RNA degradation during extraction, all glassware used was well-washed using mixed acid overnight, then rinsed thoroughly in Milli-Q water and wrapped with tinfoil and baked in a dry oven at 180 °C for at least 4 h. All disposable plastics were either new, or treated overnight in 0.3% (v/v) H_2O_2 (Andrew Industrial Ltd), then rinsed well with water and autoclaved in tinfoil. Solutions used for RNA work were not used for other purposes and clean disposable gloves were always used and regularly changed. Chemicals were dispensed by pouring, or by using spatulas that had been baked at 180 °C for at least 4 h. If pH adjustment of a solution was necessary, the pH electrode was incubated in NaOH (50 mM) for 10 to 15 min and rinsed with water. Any gel apparatus was sterilized with NaOH (0.1M) for a minimum of 20 min before rinsing with water.

2.2.2.1 Extraction of Total RNA

Hot Borate Method

Total DNA was isolated using a hot borate method (Hall *et al.*, 1978; Wan and Wilkins, 1994; Wilkins and Smart, 1996; Hunter and Reid, 2001; Moser *et al.*, 2004).

Reagents:

- DEPC treated water
- LiCl
- KCl

- sodium acetate
- nonidet (P40)
- potassium acetate
- PVP-40
- 2-mercaptoethanol
- Proteinase K (Roche)
- ethanol
- isopropanol
- isoamyl alcohol
- Borate extraction buffer: 0.2 M di-Sodium tetraborate decahydrate (Borax), 30 mM EDTA pH 8, 1% (w/v) SDS, 1% (w/v) deoxycholate (sodium salt). To dissolve, add components to pre-warmed (50 °C) RNase free water, allow to cool, then adjust the pH to 9 with NaOH, autoclave and store in 50 mL falcon tubes at -20 °C.

Borate extraction buffer was thawed to ~room temperature and put into a water bath set at 50 °C, where 2 % (w/v) PVP-40, 1 % (w/v) nonidet and 2% (w/v) 2-mercaptoethanol was then added, the mixture shaken vigorously with the cap tightly screwed on, and the water bath temperature adjusted to 85 °C.

Plant tissue was ground under liquid nitrogen with a pre-chilled pestle and mortar, while adding further liquid nitrogen to tissue as needed. Using a pre-chilled spatula, 0.3 g of the powdered tissue was transferred to a 1.5 mL microcentrifuge tube and borate extraction buffer (1 mL) pre-heated to 85 °C was added immediately. The components were mix thoroughly by vortexing at top speed (~30 s – 1 min) and left at 85 °C for 4 min. Proteinase K (0.5 mg) was added to the slurry following removal from the 85 °C water bath (rapid denaturation of proteinase K occurs at temperatures above 65 °C), mixed well, the top of the closed Eppendorf was securely wrapped with parafilm for extra protection in case of leakage and then the mixture was incubated (horizontally) at 42 °C for 1 h 30 min at 100 rpm. Immediately following incubation, 2 M KCl was added (to a final concentration of 160 mM), mixed and stored horizontally on ice for 45 min with gentle shaking of 100 rpm to allow proteins and other material to precipitate out of solution. The debris was removed by centrifugation at 20 800 x *g* for 25 min at 4 °C, after which the supernatant was transferred to a fresh tube, and 8 M LiCl (to a final concentration of 2 M) and 2-mercaptoethanol (to a final concentration of 1% (v/v)) were both added. After mixing well, the samples were incubated on ice at 4 °C overnight and the precipitated RNA collected by centrifugation at 20 800 x *g* at 4 °C for 45 min.

The pellet was resuspended in sterile water at room temperature, an equal volume of chloroform: isoamyl alcohol (24:1) added, the aqueous and organic phases mixed by vortexing and then separated by centrifugation at 20 800 x *g* for 5 min at room temperature. The upper aqueous phase was removed to a new tube and the RNA precipitated with ethanol (section 2.2.4.1), resuspended in a small volume of DEPC treated water, quantified (section 2.2.2.2) and stored at -80 °C until required.

Notes:

LiCl washes to remove pigments do not appear to be detrimental to the quantity or quality of the RNA but are probably unnecessary.

A potassium acetate precipitation step facilitates the removal of polysaccharides, residual proteins, pigments and other salt insoluble material, but the RNA yield is greatly reduced.

2-mercaptoethanol can be replaced with DTT; and Nonidet can be replaced with Igepal (Sigma)

PVP-40 was preferred to PVPP as the latter forms a matrix making recovery of the supernatant difficult.

TRI Reagent Method

This method was also assessed for the isolation of RNA in this thesis. However, none of the results presented in the thesis used RNA isolated using this method.

Reagents:

- TRI Reagent ® (Molecular Research Centre Inc., Cincinnati, OH, USA)
- Chloroform
- Isopropanol
- Ethanol
- Sodium citrate
- NaCl

Total RNA was isolated using TRI reagent (a solution of phenol and thiocyanate) according to a version of the single-step RNA isolation reagent method developed by Chomczynski and Sacchi (1987) with some modifications. Finely ground leaf tissue (0.5–1.0 g) was transferred to a 50 mL sterile screw-capped disposable polypropylene tube, and TRI reagent (5 mL) was added. The extraction mix was homogenized by shaking vigorously for 15 s, before being centrifuged at 12 000 x *g* for 1 min at 4 °C to remove extracellular membranes, polysaccharides and denatured proteins. The supernatant was transferred to a fresh tube and left at room temperature for 5 min to permit complete dissociation of nucleoprotein complexes, after which time isoamyl alcohol free chloroform (1 mL) was added, than shaken vigorously for 15 s. After keeping the suspension at room temperature for 10 min, the mixture was centrifuged for 15 min at 12 000 x *g* at 4 °C. With centrifugation, the mixture separated into a lower red phenol-chloroform phase containing proteins, an interphase containing the DNA, and the colourless aqueous phase containing RNA. The RNA containing solution was carefully pipetted into a fresh

polypropylene tube and then 1.25 mL each of isopropanol and high salt precipitation solution (0.8 M sodium citrate and 1.2 M NaCl) was added, mixed well and incubated for 5-10 min at room temperature. The tubes were then centrifuged at 12 000 x *g* for 8 min at 4 °C to pellet the RNA (white or clear pellet) while leaving polysaccharides in the supernatant. After discarding the supernatant, the RNA pellet was washed in 75% (v/v) ethanol (5-6 mL), and the tubes centrifuged at 7 500 x *g* for 5 min at 4 °C. After careful removal of the supernatant, the pellet was then air dried briefly (5 min) by inverting the tubes on clean paper towels and the pellet then resuspended in DEPC treated water (50 µL), transferred to a microcentrifuge tube and stored at -20 °C. For long-term storage, RNA was stored at -80 °C as an ethanol precipitate. This protocol was also scaled down to allow RNA isolation to be performed using microcentrifuge tubes rather than 50 mL tubes.

2.2.2.2 Quantification of RNA in Solution

RNA concentrations were determined by measuring the absorbance of each solution at 260 nm (A_{260}) and 280 nm (A_{280}) using an Ultrospec 3000 UV/visible spectrophotometer (Pharmacia Biotech). Samples were diluted appropriately and aliquots of 100 µL transferred to a slightly larger quartz cuvette and measured against a water blank. For RNA, an OD_{260} of 1.0 corresponds to approximately 40 µg mL^{-1} (Sambrook *et al.*, 1989). The RNA concentration was calculated using the following formula:

$$A_{260nm} \text{ x dilution factor x } 40 = \text{RNA concentration in } \mu g\ mL^{-1}$$

The purity of the RNA was determined by measuring the A_{260nm} / A_{280nm} ratio. Relatively pure RNA solutions have an A_{260nm} / A_{280nm} ratio of 2.0 (Sambrook *et al.*, 1989), a value that decreases with the presence of contaminants such as proteins and phenol (if used for RNA isolation).

When sample volumes were limiting a NanoDrop®ND-1000 spectrophotometer (NanoDrop Technologies) was also used to measure the absorbance of each solution at 260 nm (A_{260}) and 280 nm (A_{280}). Samples were diluted appropriately and aliquots of 2 µL were measured against a water blank.

2.2.3 Reverse Transcriptase Polymerase Chain Reaction (RT-PCR)

The prokaryotic (retroviral) enzyme 'Reverse Transcriptase' was used to synthesize the first single strand of DNA complimentary to mRNA using an oligo $d(T)_{15}$ primer. The mRNA is

then degraded and the second strand of DNA synthesized. This copy or complimentary double stranded DNA can then be used to clone into plasmid vector.

2.2.3.1 Generation of cDNA Using Reverse Transcriptase

Reagents:

- Expand reverse transcriptase (50 U μL^{-1}, Roche)
- 5 x Expand reverse transcriptase buffer (Roche)
- 0.1 M DTT (Roche)
- dNTP mix (dATP, dCTP, dGTP, dTTP, 10 mM Roche)
- RNase inhibitor (40 U μL^{-1}, Roche)
- Oligo $d(T)_{15}$ (8 mmol., 40 µg, Roche)

The first strand of complimentary DNA (cDNA) was synthesized using expand reverse transcriptase. Total RNA (5 µg; section 2.2.2.1) was adjusted to a final volume of 10 µL (with DEPC treated water if necessary), denatured with 1 µL of Oligo $d(T)_{15}$ at 70 °C for 10 min, and then immediately quenched on ice. After a brief centrifugal pulse at 4 °C to collect the contents, the tubes were placed back on ice, and the following reagents added: 4 µL of 5 x expand reverse transcriptase buffer, 2 µL of DTT, 2 µL of dNTP mix and 0.5 µL of RNase inhibitor. The contents were then gently mixed and pulse centrifuged briefly before incubating at 42 °C for 2 min, after which 1 µL of expand reverse transcriptase was added (mixed and pulse spun). The mixture was then incubated for 1 h at 42 °C. The cDNA was placed on ice to stop the reaction and used immediately for PCR amplification (section 2.2.3.2), or stored at -20 °C until required.

2.2.3.2 Amplification of cDNA by Polymerase Chain Reaction

Reagents:

- PCR master mix: *Taq* DNA polymerase, dNTPs, $MgCl_2$ and reaction buffers (Promega)
- Primers (forward and reverse)

Each primer (Sigma) was dissolved in sterile water to give a concentration of 100 µM and stored at -20 °C until required. A working stock was prepared by diluting to a concentration of 10 µM. In a 50 µL volume of PCR mixture, 2 µL of primer was used, giving a final concentration of 400 nM (for primer sequences and names refer to Figure 2.2 and Table 2.2).

ACOF1: First round forward primer (Shifted by 3 nucleotides in 5′direction for E101)

				Q H			
amino acids	D	A	C	E	N	W	G

5′ GT GAATTC GAY GCN TGY SAN AAY TGG GG 3′
***Eco*RI** 2 4 2 2 4 2 Degeneracy = 256 x

ECORI: First round reverse primer (Shifted by 12 nucleotides in 3′direction for E102)

5′ TCG TCTAGA TC RAA NCK MGG YTC YTT 3′
***Xba*I** 2 4 2 2 2 2 Degeneracy = 128 x

E101: Second round forward primer

			Q				
amino acids	A	C	E	N	W	G	F

5′ GTGAATTC GCN TGY GAR AAY TGG GGH TT 3′
***Eco*RI** 4 2 2 2 3 Degeneracy = 96 x

E102: Second round reverse primer

5′ TCG TCTAGA GYT CYT TNG CYT GRA AYT T 3′
***Xba*I** 2 2 4 2 2 2 Degeneracy = 256 x

Figure 2.2: Sequence of the Primers used in RT-PCR to Amplify Putative ACC Oxidase Sequences.

With the advent of the T-vector system (section 2.2.4.5) the restriction enzyme sites *Eco*RI and *Xba*I) are no longer necessary.

Degeneracy: M=A+C; K=T+G; R=A+G; S=C+G; W=A+T; Y=C+T; B=T+C+G; D=A+T+G; H=A+T+C; V=A+C+G; N=A+T+C+G;

Table 2.2: Primers used in this study.

Oligo Name	Primer Sequence (5′ – 3′)	T_M
AppleACO F	*Eco*RI site GAC GAC CC **GAA TTC** C ATG GCG ACT TCC CAG TTG ***Reading Frame***	83.9
AppleACO R	*Sal*I site GAC GAC **GCT GAC** TCA GGC AGT TGC AAC AGG ***Stop codon***	81.1
ORFMD2F	*Eco*RI site GAC GAC **GAA TTC** ATG GCA ACT TTCC ***Reading Frame***	71.8
ORFMD2R	*Sal*I site GAC GAC **GCT GAC** TCA CTA ATT TTG ATT TC ***Stop codon***	68.0
ORMD3F	*Bam*HI site GAC GAC **GGA TCC** ATG GAG AAC TTC C ***Reading Frame***	73.2
APEST/R	*Xho*I site GAC GAC **CTC GAG** ***TCA*** AGC AGT ACT TAT AAC TGG ACC ***Stop codon***	75.2
pProEx-1(MD1F)	*Nde*I site GAC GAC **CAT ATG** GCG ACT TTC CCA GTT GTT G ***Reading Frame***	78.7
pProEx-1(MD1R)	*Xho*I site GAC GAC **CTC GAG** TCA GGC AGT TGC AAC AGG ***Stop codon***	80.4
pProEx-1(MD2F)	*Nde*I site GAC GAC **CAT ATG** GCA ACT TTC CCA GTT GTT G ***Reading Frame***	76.6
pProEx-1(MD2R)	*Xho*I site GAC GAC **CTC GAG** TCA ATT TTG ATT TCT TTT TGT C ***Stop codon***	73.0
pProEx-1(MD3F) APEST/F	*Nde*I site GAC GAC **CAT ATG** GAG AAC TTC CCA GTT ATC AAC C M E N F P V I N ***Reading Frame***	75.1
pProEx-1(MD3R) APEST/R	*Xho*I site GAC GAC **CTC GAG** ***TCA*** AGC AGT ACT TAT AAC TGG ACC ***Stop codon***	75.2
Degen.Malus/F Degeneracy = 16X	GA**Y** TAC ATG AAG CT**S** TA**Y** **K**CT GG	58.3
F/MD-ACO2	GGA ACC CGA CAA AAA G	56.2
Degen.F.South	GA**W** GA**K** TAC AGG AA**K** **RYS** ATG AAG	57.3
Md1(rtpcr)intron2/F	GAA GAG TAC AGG AAG ACC ATG AAG	61.9
Md2(rtpcr)intron2/F	GAA GAT TAC AGG AAG ACC ATG AAG	61.7

Table 2.2 contd.

Md3(rtpcr)intron2/F	GAT GAG TAC AGG AAT GTG ATG AAG	61.3
Md1 3′- UTR	TTG TTG AGC AAA CAT TTG	58.1
Md2 3′- UTR	CTA ATA ATT TTT ATT TTA TAT AGA TAG ATT TCA AC	57.6
Md3 3′ - UTR	CAC ATT GGT TAC TTT CTA CAA CG	60.0
pGEX Forward	GGG CTG GCA AGC CAC GTT TGT G	78.7
pGEX Reverse	CCG GGA GCT GCA TGT GTC AGG G	80.4
M13 Forward	CCC AGT CAC GAC GTT GTA AAA CG	70
M13 Reverse	AGC GGA TAA CAA TTT CAC ACA GG	66
Actin Forward	GCG AAT TCT TCA CCA C**Y**A C**H**G C**Y**G A**R**C G	76
Actin Reverse	GCG GAT CCC C**R**A TCC A**R**A CAC TGT A**Y**T TTC C	76

The PCR conditions were optimized and the appropriate parameters were set on either the PTC 200 Peltier Thermal Cycler, PCR Express Thermohybaid (PCY1040) or a Sprint Hybaid. For example, the number of cycles selected (typically 20 to 35 in this thesis) determined the amountof DNA amplified. The annealing temperature was typically set 5 °C below the melting temperature (T_m) of the primers, and the length of the DNA to be amplified determined the extension time needed for complete synthesis of the PCR product. As a rule of thumb, approximately 2 min extension time was allowed per kb of DNA.

Typically, the first round PCR used 5 μL of the cDNA (synthesized as described section 2.2.3.1) mixed with 25 μL of PCR mastermix, 2 μL of each primer (forward and reverse refer to Figure 2.2 and Table 2.2), and then made up to a final volume of 50 μL with nuclease free water. For the second round PCR reaction 5 μL of the first round PCR products were used as template together with a second set of primers (forward and reverse refer to Figure 2.2 and Table 2.2). All other components in the reaction were the same as for the first PCR round.

As an example, for the amplification of ACO fragments of an estimated length of 850 bp from an appropriate first strand cDNA solution using universal degenerate primers (ECOFI and ECORI; Figure 2.2), the PCR machines were programmed for the first round PCR reaction as follows. One cycle at 94 °C for 2 min; 35 cycles at 94 °C for 30 s (denaturation), 42 °C for 30 s (annealing), and 72 °C for 1 min 15 s (extension for 850 bp); with a final incubation step at 72 °C for 5 min to complete the extension of the cDNAs, before holding at 4 °C. For the second round PCR reaction the same parameters were used except the annealing temperature was increased from 42 °C to 50 °C and the second set of universal degenerated and nested primers were used (E101 and E102; Figure 2.2).

2.2.3.3 Primers Used for In-Frame Cloning

The Amersham pGEX-6P-3 (Figure 2.3) and the Gibco-BRL pPRoEX™-1 (Figure 2.4) protein expression systems were used to over-express the genes of interest within the background of *E. coli*. This requires that the foreign DNA be inserted into the plasmid vector in the correct orientation to allow transcription of an RNA that can be translated into the protein of interest. Primers were designed (Table 2.2) in such a way that the sequences generated by PCR contained different restriction sites at their 5′ and 3′ ends. These two restriction sites could then be used to directionally clone the PCR product, in-frame, into the multiple cloning site (MCS) of the expression vector. Spacer nucleotides were sometimes added between the restriction site and the coding frame to ensure that the first three nucleotides following those encoding the N-terminal extension

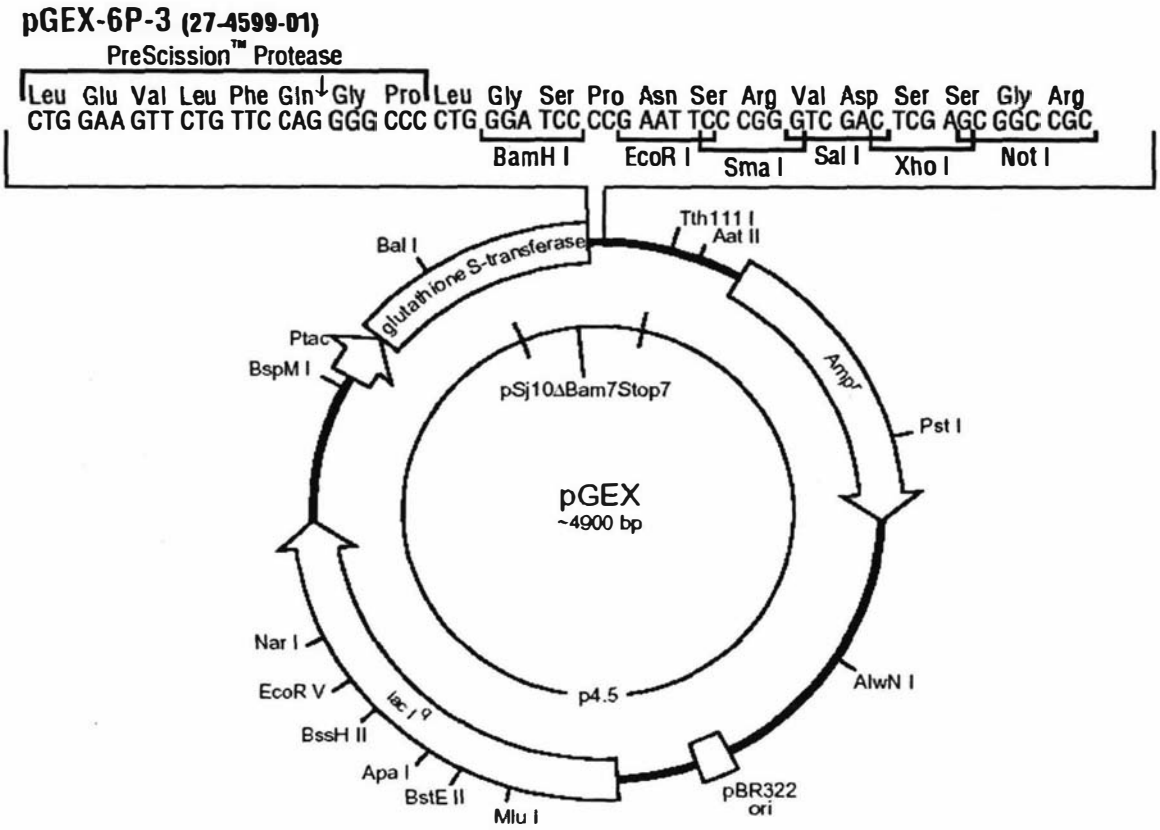


Figure 2.3: The Map and Schematic Diagram of the pGEX-6P-3 Vector and the Vector Multiple Cloning Site.

The *Eco*RI and *Sal*I sites used for inserting MD-ACO1 and MD-ACO2, and *Bam*HI and *Xho*I sites used for inserting MD-ACO3 open reading frame (ORF) sequences in-frame into the multiple cloning site (MCS) of pGEX are highlighted. The primers used for directional cloning into these sites appear in Table 2.2. Also indicated is the PreScission™ protease cleavage site from where the recombinant MD-ACO can be released from fusion with glutathione S-transferase.

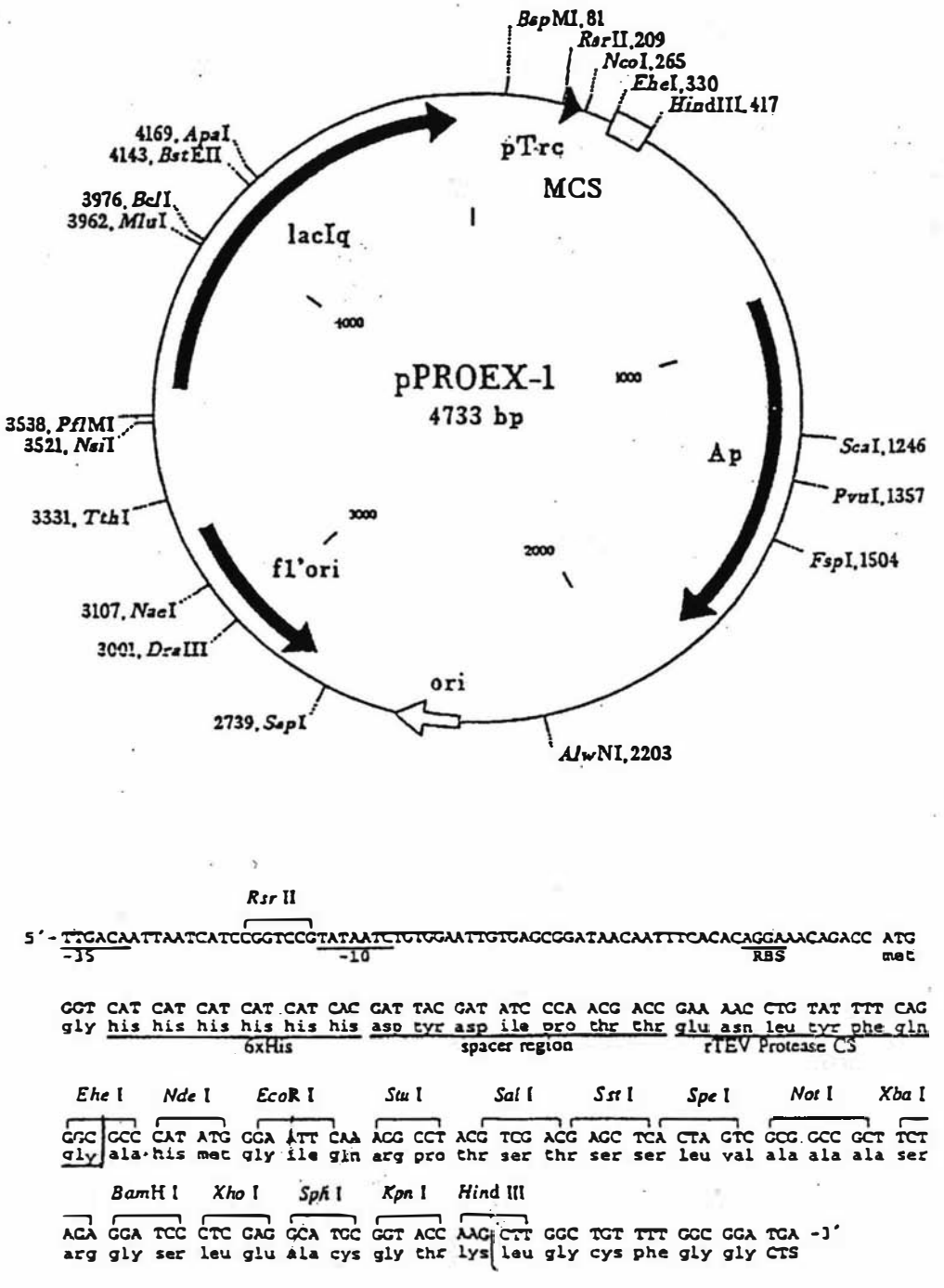


Figure 2.4: The Map and Schematic Diagram of the pProEX-1 Vector and the Vector Multiple Cloning Site.

The *Nde*I and *Xho*I sites used for inserting MD-ACO1, MD-ACO2 and MD-ACO3 open reading frame (ORF) sequences in-frame into the multiple cloning site (MCS) of pProEX-1 are highlighted. The primers used for directionally cloning into these sites appear in Table 2.2. Also indicated are the N-terminal six histidine residues that become fused to the translated sequences and hence allow purification of the fusion proteins by metal chelate affinity chromatography. The figure was reproduced from Focus 16 (4).

(of the protein of interest) coded for methionine set by the vector. At least six additional nucleotides were added to cap the restriction sites to allow the restrict enzymes to cut more effectively. Primers were designed to generate probes necessary for Southern blot analysis (Table 2.2), and primers were also designed to generate fragments for cDNA Southern analysis (Table 2.2).

2.2.3.4 Relative Quantitative RT-PCR using QuantumRNA™ 18S Internal Standards

Reagents:

- Expand reverse transcriptase (50 U μL^{-1}, Roche)
- 5 x Expand reverse transcriptase buffer (Roche)
- 0.1 M DTT (Roche)
- dNTP mix (dATP, dCTP, dGTP, dTTP, 10 mM Roche)
- RNase inhibitor (40 U μL^{-1}, Roche)
- 50 μM Random primers (Ambion)
- 18S rRNA primers: competimers (Ambion)
- 10 μM primers (Table 2.2)

Relative RT-PCR is a method for the quantitative analysis of gene expression. The assumption is that equal amounts of RNA from multiple samples, using identical PCR conditions and amplifying the same target from each sample, will result in the amount of PCR product from each reaction that is proportional to the abundance of RNA transcript in the samples. Since the expression of 18S ribosomal RNA (rRNA) is constitutively expressed (although even rRNA levels are not invariablity), it makes an ideal internal control for RNA analysis. By using QuantumRNA™ 18S Internal Standards (Ambion), with competimers, which are specially modified primers that cannot be extended, the signal for 18S rRNA can be attenuated to the level of a rare message by modulating the efficiency of the amplification of the 18S primers. A debate about using a relative quantitative RT-PCR technique to successfully demonstrate levels of specific transcripts verses conventional northern blotting is ongoing (Hengen, 1995), with some supporters finding the RT-PCR method both more valid and reliable than northern analysis (Jaakola *et al*., 2001).

Reverse transcription of RNA was carried out using total RNA (5 μg) and random primers (2 μL from a 50 μM solution) in a total volume of 10 μL, the mixture incubated for 3 min at 70 °C, quenched on ice for 2 min and collected by a brief pulse centrifugation at 4 °C. On ice, 4 μL of 5 x expand reverse transcriptase buffer, 2 μL of DTT, 2 μL of dNTP mix and 0.5 μL of RNase

inhibitor were added, the contents mixed and pulse centrifuged briefly before incubating at 42 °C for 2 min. After which, 1 μL of expand reverse transcriptase was added (mixed and pulse spun), and the reaction mix incubated for 1 h at 42 °C.

For PCR each reaction contained 2 μL of each ACO primer (forward and reverse), 4 μL of a 1:4 ratio of 18S rRNA primers to competimers mix, in 0.5 volumes of mastermix and the mixture was then made up to a total volume of 45 μL with nuclease free water. In fact, a cocktail was made up and well mixed to reduce pipetting variation and then 45 μL of the cocktail was transferred to each of the PCR tubes before 5 μL of cDNA was added and the contents mixed. The PCR parameters were the same as described earlier except the annealing temperature was raised to 55 °C.

β-actin primers (Table 2.2) were used, in the absence of non quantitative analysis, to determine whether cDNA had been generated following an RT reaction, especially where no bands occurred using primers to amplify fragments of the gene of interest.

2.2.4 Cloning of PCR Products into Plasmid Vectors

2.2.4.1 Ethanol Precipitation of DNA or RNA

Ethanol precipitation was used to concentrate nucleic acids by precipitating them out of solution and then resuspending them in the required volume. It was also used to partially purify DNA and RNA from salt solutions.

Reagents

- Sodium acetate
- Ethanol
- Isopropanol

Nucleic acid was precipitated from solution by adding a 0.1 volume of 3 M sodium acetate (pH 5.6), and either 2.5 volumes (for DNA) or 3 volumes (for RNA) of ice-cold ethanol (99.7-100 % v/v). DNA was precipitated at -20 °C for 3 h or 4 °C overnight (for maximum yield) and RNA was precipitated at -80 °C for 1 h or -20 °C overnight (for maximum yield). The nucleic acid was then pelleted by centrifugation at 20 800 x *g* for 20 min (DNA) or 30 min (RNA) at 4 °C and the supernatant discarded. After rinsing the pellet with ice-cold ethanol (75% v/v) to remove residual salts and discarding the supernatant, any residual ethanol was collected by pulse-centrifugation and removed with a micropipette. The pellet was air-dried (~ 5 min) and resuspended in sterile water (DNA) or DEPC treated water (RNA).

In some circumstances when volume quantities were limiting, 0.8 to one volume of isopropanol was added rather than ethanol and sodium acetate. However, ethanol was preferred as isopropanol is less volatile and tends to co-precipitate solutes, for example, NaCl, which can inhibit re-dissolution of the nucleic acid pellet.

2.2.4.2 Quantification of DNA

DNA concentrations were determined by measuring the absorbance of each solution at 260 nm (A_{260}) and 280 nm (A_{280}) using an Ultrospec 3000 UV/visible spectrophotometer (Pharmacia Biotech). Samples were diluted appropriately and aliquots of 100 µL transferred to a slightly larger quartz cuvette and measured against a water blank. For DNA, an OD_{260} of 1.0 corresponds to approximately 50 µg mL^{-1} of double stranded DNA (Sambrook *et al.*, 1989). The DNA concentration was calculated using the following formula:

$$A_{260nm} \times \text{dilution factor} \times 50 = \text{DNA concentration in } \mu g\ mL^{-1}$$

The purity of the DNA was determined by measuring the A_{260nm} / A_{280nm} ratio. Relatively pure DNA solutions have an A_{260nm} / A_{280nm} ratio of 1.8 (Sambrook *et al.*, 1989), a value that decreases with the presence of contaminants such as proteins, phenol and surfactants (if these are used in the nucleic acid procedures).

Relatively pure DNA solutions have A_{260nm} / A_{230nm} ratio > 2, a value that decreases with the presence of polysaccharides (Dong and Dunstan, 1996).

When sample volumes were limiting a NanoDrop®ND-1000 spectrophotometer (NanoDrop Technologies) was also used to measure the absorbance of each solution at 260 nm (A_{260}) and 280 nm (A_{280}), samples were diluted appropriately and aliquots of 2 µL were measured against a water blank.

For cloning procedures, cDNA and plasmid vector concentrations were also estimated using a High Mass Ladder or a Low Mass Ladder (Gibco BRL), where DNA samples of known concentration were run along side the unknown sample by agarose gel electrophoresis.

2.2.4.3 Agarose Gel Electrophoresis of DNA

Reagents:

- UltraPURE™ agarose (Gibco BRL)
- 10 x TAE buffer: 0.4 M Tris, 0.2 M glacial acetic acid, 10 mM EDTA pH 8

- 10 x SUDS: 0.1 M EDTA pH 8, 50 % (v/v) glycerol, 1% (w/v) SDS, 0.025% (w/v) bromophenol blue
- Ethidium bromide (10 mg mL^{-1})

Agarose gel electrophoresis is used to separate DNA fragments by size for either identification or purification. In solution (pH 8) DNA molecules are negatively charged and will migrate towards the positive electrode when an electrical current is applied. Migration is dependent on the size of the DNA fragments and their conformation both of which affect the movement of fragments in the agarose matrix. Agarose gels (0.6 % to 1.2 %) were prepared by dissolving agarose in 1 x TAE buffer by heating, allowing the solution to cool to approximately 55 °C before pouring the solution into gel-forming apparatus. For general applications, a horizontal DNA Mini Sub Cell™ (70 cm^2 gel bed, Bio-Rad) was normally used, but for Southern blot analysis a horizontal DNA Sub Cell™ (225 cm^2 gel bed, Bio-Rad) was used. DNA samples, including molecular size markers at *ca.* 0.1 μg per mm of lane width (1 Kb Plus DNA ladder, Invitrogen), were mixed with 0.1 volumes of 10 x SUDS, loaded into the pre-formed wells and separated by electrophoresis at 25 to 100 V. After electrophoresis, gels were stained with 0.1 μg mL^{-1} ethidium bromide for 10 to 20 min, and often destained (with water) for a further 20 to 30 min. The DNA fragments were visualized on a short wave $UV_{(340\ nm)}$ Transilluminator (UVP Inc., San Gabriel, CA, USA), and photographed digitally with an Alpha Imager™ 2000 Documentation and Analysis System (Alpha Innotech Corporation, San Leandro, CA, USA), or Gel Doc 2000™ (Bio-Rad).

2.2.4.4 DNA Recovery from Agarose Gels

DNA fragments were isolated from agarose gels using a spin column method with the CONCERT™ Gel Extraction Systems (Gibco BRL).

Reagents:

- CONCERT™ Gel Extraction Systems (Gibco BRL)(most concentrations not included)
- Gel Solubilizing Buffer: Sodium perchlorate, sodium acetate and TBE-solubilizer
- Wash Buffer: NaCl, EDTA and Tris-HCl (need to add ~100% ethanol)
- TE Buffer: 10 mM Tris-HCl (pH 8), 0.1 mM EDTA
- Spin cartridges, Wash tubes, Recovery tubes and Silica resin

After agarose electrophoresis, DNA fragments of interest were excised under long-wave UV light (340 nm) using a sterile scalpel blade, placed in a microcentrifuge tube, weighed (≤ 40 mg), and solubilization buffer (30 μL) added. The mixture was then incubated at 50 °C for 15 min, with shaking every 3 min for 10 s, and once the gel had dissolved, the sample was

incubated for a further 5 min. The mixture was transferred to a cartridge contained in a 2 mL Wash tube, centrifuged at 12 000 x *g* for 1 min, the flow-through solution discarded and solubilization buffer (500 µL) again added. After incubation at room temperature for 1 min, the DNA was washed by centrifugation at 12 000 x *g* for 1 min, the flow-through discarded, Wash buffer (700 µL) added and the cartridge incubated at room temperature for 5 min. Following centrifugation at 12 000 x *g* for 1 min, the flow-through was discarded and residual ethanol removed by centrifugation at 12 000 x *g* for a 1 min. The cartridge was transferred into a Recovery tube, and pre-warmed TE buffer (65 °C to 70 °C; 50 µL) was applied directly to the centre of the cartridge, the tube incubated for 1 min at room temperature, and then centrifuged at 12 000 x *g* for 2 min to collect the DNA.

2.2.4.5 DNA ligation

DNA ligation using the linearised T-vector system

The DNA fragments produced by PCR have a single deoxyadenosine attached at the 3′-ends of the duplex molecule generated by the terminal transferase activity of Taq DNA polymerase (sticky ends), which is complementary to the overhanging 3′-terminal deoxythymidines on the pGEM®-T Easy Vector developed by Promega (Figures 2.5 and 2.6).

The amount of PCR product required for ligation was determined by a 3:1 insert:vector molar ratio, calculated using the following formula:

$$\frac{\text{vector (ng) x insert (Kb)}}{\text{size of vector (Kb)}} \times \frac{3}{1} = \text{insert/PCR product (X ng)}$$

The PCR product was ligated with 50 ng of pGEM®-T Easy Vector in a reaction mix containing 5 µL of 2 x T4 DNA ligase buffer and 1 µL of T4 DNA ligase (3 weiss units μL^{-1}), in a final reaction volume of 10 µL made up with sterile water. After mixing by pipetting, the ligation reaction was incubated at 4 °C overnight.

DNA ligation using restriction digested vector

For ligations into either the pGEX-6P-3 Vector (Figure 2.3)(Amersham, Pharmacia Biotech) or the pPRoEX™-1 Vector (Figure 2.4) (GibcoBRL, Life Technologies), a 1:3 molar ratio of vector to insert was also used. The quantity of vector and PCR product was estimated visually by resolving an aliquot of plasmid and PCR product on the same 1 % (w/v) agarose gel together with either a High Mass Ladder or a Low Mass Ladder (Gibco BRL), of known concentration and estimating the concentration from the ethidium bromide staining intensities.

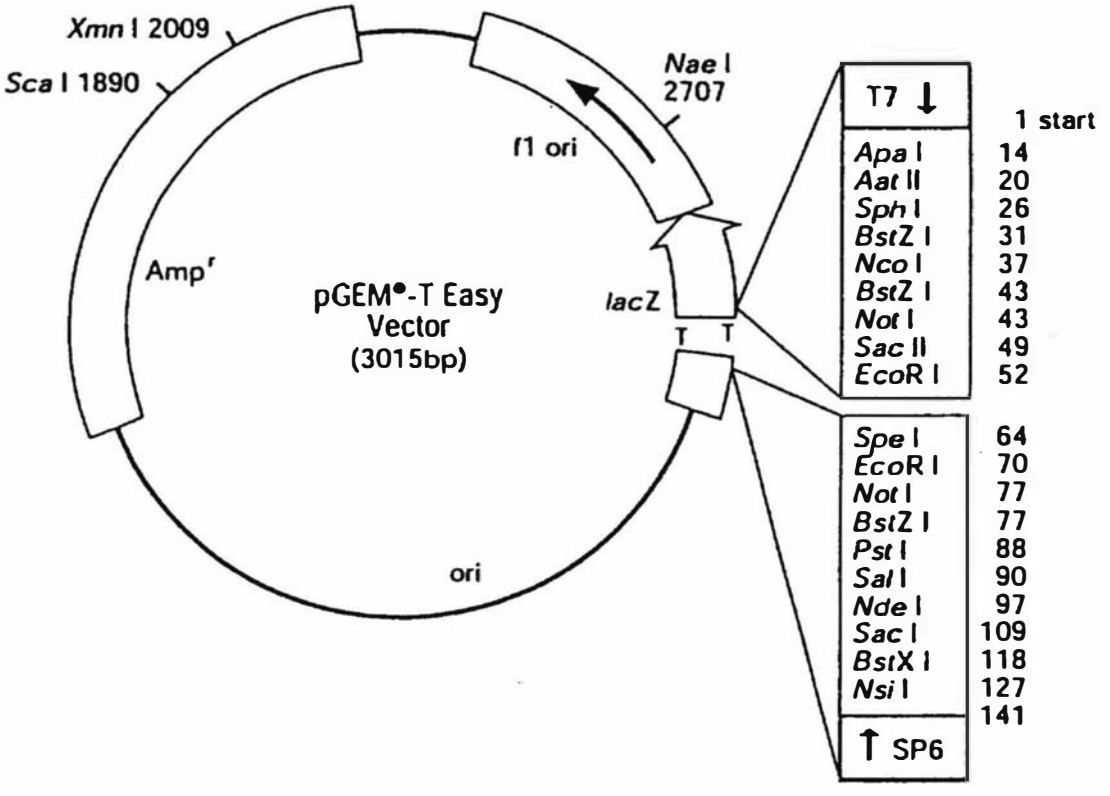


Figure 2.5: pGEM®-T Easy Vector Circle Map and Sequence Reference Points

pGEM®-T Easy Vector Sequence reference points:	
T7 RNA Polymerase transcription initiation site	1
SP6 RNA Polymerase transcription initiation site	141
T7 RNA Polymerase promoter (–17 to +3)	2999–3
SP6 RNA Polymerase promoter (–17 to +3)	139–158
multiple cloning region	10–128
lacZ start codon	180
lac operon sequences	2836–2996, 166–395
lac operator	200–216
β-lactamase coding region	1337–2197
phage f1 region	2380–2835
binding site of pUC/M13 Forward Sequencing Primer	2956–2972
binding site of pUC/M13 Reverse Sequencing Primer	176–192

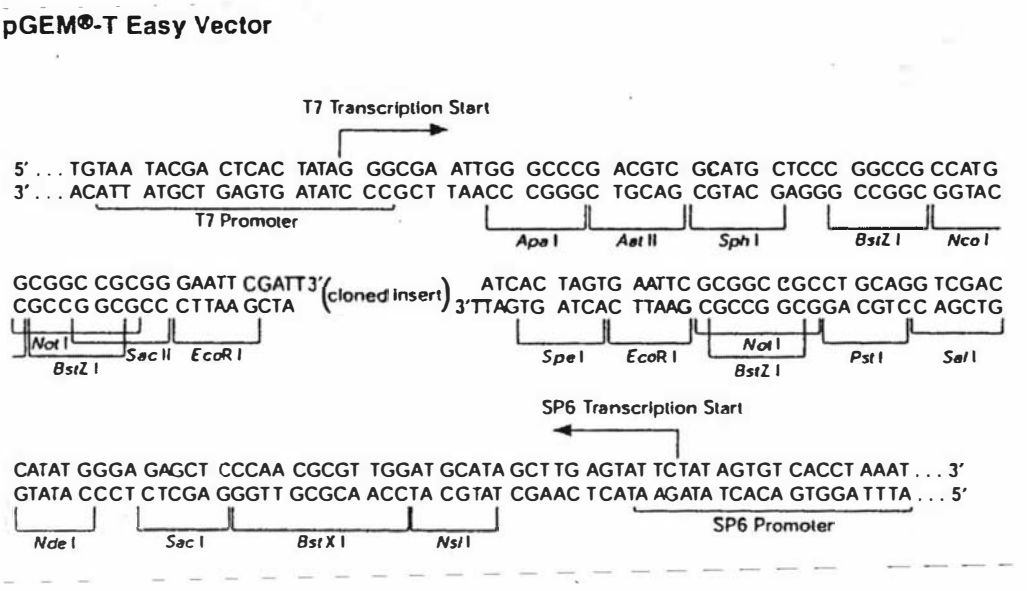


Figure 2.6 Sequence of the Promoter and Multiple Cloning Site of the pGEM®-T Easy Vector

The top strand of the sequence shown corresponds to the RNA synthesized by T7 RNA Polymerase. The bottom strand corresponds to the RNA synthesized by SP6 RNA Polymerase (from Promega, 1999).

The appropriate amount of PCR product was ligated with 10 to 50 ng of vector in a reaction mix that contained 2 µL of T4 DNA ligase (1 U μL^{-1}, Roche) and 2µL of 10 x ligation buffer (supplied with ligase), made up to 20 µL with sterile water. The ligation mix was incubated overnight at 16 °C in a PTC-200 Peltier Thermal Cycler (MJ Research Inc., Watertown, Massachusetts, 02172 USA).

2.2.4.6 Transformation of *E. coli* using the Heat Shock Method

Reagents:

- LB broth (refer section 2.2.1.1)
- X-Gal (50 mg mL^{-1}, dissolved in *N,N'*-dimethyl-formamide)

Aliquots of competent cells (section 2.2.1.2) were thawed on ice for 5 min, then 50 to 150 µL added to the ligation reaction (section 2.2.4.5), the suspension mixed by gently pipetting up and down (while remaining on ice) and then the mixture was incubated on ice for 20 min. After this time, the cells were heat-shocked at exactly 42 °C for 45 to 50 s, quenched on ice for 2 min, then 950 µL of LB broth (room temperature) was added, and the transformation mixture incubated at 37 °C for 90 min with shaking at 180 rpm. LB Amp^{100} plates (section 2.2.1.1) were

spread with 20 µL of X-Gal (50 mg mL^{-1}) and allowed to dry for 30 min at 37 °C prior to use. A 200 µL aliquot of the mix was then spread onto an LB Amp^{100} plate while the cells in the remaining mix were centrifuged at 3 000 x *g* for 1 min. Most of the supernatant was discarded and the cells resuspended in the drainings and a further 200 µL aliquot was spread onto another LB Amp^{100} plate. The plates were incubated at 37 °C overnight and then stored at 4 °C. *Lac* operon blue/white colony selection was used to identify transformants.

2.2.5 Characterization and Sequencing of Cloned DNA in *E. Coli*

2.2.5.1 Isolation of Plasmids from *E. coli* by the Alkaline Lysis Method

The quick DNA plasmid miniprep method of Sambrook *et al.*, (1989) was used.

Reagents:

- Isopropanol
- Ethanol
- Resuspension solution-A: 25 mM Tris pH 8.0 (HCl), 50 mM glucose, 10 mM EDTA
- Alkaline lysis solution-B: 0.2 M NaOH, 1% (w/v) SDS
- Neutralization solution-C: 3 M potassium acetate, 2 M glacial acetic acid

After incubating the transformant mix (refer section 2.2.4.6) on LB Amp^{100} plates overnight at 37 °C, cells from single colonies of interest were collected using sterile toothpicks and grown separately in LB broth (10 mL) and ampicillin (100 µg mL^{-1}) overnight at 37 °C with shaking (200 rpm). *E. coli* broths were transferred to microcentrifuge tubes and pelleted by centrifugation at 3 000 x *g* for 5 min at room temperature, and the supernatant discarded. After resuspending the pellet in freshly prepared solution-A (100 µL), the cells were lysed by adding freshly prepared solution-B (200 µL) and gently mixed by slow inversion, then incubated on ice for 10 min. Neutralisatization solution-C (150 µL) was added to the mixture, shaken or vortexed vigorously and then left on ice for 15 min to allow chromosomal DNA and proteins to precipitate. The precipitate was then pelleted by centrifugation at 20 800 x *g* for 5 min at room temperature and the supernatant (~ 380 µL) transferred to a fresh tube, carefully avoiding particulate matter. For a cleaner plasmid preparation, an equal volume of chloroform: isoamyl alcohol (24:1) was added to the supernatant (~ 380 µL), the aqueous and organic phases mixed by vortexing and separated by centrifugation at 20 800 x *g* for 5 min at room temperature, after which the upper aqueous phase (containing the plasmid DNA) was removed. The plasmid DNA was then precipitated by the addition of an equal volume of ice-cold isopropanol, the DNA pelleted by centrifugation at 20 800 x *g* for 5 min at room temperature and the pellet rinsed twice with ice-cold ethanol 70% (v/v), air dried for 5 min, dissolved in sterile water (40µL) and stored at -20 °C.

2.2.5.2 Plasmid Isolation from *E. coli* by the Rapid Boiling Method

A very quick DNA plasmid miniprep developed by Holmes and Quigley (1981) was used.

Reagents:

- RNase (Sigma)
- Lysozyme (Sigma)
- 3 M Sodium acetate
- Isopropanol
- Ethanol
- 10 mM Tris-HCl (pH 8.5)
- STET buffer: 8 % (w/v) Sucrose, 0.5 % (w/v) Triton X-100, 50 mM EDTA, pH8, 10 mM Tris, pH8
- Lysozyme solution: 10 mg mL^{-1} in 10 mM Tris-HCl pH 7.5
- RNase A : (10 mg mL^{-1}) pre-boiled for 15 min and stored at -20 °C

After incubating the transformant mix (refer section 2.2.4.6) on LB Amp^{100} plates overnight at 37 °C, cells from single colonies of interest were collected using sterile toothpicks and grown separately in LB broth (10 mL) and ampicillin (100 μg mL^{-1}) overnight at 37 °C with shaking (200 rpm). Following centrifugation at 3 000 x *g* to collect the cells, the supernatant was drained off and the cell pellet resuspended in STET buffer (350 μL), lysozyme solution (25 μL) added and the suspension, incubated at 37 °C for 15 min. The mixture was then boiled for 1 min and the cell debris removed by centrifugation at 20 800 x *g* for 10 min (the gelatinous pellet was removed with a toothpick). Plasmid DNA was precipitated by adding ice-cold isopropanol (400 μL) and 3 M sodium acetate (40 μL), mixing well and incubation at -20 °C for 10 to 20 min before collecting the DNA by centrifugation at 20 800 x *g* for 10 min. The supernatant was removed and the pellet rinsed in 70% ethanol before centrifugation at 20 800 x *g* for 2 min. The supernatant was removed and the pellet air-dried for 5 min, resuspended in 10 mM Tris-HCl (pH 8.5), and stored at -20 °C until required.

2.2.5.3 Digestion of DNA with Endonuclease Restriction Enzymes

Reagents:

- Restriction enzyme (Roche or Gibco BRL, Life Technologies)
- 10 x Restriction buffer
- RNase A (10 mg μL^{-1})(Sigma)
- 10 x SUDS: 0.1 M EDTA pH 8, 50%(v/v) glycerol, 1%(w/v) SDS, 0.025%(w/v) bromophenol blue

Digestion of both the plasmid vector and the PCR product in preparation for directional cloning required the use of two different restriction enzymes. The isolated plasmid (section 2.2.5.1 or 2.2.5.4) was digested with 40 U of the first restriction enzyme, in 0.1 volume of 10 x restriction buffer, 20 μg of RNase A and sterile water added to 40 μL and incubation overnight at 37 °C. Samples of both digested and undigested DNA plasmid were separated by agarose gel electrophoresis (section 2.2.4.3) to ascertain whether the enzyme had cut to completion (as determined by a wholly linear plasmid). The second restriction enzyme was then added, together with sterile water if the glycerol concentration exceeded 5% (v/v), and the reaction incubated overnight at 37 °C. If the optimal buffer used for the digestion was not common to both enzymes, then an ethanol precipitation (2.2.4.1) was necessary prior to digestion of the DNA with the second restriction enzyme. The double digested plasmid was then gel (section 2.2.4.3) and column (section 2.2.5.4) purified.

The PCR generated DNA was typically cleaned (section 2.2.5.5) prior to digestion in a reaction mix containing 80 U of the first restriction enzyme, 0.1 volume of 10 x restriction buffer and sterile water added to a final volume of 80 μL. After incubation at 37 °C overnight, the second restriction enzyme was added, together with sterile water if the glycerol concentration exceeded 5% (v/v), and the reaction incubated overnight at 37 °C. Again, if the optimal buffer used for the digestion was not common to both enzymes, the PCR products were column cleaned (2.2.5.5) prior to the second restriction digestion. The double digested PCR products were then gel (section 2.2.4.4) and column (section 2.2.5.5) purified.

To confirm the presence of an insert in a plasmid vector of the expected size, 1 to 2 μg of isolated plasmid DNA (section 2.2.5.1 or 2.2.5.2) was digested in a reaction mix containing 5 U of restriction enzyme, 0.1 volumes of 10 x restriction buffer, 10 μg RNase A with sterile water added to 10 μL, at 37 °C for 1 to 3 h. The reaction was stopped with the addition of 0.1 volumes of 10 x SUDS and then the digested DNA was resolved by electrophoresis (section 2.2.4.3). If excision of the insert required the action of two restriction enzymes, and both were able to cut effectively in a common buffer, then digestion was performed in a single reaction volume.

2.2.5.4 Purification of Plasmid DNA for Sequencing

Reagents:

- QIAprep® Spin Miniprep Kit (Qiagen Inc.)

E. coli cells, containing a plasmid ligated to a DNA sequence of interest, were collected from culture by centrifugation at 3 000 x *g* for 3 min at room temperature, the supernatant discarded

and the pellet resuspended in 250 μL of buffer P1 (containing RNase, supplied by the manufacturer), before buffer P2 (250 μL) was added to lyse the cells by gently inverting the tube 4-6 times to mix. After no longer than 5 min, 350 μL of buffer N3 (high salt) was added to stop the reaction, and the tubes were inverted immediately but gently 4-6 times to precipitate contaminating chromosomal DNA and protein. The precipitate was pelleted by centrifugation at 20 8000 x *g* for 10 min at room temperature, the supernatant transferred to a QIAprep column containing a silica gel membrane and after centrifugation at 20 800 x *g* for I min the flow through was discarded, and the DNA washed by adding 0.750 μL of buffer PE. After centrifugation at 20 800 x *g* for 1 min, the flow through was discarded, and the centrifugation was repeated to remove any residual wash buffer. The column was then transferred to a clean microcentrifuge collection tube and the DNA eluted by adding 50 μL of buffer EB (low salt) to the centre of the column and again centrifuging for 1 min at 20 800 x *g*. The plasmid DNA was separated on a 1% (w/v) agarose gel (section 2.2.4.3) to assess the quantity (section 2.2.4.2) and quality and then used immediately or stored at -20 °C until required.

2.2.5.5 Purification of PCR Products

Method I.

Reagents:

- Shrimp alkaline phosphatase (SAP), and SAP buffer (Roche)
- Endonuclease III (*Exo* III) (USB Corp., OH, USA)

PCR products to be sequenced were cleaned up to remove any RNA and primers before they were subjected to the PCR Big Dye Terminator reaction, by adding 2 μL of SAP(1U μL^{-1}), 1 μL of SAP buffer and 1 μL of *Exo*III (10U μL^{-1}) to an 0.5 volume of the PCR products (25 μL). The mixture was incubated at 37 °C for 30 min, and the SAP inactivated by incubation at 80 °C for 15 min. The PCR templates were then separated on a 1.2 % (w/v) agarose gel (section 2.2.4.3) to assess the quantity (section 2.2.4.2) and quality and then used immediately or stored at -20 °C until required.

Method II.

Reagents:

- High Pure PCR Product Purification Kit (Roche)

Following PCR amplification, the total volume for each tube was adjusted to 100 μL and 500 μL of Binding buffer added and the products mixed well. The contents were then transferred to a filter tube and centrifugated at 20 800 x *g* for 1 min at room temperature, the flow through

discarded and 500 μL of Wash buffer added. After centrifugation at 20 800 x *g* for 1min at room temperature, the flow through was discarded and the wash step was repeated using 200 μL of Wash buffer. After centrifugation, the filter tube was transferred to a clean microfuge tube, 50 – 100 μL of Elution buffer added and the PCR products collected by centrifugation at 20 800 x *g* for 1 min. The eluate was then centrifuged at 20 800 x *g* for 1 min to remove any residual glass fibres (a procedure recommended by the manufacturer), and the supernatant carefully removed. The PCR templates were then separated on a 1.2 % (w/v) agarose gel (section 2.2.4.3) to assess the quantity (section 2.2.4.2) and quality and then used immediately or stored at -20 °C until required.

2.2.5.6 Preparation for Automated Sequencing of DNA

Using the dideoxy method of DNA sequencing, the last nucleotide is always a dideoxy nucleotide. A dideoxy nucleotide is a nucleotide with a fluorescent dye attached and is known commercially as the Big Dye Terminator. The incorporation of a dideoxy nucleotide into the extension product terminates the chain and the reaction mixture contains DNA sequences of different lengths. A laser scanner on the ABI Prism automatic sequencer excites the fluorescent tag as it passes by and a detector analyzes the colour of the resulting emitted light.

Reagents:

- ABI PRISM™ Big Dye Terminator Cycle Sequencing Ready Reaction Kit (Version 3.1, Applied Biosystems)

For sequencing, the PCR assay contained DNA template (plasmid 300 ng or PCR product calculated as 2 ng for every 100 bp), 5 μL of sequencing buffer, 3.2 pmol of the appropriate primer, and 2 μL of Big Dye terminator (which contains AmpliTaq DNA Polymerase and all the required components for the sequencing reaction). The mixture was then made up to a total volume of 20 μL with sterile water, and the PCR tube containing the mixture was placed into a Peltier Thermal Cycler (MJ Research Inc.) and a one step reaction was programmed as follows: 25 cycles set at 96 °C for 10 s, then rapid thermal ramp (1 °C s^{-1}) to 50 °C, held at 50 °C for 5 s followed by rapid thermal ramp (1 °C s^{-1}) to 60 °C, held a 60 °C for 1 min 30 s. After 25 cycles, the reaction was ended and the DNA was cleaned and precipitated by the addition of 2 μL EDTA (125 mM), 2 μL of sodium acetate (3 M) and 50 μL of 100% (v/v) ethanol. After mixing well by inversion, the sample was incubated at room temperature for 15 min, and the DNA pelleted by centrifugation at 20 800 x *g* for 30 min at 4 °C, washed twice with 70% (v/v) ethanol (70 μL) and air dried.

Samples were submitted to Lorraine Berry at the Genomic Centre, Allan Wilson Centre, Massey University, and the fragments were analyzed using standard protocols with an automated ABI PRISM™ 3730 DNA Capillary Sequencer (Applied Biosystems). Universal M13 forward and reverse primers (Table 2.2) were used for the automated sequencing from the pGEM® -T Easy Vector (New England Biolab). The M13 reverse primer could be used to sequence from pPRoEX™-1. The pGEX gene specific primers (Amersham catalogue; refer Table 2.2) were ordered from Sigma.

2.2.6 DNA Sequence Analysis

2.2.6.1 Sequence Alignment

A BLAST search of the GenBank database was used to search for nucleic acid sequences and then the sequences of interest were stored within the Gene Computer Group (GCG version 11.0) Fasta programes (Accelnys Inc., San Diego, CA, USA), and used as a reference against which future sequences were compared. The electrophoretograms were edited to check whether any differences were real or caused by unincorporated dye, and the vector sequence was cut out if necessary. Many of the alignment programmes compliment each other and were used in conjunction with each other. GCG programmes such as the MAP give a choice of the best amino acid sequence from three reading frames and then the predicted polypeptide amino acid sequences from the cloned cDNA coding regions were compared with the protein sequences held in the NCBI protein databases. The programme Sequencher™ 4.2 (Genes Codes Corp., Ann Arbor, MI, USA) was used to provide an overview of how the fragments fit together and their orientation (lots of sophisticated functions but only one person can use it at a time). MT Navigator 1.0.2b3 package (Applied Biosystems Inc.), was useful for editing and comparing electrophoretograms, and for moving two or more sequences until they overlap, as with forward and reverse sequences.

Expected (E) values: a parameter that describes the number of hits one can expect to see just by chance when searching a database of a particular size. Random background noise that exists for matches between sequences, with the numbers decreasing exponentially so that the closer to zero the more significant it is (from the NCBI database).

2.2.6.2 Sequence Phylogeny

A fifty percent majority rule consensus tree was built using a heuristic search with default parameters of a β-version of the Phylogenetic Analysis Using Parsimony (PAUP* version 4.B10, Sinauer Associates Inc. Publishers, Sunderland Massachussetts© 1998 Smithsonian Institute). To view the phylogenetic tree, the software package Split Tree 4 (Huson and Bryant,

2006) was used. To edit out and appropriately label the sequences the software programme Adobe Illustrator® 8.0, (Adobe Systems Inc., USA) was used. Non parametric bootstrap values for internal splits (Felsenstein, 1985), give an indication of the strength of the signals within the data that separate the grouping of taxa on one side of the split from taxa on the other side. Hence bootstrap reduces the potential influence of stochastic error. Non parametric means the underlying programme does not assume that the distribution curve is going to be normal.

2.2.7 Southern Analysis

2.2.7.1 Isolation of Genomic DNA

Genomic DNA was isolated by a modified method based on that of Keb-Llanes *et al.*, (2002), including steps from the method of Junghans and Metziaff (1990).

Reagents

- SDS
- Potassium acetate
- Sodium acetate
- RNase A
- Phenol crystals
- Chloroform
- Isoamyl alcohol
- Ethanol
- Isopropanol
- Extraction buffer A: Hexadecyltrimethylammonium bromide (CTAB) 2 % (w/v), 100 mM Tris-HCl (pH 8), 20 mM EDTA, 1.4 M NaCl, Polyvinylpyrrolidone (PVP-40) 4 % (w/v), ascorbic acid 0.1 % (w/v), and 10 mM 2-mercaptoethanol.
- Extraction buffer B: 100 mM Tris-HCl (pH 8), 50 mM EDTA, 100 mM NaCl, and 10 mM 2-mercaptoethanol.
- Tris-buffered phenol: 6 mL Tris-HCl 1 M (pH 8), 7.5 mL NaOH 2 M, 130 mL H_2O, and 500 g commercial phenol crystals.
- TE Buffer: 10 mM Tris, 1mM EDTA (pH 8)

Approximately 4 g FW of young leaf tissue was ground to a fine powder using a pre-chilled pestle and mortar under liquid nitrogen. The powder was transferred into a 50 mL sterile screw-capped disposable polypropylene tube and 4 mL of extraction buffer A, 12 mL of extraction buffer B and 1.3 mL of SDS 20 % (w/v) were added and the mixture vortexed for 3 min. After incubation in a water bath at 65 °C for 20 min, cold (-20 °C) 5 M potassium acetate (5.5 mL)

was added and thoroughly mixed, before the mixture was transferred to microcentrifuge tubes and the debris removed by centrifugation at 15 300 x *g* for 15 min at 4 °C. After 1 mL of the supernatant was transferred to a fresh tube, 540 µL of 100% isopropanol (pre cooled to -20 °C) was added, the mixture incubated on ice for 20 min before the DNA was collected by centrifugation at 9 600 x *g* for 10 min and the supernatant discarded. The pellet was washed with 500 µL of 70 % (v/v) ethanol (pre cooled to -20 °C), followed by centrifugation at 9 600 x *g* for 1 min, pulse centrifugation and then air drying for 10 min. The pellet was resuspended in TE buffer (600 µL) then 60 µL of 3 M sodium acetate (pH 5.2) and 360 µL of 100 % (v/v) isopropanol (pre cooled to -20 °C) was added, and the mixture incubated on ice for 20 min.

Again the DNA was pelleted by centrifugation at 9 600 x *g* for 10 min, the supernatant discarded and the pellet washed with 500 µL of 70 % (v/v) ethanol (pre-cooled to -20 °C), followed by centrifugation at 9 600 x *g* for 1 min, pulse centrifugation and air drying for 10 min. The pellet was resuspended in TE buffer (600 µL), followed by the addition of 60 µL of 3 M sodium acetate (pH 5.2) and 360 µL of 100% isopropanol (pre cooled to -20 °C), and the mixture was again incubated on ice for 20 min.

The DNA was again pelleted by centrifugation at 9 600 x *g* for 10 min, the supernatant discarded and the pellet washed with 500 µL of 70 % (v/v) ethanol (pre cooled to -20 °C), followed by centrifugation at 9 600 x *g* for 1 min, pulse centrifugation and air drying for 10 min. The pellet was resuspended with 400 µL of TE buffer and 4 µL of RNase A (10 mg mL^{-1}) was added and the mixture incubated at 37 °C for 20 min. Following incubation, 200 µL of Tris-buffered phenol was added and the solution shaken for 3 min, then 200 µL of chloroform: isoamyl alcohol (24:1) was added and the solution shaken for a further 3 min. The aqueous and organic phases were separated by centrifugation at 20 800 x *g* for 10 min and the upper aqueous layer transferred to a fresh tube and the DNA precipitated with ethanol (section 2.2.4.1), resuspended and quantified (section 2.2.4.2).

2.2.7.2 Digestion of Genomic DNA

Reagents:

- *Eco*RI: 10 U μL^{-1} (Roche)
- *Hind*III: 10 U μL^{-1} (Roche)
- *Xba*I: 10 U μL^{-1} (Roche)
- 10 x Restriction buffer: (supplied with the appropriate enzyme)

Genomic DNA was digested with three restriction endonucleases. In a total volume of 600 µL containing 60 µL of 10 x restriction buffer, 10 µg of DNA was digested with 100 U of either *Eco*RI, *Hind*III or *Xba*I at 37 °C overnight (Dr Nigel Gapper, Cornell University, USA, *pers. comm.*). The digested DNA was then ethanol precipitated overnight (section 2.2.4.1), and following centrifugation at 20 800 x *g* for 20 min, washing in ice cold 75 % (v/v) ethanol and air drying for 5 min, resuspended in TE buffer (10 µL) and left at 4 °C overnight to completely dissolve the DNA (to prevent shearing the DNA by pipetting). The resuspended digests were then pooled into appropriate tubes (thus one tube contained DNA digested with *Eco*RI, another contained DNA digested with *Hind*III and the third tube contained DNA digested with *Xba*I). The reason for pooling the digested DNA was so that aliquots were taken from the same digestion mixture, thereby ensuring that all of the loading samples contained equal amounts of DNA. One tenth volume of 10 x SUDS gel loading buffer was added and the DNA samples (20 µg per lane) were fractionated on a 0.8% (w/v) agarose gel by electrophoresis at 30 V (section 2.2.4.3), for 16 to 18 h until the bromophenol dye front was *ca.* 12 cm from the origin of the gel.

2.2.7.3 Southern Blotting of Genomic DNA

Reagents:

- Depurination solution: 0.25 M HCl
- Denaturation solution: 1.5 M NaCl, 0.4 M NaOH
- Neutralizing solution: 1.0 M Tris (pH 8), 1.5 M NaCl
- Transfer buffer: (20 x SSC) 3 M NaCl, 0.3 M sodium citrate (pH 7)

Following electrophoresis (2.2.4.3), genomic DNA fragments were transferred to a nylon membrane by Southern blotting (Southern, 1975) based on the downward capillary transfer method of Chomczynski, (1992a), except for the addition of a depurination step. The agarose gel was immersed in depurination solution with gentle shaking for 10 min, rinsed twice with RO water and transferred to the denaturation solution for 1 h on a shaker. After two rinses with RO water the gel was equilibrated in neutralising buffer for 10 min on a shaker, rinsed briefly in RO water and agitated for 15 min in transfer buffer.

To transfer the DNA (refer Figure 2.7), four pieces of dry blotting paper (3MM, Whatman) were first lined up on a 4 cm high stack of paper towels, and then a gel-sized piece of blotting paper, pre-wetted with transfer buffer, was placed onto the top of the dry blotting paper. A gel-sized piece of Hybond^{TM} -N^{+} nylon membrane (Amersham), pre-soaked in transfer buffer for 5 min, was placed on top of the wet blotting paper, and then the gel was placed face-up on top of the nylon membrane, taking care to prevent air bubbles forming (by adding a small quantity of transfer buffer to the membrane and immediately laying the gel on top). Three pieces of

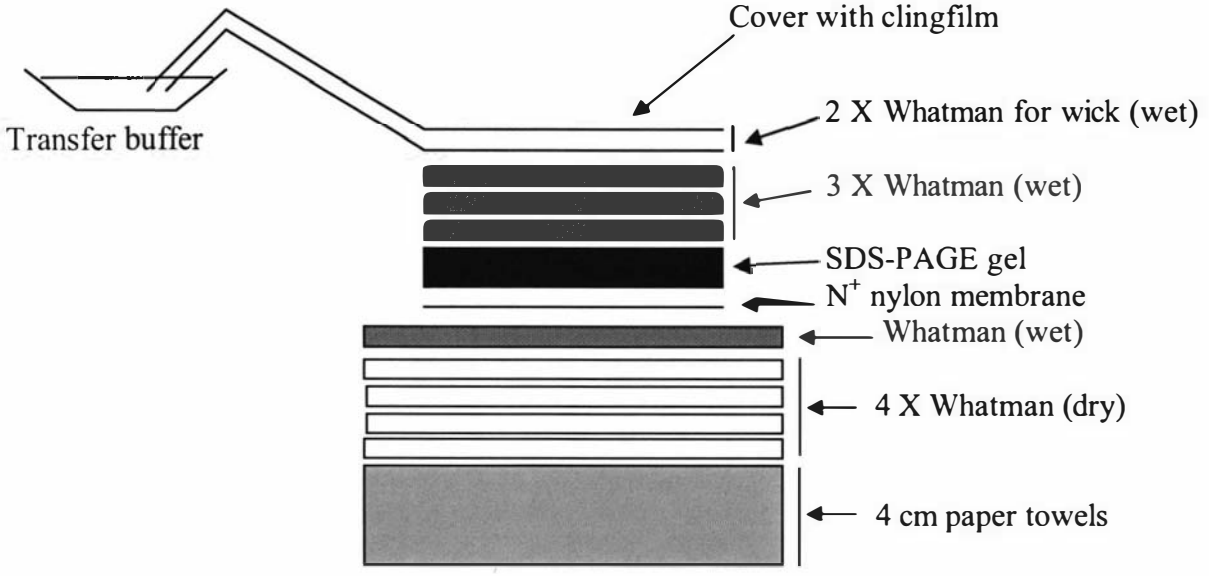


Figure 2.7: Arrangement of the Apparatus used to Transfer DNA Samples to Hybond^{TM}-N^{+} Membranes.

blotting paper, pre-wetted with transfer buffer, were placed onto the gel. A capillary wick was constructed from two pieces of longer and pre-wetted blotting paper, with the middle portion of the wick laying flat across the top of the blotting assembly and the two ends dipped into the elevated transfer buffer. After 16 h of blotting, the membrane was washed for 5 min in fresh transfer buffer to remove any gel adhering to the membrane, and then post-fixed by UV-crosslinking (UV Statalinker®2400; Stratagene, La Jolla, CA, USA) set at 1200 mJ/cm^2 (i.e. 1.2 min). The membrane was placed between two sheets of 3MM paper and allowed to dry, then sealed in a clean plastic bag and stored at 4 ℃ until required.

2.2.7.4 Southern Blotting of cDNA Fragments

DNA fragments generated by PCR were transferred to Hybond^{TM} -N^{+} nylon membrane by the downward capillary transfer method (2.2.7.3), except the gel was not depurinated, denatured or neutralised before transfer, and the transfer time was for 5 h.

2.2.7.5 Labelling DNA for Southern Analysis with [α-^{32}P] -dATP

Reagents:

- Megaprime™ DNA Labelling Kit (Amersham)
- [α-^{32}P]-dATP (Amersham)
- Reaction buffer: (supplied in kit)

DNA was labelled with [α-^{32}P]-dATP using the Megaprime™ DNA Labelling Kit (Amersham). Initially 5 μL of DNA (*ca.* 5 ng μL^{-1}) was combined with 5 μL of nonamer primers and denatured in a boiling water bath for 3 min. Following pulse centrifugation to collect the contents, 4 μL each of the unlabelled dNTPs (dGTP, dCTP, and dTTP) were added, together with reaction buffer (5 μL) and 'Klenow' polymerase (2 μL), before the final volume was adjusted to 45 μL with sterile water. The labelling reaction was initiated with 5 μL of [α-^{32}P]-dATP (specific activity 3 000 Ci mmol $^{-1}$) and continued for 15 min at 37 °C. The radiolabelled DNA was then purified through a ProbeQuant™ Sephadex G-50 Micro Column (Pharmacia Biotech). This involved vortexing the column to resuspend the Sephadex, loosening the lid, snapping off the bottom closure and centrifugation of the column in a microcentrifuge tube at 735 x *g* for 1 min to remove the void volume. The column was transferred to a new microfuge tube and the labelled sample was layered onto the Sephadex and the labelled DNA purified away from unincorporated nucleotides, reaction dyes and salts by centrifugation at 735 x *g* for 2 min. Labelled DNA collected at the bottom of the microcentifuge tube was denatured in boiling water for 2 min and then added directly to the hybridization solution (pre-equilibrated at 65 °C) bathing the membrane (2.2.7.6).

2.2.7.6 Hybridisation and Washing of DNA Blots

Reagents:

- Church hybridisation solution: 0.25 M $Na_2HPO_4.H_2O$ (pH 7.2), 7 % (w/v) SDS, 1 % (w/v) BSA fraction V, 1 mM EDTA (pH 8).
- Hybridisation wash solution: 20 mM $Na_2HPO_4.H_2O$ (pH 7.2), 5 % (w/v) SDS, 0.5 % (w/v) BSA fraction V, 1 mM EDTA (pH 8).
- 20 x SSPE: 0.2 M NaH_2PO_4 (pH 6.5), 3.6 M NaCl, 20 mM EDTA
- 2 x SSPE: 2 x SSPE (pH 6.5), 0.1 % (w/v) SDS
- 1 x SSPE: 1 x SSPE (pH 6.5), 0.1 % (w/v) SDS
- 0.2 x SSPE: 0.2 x SSPE (pH 6.5), 0.1 % (w/v) SDS
- 0.1 x SSPE: 0.1 x SSPE (pH 6.5), 0.1 % (w/v) SDS

The method used for labelling and washing of Hybond-N^+ membranes was based on that of Church and Gilbert (1984). The membrane was rolled up, nucleic acid facing inwards, and placed in a Hybaid™ screw top glass tube (Hybaid Ltd., Teddington, Middlesex, UK) containing 25 mL of Church hybridization solution, and pre-incubated in a rotary oven at 65 °C for 1 to 3 h. The denatured labelled DNA probe (section 2.2.7.5) was added to the hybridization solution and the membrane was incubated at 65 °C overnight. A series of washes were then undertaken, each at 65 °C. In the first, 100 mL of hybridization wash solution was used to wash the membrane for 20 min. This was followed by a 20 min wash in 2 x SSPE, a 20 min wash in 1 x SSPE, a 20 min wash in 0.2 x SSPE, and a final wash for 1 h in 0.1 x SSPE. The membrane was then wrapped in clingfilm and the presence of radioactivity determined using either of two methods. For the first, the membrane was placed onto a FujiFilm BAB cassette, nucleic acid facing up, and covered with a FujiFilm Imaging Plate (coated with accelerated phosphorescent fluorescent material), and the imaging plate analysed using a FujiFilm Fluoro Image Analyser FLA-5000. For the second, the membrane was placed in a cassette with an X-omatic intensifying screen and a Kodak Xar-6 X-ray film, left at room temperature for a few hours or -80 °C for days/weeks and developed in an automatic X-ray film processor (100PlusTM, All-Pro Image, Hicksville, NY, USA).

2.2.7.7 Stripping Southern Blots

Reagents:

- Stripping solution: 0.1 x SSPE, 0.1 % (w/v) SDS
- 0.1 x SSPE

Nylon membranes were stripped according to the method of Memelink *et al.*, (1994). Stripping solution was boiled for *ca.* 5 min and the solution poured onto the membrane and allowed to cool to room temperature. After discarding the solution, the procedure was repeated at least 4 times until the radioactive counts were low. The membrane was finally rinsed with 0.1 x SSPE to remove the SDS, sealed in a plastic bag and stored at 4 °C, until rehybridisation (section 2.2.7.6).

2.3 Expression, Purification, Analysis of Enzyme Activity and Protein Accumulation

cDNA ligated into the pGEX-6P-3 Vector or into the pPRoEX-1 Vector (section 2.2.4.5) and transformed into *E. coli* strain DH5α or BL-21 (section 2.2.4.6) were used in this study.

2.3.1 Preliminary Induction of Recombinant Proteins

Reagents:

- Luria-Bertani broth (section 2.2.1.1)
- Isopropyl-β-$_D$-thiogalactopyranoside (IPTG)
- Ampicillin (100 mg mL^{-1})
- SDS-PAGE gel loading buffer (2x): 100 mM Tris-HCl, pH 6.8; 20 % (v/v) glycerol; 5 % (v/v) SDS; 0.01 % (w/v) bromophenol blue.

The ability of *E. coli* transformed with an expression vector to transcribe RNA from the cDNA insert upon treatment with IPTG, and to translate the protein of interest, needed initially to be tested on a small scale.

A single colony of *E. coli* transformed with expresson vector containing the cDNA insert of interest was grown in LB broth (10 mL) and ampicillin (100 μg mL^{-1}) overnight at 37 °C with shaking (200 rpm). An aliquot of this overnight broth (0.5 mL) was then used to inoculate fresh LB/Amp^{100} broth (10 mL) and the culture incubated at 37 °C (200 rpm) until the optical density at 590 nm reached 0.5 -1.0 (about 3 h). To over-induce the expression of the foreign protein IPTG was added to a final concentration of 0.6 mM and the broth incubated (together with an un-induced control) at 37 °C for a further 3 to 5 h, during which time 1 mL samples were removed each hour from both cultures and kept on ice. At the conclusion of the sampling period the bacterial cells were collected by centrifugation at 20 800 x *g* for 30 s only, resuspended in 2 x SDS-PAGE gel loading buffer (60 μL), boiled for 4 min, centrifuged again for 3 min and loaded into a well of an SDS-PAGE gel (section 2.3.10). Usually 8 μL of sample supernatant was loaded. Following electrophoresis, the proteins in the gel were stained with coomassie brilliant blue (section 2.3.10.3) and the protein profiles examined at each time point for induction of the protein of the predicted mass.

2.3.2 Large Scale Induction of Recombinant Proteins

Reagents:

- Luria-Bertani broth (section 2.2.1.1)
- Isopropyl-β-$_D$-thiogalactopyranoside (IPTG)
- Ampicillin (100 mg mL^{-1})

From an overnight bacterial culture grown from a single colony (refer section 2.3.1), a 100 μl aliquot was used to inoculate fresh LB broth (100 mL), containing Amp^{100} (100 μg mL^{-1}), and incubated overnight at 37 °C (180 rpm). Fresh LB broths (4 x 500 mL), containing Amp^{100}

(100 μg mL^{-1}) were then inoculated with 20 mL aliquots of overnight broth (100 mL), and incubated at 37 °C (180 rpm) until $A_{590\ nm}$ = 0.5 -1.0 was reached (approximately 5 h). After this time the temperature was reduced to 18 to 20 °C, IPTG was added to a final concentration of 0.6 mM and the bacterial culture was incubated for a further 24 h at 180 rpm (Shih *et al.*, 2005).

The cells were then collected by centrifugation (Sorvall RC5-C, DuPont; rotor GS3) at 3 000 x *g* for 20 min at 4 °C, the supernatant removed and the cells resuspended in an appropriate buffer solution (refer section 2.3.3 for pGEX; or section 2.3.4 for pProEX-1), or kept at -80 °C.

Recombinant proteins were expressed at an incubation temperature of 18 to 20 °C as the result of a small scale expression study using various incubation temperatures (19 °C, 25 °C and 37 °C) indicated the recombinant proteins began to accumulate as membrane bound inclusion bodies at 25 °C, and most of the recombinant protein was in the pellet at incubation 37 °C and very little remained in the supernatant (data not shown). Many eukaryotic proteins, when expressed in bacteria, accumulate as insoluble inclusion bodies inside the cell (Marston, 1986; Rudolph and Lilie, 1996). The formation of inclusion bodies in *E. coli* can be a problem as the induced protein within the inclusion bodies is often inactive. It has been shown that lowering the incubation temperature increased the yield of correctly folded soluble protein (Schein and Noteborn, 1988; Zhang *et al.*, 1995; Xu *et al.*, 1998; Lay *et al.*, 1996; Thrower *et al.*, 2001). The extraction of protein from inclusion bodies is usually time consuming, difficult and the proteins are often denatured in the extraction process or as a result of their accumulation in the inclusion bodies.

2.3.3 Isolation of Glutathione-S-Transferase (GST) Fusion Proteins

Reagents:

- Glutathione Sepharose™ 4B (Amersham Pharmacia)
- 2 U μL^{-1} PreScission™ Protease (Amersham Pharmacia)
- Tris
- NaCl
- EDTA
- DTT
- Ascorbic acid
- Glycerol
- Modified cleavage buffer: 50 mM Tris-HCl, 100 mM NaCl, 1 mM EDTA, 1 mM DTT, 20 mM ascorbic acid, 10 % (v/v) glycerol (pH 7): stored at 4 °C for maximum of four days.

Cells of *E. coli* collected by centrifugation at 3 000 x *g* for 20 min at 4 °C (section 2.3.2), were resuspended in 30 mL of (ice-cold) modified cleavage buffer, transferred to 50 mL sterile centrifuge tubes and then the bacteria were lysed using either a French Press (Wabash Instruments, Ennerpac hydraulics) to 7 Kpsi and repeated three times, or a model Z Plus 1.1 KW Cell Disrupter (Constant Systems Ltd., Northants, UK) at 30 Kpsi (once), or by using a Virsonic digital 475 Ultrasonic cell disrupter (The VirTis Company), fitted with a 3 mm diameter probe and used at an amplitude of 14 microns (45 s on, 45 s off, repeated 6 times; with the suspension kept cooled on ice during sonication). After disruption of the cells, the debris was removed by centrifugation at 12 000 x *g* for 20 min at 4 °C (Sorvall RC5-B; rotor SS34) and the lysate used immediately.

To prepare the Glutathione Sepharose 4B (GS-4B) slurry, an aliquot of 1.33 mL was transferred to a 50 mL sterile centrifuge tube, and after centrifugation (Sorvall RT7 tabletop centrifuge; RTH 750 rotors) at 500 x *g* for 5 min, the excess ethanol was removed. The GS-4B was then resuspended in ice-cold modified cleavage buffer (12 mL) and collected by centrifugation at 500 x *g*. This step was repeated twice more and following the third wash, the GS4B was resuspended in 1 mL of modified cleavage buffer and used immediately or stored at 4 °C briefly.

The prepared GS-4B slurry was added to the cell lysate and incubated for 30 min at room temperature with gentle mixing in a rotating incubator. The glutathione S- transferase fusion protein bound to GS-4B was then collected by centrifugation at 500 x *g* for 5 min and the supernatant decanted. The resin was then washed three times with modified cleavage buffer (12 mL) with centrifugation for 5 min at 500 x *g* for 5 min. After the third wash, as much supernatant as possible was removed, 1 mL of cold modified cleavage buffer was added, the resin carefully resuspended and the contents transferred to an Eppendorf tube where 8 U of PreScission Protease was added and gently mixed. For 16 h the contents were incubated at 4 °C with slow end-over-end mixing, before centrifugation at 500 x *g* for 5 min to separate the cleaved fusion protein from the GS-4B. The supernatant containing the fusion protein was then removed and put into a new Eppendorf labelled First Eluant. A further 400 µL of modified cleavage buffer was then added to the GS-4B slurry and the resuspended GS-4B incubated at 4 °C with slow end-over-end mixing for 4 h, after which time any remaining cleaved fusion protein was separated from the GS-4B by centrifugation at 500 x *g* for 5 min. The supernatant from this 4 h incubation was then removed and put into a new Eppendorf labelled Second Eluant. The protein concentration in each eluant was determined by the Bradford protein assay (section 2.3.7), and the purity of the protein assessed by SDS-PAGE (section 2.3.10). The elutions were stored at -20 °C until required.

2.3.4 Purification of His-Tagged Proteins by Metal Chelate Affinity Chromatography

Reagents:

- Ni-NTA resin (Life Technologies)

Table 2.2: Buffers A, B and C used in Metal Chelate Affinity Chromatograph

		Concentration (mM)	
Components	**Lysis buffer (A)**	**Wash buffer (B)**	**Elution buffer (C)**
NaH_2PO_4 (pH 8.5)	50	50	50
NaCl	300	300	300
Imidazole	10	20	250
Glycerol	10 % (v/v)	10 % (v/v)	10 % (v/v)

The induced *E .coli* cells prepared in section 2.3.2 were resuspended in lysis buffer A and after cell disruption (section 2.3.3) the debris was removed by centrifugation at 12 000 x *g* for 20 min at 4 °C (Sorvall RC5-C; rotor SS34). Nickel nitrilotriacetic acid resin (Ni-NTA) chelates histidine residues and hence the His-tagged recombinant protein present in the supernatant was purified away from the bacterial protein contaminants by metal-chelate affinity chromatography.

Ni-NTA with a bed volume of 1.5 mL, was housed in a 10 mL disposable syringe barrel (Becton Dickensen) fitted with two layers of GF-A glass microfibre filter paper (Whatman) to prevent leakage of the column matrix. Prior to adding the sample, the column was pre-equilibrated with 8 to 10 volumes of Buffer A at a flow rate of 0.5 mL min^{-1}. The supernatant obtained above was gently loaded onto the column, allowed to run in, the column washed with ten volumes of Buffer A, two volumes of Buffer B, and the fusion protein eluted with ten volumes of Buffer C. The eluate was collected in 0.5 to 1 mL fractions and aliquots of each fraction analysed by SDS-PAGE (section 2.3.10) and the protein quantified (section 2.3.7) to determine which fractions contained the fusion protein. These fractions were then combined.

2.3.4.1 Cleaning of Nickel Nitrilotriacetic Acid (Ni-NTA) Resin

Ni-NTA resin was cleaned immediately after use and only reused for chelating identical recombinant isoforms. The procedures are recommended by Qiagen, based on the experiments of Hoffman-La Roche Ltd., (Basel, Switzerland).

Reagents:

- SDS
- EDTA
- ethanol
- sodium azide
- wash buffer: 0.2 M acetic acid containing 30 % (v/v) glycerol
- regeneration buffer: 6 M guanidine-HCl, 0.2 M acetic acid
- recharging buffer: 100 mM nickel sulphate ($NiSO_4$)

After each run the column was rinsed using 5 bed volumes of wash buffer followed by 3 volumes of 30 % (v/v) ethanol and then stored at 4 °C.

Following five runs the Ni-NTA was regenerated as follows: 2 column volumes of regeneration buffer, 2 column volumes of water, 3 column volumes of 2 % (w/v) SDS, 1 column volume of 25 % (v/v) ethanol, 1 column volume of 50 % (v/v) ethanol, 1 column volume of 75 % (v/v) ethanol, 5 column volumes of 100 % (v/v) ethanol, 1 column volume of 75 % (v/v) ethanol, 1 column volume of 50 % (v/v) ethanol, 1 column volume of 25 % (v/v) ethanol, 5 column volumes of water, 5 column volumes of 100 mM EDTA (pH 8), 5 column volumes of water, 2 column volumes of 100 mM $NiSO_4$ and finally, 5 column volumes of water. The Ni-NTA was then either equilibrated with 2 column volumes of Lysis Buffer A (section 2.3.4) for immediate use, or stored in 30 % (v/v) ethanol at 4 °C. If the column was to be stored for more than 1 to 2 days 0.02 % (w/v) sodium azide was included in the wash buffer (3 column volumes) and stored at 4 °C.

2.3.4.2 Cleavage of the Histidine Tag (His-Tag) from the Fusion Protein Using Tobacco Etch Virus (TEV) Protease

Removal of the affinity tag from recombinant protein was based on concern about the possible interference the His tag fusion protein expressed using the pPRoEX-1 Vector (Figure 2.4), may have on the activity of ACO. Although according to the manufacturers, the extra amino acids on the N-terminal do not affect enzyme activity (Life Technologies Gibco BRL), it seems reasonable to expect ≥ 20 extra residues (six histidine, a spacer region and the TEV protease cleavage site) to have some affect on the folding of the protein and hence enzyme activity. Thus, in some experiments, the N-terminus `His-tag' was removed using TEV protease. The TEV protease digestion assay is based on web page information from Dr DS Waugh, Protein Engineering Section, Macromolecular Crystallography Laboratory, National Cancer Institute at Frederick, MD, USA (Kapust *et al.*, 2002a; Phan *et al.*, 2002).

Reagents:

- TEV (tobacco etch virus) protease (Invitrogen)
- Buffer: 50 mM Tris-HCl, pH 8, 0.5 mM EDTA, 1 mM DTT

The N-terminal Histidine tag (His-tag) was removed by TEV protease in a 1 : 5 ratio, (1 $OD_{280\ nm}$ of TEV protease to 5 $OD_{280\ nm}$ of substrate) made up to a final volume of 140 µL with buffer, and incubated at 4 °C overnight (Nallamsetty *et al.*, 2004).

Since DTT is a strong reducing agent (reduces nickel ions), the buffer was replaced with 50 mM Tris-HCl, (pH 8) using Vivaspin concentrators (section 2.3.5). The cleaved protein was then loaded onto an Ni-NTA column (section 2.3.4) to remove the cleaved His tag, and the TEV protease which also contains a His tag (Kapust *et al.*, 2001). As only three extra amino acids remain on the N-terminal of the TEV cleaved recombinant protein, the protein elutes from the Ni-NTA column leaving the His tags chelated to the nickel.

After protein concentrations were determined (section 2.3.7), the mass of the cleaved protein was compared with the mass of the uncleaved sample, by SDS-PAGE (section 2.3.10), and then the activity of the protein was assessed (sections 2.3.8 and 2.3.9) by comparing the activities of the cleaved His tag recombinant proteins with the His tag fusion proteins.

2.3.4.3 Acetone Precipitation of Recombinant Proteins

If necessary recombinant proteins were concentrated by acetone precipitation prior to examination by western analysis. To do this, 3 volumes of (ice cold) 100 % acetone was added to the protein, mixed well and left at 20 °C for 3 h. After centrifugation at 20 800 x *g* at 4 °C for 15 min, the acetone was removed and the pellet air dried for 5 to 10 min before resuspending in either water prior to reading the optical density at 595 nm, or in SDS loading buffer prior to acrylamide gel electrophoresis.

2.3.5 Sephadex G-25 Gel Filtration Chromatography

Sephadex G-25 was used to exchange the buffer that the His-tagged protein was in (after elution from the NTA-resin) into Buffer A for FPLC. The method is modified from that described by Neal and Florini (1973).

Reagents:

- Sephadex® G-25 resin (Pharmacia Biotech)

- Gel filtration buffer: 25 mM Tris-HCl, pH 7.5; 2 mM DTT; 15 mM sodium ascorbate and 10 μM PA (Buffer A for FPLC)

To prepare the column, two layers of GF-A glass microfibre filter paper were cut into discs and placed at the bottom of a 30 mL disposable syringe barrel (Becton Dickensen). Sephadex G-25 slurry was poured into the syringe barrel and allowed to settle to provide a *ca.* 5 mL bed volume and was then pre-equilibrated with gel filtration buffer. The sample was loaded onto the column taking care not to disrupt the smooth surface of the resin, allowed to sink in, buffer added and the eluate collected in 1 mL fractions at a flow rate of *ca.* 3 mL min^{-1}. Bradfords protein assay (section 2.3.7) was used to determine the fractions which contained protein, and such fractions were pooled.

If necessary proteins were concentrated using Vivaspin concentrators (Vivascience Ltd., Hannover, Germany), with a polyethersulfone membrane and a 10 kDa cut-off. The membranes were pre-conditioned with either de-ionized water or STET buffer (8 % (w/v) Sucrose, 0.5 % (w/v) Triton X-100, 50 mM EDTA, pH 8, 10 mM Tris, pH 8), rinsed with copious amounts of de-ionized sterile water before centrifugation at 3 000 x *g* at *ca.* 4 °C.

Once used, the Sephadex G-25 was immediately placed into a clean beaker, washed with 0.2 M NaOH solution, followed by several rinses with Milli-Q water until the supernatant was pH 7, and then stored at 4 °C.

In order to retain ACO activity, the *E. coli* cells harbouring the recombinant proteins were harvested by centrifugation at 3 000 x *g* for 20 min at 4 °C (section 2.3.2), the cells disrupted (section 2.3.3), metal chelate affinity chromatography (section 2.3.4), and gel filtration chromatography were carried out within the same day and the concentrate stored at -20 °C overnight for further purification the next day.

2.3.6 Fast Protein Liquid Chromatography (FPLC)

All buffer solutions for FPLC were filtered through a 0.22 M hydrophilic polypropylene membrane filter (Gelman Sciences, Ann Arbor, MI, USA) immediately before use. Protein samples were centrifuged at 10 000 x *g* for 20 min at 4 °C prior to being loaded on to the column.

2.3.6.1 Anion Exchange Chromatography

Ion exchange chromatography separates proteins by exploiting the different net charges on proteins at a given pH, due mainly to the side chains of acidic and basic amino acids on the surface of the protein. Thus, the overall net charge distributed on the protein surface dictates the unique behaviour of a protein in an ion exchange environment. The functional groups on the matrix carry either positive (anion exchanger) or negative charges (cation exchanger) and interact with proteins principally by electrostatic attractions. These interactions depend not only on the net charge of the protein but also on the ionic strength and pH of the buffer ions, the nature of these ions, and properties of the functional ligands (Scopes, 1994). Stationary phase matrices carrying charged groups that retain their charge over a narrow pH range are regarded as weak ion exchangers, whereas those stable over a wide pH range are considered strong exchangers. Separation of proteins is achieved by their difference in equilibrium distribution between a buffered mobile phase and a stationary phase consisting of a matrix to which charged inorganic groups are attached (Roe, 1989). The bound proteins are generally eluted from the ion exchange column by increasing the buffer ionic strength (with a salt gradient). For Mono-Q beads, each quaternary amino group attached to the matrix has a single positive charge on a nitrogen atom.

Reagents:

- Buffer A: 25 mM Tris-HCl, pH 7.5; 2 mM DTT; 15 mM sodium ascorbate; 10 μM PA
- Buffer B: 1 M Na Cl; 25 mM Tris-HCl, pH 7.5; 2 mM DTT; 15 mM sodium ascorbate, 10 μM PA

The Mono-Q prepacked HR 5/5 strong anion column (Amersham/Pharmacia Biotech) was equilibrated with at least 5 volumes of buffer A at a flow rate of 0.25 mL min^{-1}. Samples were loaded onto the column, and proteins were eluted within an linear salt gradient of 100 % buffer A : 0 % buffer B to 0 % buffer A : 100 % buffer B, representing salt concentration change from 0 to 1 M NaCl, over 60 min. Fractions of 0.25 mL were collected automatically, kept on ice and assayed for protein content (section 2.3.7). The purity of recombinant ACO was assessed by SDS-PAGE (2.3.10) and western analysis (section 2.3.11). Enzyme activity was assessed (section 2.3.8 and 2.3.9) and active fractions stored at -20 °C.

2.3.6.2 Column Cleaning

The Mono-Q column was cleaned by carrying out the following steps in sequence with a reversed flow rate of 0.25 mL min^{-1}: (1) 4 mL of 1 M NaOH solution injected and then rinsed with filtered mill-Q water; (2) 4 mL of 1 M HCl solution injected and then rinsed with filtered

Mill-Q water; (3) 4 mL of 1 M NaCl solution injected and left to run overnight with filtered Mill-Q water. After cleaning the column was equilibrated with at least 10 column volumes of 20 % (v/v) ethanol and stored at room temperature.

2.3.7 The Bradford Protein Assay

Reagents:

- Coomassie Brilliant Blue R-250 concentrate dye preparation (Bio-Rad, Hercules, CA, USA)
- BSA: bovine serum albumin, Fraction V, standard grade (Serva Feinbiochemica, Heidelberg, Germany).

The protein concentration of samples was estimated with a microassay version of Bradford's method (Bradford, 1976) and Zor Selinger (1996) using a commercially available dye from Bio-Rad.

Samples containing the protein to be measured were pipetted into 96-well microtitre plates and made up to 160 µL with Milli-Q water. Bio-Rad reagent (40 µL) was then added to each sample and mixed by drawing the mixture up and down in the pipette tip. The mixtures were incubated for 10 min at room temperature, and then the absorbance values of the samples read at 595 nm using an AnthosHT II plate reader (Anthos Labtech Instruments).

A protein standard curve was constructed in triplicate using a 1 µg mL^{-1} BSA solution to determine the protein concentration of sample solutions. The samples used for protein estimation had absorbance readings in the linear region of the BSA curve (containing between 0.5 and 6.5 µg protein per 200 µL reaction). An equation was derived from the linear portion of the BSA curve and used to determine the protein concentration in the samples from their optical density values.

$$\mu g\,(\text{protein in sample}) = (OD_{595\,nm} \times 8.95) - 2.57$$

Since the equation to determine the protein concentration may vary with each batch of the Bio-Rad protein dye, as the dye concentration may be slightly different from batch to batch, a new standard curve was constructed for each batch of the dye.

2.3.8 ACC Oxidase Assay

ACO activity was measured essentially according to the method described by Ververidis and John (1991). The assay measures the enzyme activity by quantifying ethylene produced from

the substrate ACC in the presence of co-substrate sodium ascorbate and the co-factors $NaHCO_3$ and $FeSO_4$, with DTT to protect the sulfhydryl group from oxidation.

Reagents:

- ACC
- DTT
- Glycerol
- Ferrous Sulphate ($FeSO_4.7H_20$)
- Sodium ascorbate
- Sodium bicarbonate ($NaHCO_3$)
- Tri-potassium orthophosphate ($K_3PO_4.H_20$)
- Phosphoric acid (H_3PO_4)
- 100 mM phosphate buffer ($K_3PO_4.H_20$ - H_3PO_4) pH 7.5, containing 20 % (v/v) glycerol

The standard reaction mixture was made up just prior to the assay to a final concentration of 50 mM phosphate buffer (pH 7.5) containing 10% v/v glycerol, 1 mM ACC, 2 mM DTT, 30 mM sodium ascorbate (made fresh, pH 5.9 to 6.0), 20 μM $FeSO_4.7H_20$ (freshly made) and 30 mM $NaHCO_3$ (freshly made). Once all the components of the reaction mixture had been added the pH was re-adjusted if necessary. Each ACO enzyme preparation was incubated at 30 ºC for 1 min. To start the reaction, triplicate 0.2 mL enzyme samples were pipetted into 4.5 mL capacity vacutainer tubes (Becton Dickinson) containing reaction mixture (0.8 mL) pre-equilibrated at 30 ºC. The vacutainer tubes were then sealed and the reactions incubated with shaking at 180 rpm for 20 min at 30 ºC. After this time, 1 mL gas samples were removed, and the syringe needle tips were embedded in rubber to contain the evolved ethylene sample until the ethylene content was determined using gas chromatography (section 2.3.9.1).

2.3.8.1 Determination of pH Optimum

For the determination of the pH optimum, different aliquots of the standard 100 mM phosphate activity buffer containing 20 % (v/v) glycerol (section 2.3.8) were adjusted to the appropriate pH with phosphoric acid. The pH of each solution was again checked once all components of the standard reaction mixture (50 mM phosphate buffer, 10 % glycerol) had been added and adjusted if necessary. All buffers were stored at 4 ºC and the pH checked prior to being used. The enzyme activity of each isoform over the pH range was assayed as described in section 2.3.9.

2.3.8.2 Optimal Requirements for Co-Substrate and Co-Factors

The optimal requirements of each isoform for co-substrate and cofactors were determined at their optimal pHs and saturating ACC concentrations. The different concentrations used in this study for sodium ascorbate were in the range from zero to 40 mM; for $FeSO_4.7H_20$ the range varied from zero to 40 μM; and for $NaHCO_3$ the range was from zero to 60 mM. The various concentrations of sodium ascorbate, sodium bicarbonate and iron sulphate were substituted as appropriate in the ACO activity assay (section 2.3.8).

2.3.8.3 Determination of K_m, V_{max} and K_{cat}

The apparent K_m and V_{max} values of each of the ACO isoforms for their substrate, was determined by triplicate measurements of initial velocity at different ACC concentrations. The initial velocity data against ACC concentrations was graphed using the computer software programmes Microsoft Excel version 2000 (Microsoft, USA), ENZYPLOT (Walker,1997) and ENZFITTER version 2.0 (BioSoft, Cambridge, UK). The saturating ACC concentration for each isoform was determined from the graphs. Line-weaver Burk plots (Lineweaver and Burk, 1934) were used to fit the data in a defined concentration range to a straight line and K_m and V_{max} values were determined from the regression equation. The range of ACC concentrations used were determined from preliminary experiments in which different ranges of concentrations of ACC were tried. In this study, the concentrations of ACC were 0.00, 0.05, 0.1, 0.25, 0.5, 1.0, 3.0, 6.0, 10 mM. In preliminary experiments, the ACC concentrations gave a very low ACO activity for MD-ACO2 and so ACC concentrations of 15, 20 and 30 mM were tried. The activity assay was performed at the optimal pH for each isoform as described previously. The K_{cat} was determined from the equation: product (mol s^{-1}) / enzyme (mol).

2.3.8.4 Determination of Thermal Stability

To assess the thermal stability of each isoform, aliquots of each recombinant protein (1.5 mL) were put into Eppendorf tubes in triplicate and incubated at either 25 °C, 35 °C or 45 °C. Aliquots (150 μL) were taken out after 10 min, 20 min, 30 min, 60 min 90 min 120 min and 180 min and were added to the (pre-heated 30 °C) reaction mixture (section 2.3.8), the vacutainer tubes sealed and the reactions incubated and sampled as described in section 2.3.9. Aliquots of each enzyme were incubated for 1 min at 30 °C and used as the standard, each representing 100 % activity, against which the activity of the other samples were compared.

2.3.9 Ethylene Analysis

2.3.9.1 Measurement of Ethylene Using Gas Chromatography

The concentration of ethylene in gas samples was measured using a Gas Chromatograph, Model GC-8A (Shimadzu Corp., Kyoto, Japan) fitted with a flame ionization detector. The 2.5 m x 3 mm (I.D.) glass column prepacked with Porapak-Q with a mesh size of 80/100 (Alltech Associates Inc., Deerfield, Il., USA) was used for the ethylene analysis. The carrier gas was nitrogen with a flow rate of 50 mL min^{-1}. The flame as maintained by hydrogen and air at 60 kPa and 50 kPa respectively. The column was initially conditioned at 200 °C with a nitrogen carrier gas at 150 kPa, and thereafter for approximately 0.5 to 1 h before use. For measurement of samples, the oven and the injector/detector temperatures were set at 85 °C and 150 °C respectively.

A 1 mL standard calibration gas of 0.101 ppm ethylene in nitrogen (BOC Gases NZ Ltd.) was used for ethylene quantification. One mL of sample gas was injected several times onto the column and the peak retention time for ethylene was observed to be between 74 and 80 s.

2.3.9.2 Measurement of Ethylene Production in Plant Tissues

Detached intact apple leaves were weighed and then placed into 7 mL capacity glass universal bottles, the bottles were then sealed with suba-seal stoppers (Gallenkamp) and incubated at 30 °C for 20 min, after which time gas samples of 1 mL were removed. After each sampling, the evolved ethylene samples were contained in the syringe by forcing the syringe needles into a hard rubber block until measurement by gas chromatography.

2.3.9.3 Ethylene Calculations

The concentration of ethylene gas produced is expressed in nmol min^{-1} mg^{-1} for recombinant protein and for the intact apple leaves ethylene is expressed in nL g^{-1} FW h^{-1}. The concentration of ethylene in ppm was calculated by measuring the height of each sample ethylene peak (generated by the chart recorder) and comparing this measurement to the height of the ethylene peak generated with the 0.101 ppm standard gas. The number of moles the sample peaks represented could then be determined by calculating the number of moles of gas in the vacutainer tube (using the ideal gas equation) and multiplying this by the concentration of ethylene in ppm.

$$n = (PV/RT) \times ppm \times 10^{-6}$$

The Ideal Gas Equation

n	=	total number of moles of gas in the vessel
P	=	pressure (101,325 kPa)
V	=	volume (m^3)
R	=	universal gas constant, 8.314 J K^{-1} mol^{-1}
T	=	temperature (298.15 K)

Since 1 mole of ethylene occupies 22.4 L at standard temperature and pressure, multiplying by 22.4 gives the amount of ethylene in L.

2.3.10 Sodium Dodecyl Sulphate-Polyacrylamide Gel Electrophoresis (SDS-PAGE)

SDS-PAGE separates proteins electrophoretically through a polyacrylamide gel on the basis of molecular mass, and was originally described by Laemmli (1970).

2.3.10.1 Preparing and Running Linear (12 %) SDS-PAGE

Reagents:

- 40 % (w/v) acrylamide-bis stock solution (Bio-Rad)
- 2 x resolving (separating) gel buffer: 0.75 M Tris-HCl, pH 8.8; 0.2 % (w/v) SDS
- 2 x stacking gel buffer: 0.25 M Tris-HCl, pH 6.8; 0.2 % (w/v) SDS
- 2 x SDS gel loading buffer: 24 mM Tris-HCl, pH 6.8; 20 % (v/v) glycerol; 5 % (w/v) SDS; 5 % (v/v) 2-mercaptoethanol and 0.04 % (w/v) bromophenol blue (stored -20 °C)
- 5 x SDS running buffer: 0.125 M Tris, 1 M glycine, 0.5 % (w/v) SDS, pH *ca.* 8.3
- ammonium persulphate (APS) (Univar, Auburn, NSW, Australia)
- N,N,N',N-Tetramethylethylenediamine (TEMED; Reidel-de haen ag seelze)
- Prestained molecular markers, [low range (*ca.* 20.7 to 111 kDa)]: Phosphorylase B, Bovine serum albumin, Ovalbumin, Carbonic anhydrase, Soybean trypsin inhibitor and Lysozyme (Bio-Rad)

Table 2.3: Separating and Stacking Gels used for SDS-PAGE with the mini-protean® II cell (Bio-Rad)

Order of addition	Reagents	Separating gel (mL)	Stacking gel (mL)
1	**40 % (w/v) acrylamide-bis stock**	**3**	**1**
2	**2 x separating gel buffer**	**5**	**-**
2	**2 x stacking gel buffer**	**-**	**5**
3	**Mill-Q water**	**2**	**4**
4	**10 % (w/v) APS**	**0.1**	**0.1**
5	**TEMED**	**0.01**	**0.01**

The separating (resolving) gel solution (12 %) was pipetted between two glass plates until the level reached *ca.* 2.5 cm below the top of the shortest plate. An overlay of Milli-Q water was pipetted onto the separating gel to prevent atmospheric oxidation. When the separating gel had polymerised (*ca.* 30 min), the layer of Milli-Q water was discarded and the separating-stacking gel interface rinsed twice with stacking gel, the complete 4 % stacking gel solution was then pipetted onto the separating gel and the well-forming combs inserted. After about 30 min, the stacking gel had polymerised and the prepared gels were placed into the mini-protean® II cell (Bio-Rad) apparatus. Running buffer was poured into the electrophoretic tank (*ca.* 800 mL), submersing the gels, and the combs were removed carefully from the stacking gel. Protein samples were prepared by mixing the appropriate sample amount with an equal volume of 2 x SDS gel loading buffer and placing into a boiling water-bath for 3 min. The solution was then centrifuged (12 000 x *g* for 1 min at room temperature) and the supernatants pipetted into the wells of the prepared gels. The loading wells have a capacity of 40 μL with the best resolution in samples that contained between 2 and 10 μg of protein. An aliquot (8 μL) of prestained molecular markers [low range (*ca.* 19.2 to 116 kDa)] were loaded in at least one well per gel. The gels were run until the dye front had eluted from the bottom of the gel. When examining protein above 20 kDa, the gel was run until the lowest molecular weight marker (*ca.* 20 kDa) had reached the bottom of the gel, giving a greater separation between the heavier proteins. All mini-gels were run at a constant 200 V. Following electrophoresis, the gels were either stained with coomassie brilliant blue (section 2.3.10.3) or transferred to a membrane (section 2.3.11.2).

2.3.10.2 Preparing and Running Gradient (10 %-20 %) SDS-PAGE

Reagents:

- Sucrose
- 2 x stacking gel buffer: 0.25 M Tris-HCl, pH 6.8; 0.2% (w/v) SDS

Table 2.4: Separating and stacking gels used to make a 10 to 20 % linear gradient gel of acrylamide for SDS-PAGE

Reagents	Resolving Gel Heavy Solution (mL) **20 %**	Resolving Gel Light Solution (mL) **10 %**	Stacking Gel (mL)
1. **Sucrose**	**3 g**	-	-
2. **Milli-Q water**	**3.5**	**10**	**8**
3. **4 x resolving gel buffer**	**5**	**5**	-
4. **2 x stacking gel buffer**	-	-	**10**
5. **40 % (w/v) acrylamide**	**10**	**5**	**2**
6. **10 % (v/v) ASP**	**0.1**	**0.1**	**0.2**
7. **TEMED**	**0.01**	**0.01**	**0.02**

A 10 to 20 % linear gradient gel of acrylamide was prepared by mixing two solutions containing different concentrations of acrylamide, (designated heavy and light; Table 2.4), in a Hoefer SG100 gradient maker (Hoefer Scientific Instruments, San Francisco, CA, USA) and pumping the mixture using a 2120 Varioperpex®II peristalsis pump (LKB Vertriebs Ges.m.b.H., Vienna, Austria) in between two sealed glass plates (16.5 x 22 cm). After the separating gel was poured to *ca.* 20 mm below the top of the smaller glass plate, a layer of Milli-Q water was pipetted onto the surface of the gel and the gel left to polymerise overnight at 4 ºC or for 90 min at room temperature. After this time, the water was discarded, the separating gel rinsed briefly with stacking buffer, the stacking gel solution pipetted onto the separating gel, the well-forming comb inserted and the stacking gel allowed to set for *ca.* 30 min. The protein samples were prepared as described in section 2.3.10.1. Electrophoresis was conducted at 100 V through the stacking gel and 200 V through separating gel, and was usually terminated after 6 to 7 h.

2.3.10.3 Coomassie Brilliant Blue (CBB) Staining

Reagents:

- CBB stain solution: 0.1 % (w/v) Coomassie Brilliant Blue R-250, 40 % (v/v) methanol, 10 % (v/v) acetic acid.
- CBB destain solution: 30 % (v/v) ethanol

Following electrophoresis, the separated protein bands were detected by CBB staining. Gels were immersed in CBB stain for 30 min (mini gels) or overnight for larger gels with gentle shaking, followed by destaining until protein bands became visible. The gels were usually photographed or scanned immediately, and then air dried by placing between two sheets of Gel Air Cellophane Support (Bio-Rad) at room temperature.

2.3.11 Western Analysis

2.3.11.1 Production of Primary Polyclonal Antibodies to MD-ACO3

Reagents:

- Freund's adjuvant (complete and incomplete) (Difco Laboratories, Detroit, MI, USA)
- Phosphate Buffered Saline (PBS)

Polyclonal antibodies were raised against the MD-ACO3 fusion protein after purification by affinity chromatography, gel filtration and fast protein liquid chromatography (sections 2.3.4, 2.3.5 and 2.3.6). For the initial inoculation 400 μg of fusion protein (antigen) was made up to 0.6 mL with PBS and then 0.6 mL of complete Freund's was added and vortexed vigorously to form an emulsion. Rabbits (Calif. x NZ white) at the Small Animal Production Unit (SAPU), Massey University, were inoculated with the fusion protein by Debbie Chesterfield. The rabbits were boosted three times at 4 to 5 week intervals with 300 μg of fusion protein made up to 0.6 mL with PBS, and then vortexed with 0.6 mL of incomplete Freund's as described previously.

Blood was collected from the rabbits by ear bleeds performed by Debbie Chesterfield. The collected blood was left at room temperature for 3 h and allowed to clot further at 4 °C overnight. The antisera containing the antibodies was then removed from around the clot and any remaining cells were pelleted by centrifugation at 10 000 x *g* for 10 min and the serum (supernatant) removed to a fresh tube and stored at -20 °C (Hock *et al.*, 1992). The antibodies for MD-ACO1 were already available in the McManus Lab.

2.3.11.2 Electrophoretical Transfer of Proteins from Gel to PVDF Membrane

Reagents:

- Wet transfer buffer: 25 mM Tris, 190 mM glycine (pH 8.3), 10 % (v/v) methanol
- Semi-dry transfer buffer: 48 mM Tris, 39 mM glycine (pH 9.2), 20 % (v/v) methanol

Proteins separated by SDS-PAGE were electrophoretically transferred to Polyvinylidine difluoride membrane (PVDF; Perkin Elmer™, Polyscreen® or Immobilin-P) using a Trans-Blot Electrophoretic Transfer Cell (Bio-Rad), by the wet transfer method (Figure 2.8) described by

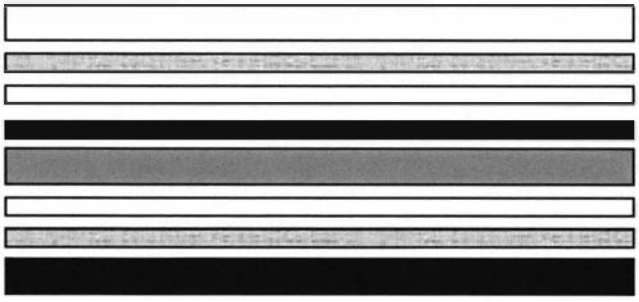
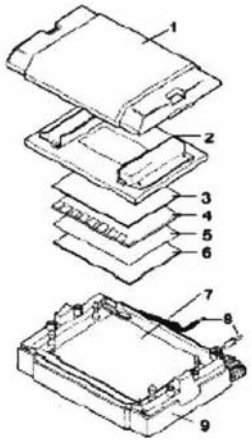


Figure 2.8: Western Blotting Apparatus: Assembly of the Electrophoretic Transfer of Proteins from an Acrylamide Gel to PVDF Membrane.



1. **safety lid**
2. **cathode assembly with latches**
3. **two pieces of Whatman filter paper**
4. **gel**
5. **PVDF membrane**
6. **two pieces of Whatman filter paper**
7. **spring-loaded anode platform, mounted on four guide posts**
8. **power cables**
9. **base**

Figure 2.9: BioRad Semi-Dry Trans-Blot Cell

Towbin *et al.*, (1979) with some modifications, or using a Semi-Dry Trans-blot®SD Electrophoretic Transfer Cell (Bio-Rad) by the method (Figure 2.9) described by Bjerrum and Schafer-Nielsen, (1986).

For the wet transfer, the cassette holder with the gel and membrane was assembled as shown in Figure 2.8. The cassette was set up while partially immersed in transfer buffer so as to exclude air bubbles which can interfere with transfer. The PVDF membrane was soaked for 15 s in 100 % methanol and then 2 min in Milli-Q water and finally 5 min in transfer buffer prior to placing on top of the gel. All wet transfers were run for 45 min at 250 mA constant current.

For the semi-dry transfer, the gel and membrane were set up on the apparatus as shown in Figure 2.9. The protein gel was soaked for 15 min in semi-dry transfer buffer, while the PVDF membrane was soaked for 15 s in 100 % (v/v) methanol, then 2 min in Milli-Q water and finally 5 min in semi-dry transfer buffer. All semi-dry transfers were run for 30 min at 12 V, with a 500 mA limit (5.5 mA cm^{-2} maximum).

2.3.11.3 Immunodetection of Proteins on PVDF Membrane

Reagents:

- Phosphate Buffered Saline: (PBS): 50 mM sodium phosphate, pH 7.4 and 250 mM NaCl
- Phosphate Buffered Saline – Tween (PBS-T): 0.5 % (v/v) Tween-20 in PBS
- Goat anti-rabbit Immunoglobulin G (IgG) conjugated to alkaline phosphatase (Sigma)
- Rabbit anti-MD-ACO (refer section 2.3.11.1)
- Substrate for alkaline phosphatase (light sensitive): 150 mM Tris-HCl, pH 9.7 containing 0.01 % (w/v) 5-bromo-4-chloro-3-indoylphosphate (BCIP), 0.02 % (w/v) *p*-nitro blue tetrazolium chloride (NBT), 1 % (v/v) dimethylsulphoxide (DMSO), 8 mM $MgCl_2$.
- I-Block™ (Tropix, Bedford, MA, USA)

Following electrophorctic transfer, the PVDF membrane was placed into a blocking solution [PBS containing 0.2 % (w/v) I-Block] for either 1 h at room temperature or 4 °C overnight. After this time the blocking solution was discarded and the membrane rinsed briefly with PBS-T. The membrane was then incubated in the primary antibody solution (either 1 in 500 dilution of anti-MD-ACO1 in PBS; or 1 in 10,000 dilution of anti-MD-ACO3 in PBS) for 1 h at 37 °C. Following incubation the antibody solution was tipped off and the membrane washed 3 times (*ca.* 3 min for each wash) with PBS-T (*ca.* 50 mL) at room temperature. The membrane was then incubated for 1 h with the secondary antibody (1 in 10,000 dilution of goat anti-rabbit IgG alkaline phosphatase conjugate) at room temperature. The membrane was then washed (3 x 10 min) with PBS-T and twice with 150 mM Tris-HCl, pH 9.7, to remove the phosphate that could

interfere with the activity of the alkaline phosphatase conjugate (by binding to the active site), (Brenna *et al.*, 1975; Zhang *et al.*, 2004). The membrane was then submerged in the substrate for alkaline phosphatase and, when sufficient colour had developed, the reaction was stopped immediately by discarding the substrate solution and rinsing the membrane several times in RO water. Each incubation step and substrate development was performed on a rocking or shaking platform (*ca.* 100 rpm). After air drying, the membrane was either scanned using a ScanJet IIcx (Hewlett Packard) with DeskScan II software (Hewlett Packard), or photographed digitally with an Alpha Imager™ 2000 Documentation and Analysis System (Alpha Innotech Corporation, San Leandro, CA, USA).

2.3.11.4 Amino Acid Sequencing of N-Terminal Peptide Sequences

Reagents:

- Transfer buffer: 10 mM 3-(cyclohexylamino)-1-propane sulfonic acid (CAPS), pH 11 containing 20 % (v/v) methanol
- PVDF Stain: 0.1 % (w/v) coomassie brilliant blue in 50 % (v/v) methanol
- Destain: 10 % (v/v) acetic acid in 50 % (v/v) methanol

Proteins for N-terminal peptide sequencing were electroblotted onto PVDF membrane following SDS-PAGE (section 2.3.10.1), based on a method by Wong *et al.*, (1993). Electrophoretic transfer of proteins from gel to PVDF membrane was conducted as described for wet transfer (section 2.3.11.2), except the transfer buffer used was 10 mM CAPS (pH 11), containing 20 % (v/v) methanol. Immediately after transfer, the membrane was stained for *ca.*10 s, destained for 3 to 4 min, rinsed thoroughly with RO water and air dried. Samples were then submitted to the Protein Microchemistry Facility, Department of Biochemistry, University of Otago for N-terminal amino acid sequence analysis.

Chapter Three RESULTS

3.1 ACC Oxidase Genes in *Malus domestica* Borkh. (Apple)

3.1.1 Molecular Cloning of Protein-Coding Regions of ACC Oxidase Genes in *Malus domestica* (cultivar: Gala).

In order to identify ACO genes expressed in the leaves of *Malus domestica* cv. Gala, apple bourse shoot leaves were analysed. Newly initiated green leaves, mature fully expanded green leaves and those at the onset of senescence (where measured chlorophyll concentration decreased significantly; data not shown) were selected and total RNA extracted. Reverse transcriptase (RT) was then used to make cDNA from the mRNA using an oligo $d(T)_{15}$ primer. ACO cDNA was amplified by the polymerase chain reaction (PCR) using degenerate oligonucleotide primers known to bind to highly conserved regions within ACO genes. The primer sequences were provided by Professor Shang Fa Yang (University of California, Davis, USA). Nested PCR primers were used to amplify ACO sequences in two rounds of PCR. The first round primers (ACOF1 and ACOR1) generated cDNA from total mRNA, and aliquots of this first round PCR were used as templates for amplification using the second round primers (E101 and E102). The sequence of the primers used in RT-PCR to amplify putative ACO gene sequences are shown as Figure 2.2.

The amplified products after the first round of PCR were unable to be detected after electrophoresis on a 1 % (w/v) agarose gel and ethidium bromide staining (data not shown). However, after two rounds of PCR, amplification products of approximately 850 bp were obtained (Figure 3.1). Total RNA without RT treatment was used as template for the two rounds of PCR to act as a control, and since no *ca.* 850 bp PCR product was amplified (Figure 3.1 lane 1), this indicates that the *ca.* 850 bp band was a genuine RT-PCR product.

The second round *ca.* 850 bp PCR products were recovered from the 1 % (w/v) agarose gel, then cloned into the pGEM®-T Easy Vector (Figure 2.5 and 2.6) and transformed into the *E. coli* strain DH5α. The white colonies from the transformation, which used LB Amp^{100} plates with IPTG and X-Gal, were picked and cultured in LB Amp^{100} broths. Plasmids were isolated (section 2.2.5.1 or 2.2.5.2), and the presence of insert of *ca.* 850 bp was confirmed by restriction enzyme digestion with E*co*RI and with S*al*I followed by agarose gel electrophoresis. Each colony was then allocated a unique identification (JEB #) and the number of colonies with and without inserts is provided as Table 3.1. Fragment of *ca.* 500 bp and 250 bp (not visible)

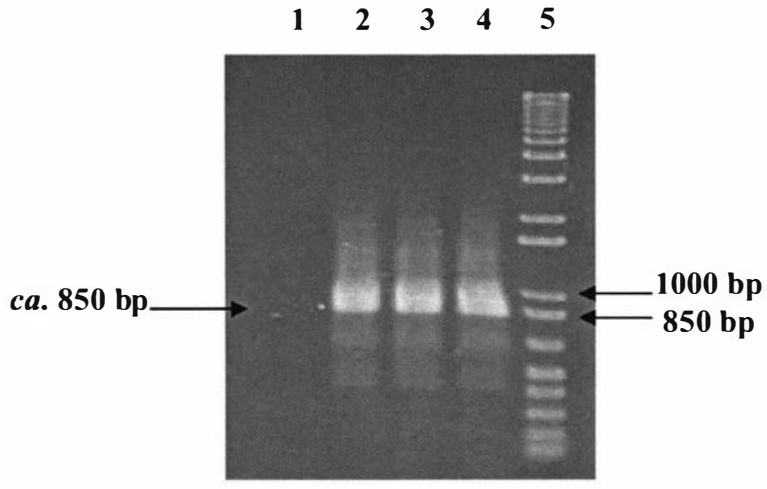


Figure 3.1: PCR Amplification of a Putative ACC Oxidase cDNA using RT-Generated cDNA Templates from Total RNA Isolated from Newly Initiated Green Leaves, Mature Green Leaves and Senescing Leaves.

Nested degenerate primers were used for two rounds of PCR amplification. PCR products were separated on 1 % (w/v) agarose gel and visualized with ethidium bromide.

Lane 1: The control using the same amount of RNA without RT-treatment as a template

Lane 2: The products from the second round PCR (newly initiated green leaves)

Lane 3: The products from the second round PCR (mature green leaves)

Lane 4: The products from the second round PCR (senescing leaves)

Lane 5: 1Kb DNA ladder (Gibco BRL). The molecular weights of two of the standards are indicated on the right of the figure. The approximate size of the amplification product is indicated by an arrow to the left of the figure.

indicated the presence of an E*co*RI restriction site within the *ca.* 850 bp insert of some of the fragments (Figure 3.2). The larger DNA fragment (*ca.* 3015 bp) is the pGEM®-T Easy Vector (Figure 2.5). Although there is only one *Sal*I restriction site in the multiple cloning site (MCS) of the pGEM®-T Easy Vector, since linearized vectors can not be supercoiled and thus run slower / heavier than a circular uncut vector, a *Sal*I restriction digest was included as an added possible indicator of the presence of an insert.

Table 3.1: Distribution of Colonies and Clones Containing ACC Oxidase Inserts From Apple Leaf Tissue.

Source of RNA	***JEB*: colonies**	**Clone (insert)**	**(no insert)**
Initial leaf	12	*JEB*:14,15,16,18,19,20,21,22	*JEB*:11,12,13,17
Fully expanded leaf	7	*JEB*:1,3,4,26,27,28	*JEB*:2
Senescing leaf	9	*JEB*:5,6,8,9,10,23	*JEB*:7,24,25
Total:	28	20	8

Vectors thought to contain an ACO insert after restriction enzyme mapping were isolated for sequencing (section 2.2.5.4) and DNA sequences were determined using an automated sequencer.

3.1.2 Confirmation of Putative ACC Oxidase cDNAs

A total of 20 clones were sequenced, the electrophoretograms (chromatograms) analysed, carefully edited and alignments made using MT Navigator, Sequencher and GCG software programes (section 2.2.6.1). Two different sequences were clearly distinguishable amongst the clones, and these were designated *JEB:α* (*JEB*:1, 3, 4, 8, 10, 18, 19, 20, 21; with an identity of >99 %) and *JEB:β* (*JEB*:5, 6, 9, 14, 15, 16, 22, 23, 26, 27, 28; with an identity of >99 %).

A National Centre or Biotechnology Information (NCBI) nucleotide comparison using the Basic Logical Alignment Search Tool (BLAST) of the Genbank database was carried out against the groups of sequences designated *JEB:α* and *JEB:β* (Table 3.2). A BLAST search against *JEB:α* (Table 3.2A) reveals the first hit to be an ACO from asian pear (*Pyrus pyrifolia*) and the second hit to be apple fruit (*Malus domestica*) ACO mRNA from the cultivar Fuji (Genbank accession AJ001646; Castiglione *et al.*, 1997a). The third hit is an ACO from *Malus sylvestris* from ripe fruit (clone *pAE12* Genbank Accession M81794; the clone *pAE12*, Genbank Accession M81794 is also reported by the same authors Dong *et al.*, 1992 as occurring in the cultivar Golden Delicious, *Malus domestica*), and the fourth hit is also from ripe fruit of Golden Delicious (designated clone *pAP4*, Genbank accession X61390; Ross *et al.*, 1992).

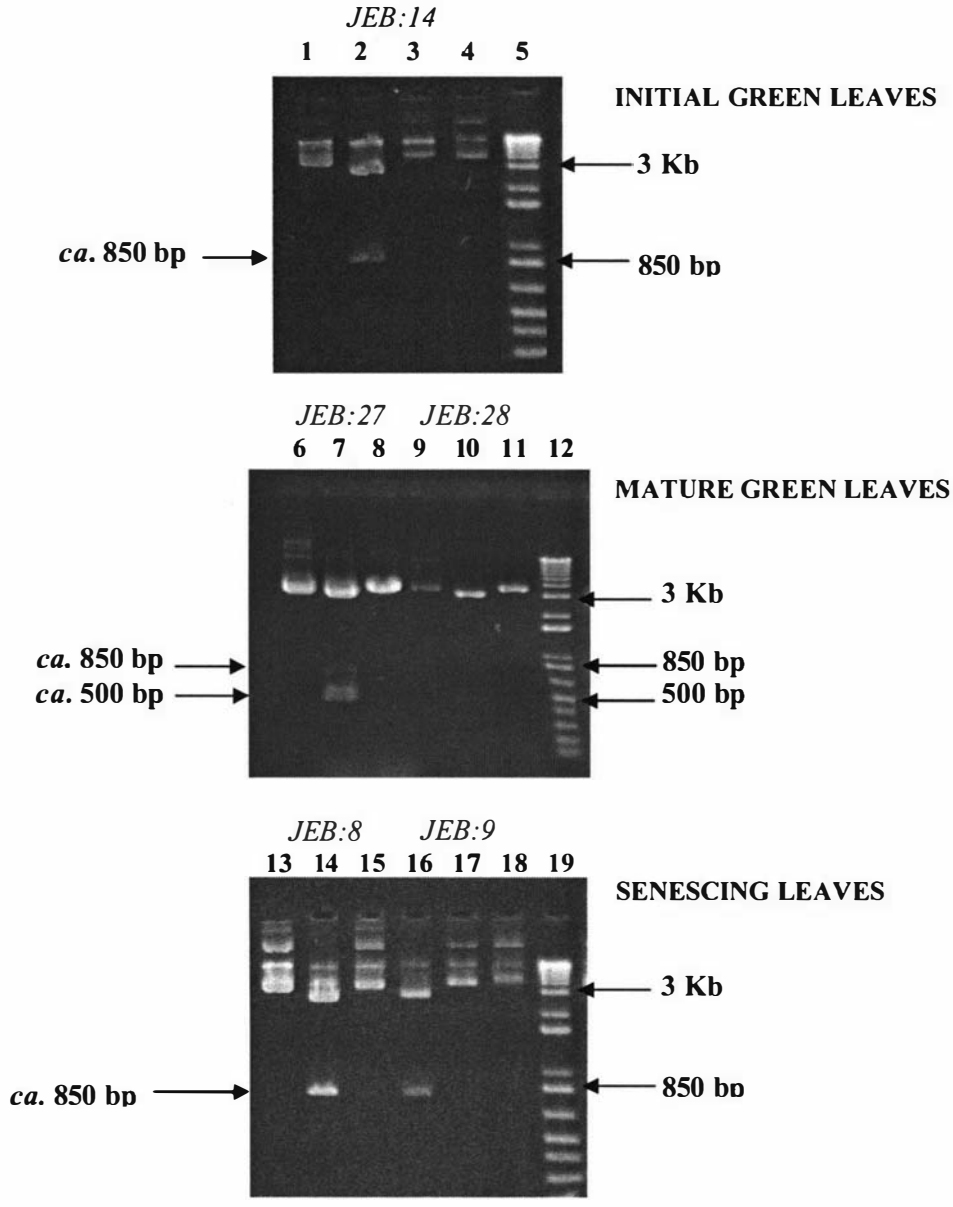


Figure 3.2: Cloning of Putative cDNAs Encoding ACC Oxidase in Newly Initiated Green Leaves, Mature Green Leaves and Senescing Leaves of *Malus domestica* Generated using RT-PCR.

Restriction digest of plasmids isolated from *E .coli* to confirm cloning of the *ca.* 850 bp cDNA fragments. Inserts obtained from *Eco*RI-digestion of plasmids containing putative ACC oxidase sequences were separated on 1 % (w/v) agarose gel and visualized with ethidium bromide.

Lane 1. Uncut/undigested clone *JEB:14*
Lane 2. Clone *JEB:14* digested using *Eco*RI
Lane 3. Clone *JEB:14* digested using *Sal*I
Lane 4. Clone *JEB:14* digested using *Sal*I
Lane 5. 1 Kb Plus DNA Ladder
Lane 6. Uncut/undigested *JEB:27*
Lane 7. Clone *JEB:27* digested using *Eco*RI
Lane 8. Clone *JEB:27* digested using *Sal*I
Lane 9. Uncut/undigested *JEB:28*
Lane 10. Clone *JEB:28* digested using *Eco*RI
Lane 11. Clone *JEB:28* digested using *Sal*I
Lane 12. 1 Kb Plus DNA Ladder
Lane 13. Uncut/undigested *JEB:8*
Lane 14. Clone *JEB:8* digested using *Eco*RI
Lane 15. Clone *JEB:8* digested using *Sal*I
Lane 16. Clone *JEB:9* digested using *Eco*RI
Lane 17. Uncut/undigested *JEB:9*
Lane 18. Clone *JEB:9* digested using *Sal*I
Lane 19.1 Kb Plus DNA Ladder

From this BLAST search, the *JEB:α* sequences closely matched other *Malus domestica* ACO sequences present in the Genbank database.

Other hits against *Malus domestica* include genomic ACO DNA with hit 8 from cv. Fuji (Genbank accession AF015787; Nam and Kim, 1998), hit 10 from cv. Golden Delicious (Genbank accession Y14005; Castiglione *et al.*, 1998), hit 11 from cv. Fuji (Genbank accession X98627; Castiglione *et al.*, 1997b) and hit 12 from cv. Granny Smith (Genbank accession AF030859; recorded in the Genbank as Ross *et al.*, 1998, but actually published in the journal Plant Molecular Biology as Atkinson *et al.*, 1998).

In contrast, a BLAST search against *JEB:β* revealed that the sequence most closely matched *Prunus armeniaca* (apricot), *Prunus mume* (Japanese apricot) and *Prunus persica* (peach) particularly (refer Table 3.2B). *Malus domestica* ACO mRNA occurs eventually as hits 22, 23 and 25 corresponding to Genbank accessions X61390 (Ross *et al.*, 1992), M81794 (Dong *et al.*, 1992) and AJ001646 (Castiglione *et al.*, 1997a) respectively. From this BLAST search the *JEB:β* group of sequences from apple seem not to be present in the NCBI Genbank database.

Table 3.2A: Results of a Nucleotide BLAST Search Against *JEB:α*, 819 bp cDNA Sequence.

Genus, species (and cultivar)	Accession number	Identities	Score (bits)	E Value
Pyrus pyrifolia mRNA	D67038	94 %	1266	0.0
Malus domestica mRNA (Fuji fruit)	**AJ001646**	93 %	1216	0.0
Malus sylvestris mRNA (***pAE12***, Golden D.)	**M81794**	93 %	1208	0.0
Malus domestica mRNA (***pAP4***, Golden D.)	**X61390**	93 %	1208	0.0
Pyrus communis mRNA	X87097	93 %	1172	0.0
Prunus persica PP-ACO2 mRNA	AB044712	87 %	790	0.0
Rosa hybrid cultivar	AF441282	86 %	726	0.0
Malus domestica genomic (Fuji)	**AF015787**	98 %	641	0.0
Prunus persica	AF129074	88 %	581	e-163
Malus domestica genomic (Golden D.)	**Y14005**	95 %	553	e-154
Malus domestica genomic (Fuji)	**X98627**	95 %	553	e-154
Malus domestica genomic (Granny S.)	**AF030859**	95 %	553	e-154
Actinidia deliciosa	M97961	83 %	462	e-127
Actinidia deliciosa mRNA	AB003514	83 %	462	e-127

Searched on 26 August, 2002 (E value; refer section 2.2.6.1)

Table 3.2B: Results of a Nucleotide BLAST Search Against *JEB:β*, 816 bp cDNA Sequence.

Genus, species (and cultivar)	Accession number	Identities	Score (bits)	E Value
Prunus armeniaca	AF026793	90 %	1034	0.0
Prunus mume PM-ACO1	AB031027	89 %	1018	0.0
Prunus persica	AF319166	89 %	1006	0.0
Prunus persica mRNA	X77232	89 %	1006	0.0
Prunus persica PP-ACO1	AB044711	89 %	970	0.0
Fagus sylvatica mRNA	AJ420190	82 %	526	e-146
Populus euramericana	AB033504	82 %	506	e-140
Fagus sylvatica	AJ420189	82 %	502	e-139
Pelargonium hortorum	U67861	82 %	460	e-126
Phaseolus lunatus	AB062359	81 %	448	e-123
Prunus persica	AF129073	91 %	442	e-121
Citrus sinensis	AF321533	81 %	412	e-112
Pelargonium hortorum	U07953	82 %	369	2e-99
Phaseolus vulgaris	AF053354	80 %	369	2e-99
Carica papaya	AY077461	79 %	365	3e-98
Passiflora edulis	AB015493	80 %	359	2e-96
Diospyros Kaki	AB038355	80 %	355	3e-95
Trifolium repens	AF115262	80 %	349	2e-93
Betula pendula mRNA	Y10749	80 %	345	3e-92
Mangifera indica mRNA	AJ297435	83 %	339	2e-90
Carica papaya	U68215	79 %	335	4e-89
***Malus domestica* mRNA (*pAP4*, Golden D.)**	**X61390**	80 %	335	4e-89
***Malus sylvestris* mRNA (*pAE12*, Golden D.)**	**M81794**	80 %	335	4e-89
Trifolium repens	AF115263	79 %	327	9e-87
***Malus domestica* mRNA** (Fuji fruit)	**AJ001646**	80 %	327	9e-87
Diospyros Kaki DK-ACO1 mRNA	AB073008	81 %	325	4e-86
Actinidia deliciosa	M97961	79 %	325	4e-86

Searched on 24 April, 2002 (E value; refer section 2.2.6.1)

Preliminary alignments found that both the mRNA (*pAP4*) from Golden Delicious fruit (Genbank accession number X61390; Ross *et al.*, 1992) and the coding regions of the genomic DNA from Granny Smith fruit (Genbank accession number AF030859; Ross *et al.*, 1998) are identical (designated as Group I). Similarly, the mRNA from Fuji fruit (Genbank accession number AJ001646; Castiglione *et al.*, 1997a) and the coding regions of the genomic DNA from Fuji (Genbank X98627; Castiglione *et al.*, 1997b) are identical (designated group II). However, the coding regions of the genomic DNA from Golden Delicious (Genbank accession Y14005; Castiglione *et al.*, 1998) and the mRNA from Fuji fruit (Genbank accession number AJ001646; Castiglione *et al.*, 1997b) differed by five base-pairs. The the coding regions of genomic DNA from Fuji (Genbank accession AF015787; Nam and Kim, 1998) differed markedly from all of the other sequences (designated Group III).

The consensus nucleotide sequence of *JEB:α* and *JEB:β* were then compared with a sequence from Golden Delicious clones *pAP4* and *pAE12* (Group I) (Genbank accession numbers X61390 and M81794 respectively; Ross *et al.*, 1992; Dong *et al.*, 1992), a sequence from Fuji (Genbank accession number AJ001646; Castiglione *et al.*, 1997a)(Group II), and the coding region of Fuji (Genbank accession number AF015787; Nam and Kim, 1998)(Group III)(Table 3.3).
Alignments using MT Navigator, sequencher and GCG software programes (section 2.2.6.1) are shown as Table 3.3A. Genbank accession numbers X61390 and M81794 are identical sequences and differ from Genbank accession number AJ001646 by five base-pairs, which is reflected in a shared nucleotide percentage identity of 99.3 % determined using Gene Computer Group (GCG) programme, Fasta (Table 3.3B), representing a difference of four amino acids. Given the small differences between the Golden Delicious (X61390, M81794) and Fuji cultivar (AJ001646) sequences, which are likely due to cultivar and/or allelic variation or nucleotide sequencing error, the three sequences are probably encoded by the same gene, and this is designated as *MD-ACO1.*

By contrast Genbank accession number AF015787 varies from both X61390:M81794 and the Fuji AJOO1646 by 56 base-pairs. Further, AF015787 has an additional 48 base-pairs at the 3′-end of the sequence compared with X61390:M81794 and the AJOO1646 sequences. Inspection of the alignments of the X61390:M81794 and AJOO1646 sequences with the AF015787 sequence in Table 3.3A show the stop codon (TGA) of the shorter sequences aligns with the nucleotide sequence CGA (coding for arginine) of the AF015787 sequence. This apparent mutation of thymidine to cytidine (or vice versa) in the AF015787 sequence probably reflects the common ancestry between these DNA sequences. A comparison of the AF015787 sequence with the other sequences (Table 3.3B) give sequence identities of 90.5 % (X61390), 90.1 % (M81794) and 90.9 % (AJ001646), indicating that AF015787 is encoded by a distinct gene, and is designated *MD-ACO2.*
The JEB:α sequence differs from the AF015787 sequence by only seven base-pairs (Table 3.3A) and shares a sequence identity of 98 % which strongly suggests that the sequences are encoded by the same gene. *JEB:α* differs from sequence X61390:M81794 by 48 base-pairs and from sequence AJOO1646 by 47 base-pairs, with sequence identities for X61390:M81794 of 93.6 % and with AJOO1646 of 94 %, which supports the view that *JEB:α* is encoded by a gene distinct from those encoding X61390:M81794 and AJOO1646. *JEB:α* and *JEB:β* sequences differ by 211 base-pairs and share a nucleotide sequence identity of 78.9 %, similar base-pair differences are found between *JEB:β* and the Genbank database sequences shown as Table 3.3A, which are also consistent with the percentage identities shared between *JEB:β* and the sequences of X61390 (79.1 %), M81794 (79.5 %), AJOO1646 (78.5 %) and AF015787 (78.5 %)(Table 3.3B). Taken together, this data clearly indicates that *JEB:β* may correspond to a distinct gene to *JEB:α*, and is designated *MD-ACO3.*

```
I    X61390:M81794  ATGGCGACTTTCCCAGTTGTTGACTTGAGCCTTGTCAATGGTGAAGAGAGAGCAGCAACCTTGGAGAAGATCAATGA
II   AJOO1646       ATGGCGACTTTCCCAGTTGTCGACTTGAGCCTTGTCAATGGTGAAGAGAGAGCAGCAACCTTGGAGAAGATCAATGA
III  AF015787       ATGGCAACTTTCCCAGTTGTTGACATGGACCTTATCAATGGTGAAGAGAGAGCAGCAACCTTGGAGAAGATCAATGA

I    X61390:M81794  TGCTTGTGAGAACTGGGGTTTCTTTGAGCTGGTGAACCATGGGATGTCTACTGAGCTTTTGGACACTGTGGAGAAG
II   AJOO1646       TGCTTGTGAGAACTGGGGTTTCTTTGAGCTGGTGAACCATGGGATGTCTACTGAGCTTTTGGACACTGTGGAGAAG
III  AF015787       TGCATGTGAGAACTGGGGTTTCTTTGAGTTGGTGAACCATGGGATATCAACTGAGCTTTTGGACACTGTGGAGAAG
     JEB: α          GCTTGCGAAAACTGGGGCTTCTTTGAGTTGGTGAACCATGGGATATCAACTGAGCTTTTGGACACTGTGGAGAAG
     JEB: β          GCGTGCGAGAACTGGGGCTTCTTTGAGCTGGTGAGTCATGGGATTCCAACTGAGTTTTTGGACACAGTGGAGAGG

I    X61390:M81794  ATGACCAAGGATCACTACAAGAAGACCATGGAGCAAAGGTTTAAGGAAATGGTGGCAGCCAAAGGCTCGACGACTG
II   AJOO1646       ATGACCAAGGATCACTACAAGAAGACCATGGAGCAAAGGTTTAAGGAAATGGTGGCAGCCAAAGGCTCGACGACTG
III  AF015787       ATGAACAAGGATCACTACAAGAAGACCATGGAGCAAAGGTTCAAGGAAATGGTGGCAGCCAAAGGCCTCGAAGCTG
     JEB: α          ATGAACAAGGATCACTACAAGAAGACCATGGAGCAAAGGTTCAAGGAAATGGTGGCAGCCAAAGGCCTCGAAGCTG
     JEB: β          CTGACAAAAGAGCACTACAAGCAGTGTTTGGAGCAAAGGTTCAAGGAGTGGTGGCCAGCATAAGGCCTTGAGGGTG

I    X61390:M81794  TCCAGTCCGAAATCCACGACTTGGACTGGGAAAGCACCTTCTTCTTGCGCCACCTTCCTTCCTCAAACATTTCCGA
II   AJOO1646       TCCAGTCCGAAATCCACGACTTGGACTGGGAAAGCACCTTCTTCTTGCGCCACCTTCCTTCCTCAAACATTTCCGA
III  AF015787       TCCAGTCCGAAATCCACTACTTGGACTGGGAAAGCACCTTCTTCTTGCGCCACCTTCCTTCCTCAAACATTTCCGA
     JEB: α          TCCAGTCCGAAATCCACGACTTGGACTGGGAAAGCACCTTCTTCTTGCGCCACCTTCCTTCCTCAAACATTTCCGA
     JEB: β          TTCAGACAGAAGTCAAAGATATGGATTGGGAAAGCACTTTCCACTTGCGCCATCTTCCTCAATCGAACATCTCTGA

I    X61390:M81794  AATCCCTGATCTCGAGGAAGAGTACAGGAAGACCATGAAGGAATTTGCAGTGGAACTGGAGAAGCTAGCTGAGAAG
II   AJOO1646       AATCCCTGATCTCGAGGAAGATTACAGGAAGACCATGAAGGAATTTGCAGTGGAACTGGAGAAGCTAGCTGAGAAG
III  AF015787       AATCCCTGATCTCGAGGAAGATTACAGGAAGACCATGAAGGAATTTGCAGTGGAATTGGAGAAGCTAGCTGAGAAG
     JEB: α          AATCCCTGATCTCGAGGAAGATTACAGGAAGACCATGAAGGAATTTGCAGTGGAATTGGAGAAGCTAGCTGAGAAG
     JEB: β          AGTACCAGATCTCAAGGATGAGTACAGGAATGTGATGAAGGAGTTTGCATTGAAATTGGAAAAATTAGCAGAGCAG

I    X61390:M81794  CTTTTGGACTTGCTGTGTGAGAATCTTGGACTCGAGAAGGGTTATCTGAAGAAGGTTTTCTATGGATCCAAGGGTC
II   AJOO1646       CTTTTGGACTTGCTGTGTGAGAATCTTGGACTCGAGAAGGGTTATCTGAAGAAGGTTTTCTATGGATCCAAGGGTC
III  AF015787       CTTTTGGACTTGCTGTGTGAGAATCTTGGACTTGAGAAGGGCTATCTGAAGAAGGCTTTCTATGGATCCAAGGGTC
     JEB: α          CTTTTGGGCTTGTTGTGTGAGAATCTTGGACTTGAGAAGGGCTATCTGAAGAAGGCTTTCTATGGATCCAAGGGTC
     JEB: β          CTGCTGGACTTGTTGTGTGAGAATCTTGGACTGGAACAAGGGTACCTTAAGAAGGCATTTTATGGAACAAAGGGAC

I    X61390:M81794  CGAATTTTGGGACCAAGGTCAGCAACTACCCTCCATGCCCCAAGCCAGACCTGATCAAGGGACTCCGGGCCCACAG
II   AJOO1646       CGAATTTTGGGACCAAGGTCAGCAACTACCCTCCATGCCCCAAGCCAGACCTGATCAAGGGACTCCGGGCCCACAG
III  AF015787       CGAATTTTGGGACCAAGGTCAGCAACTACCCTCCATGTCCCAAGCCAGACCTGATCAAGGGACTCCGGGCCCACAC
     JEB: α          CGAATTTTGGGACCAAGGTCAGCAACTACCCTCCATGTCCCAAGCCGGACCTGATCAAGGGACTCCGGGCCCACAC
     JEB: β          CAACTTTTGGCACCAAGGTGAGCAACTACCCTCCATGTCCCAACCCGACCTGATCAAGGGTCTCCAGGGCCCACAC

I    X61390:M81794  CGACGCCGGTGGCATCATCCTGCTTTTCCAGGATGACAAGGTCAGCGGCCTCCAGCTTCTCAAGGATGGTGAATGG
II   AJOO1646       CGACGCCGGTGGCATCATCCTGCTTTTCCAGGATGACAAGGTCAGCGGCCTCCAGCTTCTCAAGGATGGTGAATGG
III  AF015787       CGACGCTGGTGGTATCATCCTGCTTTTCCAGGATGACAAGGTCAGTGGCCTCCAGCTCCTCAAGGATGGTGAATGG
     JEB: α          CGACGCTGGTGGTATCATCCTGCTTTTCCAGGATGACAAGGTCAGCGGCCTCCAGCTCCTCAAGGATGGTGAATGG
     JEB: β          CGATGCCGGCGGCCTCATCTTGCTCTTCCAGGATGACAAGGTCAGTGGCCTCCAGCTCCTCAAGGACGGAGAGTGG

I    X61390:M81794  GTGGATGTCCCCCCCAATGCACCACTCCATTGTCATAAACTTAGGTGACCAGATTGAGGTGATCACCAATGGGAAGT
II   AJOO1646       GTGGATGTCCCCCCCAATGCACCACTCCATTGTCATAAACTTAGGTGACCAGATTGAGGTGATCACCAATGGGAAGT
III  AF015787       ATGGATGTCCCCCCCAGTGCACCACTCCATTGTCATCAACTTAGGTGACCAGATTGAGGTGATCACTAATGGGAAGT
     JEB: α          ATGGATGTCCCCCCCAGTGCACCACTCCATTGTCATCAACTTAGGTGACCAGATTGAGGTGATCACTAATGGGAAGT
     JEB: β          GTTGATGTGCCTCCCATGCGCCACTCCATTGTTATCAATCTTGGTGACCAACTTGAGGTGATCACCAACGGAAAGT

I    X61390:M81794  ACAAAAGTGTGATGCACCGGGTGATAGCTCAGTCGGATGGGACCAGAATGTCGATAGCCTCGTTCTACAACCCAGG
II   AJOO1646       ACAAAAGTGTGATGCACCGGGTGATAGCTCAGTCGGATGGGACCAGAATGTCGATAGCCTCGTTCTACAACCCAGG
III  AF015787       ACAAGAGTATAATGCACCGGGTGATAGCTCAGTCGGACGGAACCAGAATGTCGATAGCGTCGTTCTACAACCCGGG
     JEB: α          ACAAGAGTATAATGCACCGGGTGATAGCTCAGTCGGACGGAACCAGAATGTCGATAGCGTCGTTCTACAACCCGGG
     JEB: β          ACAAGAGTGTGGAACACAGGGTGATTGCCCAAACAGATGGCACCAGAATGTCAATAGCTTCATTCTACAACCCAGG

I    X61390:M81794  CAACGACTCATTCATCAGCCCAGCACCGGCAGTGCTTGAGAAGAAAACTGAGGACGCCCCAACTTATCCCAAGTTT
II   AJOO1646       CAACGACGCATTCATCAGCCCAGCACCGGCAGTGCTTGAGAAGAAAACTGGGGACGCCCCAACTTATCCCAAGTTT
III  AF015787       CGACGATGCGTTTATCAGCCCGGCACCGGCATTGCTGGAGGAGAAATCTGAGGTTTCCCCAACTTATCCCAAATTT
     JEB: α          CGACGATGCGTTTATCAGCCCGGCACCGGCATTGCTGGAGAAGAAATCTGAGGAAACCCCAACTTATCCCAAATTT
     JEB: β          CAGTGATGCGGTGATCTACCCAGCACCAACCCTAGTGGAGAAAGAAGCAGAGGAGAAGAATCAAGTGTACCCGAAA

I    X61390:M81794  GTGTTTGATGACTACATGAAGCTGTATTCTGGCCTGAAATTCCAAGCCAAGGAGCCAAGATTTGAAGCTATGAAGG
II   AJOO1646       GTGTTTGATGACTACATGAAGCTGTATTCTGGCCTGAAATTCCAAGCCAAGGAGCCAAGATTTGAAGCTATGAAGG
III  AF015787       TTGTTTGATGATTACATGAAGCTGTACTCTGGCCTCAAATTCCAAGCCAAGGAGCCAAGATTTGAAGCTATGAAGG
     JEB: α          TTGTTTGATGATTACATGAAGCTGTACTCTGGCCTCAAATTCCAAGCCAAAGAA
     JEB: β          TTCGTGTTCGAAGACTACATGAAGCTCTATGCTGGGGTCAAGTTCCAGGCCAAAGAG

I    X61390:M81794  CCAAGGAATCCACCCCTGTTGCAACTGCCTGA
II   AJOO1646       CCAAGGAACCCACCCCTGTTGCAACTGCCTGA
III  AF015787       CCAGGGAAACCACCCCTGTTGAAACTGCCCGAGGTCTGAGAGCCGTCCGATGGAACACGACAAAAAGAAATCAAAATTAG
```

Table 3.3B: Nucleotide Identity (%) Between *JEB:α* and *JEB:β* and ACC Oxidase Sequences from Three Cultivars of *Malus domestica*.

	X61390 Golden Delicious **fruit cortex** *(MD-ACO1)*	**M81794** Golden Delicious **ripe fruit** ***(MD-ACO1)***	**AJ001646** Fuji **fruit** *(MD-ACO1)*	**AF015787** Fuji **exons from genomic** ***(MD-ACO2)***	***JEB:α*** Gala **leaf** *(MD-ACO2)*	***JEB:β*** Gala **leaf** *(MD-ACO3)*
X61390	_	100	99.3	90.5	93.6	79.1
M81794		_	99.3	90.1	93.6	79.5
AJ001646			_	90.9	94	78.5
AF015787				_	98	78.5
JEB:α					_	78.9
JEB:β						_

As there is often wobble of the third base pair in a codon, the translated sequence may not reflect variations between nucleotide sequences, hence the putative amino acid sequence may in fact be a more meaningful indicator of whether or not sequences are encoded by distinct genes (refer Figures 3.3, 3.4 and 3.5).

From the nucleotide sequences of the groups designated *JEB:α* (813 bp) and *JEB:β* (816 bp) the deduced amino acid sequences were obtained using the Gene Computer Group (GCG) programme, Fasta (MAP function). Comparisons of the deduced amino acid sequences of *JEB:α* and *JEB:β* with those of Genbank accession numbers X61390:*pAP4* (Ross *et al.*, 1992) and AF015787 (Nam and Kim, 1998) are shown as Figure 3.3, and broadly confirm the nucleotide alignments. JEB:α and the AF015787 differ by four amino acids, whereas JEB:α and X6139 differ by 16 amino acid, while X6139 and AF015787 differ from each other, over the corresponding sequence, by 17 amino acids. Such results suggest JEB:α (cv. Gala) is encoded by the same gene as AF015787 from cv. Fuji (which has been designated MD-ACO2), and that both JEB:α and AF015787 are distinct from X61390 from cv. Golden Delicious (which is designated MD-ACO1). JEB:β differs quite markedly from X6139 (by 65 aa), JEB:α (by 68 aa) and AF015787 (by 72 aa) which strongly suggests that the JEB:β is encoded by a gene distinct from both Genbank accession numbers (X6139 and AF015787) and JEB:α (and is designated as MD-ACO3).

```
MD-ACO1: X61390      A C E N W G F F E L V N H G M S T E L L D T V E K M T K D H Y K K T
MD-ACO2: AF015787    A C E N W G F F E L V N H G I S T E L L D T V E K M N K D H Y K K T
MD-ACO2: JEB: α      A C E N W G F F E L V N H G I S T E L L D T V E K M N K D H Y K K T
MD-ACO3: JEB: β      A C E N W G F F E L V S H G I P T E F L D T V E R L T K E H Y K Q C

MD-ACO1: X61390      M E Q R F K E M V A A K G L D D V Q S E I H D L D W E S T F F L R H
MD-ACO2: AF015787    M E Q R F K E M V A A K G L E A V Q S E I H Y L D W E S T F F L R H
MD-ACO2: JEB: α      M E Q R F K E M V A A K G L E A V Q S E I H D L D W E S T F F L R H
MD-ACO3: JEB: β      L E Q R F K E L V A S K G L E G V Q T E V K D M D W E S T F H L R H

MD-ACO1: X61390      L P S S N I S E I P D L E E E Y R K T M K E F A V E L E K L A E K L
MD-ACO2: AF015787    L P S S N I S E I P D L E E D Y R K T M K E F A V E L E K L A E K L
MD-ACO2: JEB: α      L P S S N I S E I P D L E E D Y R K T M K E F A V E L E K L A E K L
MD-ACO3: JEB: β      L P Q S N I S E V P D L K D E Y R N V M K E F A L K L E K L A E Q L

MD-ACO1: X61390      L D L L C E N L G L E K G Y L K K V F Y G S K G P N F G T K V S N Y
MD-ACO2: AF015787    L D L L C E N L G L E K G Y L K K V F Y G S K G P N F G T K V S N Y
MD-ACO2: JEB: α      L D L L C E N L G L E K G Y L K K A F Y G S K G P N F G T K V S N Y
MD-ACO3: JEB: β      L D L L C E N L G L E Q G Y L K K A F Y G T K G P T F G T K V S N Y

MD-ACO1: X61390      P P C P K P D L I K G L R A H S D A G G I I L L F Q D D K V S G L Q
MD-ACO2: AF015787    P P C P K P D L I K G L R A H T D A G G I I L L F Q D D K V S G L Q
MD-ACO2: JEB: α      P P C P K P D L I K G L R A H T D A G G I I L L F Q D D K V S G L Q
MD-ACO3: JEB: β      P P C P N P D L I K G L R A H T D A G G L I L L F Q D D K V S G L Q

MD-ACO1: X61390      L L K D G E W V D V P P M H H S I V I N L G D Q I E V I T N G K Y K
MD-ACO2: AF015787    L L K D G E W M D V P P V H H S I V I N L G D Q I E V I T N G K Y K
MD-ACO2: JEB: α      L L K D G E W M D V P P V H H S I V I N L G D Q I E V I T N G K Y K
MD-ACO3: JEB: β      L L K D G E W V D V P P M R H S I V I N L G D Q L E V I T N G K Y K

MD-ACO1: X61390      S V M H R V I A Q S D G T R M S I A S F Y N P G N D S F I S P A P A
MD-ACO2: AF015787    S I M H R V I A Q S D G T R M S I A S F Y N P G D D A F I S P A P A
MD-ACO2: JEB: α      S I M H R V I A Q S D G T R M S I A S F Y N P G D D A F I S P A P A
MD-ACO3: JEB: β      S V E H R V I A Q T D G T R M S I A S F Y N P G S D A V I Y P A P T

MD-ACO1: X61390      V L E K K T E D A P T Y P K F V F D D Y M K L Y S G L K F Q A K E
MD-ACO2: AF015787    L L E E K S E V S P T Y P K F L F D D Y M K L Y S G L K F Q A K E(P)
MD-ACO2: JEB: α      L L E K K S E E T P T Y P K F L F D D Y M K L Y S G L K F Q A K E
MD-ACO3: JEB: β      L V E K E A E E K N Q V Y P K F V F E D Y M K L Y A G V K F Q A K E
```

Figure 3.3: Comparison Between the Translated Sequences of the Partial cDNAs *JEB:α* and *JEB:β* with the Corresponding ACC Oxidase Sequences as Indicated.

3.1.3 Expressed Sequence Tag (EST) Searches at HortResearch

With the *JEB:α* sequence (*MD-ACO2*) and the *JEB:β* (*MD-ACO3*) sequence proposed to correspond to different ACO genes, the next step was to search the EST library from apple constructed by HortResearch to identify homologous sequences (and therefore full length cDNA clones). The Genbank accession number X61390 sequence (clone *pAP4*; Ross *et al.*, 1992) (designated *MD-ACO1*) had already been gifted to the McManus laboratory.

Searching for the ESTs with the closest matches to *MD-ACO2* and *MD-ACO3* began with aligning and comparing the contigs using sequencher, MT Navigator and GCG computer programes to assess their identities and/or orientation(s). Once selected a full bidirectional sequencing of the ESTs with the closest match to *JEB:α* or *JEB:β* was received from HortResearch.

Searching for the ESTs with the closest matches to *JEB:α* found the closest alignments were in fact with Genbank accession numbers X61390 (Ross *et al.*, 1992), M81794 (Dong *et al.*, 1992) and AJOO1646 (Castiglione *et al.*, 1997a), but with only a nucleotide identity of 90 %, and so it was therefore assumed that JEB:α was not in the HortResearch EST library. An attempt was then made to obtain the 3′-UTR sequence from *JEB:α* using 3′-RACE (data not shown), but as this was unsuccessful, a decision was then made to interrogate the HortResearch EST databank further using only the 3′-UTR (138 bp) of the Genbank accession number AF015787 (Nam and Kim, 1998) gene sequence. A sequence of 623 bp, designated as EST 153710, was the best hit/match and an aliquot of the vector containing the sequence was requested. The identity values of EST 153710 and each of the sequences is shown as Table 3.4. *JEB:α* : AF015787 share a high sequence identity of 97.6 %, followed by X61390 (*pAP4*; 86.6 %) and then *JEB:β* (78.5 %).

Table 3.4: Identity (%) Between EST 153710 and the cDNA X61390 (*pAP4*), *JEB:α* :AF015787 and *JEB:β*.

	X61390 : *pAP4* (*MD-ACO1*)	***JEB:α* : AF015787 (*MD-ACO2*)**	***JEB:β* (*MD-ACO3*)**
EST 153710	86.6% (623 bp)	97.6% (615 bp)	78.5% (428 bp)

An alignment of the deduced amino acid sequence of AF015787 with those of EST 153710 (refer Figure 3.4) shows a difference of three amino acids over the length of the sequence, while JEB:α (*MD-ACO2*) seems to be an exact match (with EST 153710) over the 834 bp sequence. After further interrogation of the HortResearch EST databank using both EST 153710 and *JEB:α*, a sequence of 1,230 bp designated EST 120223 extending from the 5′-UTR and matching the entire length of both EST 153710 and *JEB:α* was found. A comparison of the amino acid sequences of EST 120223 with both EST 153710 and *JEB:α*, as well as AF015787 is shown as Figure 3.4.

```
AF015787    M A T F P V V D M D L I N G E E R A A T L E K I N D A C E N W G F F E L V
EST 120223  M A T F P V V D M D L I N G E E R A A T L E K I N D A C E N W G F F E L V
JEB: α                                                  A C E N W G F F E L V

AF015787    N H G I S T E L L D T V E K M N K D H Y K K T M E Q R F K E M V A A K G
EST 120223  N H G I S T E L L D T V E K M N K D H Y K K T M E Q R F K E M V A A K G
JEB: α      N H G I S T E L L D T V E K M N K D H Y K K T M E Q R F K E M V A A K G

AF015787    L E A V Q S E I H Y L D W E S T F F L R H L P S S N I S E I P D L E E D Y R K
EST 120223  L E A V Q S E I H D L D W E S T F F L R H L P S S N I S E I P D L E E D Y R K
JEB: α      L E A V Q S E I H D L D W E S T F F L R H L P S S N I S E I P D L E E D Y R K

AF015787    T M K E F A V E L E K L A E K L L D L L C E N L G L E K G Y L K K V F Y G
EST 120223  T M K E F A V E L E K L A E K L L D L L C E N L G L E K G Y L K K A F Y G
JEB: α      T M K E F A V E L E K L A E K L L D L L C E N L G L E K G Y L K K A F Y G

AF015787    S K G P N F G T K V S N Y P P C P K P D L I K G L R A H T D A G G I I L L F
EST 120223  S K G P N F G T K V S N Y P P C P K P D L I K G L R A H T D A G G I I L L F
EST 153710                                  K P D L I K G L R A H T D A G G I I L L F
JEB: α      S K G P N F G T K V S N Y P P C P K P D L I K G L R A H T D A G G I I L L F

AF015787    Q D D K V S G L Q L L K D G E W M D V P P V H H S I V I N L G D Q I E V I
EST 120223  Q D D K V S G L Q L L K D G E W M D V P P V H H S I V I N L G D Q I E V I
EST 153710  Q D D K V S G L Q L L K D G E W M D V P P V H H S I V I N L G D Q I E V I
JEB: α      Q D D K V S G L Q L L K D G E W M D V P P V H H S I V I N L G D Q I E V I

AF015787    T N G K Y K S I M H R V I A Q S D G T R M S I A S F Y N P G D D A F I S P A
EST 120223  T N G K Y K S I M H R V I A Q S D G T R M S I A S S Y N P G D D A F I S P A
EST 153710  T N G K Y K S I M H R V I A Q S D G T R M S I A S F Y N P G D D A F I S P A
JEB: α      T N G K Y K S I M H R V I A Q S D G T R M S I A S F Y N P G D D A F I S P A

AF015787    P A L L E E K S E V S P T Y P K F L F D D Y M K L Y S G L K F Q A K E P R F
EST 120223  P A L L E K K S E E T P T Y P K F L F D D Y M K L Y S G L K F Q A K E P R F
EST 153710  P A L L E K K S E E T P T Y P K F L F D D Y M K L Y S G L K F Q A K E P R F
JEB: α      P A L L E K K S E E T P T Y P K F L F D D Y M K L Y S G L K F Q A K E

AF015787    E A M K A R E T T P V E T A R G L R A V R W N T T K R N Q N
EST 120223  E A M K A R E T T P V E T A R G L R A V R W N T T K R N Q N
EST 153710  E A M K A R E T T P V E T A R G L R A V R W N P T K R N Q N
```

Figure 3.4: Comparison of the Deducted Amino Acid Sequences of *JEB: α* (*MD-ACO2*) with Genbank Accession Number AF015787 and EST 120223 and EST 153710. Variations of specific amino acid residues are shown in bold.

A further interrogation of the HortResearch EST databank using the nucleotide sequence of the group designated *JEB:β* (*MD-ACO3*) found two ESTs (designated 192136 and 179706) which closely matched the *JEB:β* sequence (Identities are shown in Table 3.5). The *JEB:β* sequence shares a high identity with the ESTs (98 %) whilst both X61390 (*pAP4*; 78 %) and AF015787 (JEB:α; 77.3 %) share a much lower comparative identity.

Table 3.5: Identity (%) Between ESTs (192136 and 179706) and the cDNA *pAP4*, *JEB:α* and *JEB:β* Sequences.

	X61390 : *pAP4* (*MD-ACO1*)	***JEB:α* : AF01578 (*MD-ACO2*)**	***JEB:β* (*MD-ACO3*)**
EST 179706[1]	78%	77.3%	98%
EST 192136			

[1]EST 179706 & EST 192136 share an identity of 99.2%

Since the deduced amino acid sequences of EST 179706 and EST 192136 are identical to each other (Figure 3.5), they are probably the same gene. As the deducted 272 amino acids comprising the *JEB:β* sequence matches the EST sequences so well (98 % identity) it is likely that *JEB:β* (*MD-ACO3*) is the same *Malus domestica* ACO isoform as EST 179706 and 192136.

3.1.4 Summary of gene nomenclature

Each of the three *Malus domestica* ACO sequences were therefore designated as follows: Genbank accession number X61390 (*pAP4* ; Ross *et. al.*, 1992) and the corresponding genomic DNA sequence Genbank accession number AF030859 (Ross *et al.*, 1998; Atkinson *et al.*, 1998) as *MD-ACO1*; EST 120223 and the corresponding genomic DNA sequence Genbank accession number AF015787 (Nam and Kim, 1998) as *MD-ACO2* (cloned in this thesis as *pJEB:α*), and EST 179706 and 192136 are designated *MD-ACO3* (cloned in this thesis as *pJEB:β*).

```
EST 179706    MENFPVINLESLNGEGRKATMEKIKDACENWGFFELV
EST 192136    MENFPVINLESLNGEGRKATMEKIKDACENWGFFELV
JEB:β                                 ACENWGFFELV

EST 179706    SHGIPTEFLDTVERLTKEHYKQCLEQRFKELVASKGLE
EST 192136    SHGIPTEFLDTVERLTKEHYKQCLEQRFKELVASKGLE
JEB:β         SHGIPTEFLDTVERLTKEHYKQCLEQRFKELVASKGLE

EST 179706    GVQTEVKDMDWESTFHLRHLPQSNISEVPDLKDEYRN
EST 192136    GVQTEVKDMDWESTFHLRHLPQSNISEVPDLKDEYRN
JEB:β         GVQTEVKDMDWESTFHLRHLPQSNISEVPDLKDEYRN

EST 179706    VMKEFALKLEKLAEQLLDLLCENLGLEQGYLKKAFYG
EST 192136    VMKEFALKLEKLAEQLLDLLCENLGLEQGYLKKAFYG
JEB:β         VMKEFALKLEKLAEQLLDLLCENLGLEQGYLKKAFYG

EST 179706    TKGPTFGTKVSNYPPCPNPDLIKGLRAHTDAGGLILLF
EST 192136    TKGPTFGTKVSNYPPCPNPDLIKGLRAHTDAGGLILLF
JEB:β         TKGPTFGTKVSNYPPCPNPDLIKGLRAHTDAGGLILLF

EST 179706    QDDKVSGLQLLKDGEWVDVPPMRHSIVINLGDQLEVIT
EST 192136    QDDKVSGLQLLKDGEWVDVPPMRHSIVINLGDQLEVIT
JEB:β         QDDKVSGLQLLKDGEWVDVPPMRHSIVINLGDQLEVIT

EST 179706    NGKYKSVEHRVIAQTDGTRMSIASFYNPGSDAVIYPAP
EST 192136    NGKYKSVEHRVIAQTDGTRMSIASFYNPGSDAVIYPAP
JEB:β         NGKYKSVEHRVIAQTDGTRMSIASFYNPGSDAVIYPAP

EST 179706    TLVEKEAEEKNQVYPKFVFEDYMKLYAGVKFEAKEPR
EST 192136    TLVEKEAEEKNQVYPKFVFEDYMKLYAGVKFEAKEPR
JEB:β         TLVEKEAEEKNQVYPKFVFEDYMKLYAGVKFQAKE

EST 179706    FEAMKAVEIKASFGLGPVISTA
EST 192136    FEAMKAVEIKASFGLGPVISTA
JEB:β
```

Figure 3.5: Comparisons of the Deduced Amino Acid Sequences of *JEB:β* (*MD-ACO3*) with EST 179706 and EST 192136.

3.1.5 Genomic structure of the *Malus domestica* ACC oxidase genes

The identities of the *MD-ACO1* (Ross *et al.*, 1998; Atkinson *et al.*, 1998) and *MD-ACO2* (Nam and Kim, 1998) genes are compared over the whole genomic sequence. As the genomic sequence of *MD-ACO3* is unavailable the intron distribution is unknown. However, the open reading frame of *MD-ACO3* is compared with *MD-ACO1* and *MD-ACO2* by following the beginning and the ending of each exon with the corresponding codon for the *MD-ACO1* and *MD-ACO2* exons at the boundary with the intron (Figure 3.6). Not surprisingly the identities between each of the exons of *MD-ACO1* and *MD-ACO2* is high. However, over the three introns the identity is lower (Table 3.6).

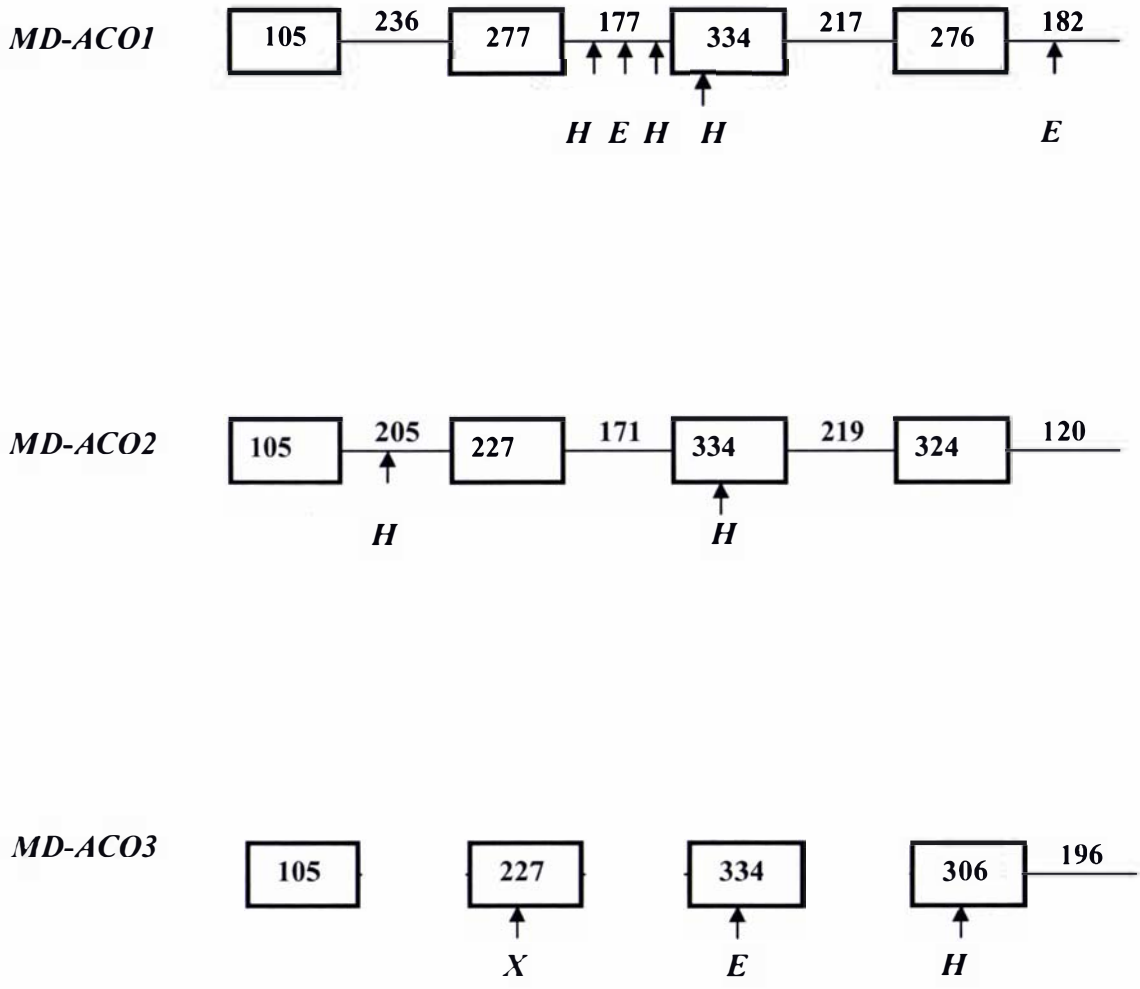


Figure 3.6: Gene Structure of *MD-ACO1* and *MD-ACO2*, with the Exon Length of *MD-ACO3* Indicated.

The boxes indicate the exon sequences and the numbers represent DNA sequence length in base pairs. The lines between the boxes represent the intron sequences, and the numbers indicate DNA length in base pairs. Restriction enzyme sites within each of the exons and introns is indicated as: ***X*** = *Xba*I, ***E*** = *Eco*RI and ***H*** = *Hind*III.

A

Exon-1	*MD-ACO1*	*MD-ACO2*	*MD-ACO3*
MD-ACO1	-	94.3 %	77.1 %
MD-ACO2		-	77.1 %
MD-ACO3			-

B

Exon-2	*MD-ACO1*	*MD-ACO2*	*MD-ACO3*
MD-ACO1	-	96.5 %	78 %
MD-ACO2		-	77.4 %
MD-ACO3			-

C

Exon-3	*MD-ACO1*	*MD-ACO2*	*MD-ACO3*
MD-ACO1	-	96.1 %	86.6 %
MD-ACO2		-	83.5 %
MD-ACO3			-

D

Exon-4	*MD-ACO1*	*MD-ACO2*	*MD-ACO3*
MD-ACO1	-	89.2 %	75.2 %
MD-ACO2		-	73 %
MD-ACO3			-

E

Intron-1	MD-ACO1	MD-ACO2	MD-ACO3
MD-ACO1	-	86.4%	
MD-ACO2		-	
MD-ACO3			-

F

Intron-2	MD-ACO1	MD-ACO2	MD-ACO3
MD-ACO1	-	79.2%	
MD-ACO2		-	
MD-ACO3			-

G

Intron-3	MD-ACO1	MD-ACO2	MD-ACO3
MD-ACO1	-	76.4%	
MD-ACO2		-	
MD-ACO3			-

H

Genomic	*MD-ACO1*	*MD-ACO2*
MD-ACO1	-	88.6 % (100 %)
MD-ACO2		-
MD-ACO3	genomic sequence unavailable	

All three *MD-ACOs* share the same nucleotide length over the first three exons (Figure 3.6), and *MD-ACO1* and *MD-ACO2* each have a *Hind*III restriction site in exon 3. An examination of the three introns, however, strongly suggests *MD-ACO1* and *MD-ACO2* are encoded by different genes. Not only do they not share the same nucleotide length, but they each have different restriction sites within their introns. For example, there are two *Hind*III and an *Eco*RI restriction site in intron -2 in the *MD-ACO1* gene, not found in the *MD-ACO2* gene. Further, a *Hind*III restriction site in intron -1 of *MD-ACO2* is not present in *MD-ACO1*.

3.1.6 Sequence Analysis of ACC Oxidase from *Malus domestica*

3.1.6.1 Nucleotide Sequence Identities Amongst the ORF of *MD-ACO1*, *MD-ACO2* and *MD-ACO3*

Using the Gene Computer Group (GCG) programme, Fasta, identities between the ACO transcripts (refer Table 3.7A and 3.7B) show the identity between the entire open reading frames (ORF) of *MD-ACO1* and *MD-ACO2* (93.9 %) is greater than between the 3′-UTR sequences (69.5 %) which further supports the hypothesis of these being two distinct *MD*-ACO genes. This is consistent with white clover ACO studies (Hunter *et.al.*, 1999) where greater identity was found over the coding region (> 90 %) than the 3′-UTR (~70 %). Whereas the identities between the ORF transcripts of *MD-ACO3* and both *MD-ACO1* (78.5 %) and *MD-ACO2* (77.8 %) are almost as low as the identities between the *MD-ACO3* transcripts for the 3′-UTR of *MD-ACO1* (68.4 %) and *MD-ACO2* (69.5 %). Identities between the MD-ACO amino acid sequences (Table 3.7C) reflects the percentage identities of the nucleotide sequences, but there is more apparent differentiation between the three proteins.

3.1.6.2 NCBI Nucleotide Database BLAST Analysis of the Entire ORF for Each of the ACC Oxidase Sequences

The results of NCBI nucleotide Blast searches for each of the ACO transcripts is shown as Table 3.8.

The first four hits against the *MD-ACO1* sequence, are *Malus domestica* ACO mRNA for the *MD-ACO1* sequence, Genbank accession numbers X61390 (Ross *et al.*, 1992), M81794 (Dong *et al.*, 1992), DQ137848 and AJ001646 (Castiglione *et al.*, 1997a), followed by *Pyrus pyrifolia* and *Pyrus communis*. The first genomic DNAs are *Malus domestica* hit numbers 12, 13 and 14 Genbank accession numbers X98627 and Y14005 (Castiglione *et al.*, 1997b; 1998) and AF030859 (Ross *et al.*, 1998) all *MD-ACO1*, interrupted by *Prunus persica*, followed by hit number 16 Genbank accession AF015787 (Nam and Kim, 1998), the *MD-ACO2* sequence (Table 3.8A).

Table 3.7 (A): Open Reading Frame Nucleotide Sequence Identities of *MD-ACO1*, *MD-ACO2* and *MD-ACO3*

	MD-ACO1	*MD-ACO2*	*MD-ACO3*
MD-ACO1	-	93.9%	78.5%
MD-ACO2		-	77.8%
MD-ACO3			-

Table 3.7 (B): Nucleotide Sequence Identities of the 3´-UTR of *MD-ACO1*, *MD-ACO2* and *MD-ACO3*

	MD-ACO1	*MD-ACO2*	*MD-ACO3*
MD-ACO1	-	69.5%	68.4%
MD-ACO2		-	71%
MD-ACO3			-

Table 3.7 (C): Translated Amino Acid Sequence Identities of MD-ACO1, MD-ACO2 and MD-ACO3

	MD-ACO1	MD-ACO2	MD-ACO3
MD-ACO1	-	92.04%	80.57%
MD-ACO2		-	75.16%
MD-ACO3			-

Table 3.8A: Results of a Nucleotide BLAST Search Against the *Malus domestica* ACC Oxidase (*MD-ACO1)* 942 bp cDNA Entire Open Reading Frame Sequence.

Genus and species	Accession number	Identities	Score (bits)	E Value
Hit 1:*MD-ACO1* mRNA (ripe fruit cortex)	**X61390**	100 %	1867	0.0
Hit 2:*MD-ACO1* mRNA (ripe fruit)	**M81794**	100 %	1867	0.0
Hit 3:*MD-ACO1* mRNA	DQ137848	99 %	1852	0.0
Hit 4:*MD-ACO1* mRNA (fruit)	**AJ001646**	99 %	1828	0.0
Pyrus pyrifolia mRNA (fruit)	D67038	98 %	1719	0.0
Pyrus communis mRNA (ripe fruit)	X87097	97 %	1643	0.0
Pyrus communis mRNA (fruit mesocarp)	AJ504857	96 %	1608	0.0
Pyrus pyrofolia mRNA (immature fruit)	AB042111	94 %	1455	0.0
Hit 9:*Malus domestica* mRNA	DQ137850	99 %	1245	0.0
Prunus persica mRNA *(ppACO2)* (fruit)	AB044712	86 %	743	0.0
Rosa hybrid mRNA	AF441282	86 %	737	0.0
Hit 12:*MD-ACO1* genomic DNA	**X98627**	100 %	672	0.0
Hit 13:*MD-ACO1* genomic DNA	**Y14005**	100 %	672	0.0
Hit 14:*MD-ACO1* genomic DNA	**AF030859**	100 %	672	0.0
Prunus persica linear DNA	AF129074	88 %	573	1e-160
Hit 16:*MD-ACO2* genomic DNA	**AF015787**	96 %	569	6e-159
Hit 29: *MD-ACO3* mRNA	**ABO86888**	81 %	361	3e-96

Searched on 27 August 2006 (E value; refer section 2.2.6.1)

The first two hits against *MD-ACO2* are *Pyrus pyrifolia* mRNA followed by *Malus domestica* ACO mRNA Genbank accession numbers X61390 (*pAP4*; Ross et al., 1992), M81794 (*pAE12*; Dong *et al.*, 1992) and AJ001646 (Castiglione *et al.*, 1997a) and DQ137848, all *MD-ACO1* sequences. The first genomic DNA is hit number 12, which is Genbank accession AF015787 (Nam and Kim, 1998) the *MD-ACO2* sequence, interrupted by *Prunus persica*, followed by Genbank accessions X98627, Y14005 (Castiglione *et al.*, 1997b; 1998) and AF03859 (Atkinson *et al.*, 1998) all *MD-ACO1* sequences (Table 3.8B).

For *MD-ACO3*, the first hit is *Malus domestica* ACO mRNA (cv. Fuji), Genbank accession AB086888 (Hatsuyama *et al.*, 2002) with 99 % identity over the entire coding sequence, and exactly the same amino acid sequence as *MD-ACO3* (although the sequence is designated as *MD-ACO2* in the Genbank database). This sequence was deposited on 25.12.02, and so was not available for the initial catagorization of the *JEB:α* and *JEB:β* sequences (e.g. Table 3.2, searched on 26.08.02 and 24.04.02 respectively). *Malus domestica* ACO mRNA occurs again at hit numbers 44 and 45, Genbank accessions DQ137848 and X61390 (*pAP4*; Ross *et al.*, 1992) respectively, both *MD-ACO1* sequences, and genomic apple ACO occurs as hit 77 Genbank accession AF015787 (Nam and Kim, 1998), the *MD-ACO2* sequence (Table 3.8C).

Table 3.8B: Results of a Nucleotide BLAST Search Against the *Malus domestica* ACC Oxidase (*MD-ACO2)* 990 bp cDNA Entire Open Reading Frame Sequence.

Genus and species	Accession number	Identities	Score (bits)	E Value
Pyrus pyrifolia mRNA (immature fruit)	AB042111	97 %	1786	0.0
Pyrus pyrifolia mRNA (fruit)	D67038	94 %	1513	0.0
Hit 3:*MD-ACO1* mRNA (ripe fruit cortex)	**X61390**	94 %	1489	0.0
Hit 4:*MD-ACO1* mRNA (ripe fruit)	**M81794**	94 %	1489	0.0
Hit 5:*MD-ACO1* mRNA (fruit)	**AJ001646**	94 %	1463	0.0
Hit 6:*MD-ACO1* mRNA	DQ137848	94 %	1447	0.0
Pyrus communis mRNA (ripe fruit)	X87097	93 %	1421	0.0
Pyrus communis mRNA (fruit mesocarp)	AJ504857	93 %	1394	0.0
Hit 9:*Malus domestica* mRNA	DQ137850	95 %	1047	0.0
Prunus persica mRNA *(ppACO2)* (fruit)	AB044712	87 %	799	0.0
Rosa hybrid mRNA	AF441282	86 %	739	0.0
Hit 12:*MD-ACO2* genomic DNA	**AF015787**	99 %	664	0.0
Prunus persica linear DNA	AF129074	88 %	505	1e-169
Hit 13:*MD-ACO1* genomic DNA	**X98627**	96 %	577	3e-161
Hit 14:*MD-ACO1* genomic DNA	**Y14005**	96 %	577	3e-161
Hit 15:*MD-ACO1* genomic DNA	**AF030859**	96 %	533	3e-161
Hit 29: *MD-ACO3* mRNA	**AB086888**	81 %	341	3e-90

Searched on 27 August, 2006 (E value; refer section 2.2.6.1)

Table 3.8C: Results of a Nucleotide BLAST Search Against the *Malus domestica* ACC Oxidase (*MD-ACO3)* 966 bp cDNA Entire Open Reading Frame Sequence.

Genus and species	Accession number	Identities	Score (bits)	E Value
Hit 1: *MD-ACO3* mRNA	**AB086888**	99 %	1877	0.0
Pyrus pyrifolia mRNA	AB042107	99 %	1844	0.0
Pyrus pyrifolia mRNA	AB042105	94 %	1518	0.0
Pyrus pyrifolia mRNA	AB042106	94 %	1503	0.0
Prunus persica mRNA	X77232	90 %	1168	0.0
Prunus persica mRNA	AF319166	90 %	1168	0.0
Prunus armeniaca mRNA	AF026793	90 %	1168	0.0
Prunus mume mRNA	AB031027	90 %	1160	0.0
Prunus persica mRNA *(pp ACO1)*	AB044711	90 %	959	0.0
Fragaria ananassa mRNA	AY706156	85 %	747	0.0
Fagus sylvatica mRNA	AJ420190	83 %	644	0.0
Morus alba mRNA	DQ785807	84 %	630	2e-177
Fragaria ananassa mRNA	AJ851828	85 %	617	3e-173
Populus euramericana mRNA	AB033504	83 %	585	1e-163
Hit 15: *Betula pendula* mRNA -	AY154649	83 %	571	9e-159
Hit 44: *MD-ACO1* mRNA	DQ137848	81 %	571	9e-159
Hit 45:*MD-ACO1* mRNA (ripe fruit cortex)	**X61390**	81 %	345	7e-94
Hit 77:*MD-ACO2* genomic DNA	**AF015787**	80 %	224	4e-55

Searched on 27 August 2006 (E value; refer section 2.2.6.1)

3.1.6.3 Analysis of the Deduced Translational Sequences of Each of the ACC Oxidase Proteins

From a deduced translation of each of the three ACO open reading frames (ORFs), amino acid sequences were aligned and compared (Figure 3.7).

Enzyme activity requires that some specific amino acid residues be conserved. Apple ACO has been observed to require the residues H^{177}, D^{179} and H^{234} to bind iron in the active site (Shaw *et al.*, 1996; Kadyrzhanova *et al.*, 1997; 1999), and R^{244}, S^{246} and T^{157} as binding sites for the ACC carboxyl group (Kadyrzhanova *et al.*, 1999; Dilley *et al.*, 2003; Seo *et al.*, 2004). Also in apple ACO, the lysine residues K^{158}, K^{230} or K^{292} are strongly implicated for ascorbate activation (Kadyrzhanova *et al.*, 1999; Dilley *et al.*, 2003) and residue R^{175} has been proposed to bind directly to $NaHCO_3$ (Dilley *et al.*, 2003). Eight lysine residues (K^{72}, K^{144}, K^{158}, K^{172}, K^{199}, K^{230}, K^{292} and K^{296}) observed in apple ACO are conserved in other species (Kadyrzhanova *et al.*, 1997; 1999), and like K^{158}, K^{230} or K^{292} the other five lysine residues (K^{72}, K^{144}, K^{172}, K^{199}, K^{296}) may possibly also be involved in ascorbate binding. For apple ACO residues in the C-terminus, E^{297}, R^{299} and E^{301} are important for enzyme activity, and particularly R^{299} which may be involved in the mechanism of CO_2 activation (Kadyrzhanova *et al.*, 1999). Also three conserved cysteine residues C^{28}, C^{133} and C^{165} have been observed of which the C^{28} residue only is important for catalysis (Kadyrzhanova *et al.*, 1997; 1999), MD-ACO3 contains a fourth cysteine residue at position 60 (C^{60}).

In other species residues H^{39}, H^{56}, Q^{78}, E^{80}, D^{83}, H^{94}, H^{211}, F^{250}, N^{252}, Y^{285}, Y^{289} (and from residues E^{302} and M^{304} in the C-terminus) are important for ACO catalytic activity (Tayeh *et al.*, 1999; Zhang *et al.*, 1997; Zhang *et al.*, 2004b), and are present in the MD-ACOs. Stabilization of the double stranded beta sheet (DSBS) by residues F^{33}, I^{184}, L^{186}, F^{187}, Q^{188}, L^{195}, L^{197}, V^{206}, V^{214}, V^{215}, V^{236}, F^{250} and other residues necessary for the stabilisation of the secondary structure of *Petunia hybrida* ACO are Y^{57}, R^{64}, L^{68}, A^{79}, M^{84}, D^{85}, W^{86}, D^{219}, E^{222}, K^{279}, Y^{285}, L^{288}, F^{294}, K^{297}, R^{300}, M^{304} (Zhang *et al.*, 2004b), and all of these residues are present in the MD-ACO isoforms.

One of the protein cleavage sites observed by Zhang *et al.*, (2004b) between L^{186} and F^{187} is present in all MD-ACO isoforms. However, the second cleavage site between V^{214} and V^{215} is absent, but rather the isoleucine residue occurs at position 215 (I^{215}) instead of a valine residue (V^{214}) are observed in the MD-ACOs.

The presence of all of these residues supports the probability that *MD-ACO1*, *MD-ACO2* and *MD-ACO3* transcripts will encode functional ACOs.

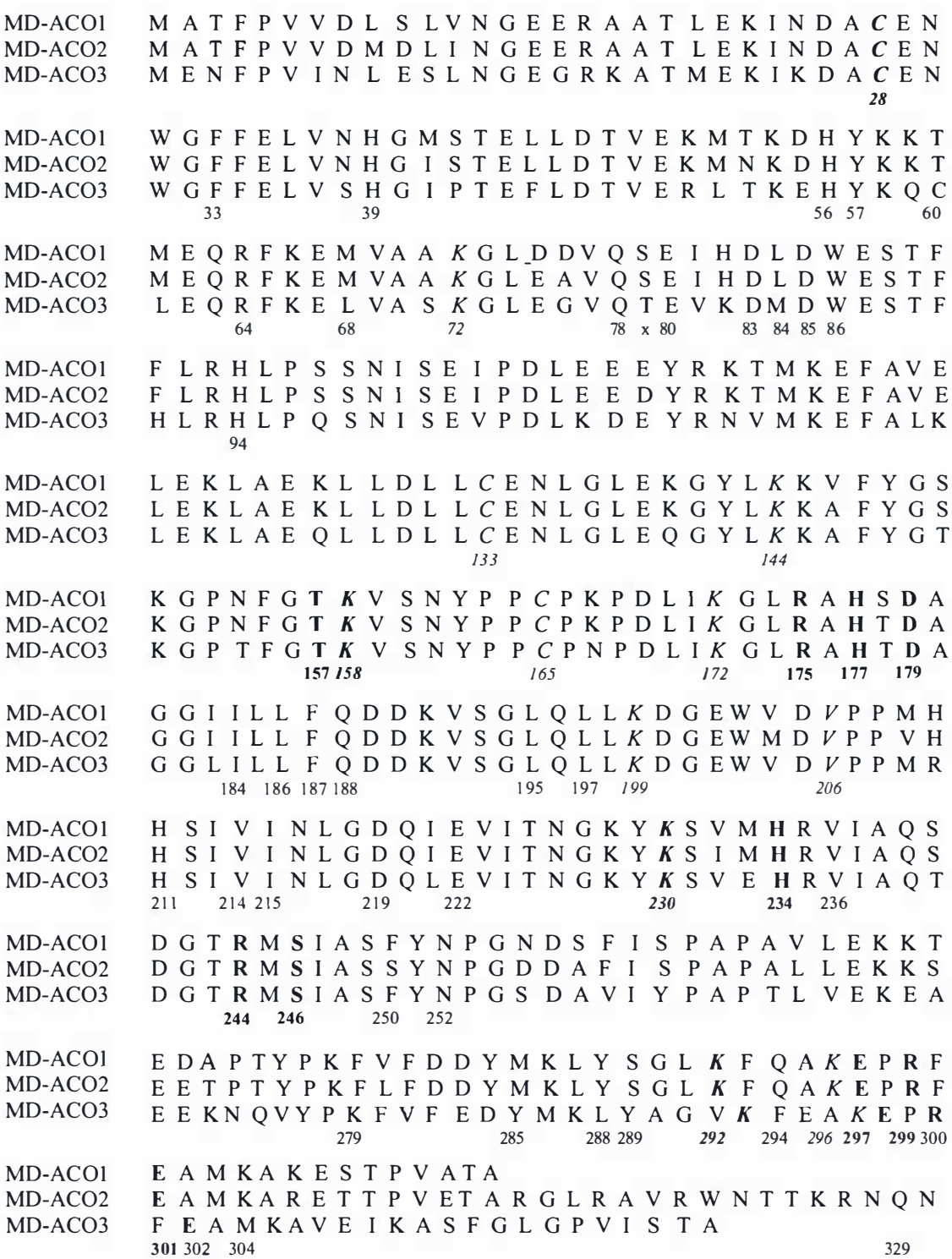


Figure 3.7: Comparison of the Deduced Amino Acid Sequences of the Open Reading Frames of MD-ACO1, MD-ACO2 and MD-ACO3.

Amino acids important for apple ACO activity are in bold, and the conserved lysines and cysteines are italicized. Amino acids important for the activity and for the stabilization of the ACO secondary structure in other species, are also indicated.

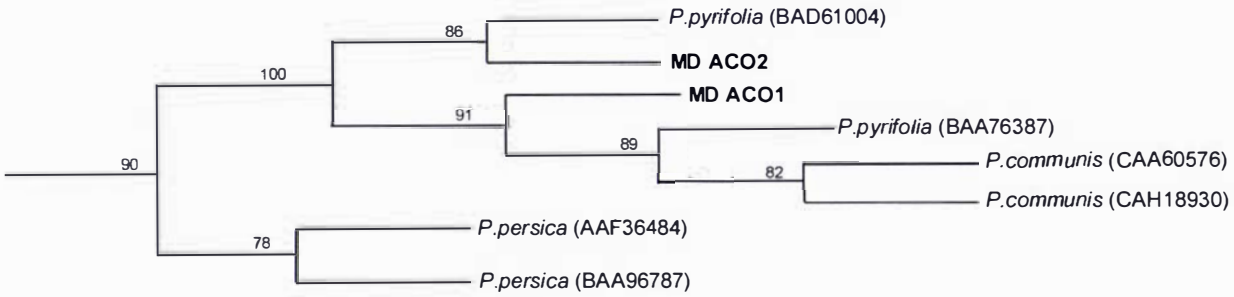
A phylogenetic tree constructed from an alignment of eighty five ACO sequences obtained from the NCBI protein database with the deduced amino acid sequences for *MD-ACO1*, *MD-ACO2* and *MD-ACO3* over the entire open reading frame is shown as Appendix 1A and the full name of each entry as Appendix 1B. As the phylogenetic tree is so large it is convenient to only show the *MD-ACO1* and *MD-ACO2* groupings from the tree (Figure 3.8A), and the groupings around *MD-ACO3* (Figure 3.8B) separately. Clearly, *MD-ACO3* is encoded from a gene distinct as the major splits of the tree are far removed from those of both *MD-ACO1* or *MD-ACO2* (Appendix 1A). Also there is reasonable evidence that *MD-ACO1* and *MD-ACO2* are each encoded by distinct genes as they are two splits apart on the tree (Figure 3.8A). *MD-ACO1* and *MD-ACO2* are grouped with *PP-ACO2* (peach fruit, unspecified developmental state), while *MD-ACO3* is grouped with *PP-ACO1* (from softening, ripening and wounded fruit). Interestingly, *PC-ACO1* (European pear) and *JP-AOX1* and *PP-AOX4* (Asian pear) associate with *MD-ACO1* and *MD-ACO2* which are expressed in immature and unripe mature fruit; in contrast to *PP-AOX2A*, *PP-AOX2B* and *JP-AOX3* (Asian pear) which associate with *MD-ACO3* and are expressed in ripe fruit tissue.

3.1.7 Confirmation by Southern Analysis that *MD-ACO3* is Encoded by a Gene Distinct from *MD-ACO1*and *MD-ACO2*

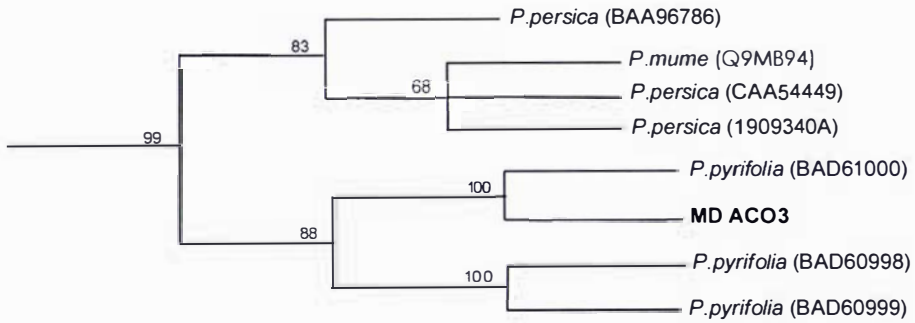
Prior to Southern analysis of *MD-ACO1*, *MD-ACO2* and *MD-ACO3*, the specificity of these genes as gene-specific probes was examined. This was undertaken because they are similar in nucleotide sequence (Table 3.7), particularly *MD-ACO1* and *MD-ACO2* (ORF 93.9 %), and so have the potential to cross-hybridise. Therefore, the probes were designed to include the 3′ terminal end of the ORF and some 3′-UTR (but do not include any restriction sites) and hence advantage was taken of the lower identity between their 3′-UTR sequences (Table 3.7B), as well as the variation in their ORF lengths (Figure 3.7). The *MD-ACO1* probe (182 bp) shares a 71.1 % identity with the *MD-ACO2* probe (145 bp) with a 135 bp overlap, and shares a 59.1 % identity with the probe for *MD-ACO3* (273 bp) with a 257 bp overlap. The *MD-ACO3* probe shares 64.4 % identity with the *MD-ACO2* probe with a 64 bp overlap. The blots were hybridized with [α-^{32}P]-dATP labelled *MD-ACO1*, *MD-ACO2* or *MD-ACO3* sequences and then washed at high stringency (0.1 x SSPE, 0.1 % (w/v) SDS at 65 °C). No cross-hybridization was detected between any of the three ACO sequences (Figure 3.9). Such washing conditions were then used in subsequent DNA and RNA blot analysis.

Southern analysis was performed using genomic DNA isolated from *Malus domestica* (section 2.2.7.1). Firstly, to examine whether the genomic DNA was completely digested (indicated by a smear rather than distinct bands), aliquots (100 ng) of digested genomic DNA were separated on agarose 1 % (w/v) by electrophoresis on a mini gel and visualised by ethidium bromide

A


P.pyrifolia (BAD61004)
86
MD ACO2
100
MD ACO1
91
P.pyrifolia (BAA76387)
89
P.communis (CAA60576)
90
82
P.communis (CAH18930)
P.persica (AAF36484)
78
P.persica (BAA96787)

B


P.persica (BAA96786)
83
P.mume (Q9MB94)
68
P.persica (CAA54449)
P.persica (1909340A)
99
P.pyrifolia (BAD61000)
100
MD ACO3
88
P.pyrifolia (BAD60998)
100
P.pyrifolia (BAD60999)

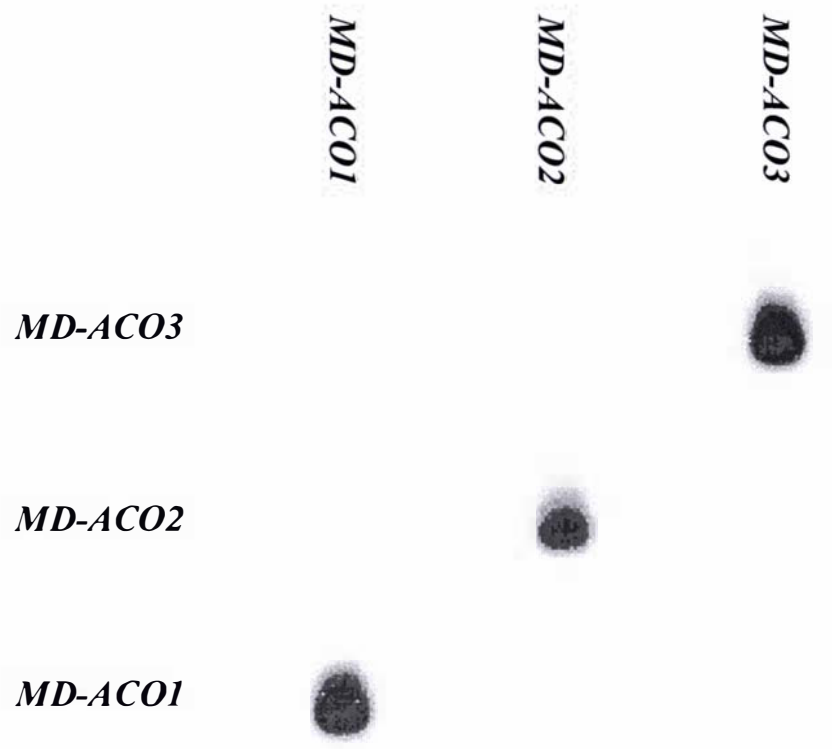


Figure 3.9: Specificity of *MD-ACO1*, *MD-ACO2* and *MD-ACO3* as Probes in Blotting Analysis

Each lane contains 50 ng of *MD-ACO1*, *MD-ACO2* and *MD-ACO3* cDNA sequences as indicated. The blots were hybridized with ^{32}P labelled cDNA probes *MD-ACO1*, *MD-ACO2* and *MD-ACO3* as indicated, and washed at high stringency (0.1 x SSPE, 0.1 % (w/v) SDS at 65 ºC).

staining (Figure 3.10A). As ethidium bromide may interfere with the transfer of DNA from gel to Hybond^{TM}-N^{+} membrane, for Southern analysis, the agarose gels were not stained with ethidium bromide. For Southern analysis aliquots (25 μg) of restriction enzyme digested genomic DNA (section 2.2.7.2)„ were separated on 0.8 % (w/v) agarose gel by electrophoresis (section 2.2.4.3) at 30 V for 18 h, and then transferred onto the Hybond^{TM}-N^{+} membrane (section 2.2.7.3).

Southern analysis confirmed that *MD-ACO3* was encoded by a gene distinct from both *MD-ACO1* and *MD-ACO2* genes as the hybridization pattern is clearly very distinct (Figure 3.10B). Although the fragment sizes for *MD-ACO1* and *MD-ACO2* were similar in the *Eco*RI, *Hind*III and *Xba*I lanes, *MD-ACO2* has fewer and less intense bands overall.

Digestion with *Eco*RI reveals a fragment which strongly hybridises to *MD-ACO1* (at *ca.* 2.5 kb), but appears not to hybridise to *MD-ACO2* or *MD-ACO3.* However, hybridization of both *MD-ACO1* and *MD-ACO2* to fragments of *ca.* 5.0 kb and 8.0 kb is observed, and *MD-ACO1* also hybridizes to larger fragments of *ca.* 10.5 kb and 12 kb. Although a number of fragments have lightly hybridised to *MD-ACO3*, they are rather indistinct smears which descend to approximately 2.9 kb, but predominantly larger fragments (of more than 8 kb). Digestion with *Hind*III revealed only one fragment which hybridised strongly with *MD-ACO2* (of *ca.* 1.9 kb), compared to two fragments which hybridised strongly with *MD-ACO1* (of *ca.* 1.5 and 1.9 kb), and fragments of *ca.* 3.3 kb, 5 kb and 6 kb hybridize with *MD-ACO3.* The *MD-ACO3* probe has strongly hybridized to a single fragment cut with *Xba*I (of *ca.* 5.1 kb), the *MD-ACO1* and *MD-ACO2* hybridization patterns are less distinct. For example, one fragment which hybridised lightly but distinctly with *MD-ACO2* of *ca.* 15 kb, and a number of fragments which hybridised with *MD-ACO1* are barely detectable against the smear which descends to approximately 6 kb, nevertheless a fragment of *ca.* 15 kb is faintly distinguishable. There are other, less intense bands, even at high stringency which may suggest the presence of sequences related but not totally identical to *MD-ACO1*, *MD-ACO2* and *MD-ACO3.* It should be noted that the probe sequence for all of the *MD-ACO*s do not contain restriction digestion sites for *Eco*RI, *Hind*III or *Xba*I. Although both *MD-ACO1* and *MD-ACO2* have *Hind*III restriction sites at the same site in the third exon (Figure 3.6), *MD-ACO2* also has a *Hind*III site within the first intron, giving a fragment of 630 bp. However, *MD-ACO1* has three *Hind*III restriction sites (Figure 3.6): there is 70 bp between the two *Hind*III sites within intron two, 130 bp between the downstream *Hind* III site within intron 2 and the *Hind*III site within exon 3, making a total of 200 bp between the upstream *Hind*III site within intron 2 and the *Hind*III site within exon 3. There are 1,340 bp between *Eco*RI restriction sites within the *MD-ACO1* genomic sequence between intron 2 and the 3′-UTR. The probes for each of the *MD-ACO*s are specific (Figure 3.9)

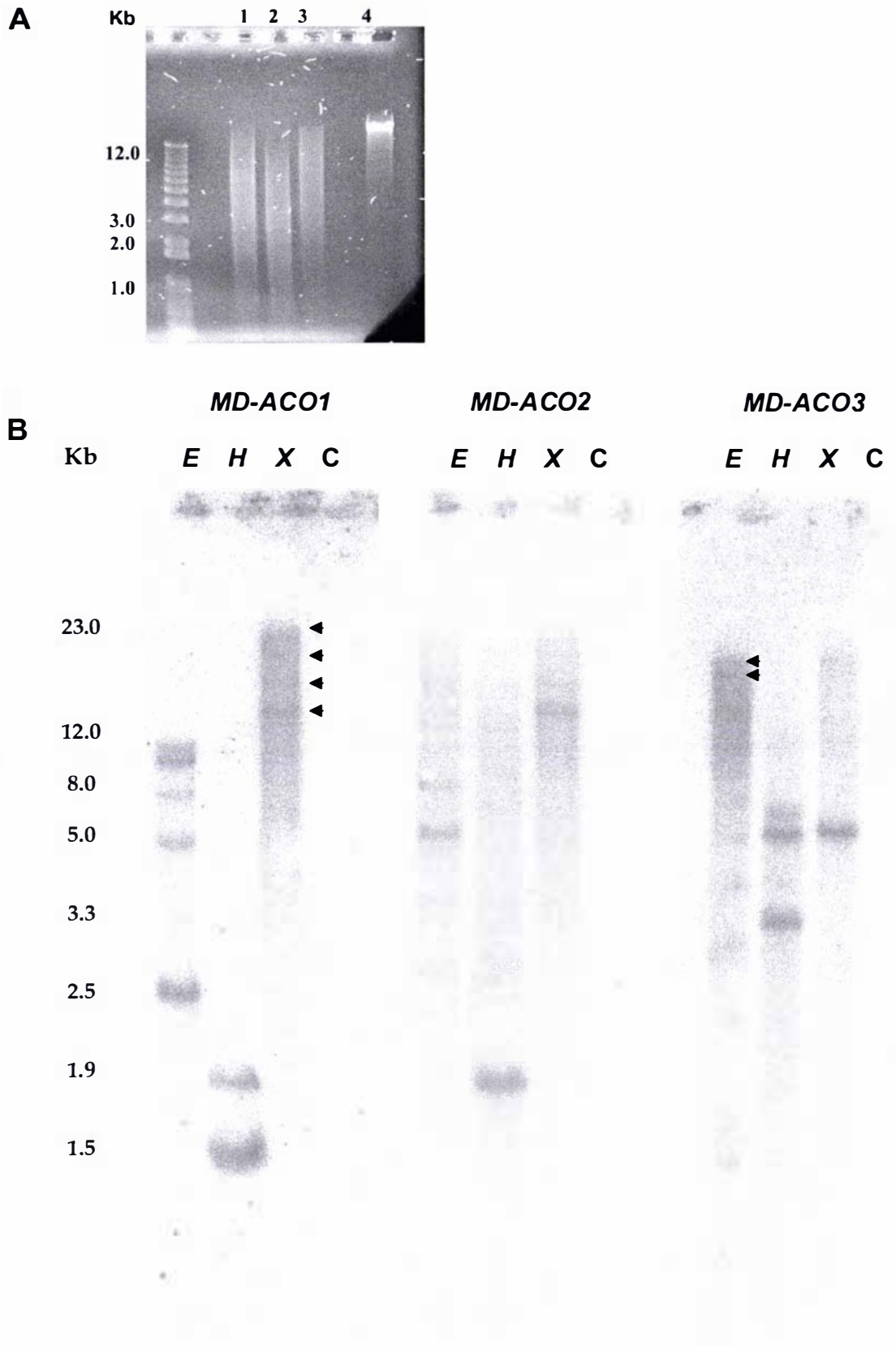


Figure 3.10: Southern Analysis of *Malus domestica* Genomic DNA

A. Digested DNA visualised by ethidium bromide staining (mini-gel)

B. Hybridisation pattern of ^{32}P labelled *MD-ACO1*, ^{32}P labelled *MD-ACO2*, ^{32}P labelled *MD-ACO3*. Lane 1: digested with *EcoRI* (E), Lane 2: digested with *HindIII* (H), Lane 3: digested with *Xba* I (X), Lane 4: undigested DNA control (C). Molecular sizes are indicated. FujiFilm Fluoro Image Analyser FLA-5000.

and the same digestion mixture was aliquoted for each of the *MD-ACO*s for each of the three restriction digestions. Even though Gala apple has 34 chromosomes and the haploid number is 17 (Westwood, 1993), and is thought to be a functional diploid (Korban *et al.*, 2004), it is usually classified as an allopolyploid (Newcomb *et al.*, 2006) or ancient tetraploid, and so allelic forms of the genes may differ. However, the possibility that *MD-ACO1* and *MD-ACO2* are encoded by distinct genes can not be ruled out, and will be evaluated further in the Discussion section.

3.1.8 Evidence that Three Members of the *MD-ACO* Multi-gene Family are Differentially Expressed *In Vivo*.

A Virtual Northern was supplied by Dr Andrew Allen, HortResearch in Auckland, (Figure 3.11), and was compiled from data gathered by HortResearch for the construction of an expressed sequenced tags (ESTs) library. In this analysis EST 179706 and EST 192136 (*MD-ACO3*) are closely associated with leaf tissue rather than the fruit tissue (fruit stored @ 0.5 °C for 24 h), EST 153710 (*MD-ACO2*) is expressed in the fruit tissue and spur buds, while *MD-ACO1* (clone *pAP4*) is expressed only in fruit tissue in this data set.

Figure 3.11: Virtual Northern: The Cultivar and Tissue Type from which the *MD-ACO1*, *MD-ACO2* and *MD-ACO3* EST Sequences were Generated and Days After Full Bloom (DAFB) is also indicated.

cDNA sequence	Cultivar and tissue type from which the RNA was extracted.
EST 179706 (*MD-ACO3*)	Gala seedling leaves infected with Venturia inaequalis Gala pre-opened vegetative bud
EST 192136 (*MD-ACO3*)	Gala fruit stored @ 0.5°C for 24 h Gala seedling leaves infected with Venturia inaequalis Pinkie expanding leaf Gala partially senescing leaf
EST 153710 (*MD-ACO2*)	Apple fruit cortex, tree ripened fruit 150 DAFB Apple skin peel, tree ripened fruit 150 DAFB Gala 126 DAFB fruit cortex Spur buds from OFF Pacific Rose trees Gala fruit stored for 24 h under low oxygen/high CO2
clone *pAP4* cDNA (*MD-ACO1*)	Gala fruit stored for 24h under low oxygen/high CO_2 Apple fruit cortex, tree ripened fruit 150 DAFB Apple skin peel, tree ripened fruit 150 DAFB Gala 126 DAFB fruit cortex

To ascertain in which apple tissue *MD-ACO1*, *MD-ACO2* and *MD-ACO3* were transcribed, RNA was extracted (section 2.2.2.1) from the tissue of initial leaf (collected on 15.10.03), mature fully expanded leaf (collected on 07.04.04), young fruit (~ 2 cm diameter, collected on 16.12.03) and mature fruit (collected on 23.02.04). An RT reaction using an oligo $d(T)_{15}$ primer generated cDNA was used as template, followed by a 30 cycle PCR amplification at an annealing temperature of 55 °C, using gene-specific primers (refer Table 2.2) for the putative *MD-ACO1* [pProEx-1(MD1F) and pProEx-1(MD1R)], *MD-ACO2* [pProEx-1(MD2F) and pProEx-1(MD2R)], and *MD-ACO3* [pProEx-1(MD3F) and pProEx-1(MD3R)]. Fragments generated by RT-PCR were separated by agarose gel electrophoresis (section 2.2.4.3) and visualised using ethidium bromide staining (Figure 3.12).

Using this degree of sensitivity, *MD-ACO1*, *MD-ACO2* and *MD-ACO3* appear to have different expression patterns *in vivo*. Primers specific for *MD-ACO1* amplified products from mature apple fruit tissue (Figure 3.12), and less intensely from young apple fruit tissue. In contrast, primers specific for *MD-ACO2* amplified products from each apple tissue examined, young leaf, mature leaf, young fruit and mature fruit, while *MD-ACO3* gene specific primers amplified products from all tissues but less intensely from mature fruit.

Primers were designed to generate PCR produces, to be used in relative quantitative RT-PCR (section 2.2.3.4), and as targets for the hybridization of probes in cDNA Southern blot analysis (sections 2.2.7.4, 2.2.7.5 and 2.2.7.6). Primers were designed in such a way as to span the second intron-exon boundaries of the target mRNA (Table 2.2), and thus prevent amplification of the target region from any contaminating genomic DNA that may be present in the template RNA. Although any PCR product so produced would probably be distinquishable by its larger size, such a control reduces ambiguity and leaves all of the reaction mixture available for amplification of the RNA template.

Semi-quantitative RT-PCR (section 2.2.3.4) was used to examine the variation in the abundance of *MD-ACO1*, *MD-ACO2* and *MD-ACO3* transcripts in apple tissue from young leaf, mature leaf, young fruit and mature fruit. Random primers were used to generate cDNA from total RNA extracts and particular care was taken to ensure that the amount of RNA used in each of the RT reactions was exactly the same, thus allowing a comparison to be made across the different apple tissues. Since the expression of ribosomal RNA is invariant, it can provide a credible quantitative internal control. *MD-ACO* fragments were then amplified in one PCR round of 25 cycles at an annealing temperature of 55 °C, using gene-specific forward primers MD-ACO1, Md1(rtpcr)intron2/F; MD-ACO2, Md2(rtpcr)intron2/F and MD-ACO3, Md3 (rtpcr)intron2/F (Table 2.2) which span the exon-intron boundaries of the second intron and

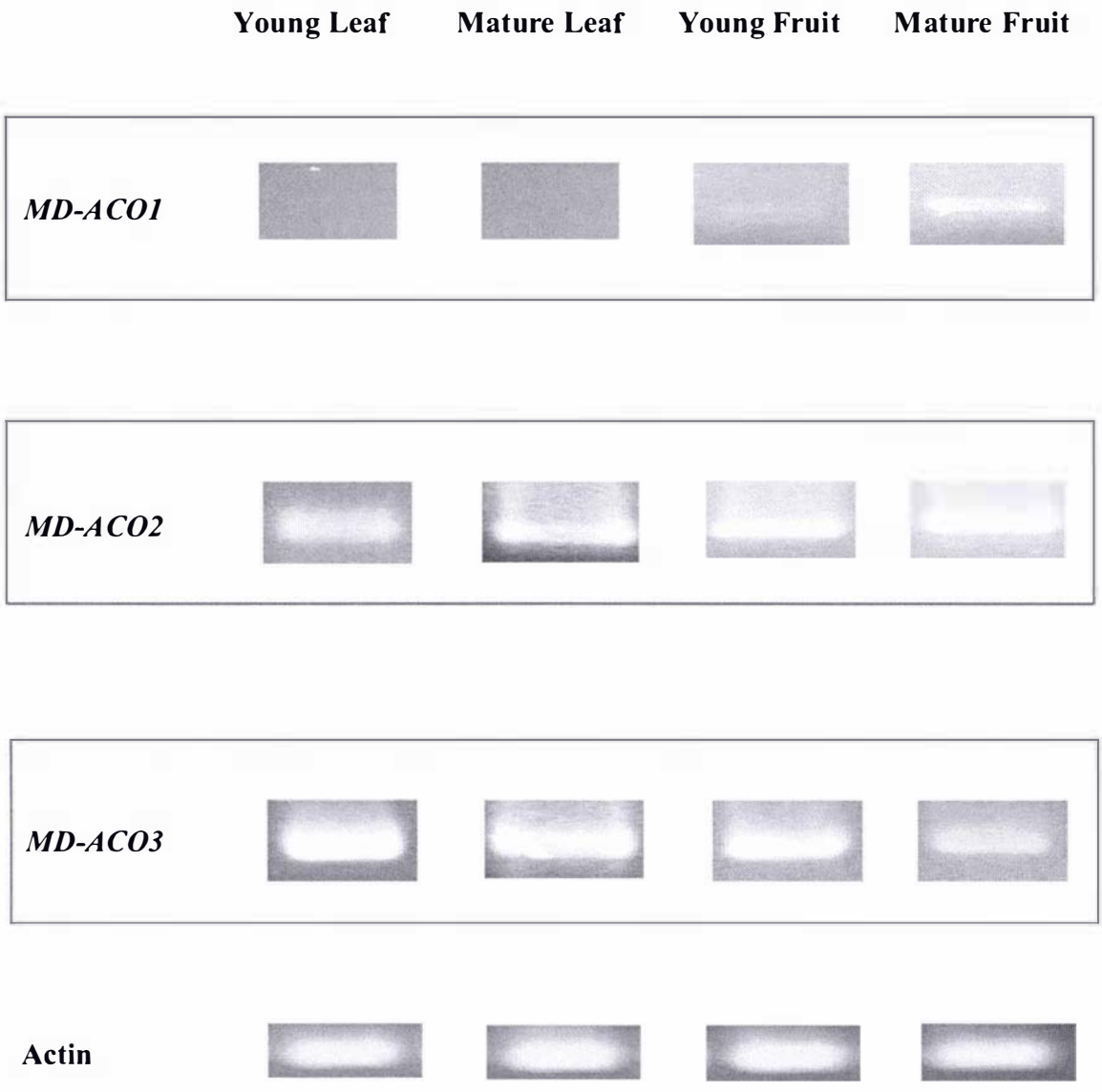


Figure 3.12: Evidence that *MD-ACO1*, *MD-ACO2* and *MD-ACO3* are Expressed Differentially *In Vivo*.

Fragments were generated by RT-PCR, using an oligo d(T)15 primer for the RT reaction and gene-specific primers (as indicated) for thirty PCR cycles at an annealing temperature of 55 °C, and visualised using ethidium bromide staining. Lane 1: young leaf, Lane 2: mature leaf, Lane 3: young fruit, Lane 4 mature fruit. Primers used *MD-ACO1*, pProEx-1(MD1F) and pProEx-1(MD1R); *MD-ACO2*, pProEx-1(MD2F)and pProEx-1(MD2R), and *MD-ACO3*, pProEx-1(MD3F) and pProEx-1(MD3R).

gene-specific reverse primers (MD-ACO1, Md1 3′-UTR; MD-ACO2, Md2 3′-UTR and MD-ACO3, Md3 3′-UTR; Table 2.2)(Figure 3.13). Primers were used at a final concentration of 400 nM (section 2.2.3.2), as well as a mixture of a 1:4 ratio of 18S rRNA primers : competimers (section 2.2.3.4) at a final concentration of 800 nM in the standard PCR reaction mixture.

Quantitative analysis of *MD-ACO1, MD-ACO2* and *MD-ACO3* gene expression is shown as Figure 3.14, and the amplification products of the expected sizes are indicated for ribosomal RNA (315 bp), *MD-ACO1* (800 bp), *MD-ACO2* (790 bp) and *MD-ACO3* (800 bp). Primers specific for *MD-ACO1* amplified products from mature apple fruit tissue (Figure 3.14), and less intensely from young apple fruit tissue, with no visible band for either young or mature green leaf tissue. By contrast, primers specific for *MD-ACO2* amplified products from each apple tissue, but with a greater intensity in the fruit tissue whilst *MD-ACO3* gene specific primers amplified products in all tissues, although less intensely in tissue from mature fruit.

A decision was made to further investigate the gene expression of *Malus domestica* using cDNA Southern blot analysis and X-ray film imaging. Southern blot analysis is very sensitive, and allows the use of fewer PCR cycles to ensure that each reaction is compared on the linear part of the curve in terms of rate of amplification.

An RT reaction using an oligo $d(T)_{15}$ primer (rather than random primers necessary for relative quantitative RT-PCR when using the S18 ribosomal controls) was used to generate cDNA from total RNA extracted from young leaf, mature leaf, young fruit and mature fruit, and was followed by two PCR amplification rounds of 20 cycles each, at an annealing temperature of 55 °C, using the forward degenerate primer (Degen.F.South; Table 2.2) and gene-specific 3′-UTR primers (Md1 3′-UTR, Md2 3′-UTR and Md3 3′-UTR; Table 2.2)(data not shown). DNA sequencing confirmed the sequences (*ca.* 815 bp) to be ACO. Originally it was intended to use degenerate primers for the cDNA Southern analysis so that exactly the same cDNA mixture can be challenged by each individual probe sequence of *MD-ACO1*, *MD-ACO2* and *MD-ACO3* (Table 2.2) in separate hybridization reactions, and also since only one set of primers is used, any variability amongst primers is controlled for. However, a true degenerate reverse primer could not be developed in the 3′-UTR due to the lack of conserved regions between all three *MD-ACO* genes, and multiple T nucleotides serve as a poor primer (Frohman *et al.*, 1988), so a semi-degenerate primer was made up of a mixture of the same three gene-specific reverse primers (Md1 3′-UTR, Md2 3′-UTR and Md3 3′-UTR; Table 2.2) used in Figure 3.14. The reverse primer concentration in each PCR reaction mixture was the usual *ca.* 400 nM (section 2.2.3.2).

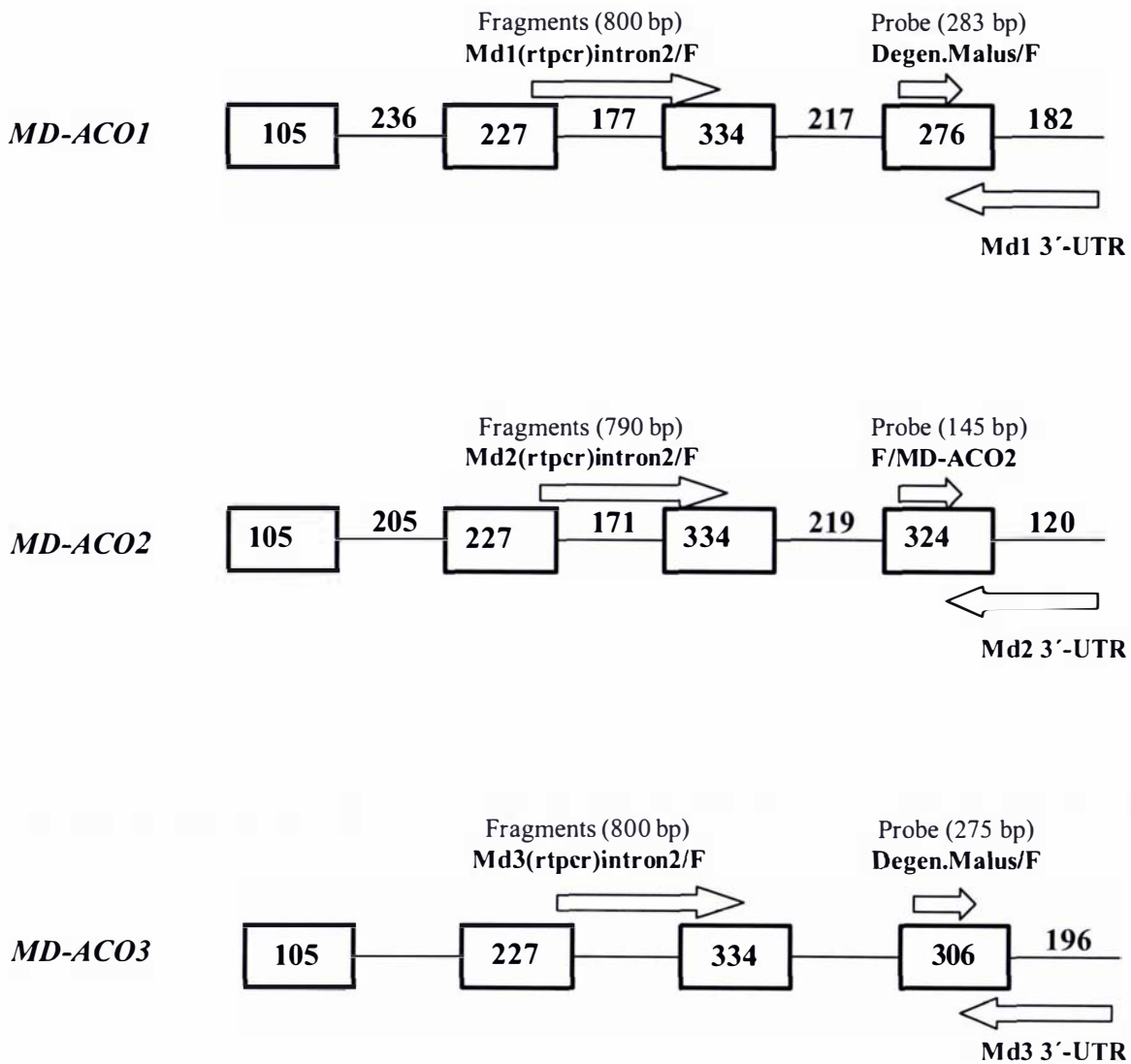


Figure 3.13: The position of the forward intron spanning primers of *MD-ACO1*, *MD-ACO2* and *MD-ACO3*, the forward position of the probe primers, and the reverse 3′-UTR primers used for both fragments and probes.

The boxes indicate the exon sequences and the numbers represent DNA sequence length in base pairs. The lines between the boxes represent the intron sequences, and the numbers indicate DNA. Intron spanning forward primers are indicated, the primer sequence on the second exon is length in base pairs continuous with the sequence on the third exon so that the entire second intron sequence is completely excluded. The reverse primers are in the 3′-UTR and run into the fourth exon. The forward primers for the probes are also indicated. For the nucleotide sequences refer to Table 2.2.

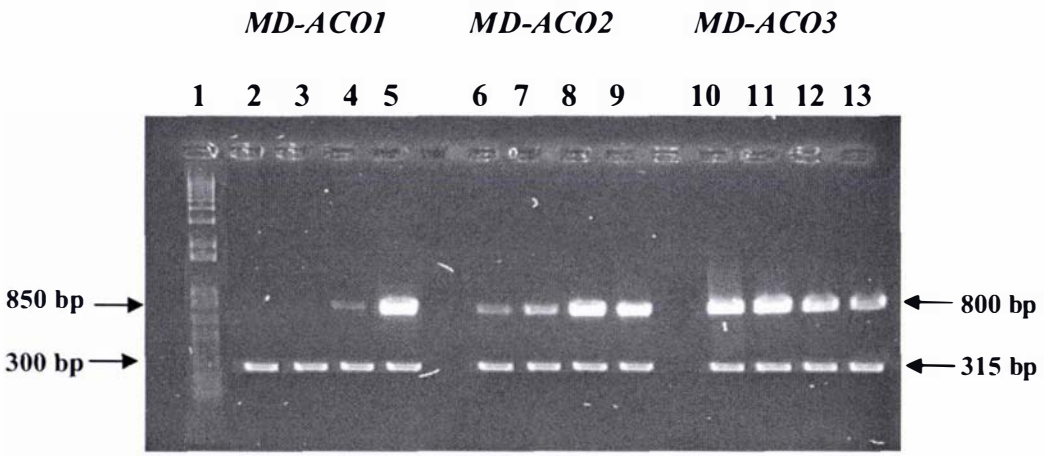


Figure 3.14: Relative Quantitative RT-PCR Analysis of *MD-ACO1*, *MD-ACO2* and *MD-ACO3* Differential Expression *In Vivo*.

Lane 1: 1Kb DNA ladder (Gibco BRL), Lanes 2, 6 and 10: RNA extracted from young leaf tissue, Lanes 3, 7 and 11: RNA extracted from mature leaf tissue, Lanes 4, 8 and 12: RNA extracted from young fruit tissue, Lanes 5, 9 and 13: RNA extracted from mature fruit tissue. Two of the DNA standards are indicated on the left of the figure. The approximate size of the amplification products are indicated by arrows to the right of the figure (18S ribosomal RNA *ca.* 315 bp; putative MD-ACOs *ca.* 790 to 800 bp), and visualized using ethidium bromide staining.

cDNA was generated from total RNA extracted from young leaf, mature leaf, young fruit and mature fruit by an RT reaction using an oligo $d(T)_{15}$ primer. Twenty PCR cycles were used to amplify the fragments of interest using the degenerate forward primer Degen.F.South (Table 2.2) and the semi-degenerate reverse primer, at an annealing temperature of 55 °C. As DNA hybridization is much more sensitive than ethidium bromide staining, one PCR amplification round was used and 20 or 30 PCR cycles. Univeral actin primers were used as a control. Aliquots (15 µL) of cDNA from each tissue were separated on 1 % (w/v) agarose on three separate mini-gels by electrophoresis at 80 V (section 2.2.4.3) for *ca.* 1 h 30 min, and the fragments then transferred on to the Hybond^{TM}-N^+ membrane (section 2.2.7.4). Triplicate blots containing the same cDNA mixtures from apple tissue (young leaf, mature leaf, young fruit and mature fruit) were probed with [α-^{32}P]-dATP labelled *MD-ACO1*, *MD-ACO2* or *MD-ACO3* sequences and then washed at high stringency.

MD-ACO1, *MD-ACO2* and *MD-ACO3* are differentially expressed as confirmed by cDNA Southern analysis (Figure 3.15). *MD-ACO1* appears to be specific to the fruit tissue as no *MD-ACO1* transcript was detected in the leaves. *MD-ACO2* and *MD-ACO3* are expressed in all tissue, but for *MD-ACO2* the bands are more intense in fruit tissue, whilst for *MD-ACO3* the bands are more intense in the leaf tissue. The expression data (Figures 3.12, 3.14 and 3.15) reflects the virtual northern data (refer Figure 3.11), in that *MD-ACO1* is expressed in apple fruit tissue and is not detected in leaf tissue. *MD-ACO2* and *MD-ACO3* are expressed in both leaf and fruit tissue, but whereas *MD-ACO2* is more abundant in fruit tissue, *MD-ACO3* is expressed predominantly in leaf tissue.

In summary, therefore, the semi-quantitative RT-PCR analysis (Figure 3.14) and the cDNA Southern analysis (Figure 3.15) confirm the following differential expression patterns. *MD-ACO1* occurs predominantly in mature fruit tissue with some expression in young fruit tissue. *MD-ACO2* occurs predominantly in fruit tissue but also in leaf tissue. *MD-ACO3* occurs predominantly in young leaf tissue but also in fruit tissue.

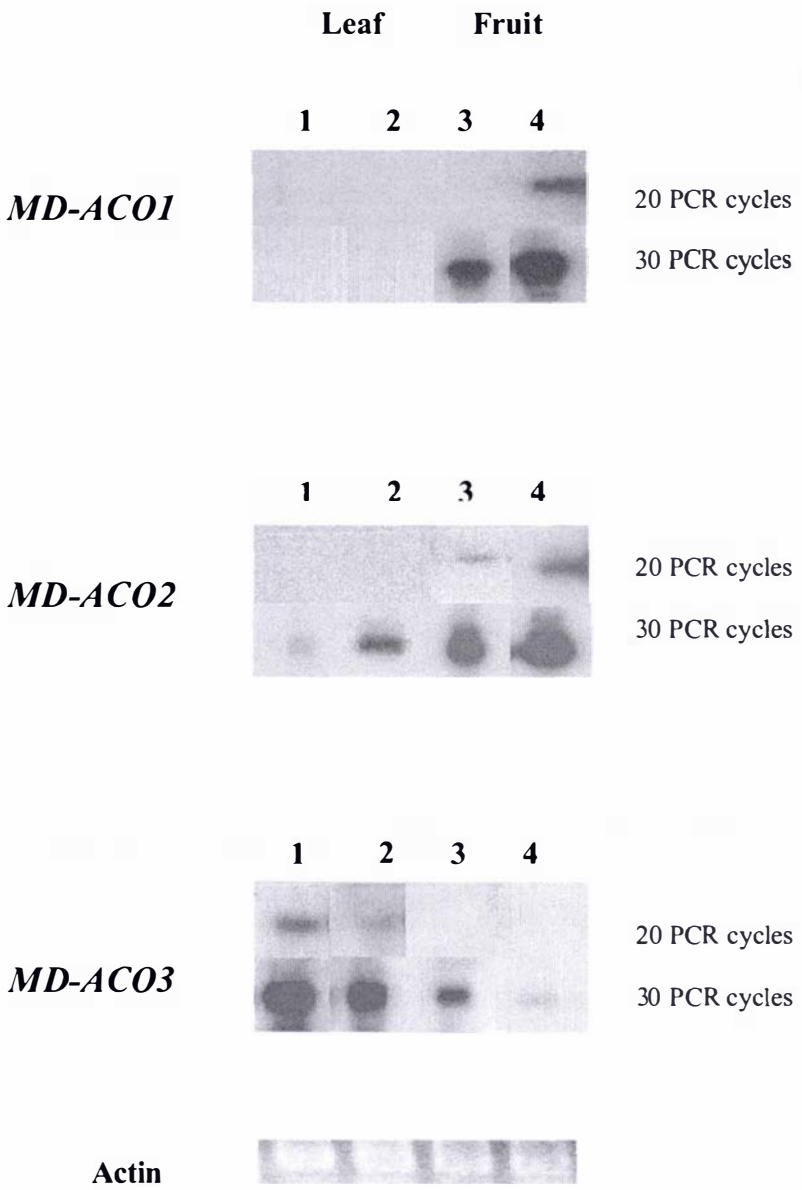


Figure 3.15: Confirmation that *MD-ACO1*, *MD-ACO2* and *MD-ACO3* are Differentially Expressed *In Vivo* using cDNA Southern Analysis.

Fragments generated by RT-PCR, using an oligo d(T)15 primer for the RT reaction and degenerate primers, for either one round of 20 PCR cycles, or one round of 30 PCR cycles (as indicated). Hybridisation of ^{32}P labelled *MD-ACO1*, ^{32}P labelled *MD-ACO2*, ^{32}P labelled *MD-ACO3* are indicated. Lane 1: young green leaf, Lane 2: mature green leaf, Lane 3: young fruit and Lane 4: mature fruit. Fragment sizes are *ca.* 790 to 800 bp. Kodak Xar-6 X-ray film and developed in an automatic X-ray film processor.

3.2 Expression and Characterization of MD-ACO1, MD-ACO2 and MD-ACO3 as Recombinant Proteins

3.2.1 Protein Expression of MD-ACO1, MD-ACO3 and MD-ACO3

3.2.1.1 Expression of Recombinant Protein in *E. Coli*

The open reading frame (ORF) sequences were directionally cloned into the pGEX expression vector (Figure 2.3) using gene-specific primers designed to incorporated restriction enzyme sites (Table 2.2). Primers used to select the ORF from the *pAP4* plasmid template contained the *Eco*RI restriction site in the forward primer and the *Sal*I restriction site in the reverse primer (had already been cloned in the McManus lab). Primers used to select the putative *MD-ACO2* ORF from the plasmid template (EST 120223) contained the *Eco*RI restriction site in the forward primer and the *Sal*I restriction site in the reverse primer. Primers used to select the ORF from the putative MD-ACO3 ORF (EST 192136 and 179706) plasmid template contained the *Bam*H1 restriction site in the forward primer and the *Xho*I restriction site in the reverse primer. Following one round of PCR amplification, the fragments were separated on 1 % (w/v) agarose gel and visualized with ethidium bromide (data not shown). Each of the cDNA fragments contains the ORF (*MD-ACO1*, 942 bp; *MD-ACO2*, 990 bp and *MD-ACO3*, 966 bp), plus the extra nucleotides comprising the cap, the restriction site and any additional nucleotides necessary to ensure the first ATG codon (encoding methionine) is in-frame, to give final PCR product sizes for *MD-ACO1* of 972 bp, *MD-ACO2* of 1,017 bp and *MD-ACO3* of 993 bp.

The ORFs of *MD-ACO1*, *MD-ACO2* and *MD-ACO3* were expressed as a translational fusion with glutathione-S-transferase (GST) in *E. coli* (initially strain DH5α and then strain BL-21) using the pGEX expression vector. Following cleavage of GST from the recombinant protein, using PreScission™ Protease (Amersham Pharmacia), the protein was examined using either SDS-PAGE stained with coomassie or transferred to a membrane for western analysis. A comparison of each of the three MD-ACO proteins is shown as Figure 3.16. The gene products of *MD-ACO1* (35.84 kDa) and *MD-ACO2* (37.99 kDa) are migrating as expected. However, the (putative) MD-ACO3 (encoded from EST 192136 and 179706) appears to have a lower molecular mass which is inconsistent with the expected weight determined by the sequence of amino acids between the PreScission Protease cleavage site and the stop codon of 36.8 kDa (refer Table 3.9). Also inconsistent with autocleavage between lysine at position 186 and phenylalaline at position 187 (Zhang *et al.*, 2004b), which would be expected to generate fragments of 26.2 kDa and 10.60 kDa.

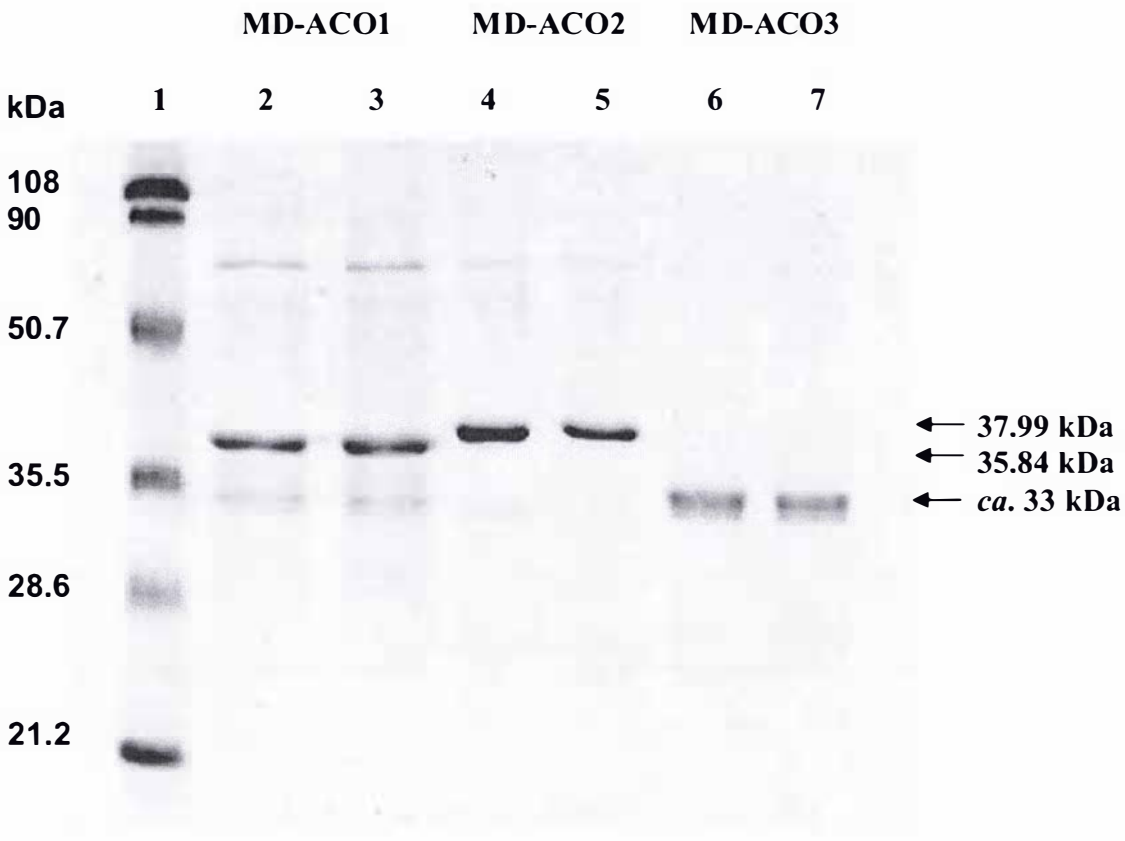


Figure 3.16: MD-ACO1, (Putative) MD-ACO2 and (Putative) MD-ACO3 Expressed in *E. coli* (strain BL-21) using the pGEX Expression Vector.

Recombinant proteins were separated using SDS-PAGE and stained with coomassie brilliant blue. Each lane was loaded with 4 µg of protein. Lane 1: Calibrated low range molecular weight marker (BioRad), Lanes 2 and 3: recombinant MD-ACO1 (35.84 kDa), Lanes 4 and 5: putative recombinant MD-ACO2 (37.99 kDa), Lanes 6 and 7: putative recombinant MD-ACO3 (*ca.* 33 kDa). The mass of each protein as indicated on the right of the figure are calculated from the translated sequence.

Table 3.9: A Comparison of MD-ACO1, (Putative) MD-ACO2 and (Putative) MD-ACO3: including number of base-pairs, number of amino acids, protein mass and theoretical pI.

	MD-ACO1	MD-ACO2	MD-ACO3
Base-pairs (bp)	942	990	966
Amino acids (aa)	314	330	322
Molecular mass (kDa)	35.35	37.50	36.314
pI (theoretical)	5.24	5.52	5.28
Modified Molecular Masses			
[1](+4 or +7 aa) pGEX kDa	35.84	37.99	36.797
(+24 aa) pProEX-1 kDa	38.53	40.39	39.263
(+3 aa) His-tag removed	36.47	38.65	37.71

[1]MD-ACO1 and MD-ACO2 have 7 extra amino acids (from the *Eco*RI site in the MCS), and MD-ACO3 has 4 extra amino acids (from the *Bam*HI site in the MCS).

MD-ACO1 is not deemed 'putative' as validation of the amino acid sequence or an MD-ACO had been confirmed previously by sequencing the protein (McManus and Scott *pers comm.*). Similarly, the MD-ACO2 protein was sequenced and found to have the N-terminal sequence M A T F P V V D M D which distinguishes the sequence from the MD-ACO1 amino acid sequence of M A T F P V V D L S (refer Figure 3.7). Further, the predicted masses of MD-ACO1 and MD-ACO2 do differ (Table 3.9) and the recombinant proteins did differ in mass after separation using SDS-PAGE (Figure 3.16). Therefore, there is good evidence that MD-ACO2 is the gene product of *MD-ACO2*. To clarify the discrepancy in molecular mass, the < 36.8 kDa MD-ACO3 protein was also prepared for amino acid N-terminal sequence analysis (section 2.3.11.4) on PVDF membrane, stained with coomassie brilliant blue (data not shown), and sent to the Protein Microchemistry Facility of the Department of Biochemistry at Otago University. The N-terminal amino acid sequence M E N F P V I N L E was confirmed and is in agreement with the deduced amino acid sequence for MD-ACO3 (Figure 3.7). This suggests firstly that MD-ACO3 is the gene product of *MD-ACO3* (and therefore the 'putative' term can be dispensed with) and also that the truncation of MD-ACO3 was not within the N-terminal region of the protein. Since studies have shown that truncation of the carboxyl end of ACO results in loss of enzymatic activity (Zhang *et al.*, 2004b), and the enzyme is prone to fragmentation and backbone auto-cleavage (Zhang *et al.*, 1997), an activity assay of each of the MD-ACOs was undertaken in order to support the hypothesis that the MD-ACO3 was truncated at the carboxyl terminus. After expression in pGEX, both MD-ACO1 and MD-ACO2 are active

(refer Figure 3.17), whereas the MD-ACO3 is clearly inactive which may suggest polypeptide chain cleavage within the C-terminus domain.

As a consequence of the apparent MD-ACO3 truncation in the pGEX vector, the *MD-ACO3* ORF sequence was directionally cloned into the pProEX-1 expression vector (Figure 2.4) using gene-specific primers designed with restriction enzyme sites (Table 2.2). A comparison of the molecular mass of MD-ACO3 expressed in *E. coli* (strain BL-21) using the pGEX vector, with a preliminary induction (section 2.3.1) of recombinant MD-ACO3 expressed in *E. coli* (strain BL-21) using the pProEX-1 vector is shown as Figure 3.18. Aliquots (7 µg) of recombinant protein were separated using a 10 to 20 % gradient gel (section 2.3.10.2), and MD-ACO3 expressed in the pGEX vector is estimated to be *ca.* 33 kDa (Figure 3.18, Lane 2). Since the gene product of *MD-ACO3*, expressed using the pProEX-1 vector (Figure 3.18, Lane 3 uninduced and Lane 4 induced with IPTG) is now migrating as expected (39.3 kDa), it was decided that the ORF sequences of *MD-ACO1* and *MD-ACO2* should also be cloned into the pProEX-1 expression vector. For comparative kinetic analysis of MD-ACO1, MD-ACO2 and MD-ACO3, the expression of all three enzymes in the same expression system is necessary to control for any variation there may be in enzyme activity due to the different expression vector systems.

3.2.1.2 Purification of His-Tagged Fusion Proteins

MD-ACO1, MD-ACO2 and MD-ACO3 expressed in *E. coli* (strain BL-21), using the pProEX-1 vector, were separated from bacterial protein contaminants by metal chelate chromatography (section 2.3.4). Following SDS-PAGE and coomassie staining or western blot analysis, bands of the expected mass were detected for MD-ACO1 (38.53 kDa), for MD-ACO2 (40.39 kDa) and for MD-ACO3 (39.26 kDa) (asterisks in Figure 3.19).

However, significant unexpected bands were also detected by coomassie staining and by Western blot analysis. An ACO assay was undertaken for each of the three MD-ACOs of the expected mass, together with the unexpected lower mass proteins that were also recognised by the MD-ACO1 and MD-ACO3 antibodies (see section 3.2.2)(▲ in Figure 3.19) after these were separated using Mono-Q anion exchange chromatography (see Figure 3.20). Ethylene measurement by gas chromatography determined all three MD-ACO proteins of the expected mass to be active. In contrast the lower molecular mass proteins were inactive. As more intense staining of the non active *ca.* 36 kDa protein occurs for MD-ACO3 than for either MD-ACO1 or MD-ACO2 (Figure 3.19) N-terminal amino acid sequencing of this protein was performed. A sequence of M E N F P V I N L was obtained which aligns with the N-terminus of MD-ACO3 thereby confirming the sequence to be MD-ACO3, and suggesting that the

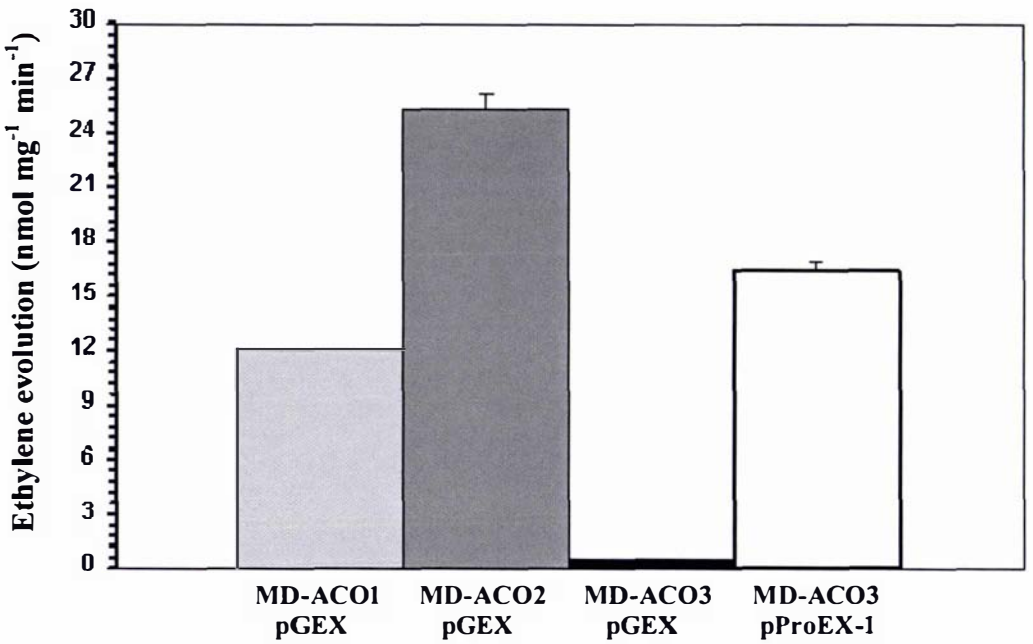


Figure 3.17: Specific Activities of Recombinant MD-ACO1, MD-ACO2 and MD-ACO3 Expressed in the pGEX Vector

Ethylene evolution was determined by gas chromatography in parts per million (ppm), and converted to nmol mg^{-1} min^{-1} from which the specific activities of each enzyme were calculated. The standard ACO assay reaction mixture was used. The specific activity of the MD-ACO3 expressed in the pProEX-1 expression vector (Figure 2.4) is also included as a comparison. Values and means ● SE (n = 6).

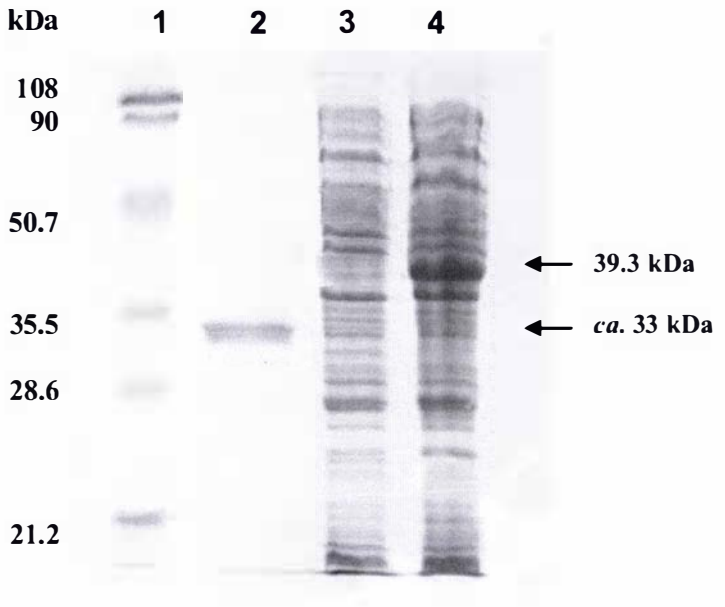


Figure 3.18: Comparison of the Molecular Mass of Recombinant MD-ACO3 Expressed using the pGEX Vector with MD-ACO3 Expressed using the pProEX-1 Vector, after Separation on a 10 to 20 % SDS-PAGE Gradient Gel.

Aliquots (7 μg) of recombinant protein were separated using the gradient gel SDS-PAGE system. Lane 1: Calibrated low range molecular weight marker (BioRad), Lane 2: MD-ACO3 expressed in *E. coli* using pGEX, Lane 3: uninduced MD-ACO3 expressed in *E. coli* using pProEX-1, Lane 4: induced MD-ACO3 expressed with IPTG in *E. coli* using pProEX-1. The estimated molecular weights of MD-ACO3 are indicated to the right.

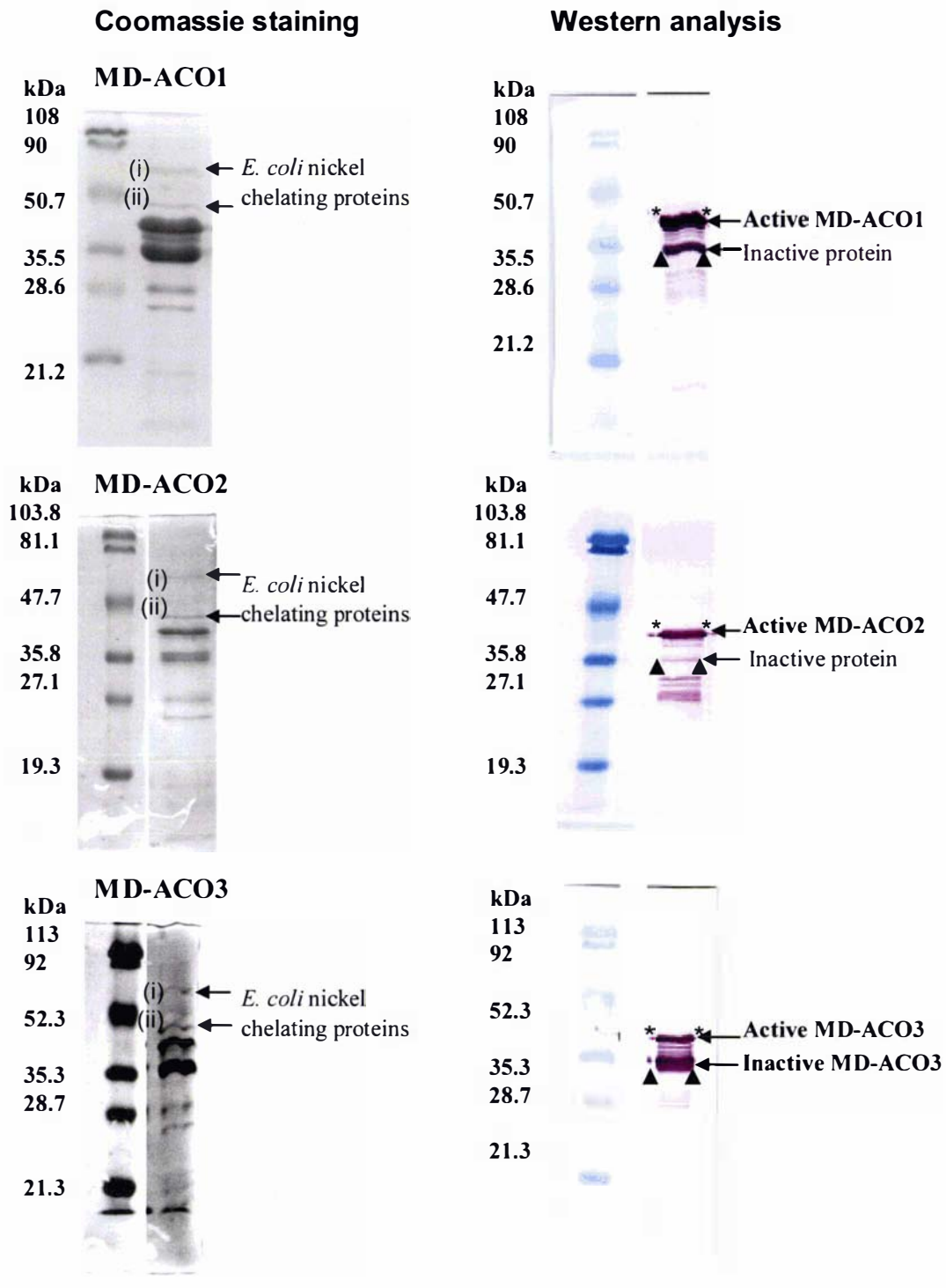


Figure 3.19: SDS-PAGE of MD-ACO1, MD-ACO2 and MD-ACO3 Following Metal Chelate Chromatography.

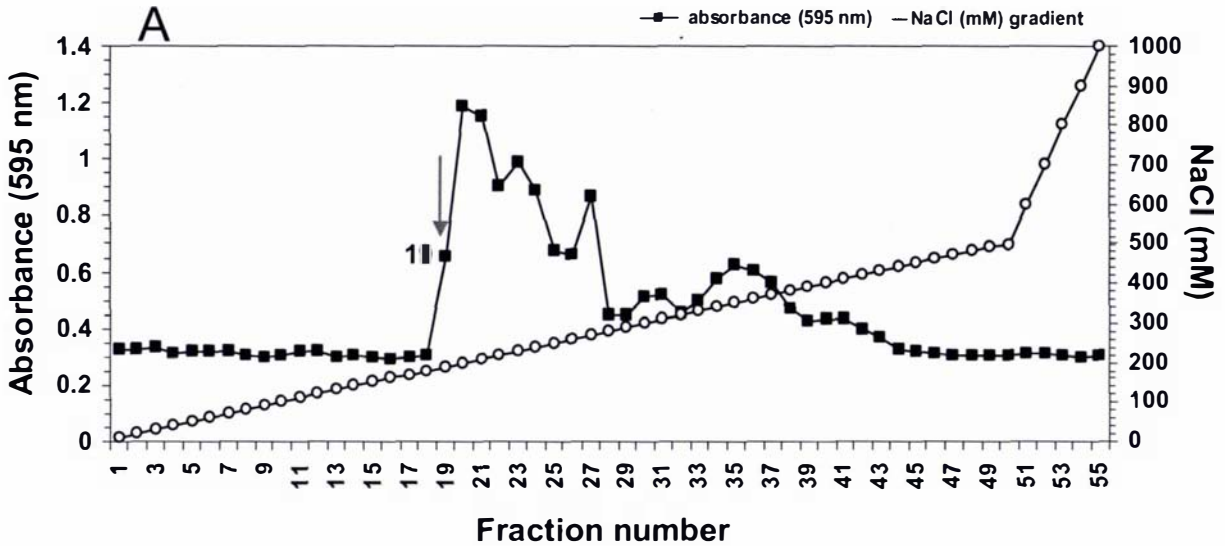
For coomassie staining each lane contains 4 µg of protein and for western analysis each lane contains 0.4 µg of protein. The calibrated low molecular weight marker is shown and the nickel chelating *E. coli* proteins as well as the active and inactive MD-ACO fragments are indicated. The separated MD-ACO1 and MD-ACO2 recombinant proteins were challenged with the anti-MD-ACO1 antibody. The separated MD-ACO3 recombinant protein was challenged with anti-MD-ACO3 antibody.

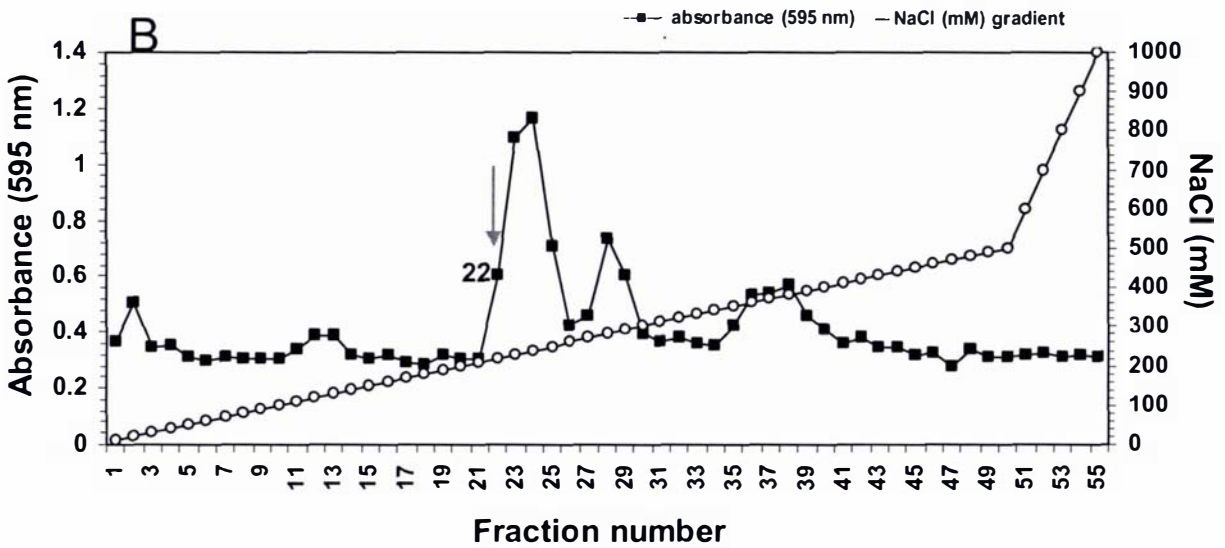
truncation occurred again through the C-terminal domain. The reason for this apparent degradation of MD-ACO3 in particular is unclear, even though all three isoforms contain an autocleavage site (between L^{186} and F^{187}; Zhang *et al.*, 2004b). Such a cleavage would leave recombinant MD-ACO3 fragments of *ca.* 26.2 kDa and *ca.* 10.60 kDa, and although there are some bands at approximately *ca.* 26.2 kDa, fragmentation appears to occur predominantly at *ca.* 36 kDa.

Following N-terminal amino acid sequencing of the higher mass bands (*ca.* $\geq$ 45 kDa) visible on the coomassie stained gels and undetectable by western analysis (Figure 3.19) the proteins were determined to be the nickel chelating *E. coli* proteins, succinylornithine transaminase (i) and glucosamine-fructose-6-phosphate aminotransferase (ii).

As indicated previously the recombinant proteins were to be used for kinetic analysis and so it was necessary to separate the active protein from the inactive protein fragments using fast protein liquid chromatography (FPLC). Following desalting through a G-25 packed column (section 2.3.5), the MD-ACO1, MD-ACO2 and MD-ACO3 samples were individually injected onto a Mono Q column using the FPLC (section 2.3.6) under exactly the same conditions, using the same buffers and salt gradient at pH 7.5. The Bradford Protein assay (section 2.3.7) was used to determine which fractions contained protein (Figure 3.20 A, B and C). In order to ascertain which fractions contained active recombinant ACO, and whether the inactive MD-ACO protein fragments had been successfully separated, western blot analysis was used. Further, to determine whether the nickel chelating contaminants had also been separated from the active ACO, the acrylamide gels were stained with coomassie following SDS-PAGE. Protein concentrations were determined from a standard equation (section 2.3.7), and then diluted ten fold to give 0.4 μg of protein per lane for the western blot analyses and 4 μg per lane of protein for the coomassie stained acrylamide gels (data not shown).

Active recombinant ACO began to elute from the anion exchange column at a slightly different salt concentration for each isoform. For example, MD-ACO1 began eluting at 180 mM of NaCl (collected in fraction 19; Figure 3.20A), MD-ACO2 began eluting at 210 mM of NaCl (collected in fraction 22; Figure 3.20B), and MD-ACO3 began eluting at 190 mM of NaCl, (collected in fraction 20; Figure 3.20C). All three of the MD-ACO proteins were eluted within a linear salt gradient representing a NaCl concentration change of 0 to 1M NaCl over 60 min (under exactly the same conditions, i.e. buffers and FPLC programme). The NaCl concentration at which MD-ACO1 (180 mM), MD-ACO2 (210 mM) and MD-ACO3 (190 mM) eluted from the Mono Q column is compared in Table 3.10 with the estimated isoelectric point (pI; ExPASy) of each of the *Malus domestica* ACO isoforms.


A
absorbance (595 nm)
NaCl (mM) gradient
Absorbance (595 nm)
NaCl (mM)
Fraction number
11


B
absorbance (595 nm)
NaCl (mM) gradient
Absorbance (595 nm)
NaCl (mM)
Fraction number
22

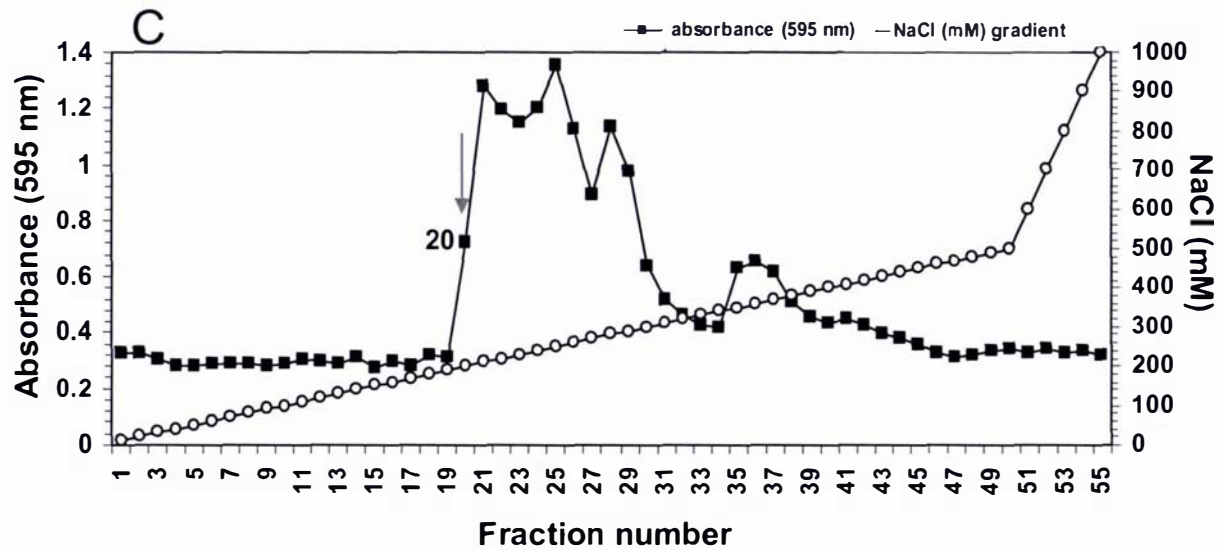

C
absorbance (595 nm)
NaCl (mM) gradient
Absorbance (595 nm)
NaCl (mM)
Fraction number
20

Table 3.10: NaCl Concentration at which MD-ACO1, MD-ACO2 and MD-ACO3 Elute from the Mono Q Column at pH 7.5, Compared with the Estimated pI of Each of the Proteins:

	NaCl (mM)	Theoretical pI
MD-ACO1	180-210	5.24
MD-ACO2	210-240	5.52
MD-ACO3	190-220	5.28

Fractions containing the separated active recombinant ACO were used for subsequent kinetic analysis (Figure 3.21).

3.2.2 Characterization of Polyclonal Antibodies Raised Against MD-ACO Fusion Proteins

Initially, polyclonal IgG antibodies raised against MD-ACO1 (translational product of *pAP4*; Ross *et al.*, 1992) were used for western blot analysis to examine whether they would recognise the ACO protein in apple fruit and leaf tissue. Proteins from apple fruit showed strong recognition at a molecular mass of *ca.* 35.8 kDa (lanes 3, 4 and 5; Figure 3.22) following ACO extraction using 1 % (v/v) Triton. In contrast, only a barely perceptible band appeared in mature fully expanded green leaf tissue extracts (lane 1; Figure 3.22) and senescent leaf tissue extracts (lane 2; Figure 3.22). Further western blot analysis using only apple leaf samples (initial leaf, mature fully expanded green leaf and senescent leaf tissue) showed antibody recognition at higher weights after over 30 min of development time, and bands were imperceptable at 35.35 kDa (data not shown). These results suggested either that the antibodies raised against MD-ACO1 (translational product of *pAP4*; Ross *et al.*, 1992) were best at recognising this isoform, and that the ACO isoform(s) in leaf tissue were distinct MD-ACO proteins, or that the MD-ACO1 was expressed at very low levels in apple leaf tissue.

Antibodies were also raised in this thesis against the recombinant MD-ACO3 isoform (refer section 2.3.11.1) and used for western blot analysis to examine whether they would recognise the ACO protein in apple leaf tissue. Apple leaf samples (Lanes 4, 5 and 6; Figure 3.23) showed antibody recognition at the expected weight of MD-ACO3 (36.3 kDa), and also apple fruit samples (Lanes 7 and 8; Figure 3.23) showed antibody recognition but at a slightly lower molecular mass. This is not unexpected as climacteric apple fruit is known to accumulate a great abundance of ACO (Dong *et al.*, 1992; Dilley *et al.*, 1993), and hence the MD-ACO3

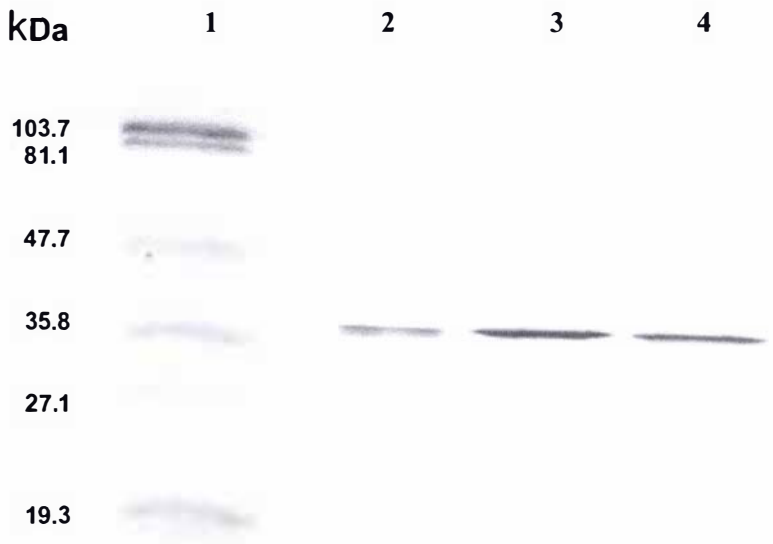


Figure 3.21: Recombinant His-tagged Proteins after Purification by Metal Chelate Affinity Chomatography, Sephadex G-25 and Anion Exchange Chromatography.

Apple recombinant ACC oxidase fractions used for kinetic analysis. SDS-PAGE stained with coomassie brilliant blue. Each lane contains 4 μg of protein. Lane 1: Calibrated low range molecular weight marker (BioRad), Lane 2: recombinant MD-ACO1 from fraction 20, Lane 3: recombinant MD-ACO2 from fraction 19, Lane 4: recombinant MD-ACO3 from fraction 22 (refer Figure 3.20).

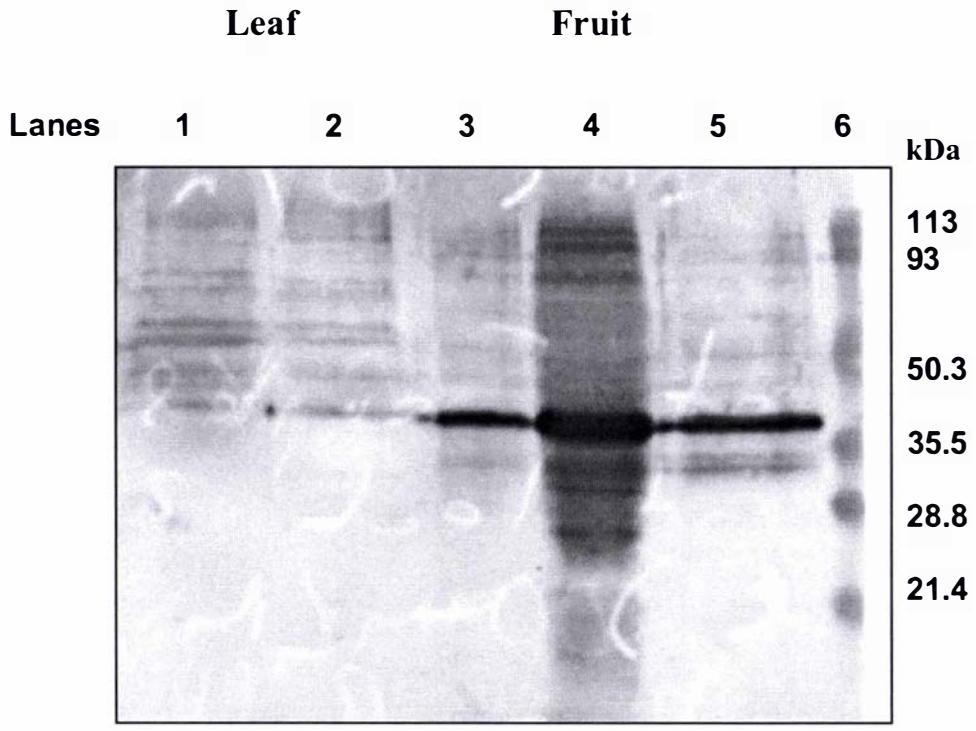


Figure 3.22: Detection of ACC Oxidase in Apple Fruit and Apple Leaves using Antibody Raised Against MD-ACO1 on Western Blot

10 μg of protein was loaded per well and ACC oxidase was detected using antibody raised against recombinant MD-ACO1 in rabbit, and then using an anti-goat secondary antibody conjugated to alkaline phosphatase. Lane 1. Mature fully expanded green leaf tissue; Lane 2. Senescent leaf tissue; Lane 3. Fruit supernatant; Lane 4. Fruit pellet; Lane 5. Fruit pellet extracted using 1% Triton (v/v); Lane 6. SDS-PAGE (low range) standards.

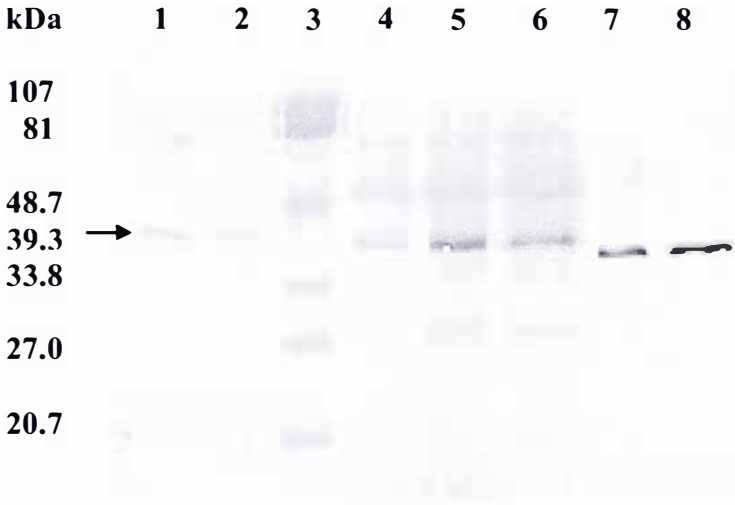


Figure 3.23: Detection, using Western Analysis, of ACC Oxidase in Apple Fruit and Apple Leaves by an Antibody Raised Against MD-ACO3

Lane 1: Recombinant MD-ACO3 (5.0 μg of protein per well), Lane 2: Recombinant MD-ACO3 (2.5 μg of protein per well), Lane 3: SDS-PAGE (low range) standards, Lane 4: Leaf tissue (extracted in 0.1 % Triton and 2 mM DTT) (10 μg of protein per well), Lane 5: Leaf tissue (extracted in 1.0 % Triton) (10 μg of protein per well), Lane 6: Leaf tissue (extracted in 10 mM DTT) (10 μg of protein per well), Lane 7: Fruit tissue (extracted in 0.5 % Triton) (10 μg of protein per well), Lane 8: Fruit tissue (extracted in 1.0 %Triton) (10 μg of protein per well).

antibody may also be recognising a MD-ACO isoform of a lower molecular mass in the fruit tissue. Antibodies were not raised against the recombinant MD-ACO2 isoform as the MD-ACO1 and MD-ACO2 isoforms are relatively similar in terms of amino acid sequence and it was considered that any accumulation of MD-ACO2 protein would be recognised by the antibody raised against the MD-ACO1 isoform. The cross-reactivity of the MD-ACO1 and MD-ACO3 antibodies was examined using recombinant proteins. At high concentrations of separated recombinant protein, both MD-ACO1 and MD-ACO3 antibodies did cross-react and recognise MD-ACO1, MD-ACO2 and MD-ACO3. To produce antibodies that could discriminate between these two isoforms, either monoclonal antibodies are necessary or polyclonal antibodies produced to specific peptides. Both of these approaches were outside the scope of this thesis.

3.2.2.1 Protein Accumulation of MD-ACO1/MD-ACO2 and MD-ACO3 in Apple Tissue

In order to confirm the accumulation pattern of the MD-ACO isoforms as determined by the antibodies available, ACO was extracted (section 2.1.4) from the following apple tissues using 1 % (v/v) Triton: initial apple leaf (collected on 16.12.03), mature fully expanded apple leaf (collected on 07.04.04), young fruit (~ 2 cm diameter, collected on 16.12.03) and mature fruit (collected on 23.02.04). Aliquots of apple tissue extract containing 20 μg of protein were examined by western analysis (section 2.3.11) using antibodies raised against the gene products of *MD-ACO1* and *MD-ACO3* (refer section 2.3.11.1). The results indicate that in apple, the accumulation of ACO is tissue specific (Figure 3.24). Antibodies raised against MD-ACO1 recognise protein predominantly in the mature apple fruit extract (Figure 3.24A; lane 3), while antibodies raised against MD-ACO3 recognise protein predominantly in young leaf tissue (Figure 3.24B, Lane 4), and also in young fruit and mature leaf tissue (Figure 3.24B, Lanes 2 and 5).

3.2.2.2 Protein Analysis: Removal of the His-Tag

Prior to kinetic analysis of the three apple ACOs, an experiment to determine the effect of His-tag removal on recombinant MD-ACO2 and recombinant MD-ACO3 activity was undertaken (Figure 3.25). The extra 24 amino acids comprising the hexahistidine tag, spacer region and the TEV protease cutting site was removed using TEV protease (refer section 2.3.4.2), leaving only 3 additional amino acids on the N-terminal end of the proteins. Although TEV protease is maximally active at 34 °C and typically overnight, Nallamsetty *et al.* (2004) recommend performing the digest at room temperature (20 °C) or 4 °C overnight. TEV protease is only three-fold less active at 4 °C than at 20 °C (Nallamsetty *et al.*, 2004), but given the well



Figure 3.24: Accumulation of MD-ACO1/MD-ACO2 and MD-ACO3 in Various Tissues of Apple.

Western blot analysis using antibodies raised against MD-ACO1 (A) and antibodies raised against MD-ACO3 (B). Lane 1: Prestained low range molecular markers (Bio-Rad), Lane 2: young fruit tissue, Lane 3: mature fruit tissue, Lane 4: young leaf tissue, Lane 5: mature leaf tissue. All tissue samples were extracted in 1 % (v/v) Triton.

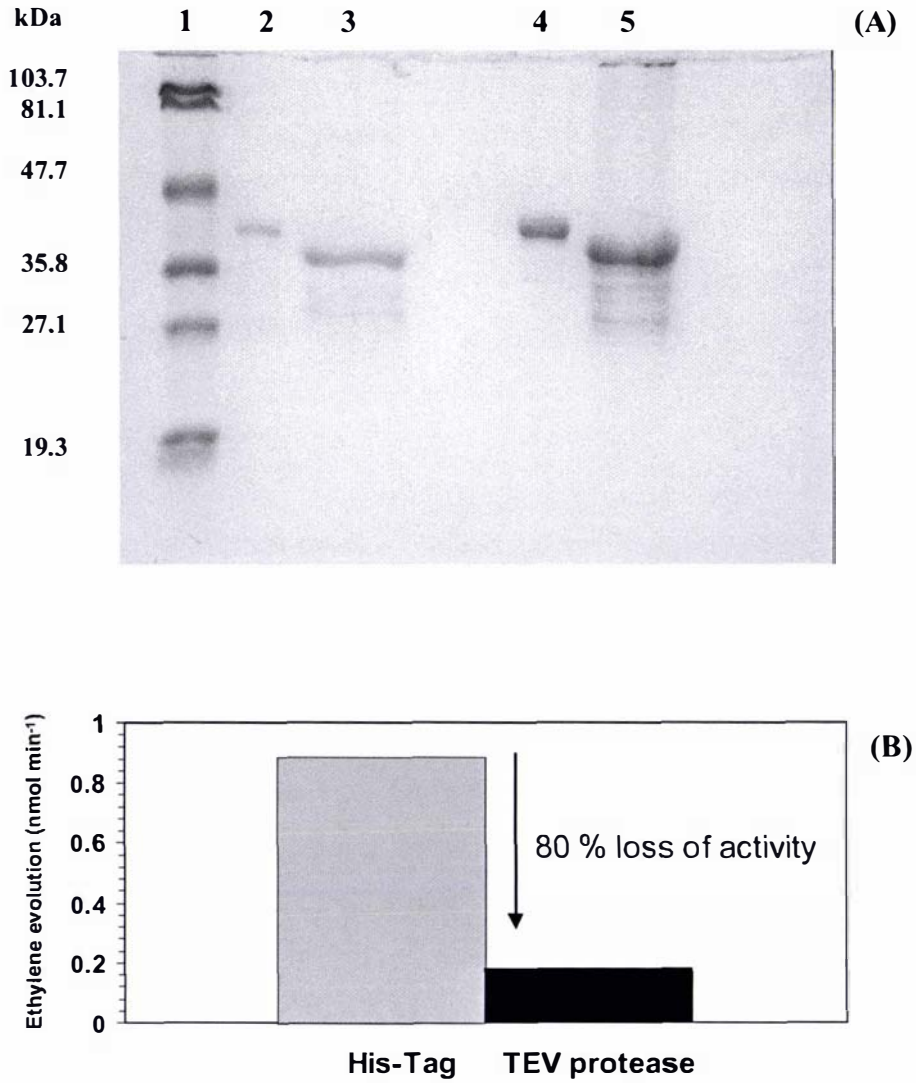


Figure 3.25: Cleavage of the Histidine Tag from Recombinant MD-ACO2 and MD-ACO3 using Tobacco Etch Virus (TEV) Protease, and Subsequent Evaluation of Enzymatic Activity

(A) SDS-PAGE stained with coomassie brilliant blue. Aliquots of *ca.* 5 μg of sample per lane. Lane 1: Calibrated low range molecular weight marker (BioRad), Lane 2: MD-ACO2 uncleaved control (expected molecular mass *ca.* 40.39 kDa), Lane 3: MD-ACO2 cleaved with TEV protease (expected molecular mass *ca.* 39.26 kDa), Lane 4: MD-ACO3 uncleaved control (*ca.* 40.39 kDa) Lane 5: MD-ACO3 cleaved with TEV protease (*ca.* 37.71 kDa). (B) Recombinant MD-ACO3 activity prior to the removal of the histidine-tag or after cleavage of the histidine tag (ACO activity is expressed in ppm as indicated).

published instability of ACO (Poneleit and Dilley, 1992; Pirrung *et al.*, 1993; Dupille *et al.*, 1993) the digestion was incubated at 4 °C overnight. Samples separated by SDS-PAGE and stained using coomassie brilliant blue (Figure 3.25A) indicate the digestion went to completion, as both the uncleaved His-tag controls of recombinant MD-ACO2 (*ca.* 40.39 kDa) and recombinant MD-ACO3 (*ca.* 39.3 kDa) as well as the TEV protease cleaved recombinant MD-ACO2 (*ca.* 38.65 kDa) and recombinant MD-ACO3 (*ca.* 37.71 kDa) separate to the expected molecular mass (Table 3.9).

Fragmentation of the proteins incubated at 4 °C with TEV protease is apparent compared to the untreated controls (Figure 3.25A). An ACO activity assay was then undertaken to determine whether the enzymatic activity of MD-ACO3 was changed as a result of His-tag removal. Compared to the uncleaved His-tag fusion MD-ACO3 control, the His-tag cleaved MD-ACO3 was determined to be 80 % less active (Figure 3.25B). As the enzymatic activity is compromised kinetic analysis was therefore undertaken without the removal of the His-tags.

3.2.3 Kinetic Properties of MD-ACO1, MD-ACO2 and MD-ACO3

3.2.3.1 Optimal Substrate and Co-factor Requirements for MD-ACO Activity

An investigation into the kinetic parameters of each of the recombinant ACO isoforms in *Malus domestica* was undertaken to compare any possible differences that may exist between the activities of the enzymes under different ACO assay conditions. These may in turn reflect the physiological conditions under which each of the isoforms is optimally active, and thus give some indication as to their possible physiological role(s)/function(s) in the plant. Each of the experiments was performed in triplicate, for each of the isoforms, and the same experiment for all three isoforms was conducted on the same day, in parallel, under exactly the same experimental conditions where appropriate.

Prior to a detailed analysis of the co-substrate and co-factor requirements, the reaction rates (nmol min^{-1}) of each of the enzymes was examined as a function of the amount of enzyme used in the ACO assay (section 2.3.8). The maximum velocity (V_{max}) of each of the MD-ACO isoforms increased as the amount of enzyme increased (Figure 3.26). MD-ACO1 (5 μg = V_{max} 0.073 nmol min^{-1}, and 10 μg = 0.152 nmol min^{-1}), MD-ACO2 (5 μg = V_{max} 0.055 nmol min^{-1}, and 10 μg = 0.129 nmol min^{-1}) and MD-ACO3 (5 μg = V_{max} 0.090 nmol min^{-1}, and 10 μg = 0.189 nmol min^{-1}).

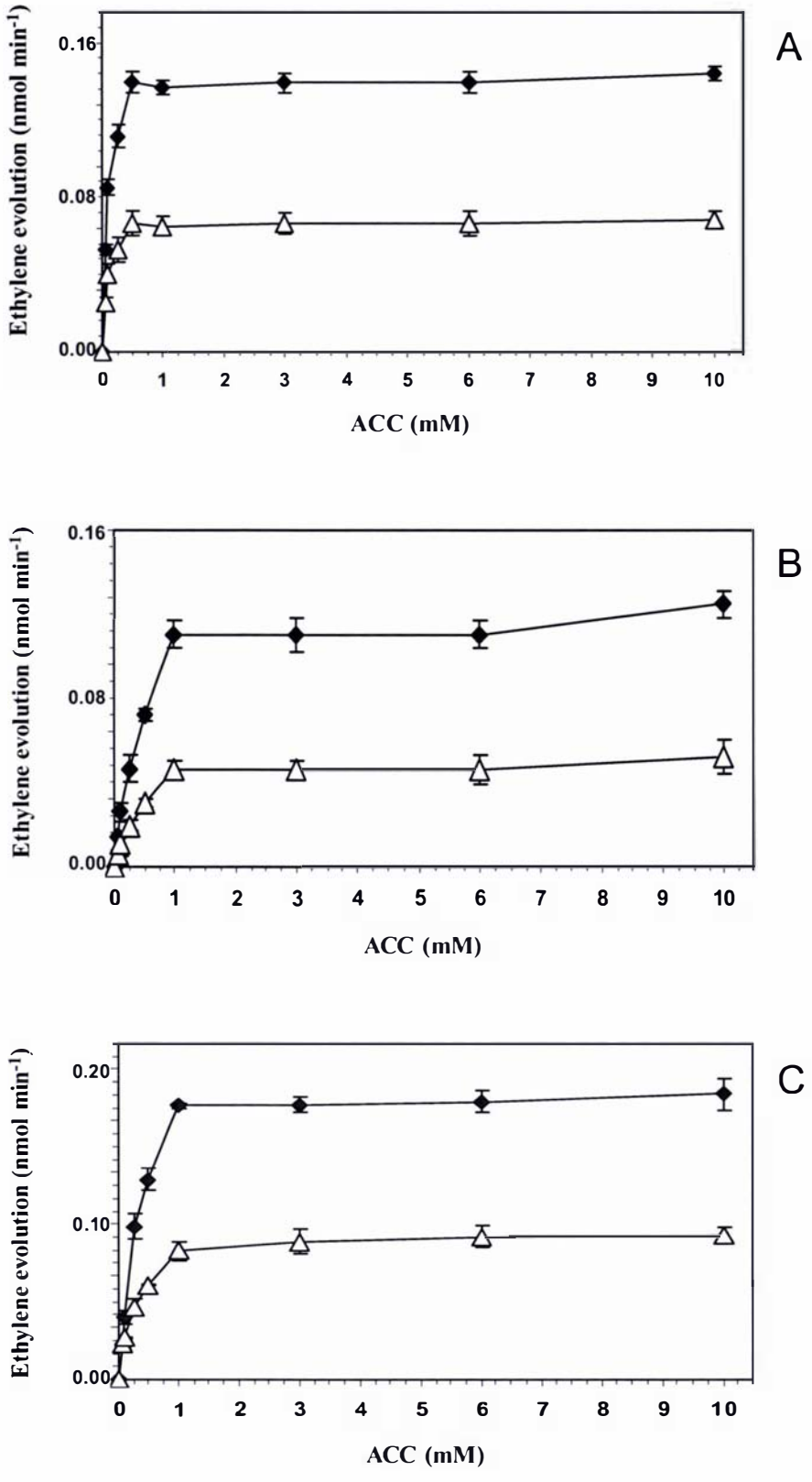


Figure 3.26: Effect of MD-ACO Concentration on the V_{max}

of MD-ACO1 (A), MD-ACO2 (B) and MD-ACO3 (C)

10 µg of enzyme —◆— , and 5 µg of enzyme —△— .

The optimal requirements of each isoform for co-substrate and cofactors were then determined at their optimal pHs and saturating ACC concentrations as described in section 2.3.8.1 and 2.3.8.2. The results from these studies are summarized as Table 3.11.

From the literature, a number of similar studies (Dong *et al.*, 1992b; Poneleit and Dilley, 1993; Mizutani *et al.*, 1995) have focussed on the role of CO_2 (as $NaHCO_3$). Therefore, the role of $NaHCO_3$ was examined more closely. With the omission of sodium bicarbonate from the ACO assay, the enzyme activity was determined over various ACC concentrations for each of the MD-ACO isoforms. In these assays enzyme activity decreased more than two-fold compared to the standard ACO assay containing $NaHCO_3$ (30 mM) *in vitro* (Figure 3.27).

3.2.3.2 The Michaelis-Constant (K_m) and Maxium Velocity (V_{max}) of the MD-ACO Isoforms for ACC

The dependence of MD-ACO1, MD-ACO2 and MD-ACO3 activity on the concentration of ACC, assayed at the optimal pH (pH 7.5) and using the standard concentrations of sodium ascorbate (30 mM), ferrous iron (20 μM) and sodium bicarbonate (30 mM), exhibited Michaelis Menten kinetics (Figures 3.28). Enzyme activity of isoform MD-ACO1 approached saturation at an ACC concentration of 0.5 mM while, isoforms MD-ACO2 and MD-ACO3 were saturated at an ACC concentration of 1 mM (Figure 3.28). The apparent K_m and V_{max} were determined from Lineweaver-Burk plots (Figures 3.28). The apparent K_m of MD-ACO1 (89.39 μM) indicates that this isoform has a higher affinity for its substrate ACC than either MD-ACO2 (401.03 μM) by more than 4 fold, and MD-ACO3 (244.5 μM) by approximately 2.5 fold. MD-ACO2 has a lower V_{max} (12.94 nmol of ethylene mg^{-1} min^{-1}) than the V_{max} of MD-ACO1 (15.15 nmol of ethylene mg^{-1} min^{-1}) and MD-ACO3 (18.94 nmol of ethylene mg^{-1} min^{-1}) which are similar. These values are also consistent with the V_{max} and K_m values obtained using the Eadie Hofstee regression (data not shown). K_{cat} values [ethylene evolution (mol s^{-1}) / MD-ACO (mol)] (refer Table 3.12), revealed MD-ACO3 (9.14×10^{-2}) to have the higher turnover rate compared to MD-ACO1 (6.6×10^{-2}) and the very sluggish MD-ACO2 (3.44×10^{-2}). The K_{cat}/K_m (μM s^{-1}) is a useful means for comparing activities between enzymes, and values 7.38×10^{-4} μM s^{-1} MD-ACO1, 0.86×10^{-4} μM s^{-1} MD-ACO2 and 3.8×10^{-4} μM s^{-1} MD-ACO3 were calculated. The results of this study indicate that the three MD-ACO isoforms have different kinetic properties, and will be analysed in the discussion.

Table 3.11: Summary of Substrate and Co-factor Requirements for MD-ACO1 MD-ACO2 and MD-ACO3 for Optimal Activity

	MD-ACO1	MD-ACO2	MD-ACO3
pH			
Activity range	6.5 – 8.0	6.5 -8.5	6.5 – 8.0
Optimal range	7.0 -7.5	7.5 - 8.0	7.0 - 8.0
Optima	7.2	7.8	7.5
Ascorbate			
(absolute requirement)			
Optimal concentration	30 mM	30 mM	30 mM
50 % inhibition	40 mM	40 mM	40 mM
$FeSO_4.7H_20$			
Optimal range	15 – 25 μM	15 – 25 μM	15 – 25 μM
Maximum activity	20 μM	15 μM	20 μM
≥ 70 % Inhibition	40 μM	40 μM	40 μM
$Na^+HCO_3^-$			
[1] 30 to 40 % activity	0 mM	0 mM	0 mM
Optimal range	20 – 40 mM	20 – 40 mM	10 – 40 mM
Maximum activity	30 mM	30 mM	30 mM
70 – 100 % inhibition	60 mM	60 mM	60 mM

[1] refer Figure 3.27

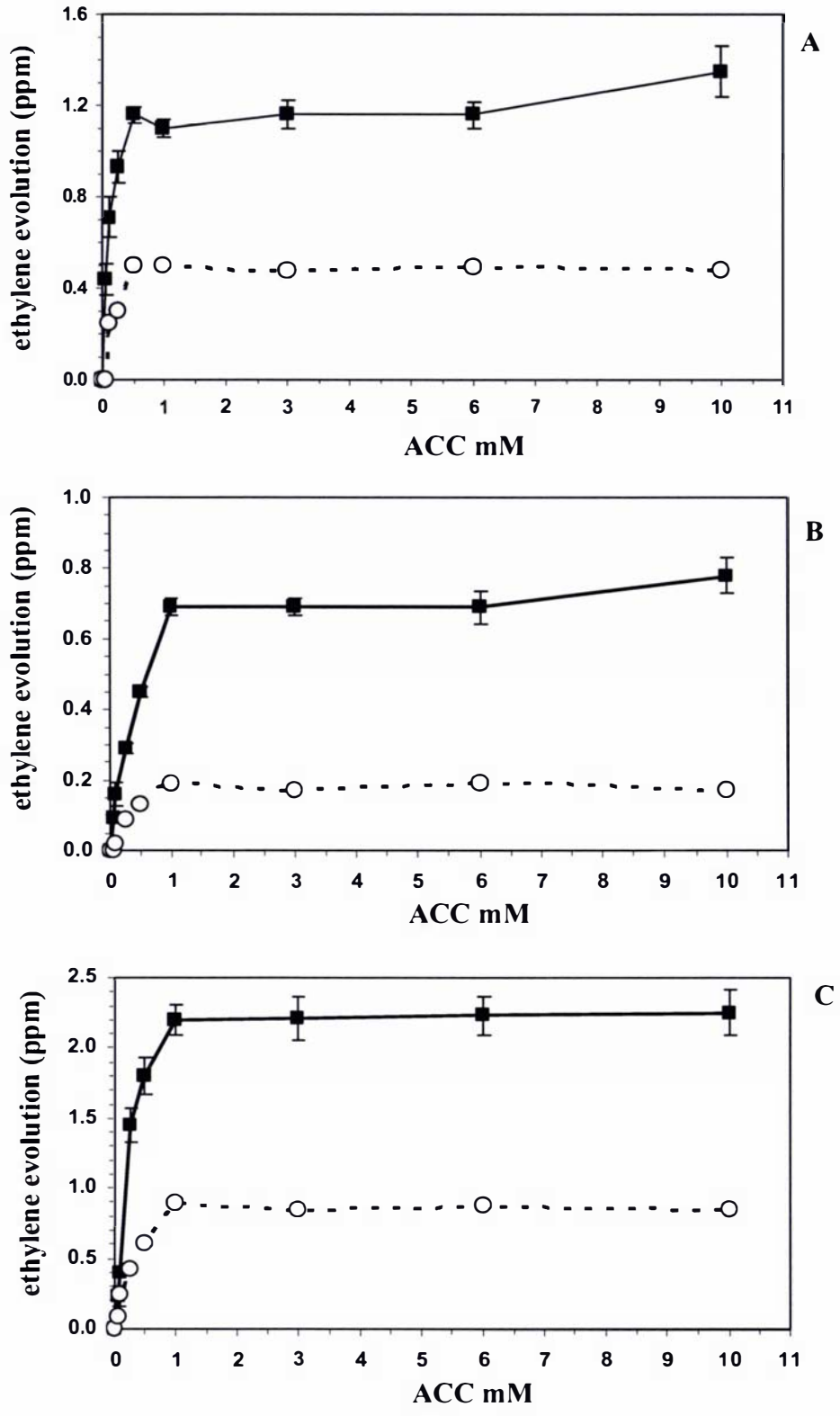


Figure 3.27: Activity Assays of MD-ACO1, MD-ACO2 and MD-ACO3 Without the Presence of Sodium Bicarbonate ($NaHCO_3$) in the Reaction Mixture.

A: MD-ACO1; B: MD-ACO2; C: MD-ACO3. Values and means ± SE (n=3)

NaHCO3 (+) NaHCO3 (-)

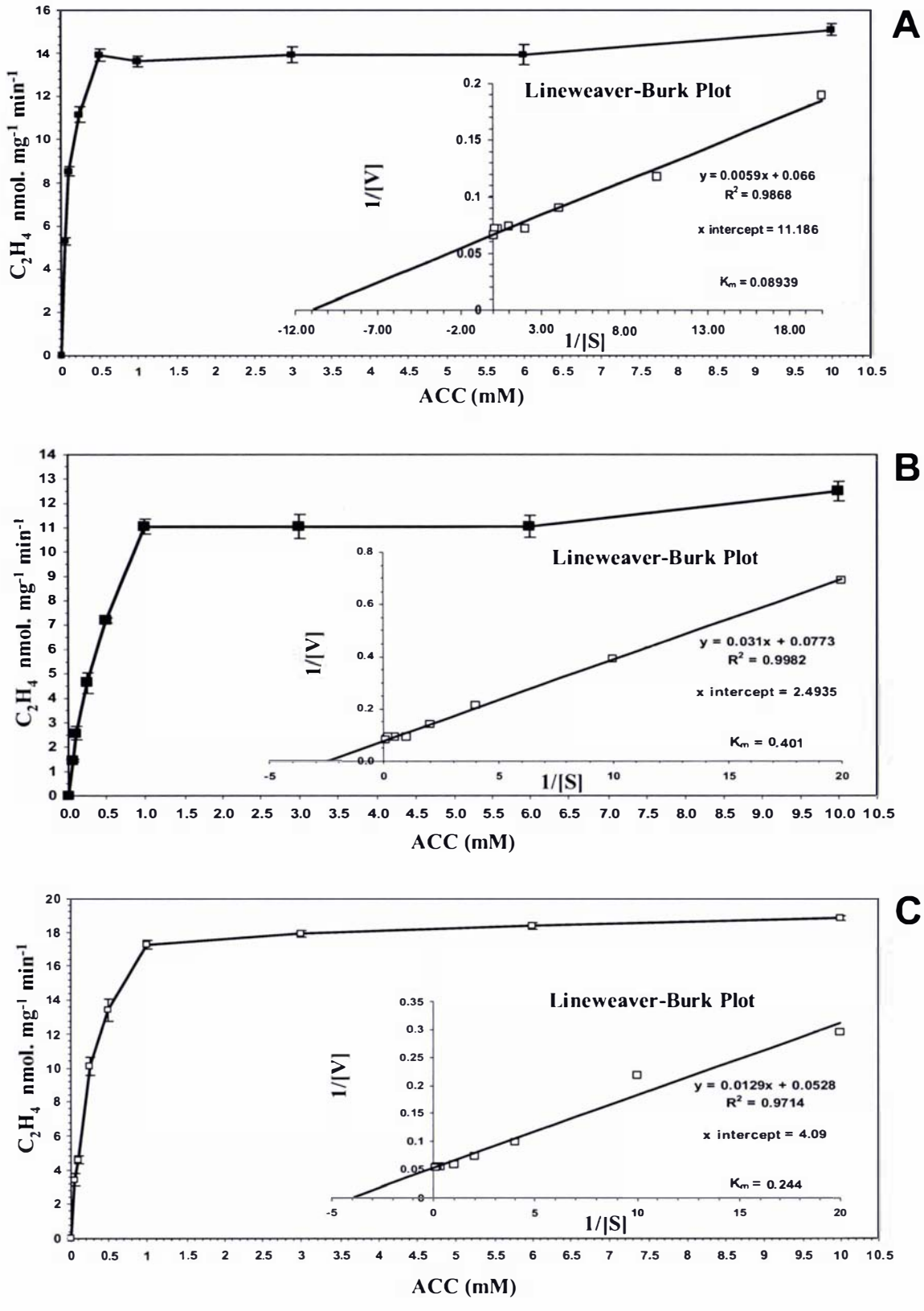


Figure 3.28: Recombinant MD-ACO1(A), MD-ACO2 (B) and MD-ACO3 (C) Activity as a Function of ACC Concentration. Each inset is the Lineweaver-Burk (double reciprocol) plot. Values and means ± SE (n = 6).

Table 3.12: Summary of Kinetic Properties of MD-ACO1 MD-ACO2 and MD-ACO3

	MD-ACO1	MD-ACO2	MD-ACO3
K_m (μM)	89.39 ± 9.7	401.03 ± 22.1	244.5 ± 14.2
V_{max} (nmol mg^{-1} min^{-1})	15.15 ± 0.73	12.94 ± 0.97	18.94 ± 0.69
K_{cat} s^{-1}	6.6 x 10^{-2}	3.44 x 10^{-2}	9.14 x 10^{-2}
K_{cat}/K_m (μM s^{-1})	7.38 x 10^{-4}	0.86 x 10^{-4}	3.8 x 10^{-4}

Values and means ± SE (n = 6).

3.2.3.3 Assessment of Some Kinetic Parameters Using the Same ACC Oxidase Isoform Generated in Two Different Expression Vector Systems

An anecdotal observation made during the kinetic study was that ACO activity was higher in the product of the pGEX vector than using the pProEx-1 expression vector. To examine this more closely an assessment of some of the kinetic parameters of the recombinant MD-ACO1 and MD-ACO2 expressed using the pGEX expression vector was undertaken and compared with the pProEX-1 expression. MD-ACO1, when expressed using the pGEX expression vector had a K_m value of 82.74 μM, a V_{max} of 17.73 nmol mg^{-1} min^{-1} and approached saturation at an ACC concentration of 0.5 mM which was very similar to MD-ACO1 expressed using the pProEX-1 expression vector. By contrast, the V_{max} of MD-ACO2 (18.38 nmol mg^{-1} min^{-1}) expressed using the pGEX expression vector is much higher than MD-ACO2 (12.94 nmol mg^{-1} min^{-1}) expressed using the pProEX-1 vector. Further, MD-ACO2 expressed using the pGEX expression vector has a lower K_m (91.91 μM) compared to MD-ACO2 expressed using the pProEx-1 expression vector, and approached saturation at ACC concentrations of 0.5 mM (Figure 3.29). The results are summarized in Table 3.13.

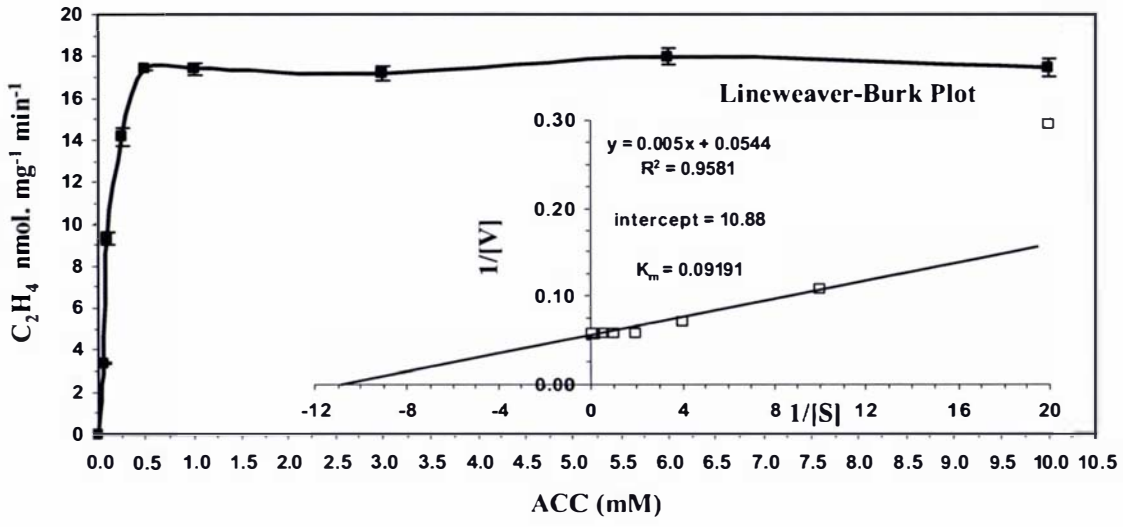


Figure 3.29: Recombinant MD-ACO2 Activity as a Function of ACC Concentration, Expressed in the pGEX Vector. Inset is the Lineweaver-Burk (double reciprocol) plot. Values and means ± SE (n = 6).

Recombinant MD-ACO1 not shown: (refer Table 3.13)

Table 3.13: Some Kinetic Properties using the pGEX and pProEx-1 Expression Vectors

	MD-ACO1		MD-ACO2	
	pGEX	pProEx-1	pGEX	pProEx-1
K_m (μM)	82.74 ± 8.1	89.39 ± 9.7	91.91 ± 13.0	401.03 ± 22.1
V_{max} (nmol)	17.73 ± 0.53	15.15 ± 0.73	18.38 ± 0.64	12.94 ± 0.97
ACC (mM)	0.5	0.5	0.5	1.0

Both the V_{max} and K_m values obtained for MD-ACO1 and MD-ACO2 expressed in the pGEX vector are consistent with the calculations using the Eadie-Hofstee regression plot (not shown).

3.2.3.3 Thermostability of MD-ACO1, MD-ACO2 and MD-ACO3

No significant difference in thermostability was found in this study between the MD-ACO isoforms. Two separate studies were carried out using the same temperatures, time of sampling and batch of enzyme samples. For each, study three aliquots of each isoform was used for each incubation temperature (25 °C, 35 °C and 45 °C), which required very rapid sampling and the need to store samples at 4 °C prior to the ACO assay to determine enzymatic activity using the gas chromatography (GC). As the incubation temperature increased the activities of all three isoforms decreased. Similarly, as the time of incubation lengthened the activities of all three isoforms also decreased (both temperature and time are therefore negatively correlated with apple ACO activity), (trend-lines representing the percentage of enzyme activity lost are shown as Figure 3.30). For example, following incubation at 25 °C the activity of all three isoforms reduced by approximately 50 % in 30 min (Figure 3.30A), which represents a half-life (L½) of 30 min at 25 °C (Figure 3.30A). The half-life of all three isoforms at 35 °C is approximately 13 min and 30 seconds (Figure 3.30B), and the half-life of all three isoforms at an incubation temperature of 45 °C is approximately 5 minutes and 50 seconds (Figure 3.30C), in these studies. A summary of the percentage of enzyme activity lost after incubation at 25 °C, 35 °C and 45 °C for each of the sampling times is shown in Table 3.14.

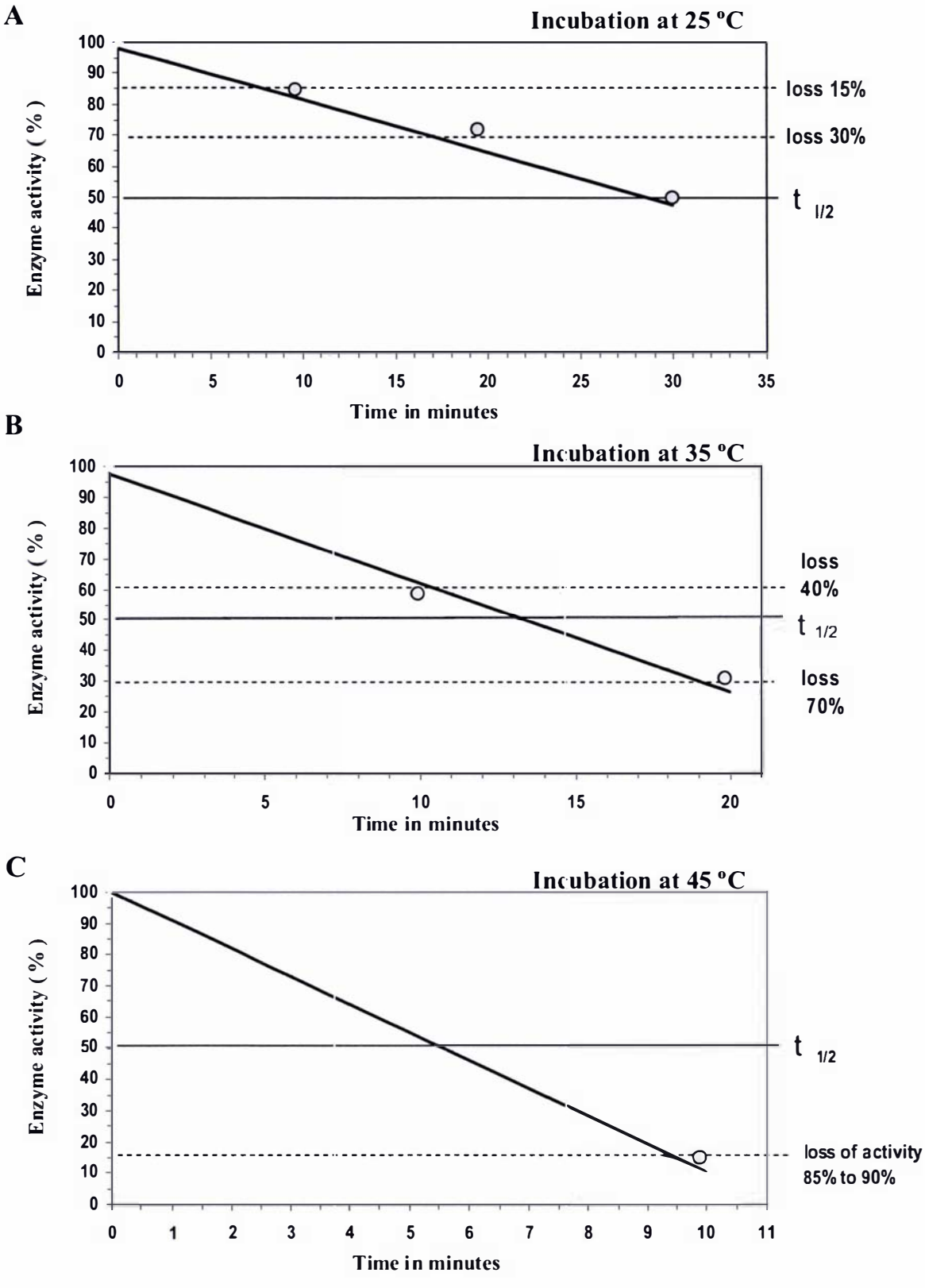


Figure 3.30: Thermal Stability of *Malus domestica* ACC Oxidase at Incubation Temperatures of 25 °C, 35 °C and 45 °C.

The percentage of enzyme activity is shown for each incubation temperature, 25 °C (A), 35 °C (B), and 45 °C (C). Each trendline represents pooled data for MD-ACO1, MD-ACO2 and MD-ACO3 ACC oxidase activity (as a percentage) as a function of time in minutes. (n = 18)

Table 3.14: Summary of Thermal Stability of *Malus domestica* ACC Oxidases at Incubation Temperatures of 25 °C, 35 °C and 45 °C.

The data are presented as a percentage of the enzyme activity lost at each temperature and at each time (min.) of sampling. Data are pooled for MD-ACO1, MD-ACO2 and MD-ACO3.

Temperature	10 min	20 min	30 min	60 min
25 °C	15 ± 4 %	30 ± 5 %	50 ± 5 %	75 ± 2 %
35 °C	40 ± 3 %	70 ± 6 %	80 ± 3 %	
45 °C	85 – 90 %			

Values and means ± SE (n = 18)

3.3 ACC Oxidase Gene Expression in the Bourse Shoot Leaves of Apple

For information about bourse shoot leaves refer section 1.6, and for the harvesting of leaf tissue samples refer section 2.1.

3.3.1 Physiological Measurements, MD-ACO Protein Accumulation and Gene Expression During Leaf Development

3.3.1.1 Change in Chlorophyll Concentration

Total chlorophyll (chlorophyll *a* and *b*) concentration was determined in this study as an indicator of the developmental status (maturation and senescence) of leaves (Smart, 1994; Thomas, 1997; Hunter *et al*., 1999; Buchanan-Wollaston *et al*, 2003).

Early in the season as the bourse shoots were still growing it was unclear which buds would have an initial leaf on the day of sampling, which bourse shoots would have 5 bourse shoot leaves, and as the season progressed in order to collect samples from bourse shoots of the same approximate length and with the same approximate number of leaves, tagging was carried out on the day of sampling and samples were collected at 11 am. Bourse shoot leaf samples collected early in the season from initial leaf tissue following bud break (collected on 15.10.03) and from the second youngest leaf from the bourse shoot tissue (collected on 23.10.03) have lower chlorophyll levels than leaf tissue collected as the 2003/2004 growing season progressed (Figure 3.31). Leaf samples collected on 21.11.03 were from bourse shoots of approximately 10 cm in length, which had five leaves. All five bourse shoot leaves were collected, and each leaf categorized according to its position on the bourse shoot. For example, the initial leaf is labelled leaf one through to the fifth leaf which is labelled leaf five. Total chlorophyll levels increased from the initial leaf (343 $\mu g\ g^{-1}$ FW) to the basal leaf (1022.25 $\mu g\ g^{-1}$ FW), as the newly initiated leaf unfolded and expanded over the five developmental stages sampled (Figure 3.31). As the leaves matured chlorophyll *a* concentration increased more rapidly than chlorophyll *b* concentration, which is indicated by the ratio of chlorophyll *a:b* changing from 1.85 in the initial leaf to 2.06 at the basal leaf (from tissue collected on 21.11.03). Tissue collected from initial, middle and basal leaf tissue at mid season (collected on 18.12.03 and 29.01.04) have similar chlorophyll content, with perhaps some decline in the basal leaf tissue for both days (Figure 3.31). The data coincides with the expected mature fully expanded green leaf status at mid season and the end of bourse shoot extension at mid to late January.

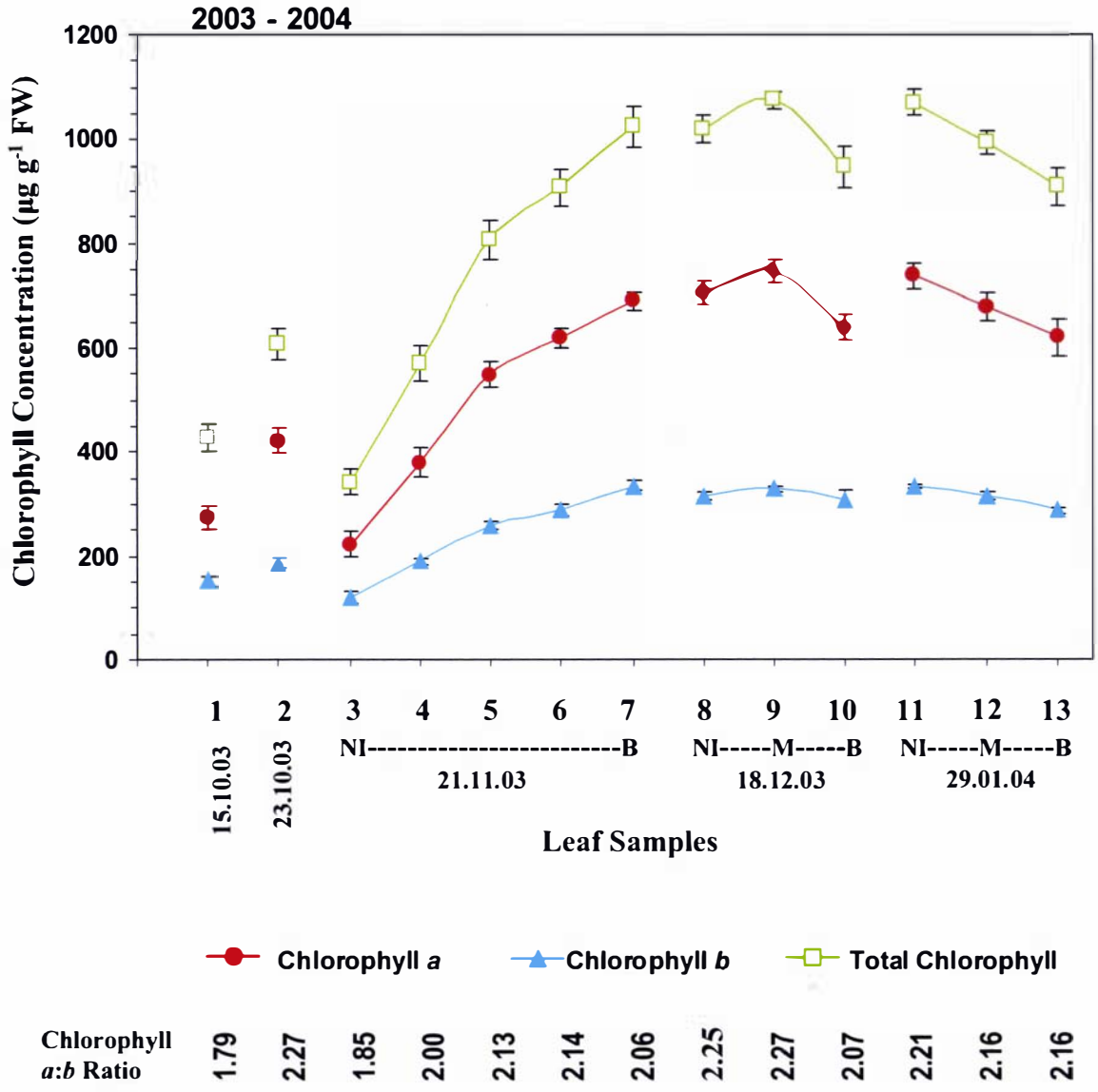


Figure 3.31: Changes in Chlorophyll Concentration as an Indicator of Leaf Maturation in *Malus domestica*.

Sample 1: Initial leaf (15.10.03), Sample 2: Second to youngest leaf (23.10.03), Samples 3 to 7: Leaves from newly initiated to basal are shown for (21.11.03), Samples 8 to 10: Leaves from newly initiated, middle and basal (18.12.03), Samples 11 to 13: Leaves from newly initiated, middle and basal (29.01.04). Symbols mean: Newly initiated (NI), middle (M) and basal (B). Values are means ± SE (n = 3).

To measure changes in chlorophyll concentration later in the season when the bourse shoot growth had terminated, pre-tagged fruiting and non fruiting bourse shoots (15 trees; ~7 tags per tree) at approximately 50 cm in length were pooled and used for this study. Leaves 5, 6 and 7 (counting from the apical end towards the basal end) were shown by statistical analysis (a one way analysis of variance) not to be significantly different at the $p = 0.05$ level (data not shown). Therefore, leaves 5 to 7 from each bourse shoot were collected during this study, including for the photosynthetic measurements, for the protein accumulation and for the gene expression studies, with the leaf samples collected at approximately 11 am. Chlorophyll concentration in leaf tissue collected from mid-season through to senescence (4.03.03 to 26.05.03) decreased as the leaves aged (Figure 3.32). Chlorophyll *a* concentration declines in very close synchrony with the decrease of total chlorophyll levels. In this study chlorophyll *a* degraded more quickly than chlorophyll *b* from 04.03.03 to 04.04.03 reflected in the chlorophyll *a* to *b* ratios of 2.30 to 2.13 (Figure 3.32), but then increased from 14.04.03 to 02.05.03 before the ratio again decreased from 2.05.03 to 26.05.03.

In sampling in 2004, chlorophyll content determined through to senescence (29.01.04 to 26.04.04) (Figure 3.33A) followed the 2003 decline in chlorophyll levels as the leaves aged, notably from 29.03.04 to 22.04.04, as reflected in the chlorophyll *a*:*b* ratio of 3.56 to 1.71. In 2005, chlorophyll concentrations prior to fruit harvest (15.02.05 and 01.03.05) and post fruit harvest (16.03.05, 30.03.05 and 07.04.05) also trended downwards gradually, but sampling ceased prior to the completion of senescence so that the chlorophyll content is unable to be compared directly with the other seasons (Figure 3.33B). The leaves of apple entered senescence at different times over the three seasons examined in this study, and also at different times within the same season (as judged by leaf colour change, and necrosis), probably as a consequence of their individual micro-environments. This may have resulted in a greater variability of chlorophyll levels amongst the ageing leaves, both within seasons and between seasons.

3.3.1.2 Photosynthesis Measurements

Assessment of the leaf carbon assimilation status of apple leaves from mid season through senescence in 2003 was undertaken using a portable photosynthetic system (PP Systems, Haverhill, MA, USA), in the field at approximately 11 am each day of sampling. Physiological measurements of net photosynthesis (pn; μmol m^2 s^{-1}), stomatal conductance (mmol m^2 s^{-1}) and evaporation representing transpiration (mmol m^2 s^{-1}) were used for comparisons. Leaf carbon assimilation decreased from mid-season through to senescence, in concert with a decrease in chlorophyll concentrations in the leaf tissue (Figure 3.34). As expected, evaporation mimics

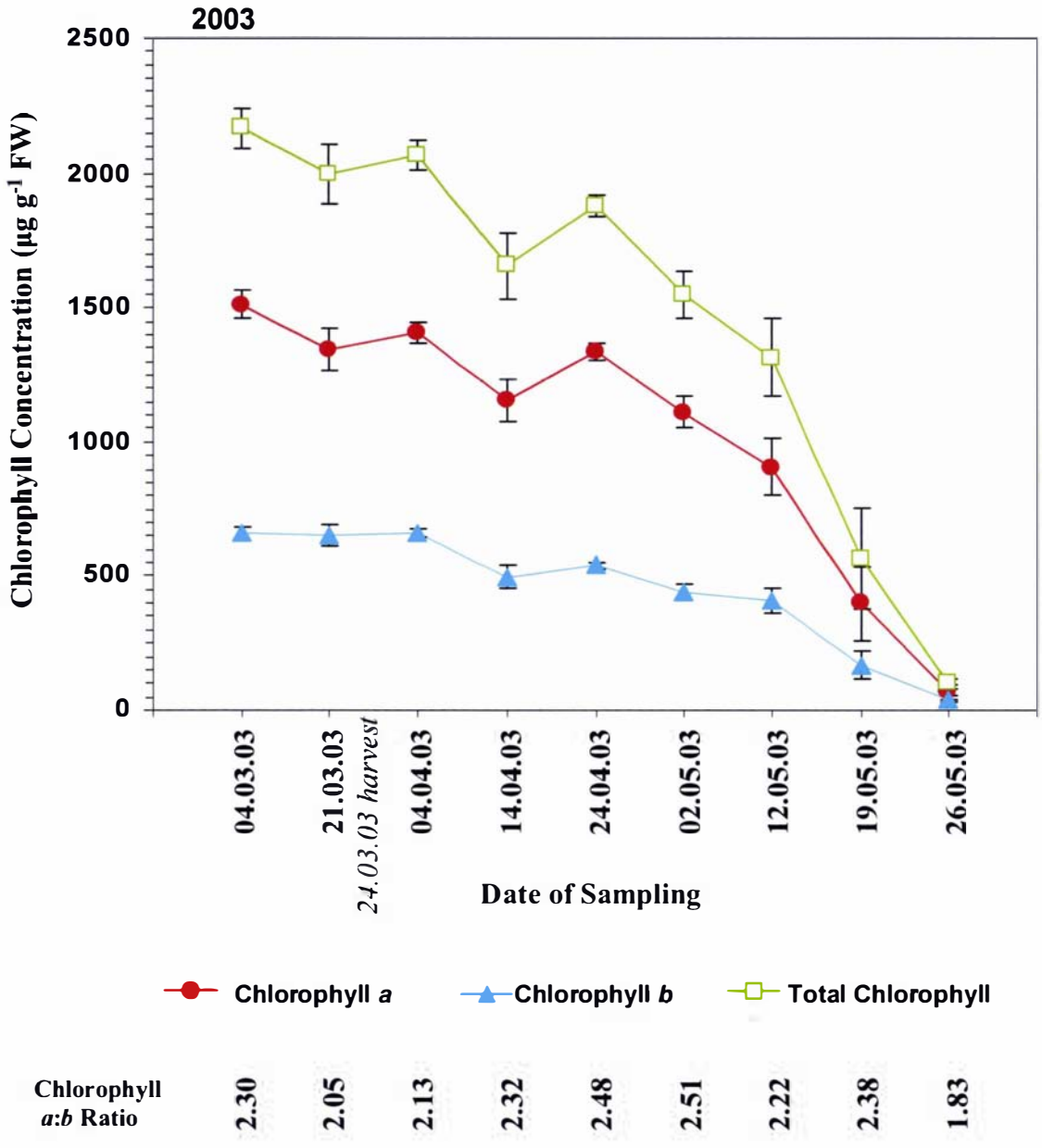


Figure 3.32: Changes in Chlorophyll Concentration as an Indicator of Leaf Senescence in *Malus domestica*.

The date indicates the day the sample was collected, and also the chlorophyll *a* to chlorophyll *b* ratios are indicated. Values are means ± SE (n = 3).

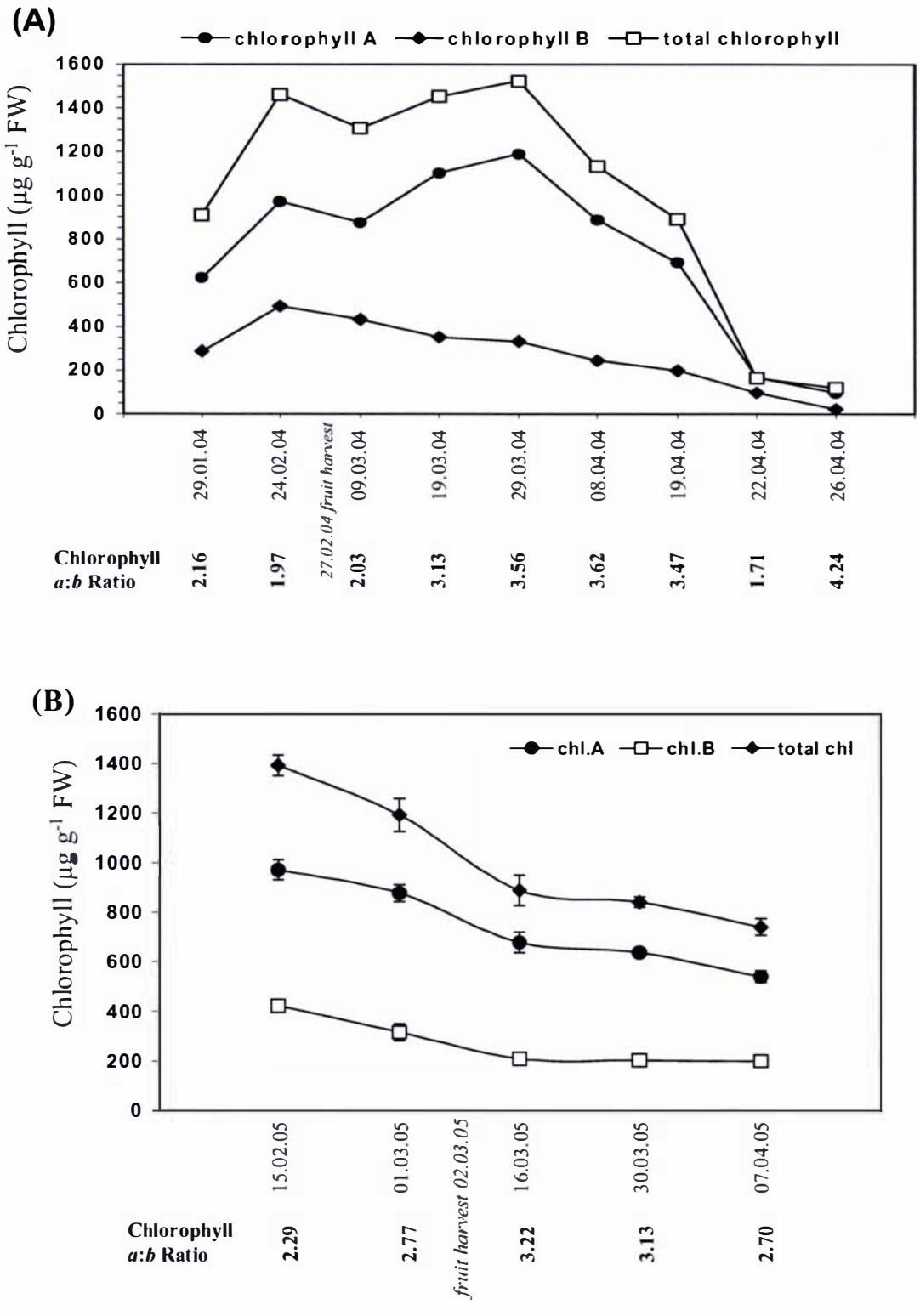


Figure 3.33: Chlorophyll Concentration as an Indicator of Leaf Senescence in *Malus domestica*.

A: Chlorophyll concentrations for 2004; **B:** Chlorophyll concentrations for 2005.

The date indicates the day the sample was collected, and the chlorophyll *a* to chlorophyll *b* ratios are indicated. Values are means ± SE (n = 3).

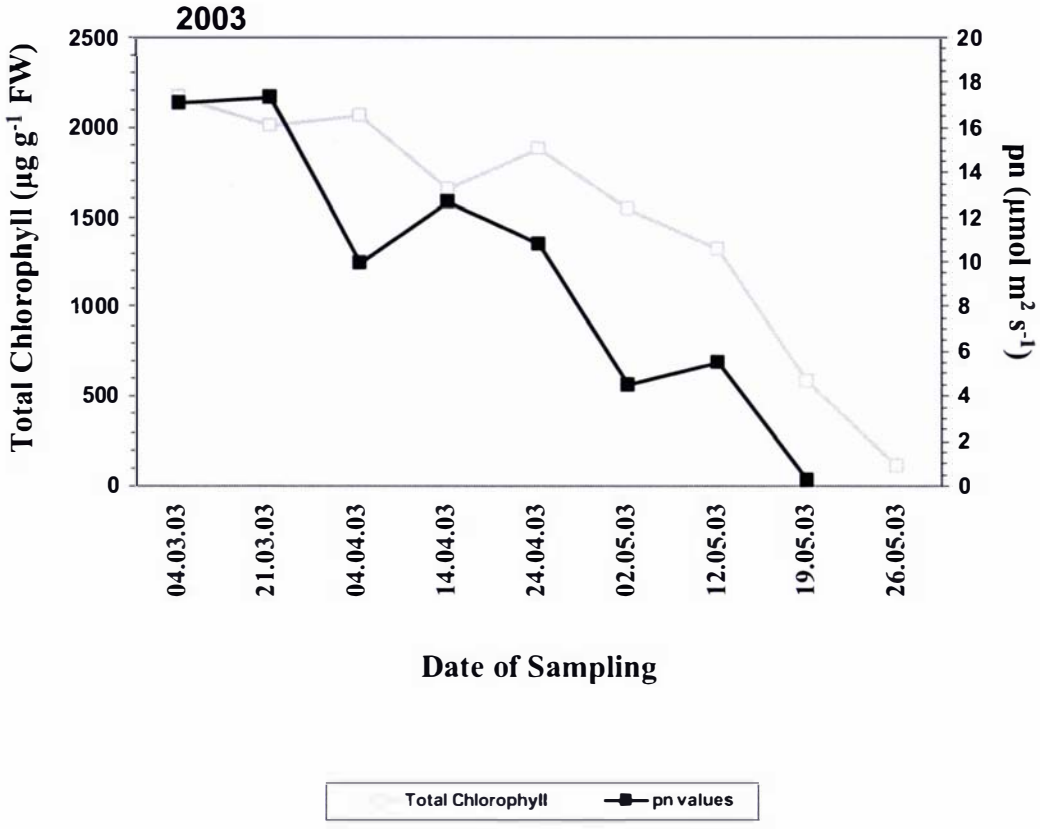


Figure 3.34: Leaf Carbon Assimilation in *Malus domestica* as an Indicator of Leaf Senescence.

Leaf carbon assimilation or net photosynthesis (pn) measured in µmol m^2 s^{-1} using the portable photosynthetic system on the same days and at the same time as samples were collected for chlorophyll extraction and analysis.

stomatal conductance with the levels of both dropping immediately following fruit harvest (24.03.03), and then becoming elevating a few weeks prior to leaf necrosis (data not shown).

An attempt was made to assess ethylene evolution levels from leaves harvested at the same time as those collected for chlorophyll extraction. Four hours after detachment the leaves were sealed in containers and incubated at 30 °C for 20 min after which a 1 mL gas sample was analysed for ethylene concentration using the GC. However, ethylene evolution was inconsistent and uninterpretable (data not shown) and so these determinations were not continued.

3.3.1.3 Protein Accumulation and Gene Expression

ACO protein accumulation in apple leaf tissue (collected at the beginning of the season to mid-season) was examined using western blot analysis with either the MD-ACO1 antibody (Figure 3.35) or MD-ACO3 antibody (Figure 3.36). Recognition of proteins of the expected molecular mass (35.35 kDa) were not apparent using the MD-ACO1 antibody for the apple leaf samples (Lanes 3 to 7 and 10 to 14; Figure 3.35), although recognition of an immunoreactive ACO from fruit is observed clearly (Lanes 2 and 9; Figure 3.35). Therefore, accumulation of MD-ACO1 in leaf tissue was not studied further in this thesis. In contrast, recognition was observed in the same apple leaf extracts using the antibody raised against MD-ACO3 (Lanes 1 & 2, 4 to 8 and 10 to 12; Figure 3.36), except in extracts from 29.01.04 leaf tissue (Lanes 14 to 16; Figure 3.36) where bands are not clearly distinguishable.

During leaf maturation and senescence, protein accumulation and gene expression of ACO was also examined. To look at protein accumulation, leaf samples collected from 4.03.03 to 26.05.03 were examined using western blot analysis with antibodies raised against MD-ACO3 (Figure 3.37). In these experiments, bands of a higher mass, than for the immunoreactive ACO from fruit tissue, appeared in the leaf tissue samples collected prior to fruit harvest (indicated with an asterisk on Figure 3.37; Lanes 3 and 4), whereas no antibody recognition is apparent in the leaf samples collected after fruit harvest (Figure 3.37; Lanes 5 to 11). This data suggests that antibody raised against MD-ACO3 is recognising a protein distinct from the fruit-associated MD-ACO1 protein, and that transcription and/or translation of this protein may be terminated when the fruit is removed from the apple tree *en masse*.

To examine ACO gene expression from mid season through to senescence, total RNA was extracted from leaf tissue collected from 04.03.03 to 26.05.03. Northern blot analysis was largely unsuccessful due to the degradation of RNA, particularly during the senescent stages.

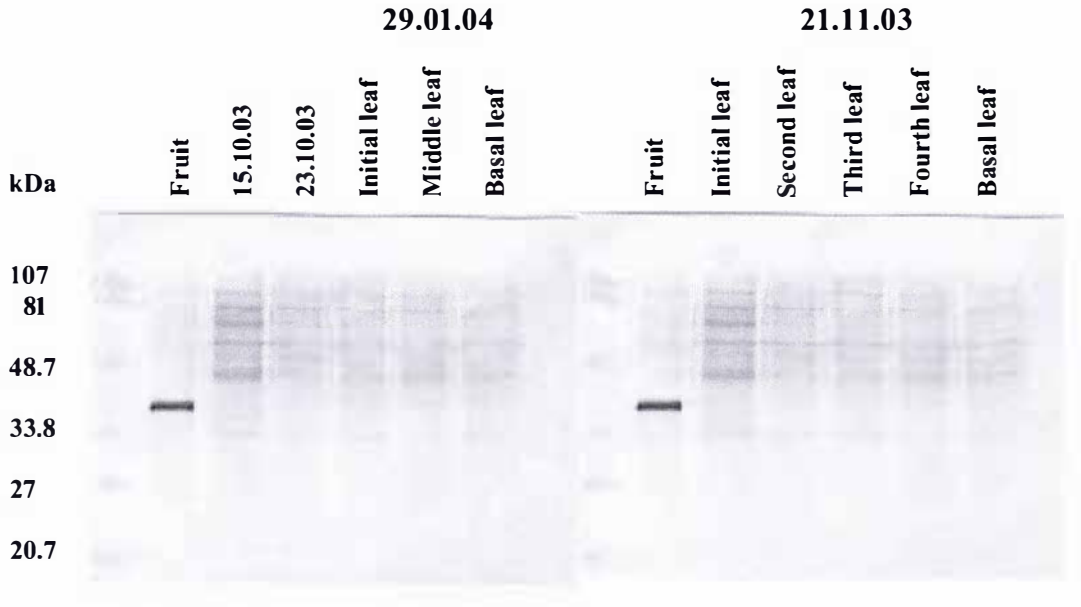


Figure 3.35: ACC Oxidase Accumulation in the Leaves of *Malus domestica,* from Early to Mid-Season, using Antibodies Raised Against Recombinant MD-ACO1

For apple leaf tissue, 20 μg of protein per well was loaded, while 10 μg of protein per well was loaded of apple fruit tissue. Antibody recognition was determined using a goat anti-rabbit alkaline phosphatase conjugated secondary antibody. Lanes 1 and 8: SDS-PAGE (low range) standards, Lane 2 and 9: apple fruit tissue, Lane 3: apple leaf tissue (15.10.03), Lane 4: apple leaf tissue (23.10.03), Lane 5: initial leaf tissue (29.01.04), Lane 6: middle (5, 6 or 7) leaf (29.01.04), Lane 7: basal leaf tissue (29.01.04), Lane 10: initial leaf tissue (21.11.03), Lane 11: second leaf (21.11.03), Lane 12: third leaf (21.11.03), Lane 13: fourth leaf (21.11.03), Lane 14: basal leaf tissue (21.11.03).

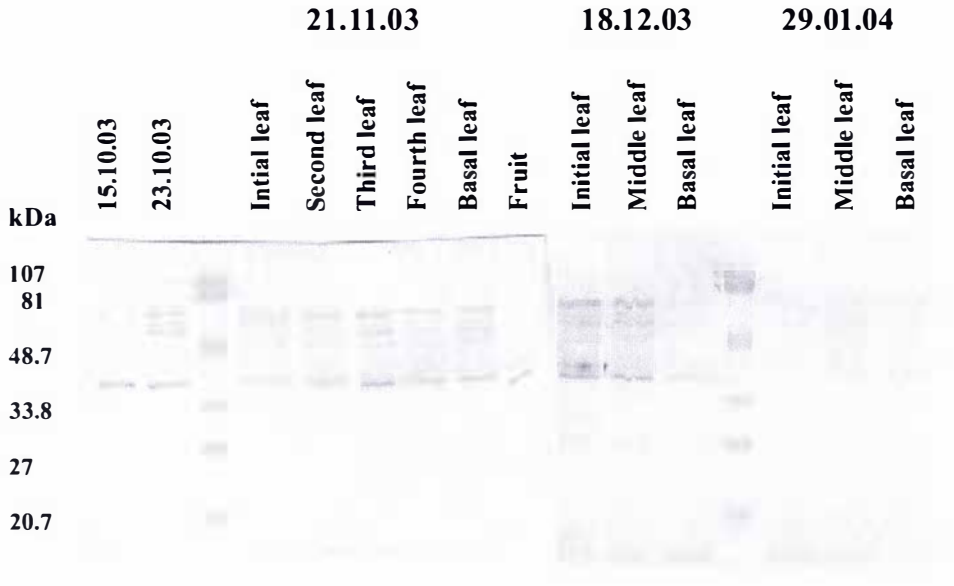


Figure 3.36: ACC Oxidase Accumulation in the Leaves of *Malus domestica*, from Early to Mid-season, using Antibodies Raised Against MD-ACO3

For apple leaf tissue, 20 μg of protein per well was loaded, while 10 μg of protein per well was loaded of apple fruit tissue. Antibody recognition was determined using a goat anti-rabbit alkaline phosphatase conjugated secondary antibody. Lane 1: apple leaf tissue (15.10.03), Lane 2: apple leaf tissue (23.10.03), Lane 3: SDS-PAGE (low range) standards, Lane 4: initial leaf tissue (21.11.03), Lane 5: second leaf (21.11.03), Lane 6: third leaf (21.11.03), Lane 7: fourth leaf (21.11.03), Lane 8: basal leaf tissue (21.11.03), Lane 9: apple fruit tissue (not very clear), Lane 10: initial leaf tissue (18.12.03), Lane 11: middle (5, 6 or 7) leaf (18.12.03), Lane 12: basal leaf tissue (18.12.03), Lane 13: SDS-PAGE (low range) standards, Lane 14: initial leaf tissue (29.12.03), Lane 15: middle (5, 6 or 7) leaf (29.12.03), Lane 16: basal leaf tissue (29.12.03).

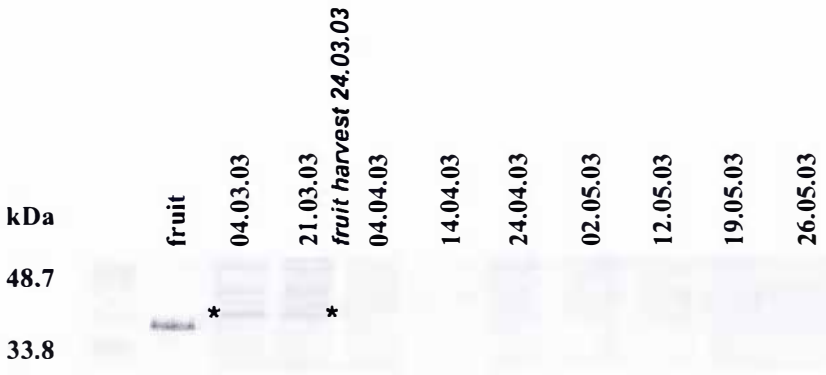


Figure 3.37: Changes in ACC Oxidase Protein Accumulation in Leaf Tissue from Mid-Season Through to Senescence (2003) in *Malus domestica*.

Examination of protein accumulation using western blot analysis (40 μg protein per lane), of leaf tissue collected at approximately 11 am on the day of sampling (dates are indicated including the date of fruit harvest). Apple fruit tissue extracts are also included. Western analysis using antibodies raised against MD-ACO3.

Relative quantitative RT-PCR (section 2.2.3.4) was undertaken to determine whether cDNA Southern blot analysis would be a viable alternative to northern analysis, and some early season initial leaf samples (collected on 15.10.03, 23.10.03 and 21.11.03) were included. Using this approach bands of the expected size appeared after the first PCR amplification round (29 cycles) when primers for either *MD-ACO2* (fragments 790 bp) or *MD-ACO3* (fragments 800 bp) were used. When *MD-ACO1* primers were used, no PCR products were detected (Figure 3.38), even after a second round of PCR amplification. However, fragments were clearly visible when the same *MD-ACO1* primers were used to amplify fragments from apple fruit tissue following an RT reaction (data not shown). Ribosomal RNA (18S) was used as a control and appeared on all of the gels at the expected fragment size of 315 bp (Figure 3.38).

Following cDNA Southern blot analysis on the same tissue extracts (collected from 04.03.03 to 26.05.03 and used for relative quantitative RT-PCR; data not shown), both *MD-ACO2* and *MD-ACO3* probes hybridized with cDNA fragments at the expected size of 790 bp and 800 bp respectively, prior to apple fruit harvest (Figure 3.38). However, such hybridization is not evident after the removal of the fruit from the trees. One round of PCR amplification (30 cycles) of the cDNA transcripts (from the cDNA mix used to amplify fragments for cDNA Southern analysis) using universal primers for β-actin (Table 2.2) generated fragments of *ca.* 250 bp. Taken together the data indicates either that *MD-ACO1* is uninduced in leaf tissue or that the quantities of *MD-ACO1* transcript are lower in leaf tissue than the sensitivity of the systems used and hence unable to be detected. In contrast both *MD-ACO2* and *MD-ACO3* are expressed in initial leaf tissue and mature green fully expanded leaf tissue, but the expression of both isoforms is undetectable in leaf tissue collected after the fruit has been harvested *en masse.*

A further study from mid-season through senescence was undertaken during 2004 (collected from 29.01.04 to 26.04.04; Figure 3.39A) and, then in 2005, two samples were collected prior to fruit harvest on the 02.03.05 (15.02.05 and 01.03.05; Figure 3.39B) and two samples were collected post fruit harvest (16.03.05 and 30.03.05; Figure 3.39B). Both the 2004 and the 2005 data corroborates the 2003 data in so far as ACO gene expression is not detectable after fruit harvest. As cDNA fragments were generated using actin primers (Table 2.2) ACO was probably not present in the total RNA extracted from leaf tissue. However, evidence of ACO gene expression prior to fruit harvest is very unconvincing for the 2005 data, although the recognition of protein at a lower mass (*ca.* 33.8 and 27 kDa) by the MD-ACO antibody is evident (Figure 3.39B). This may be degraded/ fragmented MD-ACO3, or another isoform, since recognition of any protein is very faint.

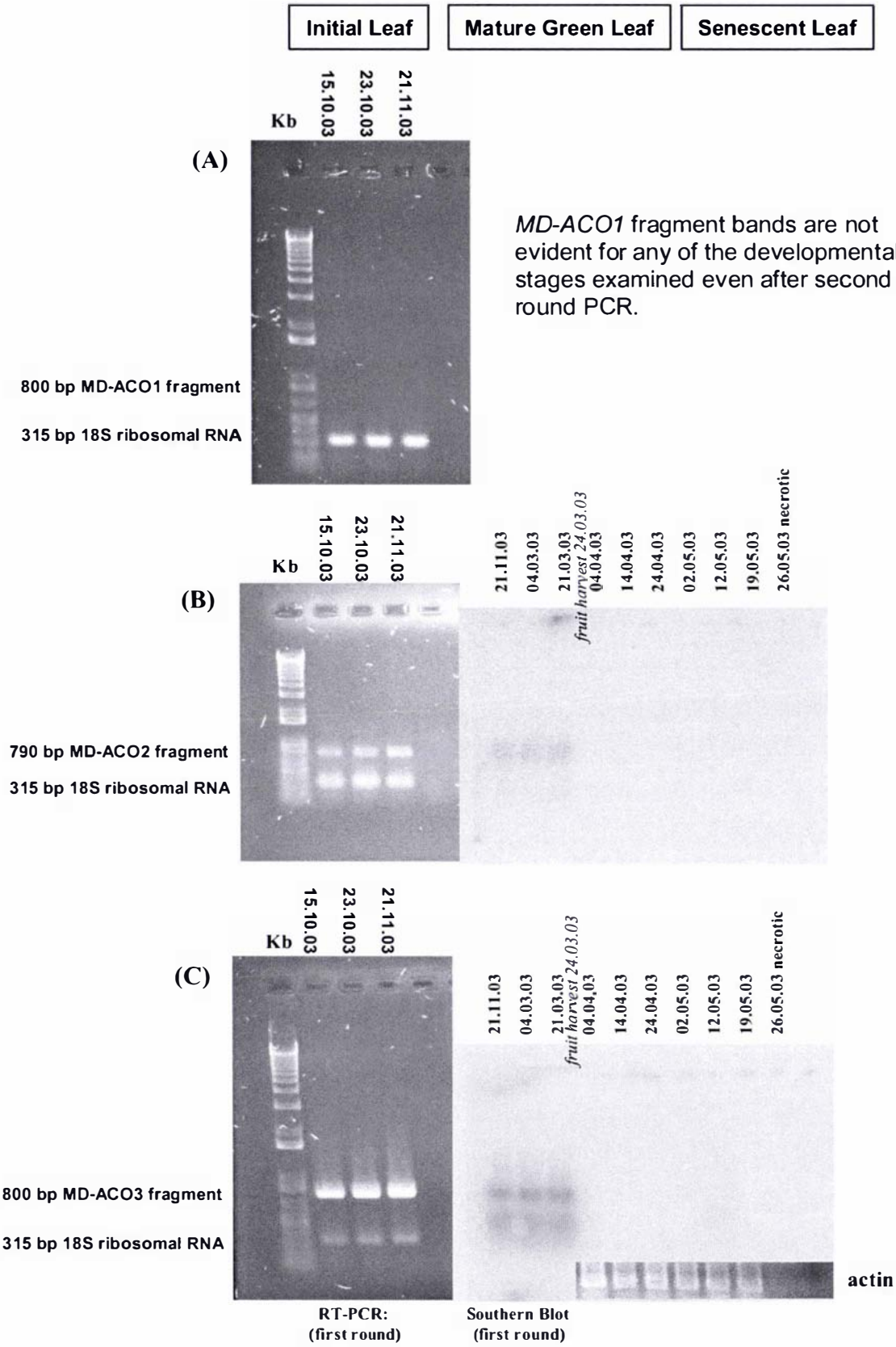


Figure 3.38: RT-PCR Analysis and cDNA Southern Blot Analysis of ACC Oxidase Gene Expression (2003).

(A) Primers used to amplify *MD-ACO1* fragments, (B) Primers used to amplify *MD-ACO2* fragments and (C) Primers used to amplify *MD-ACO3* fragments. cDNA Southerns were washed at high stringency.

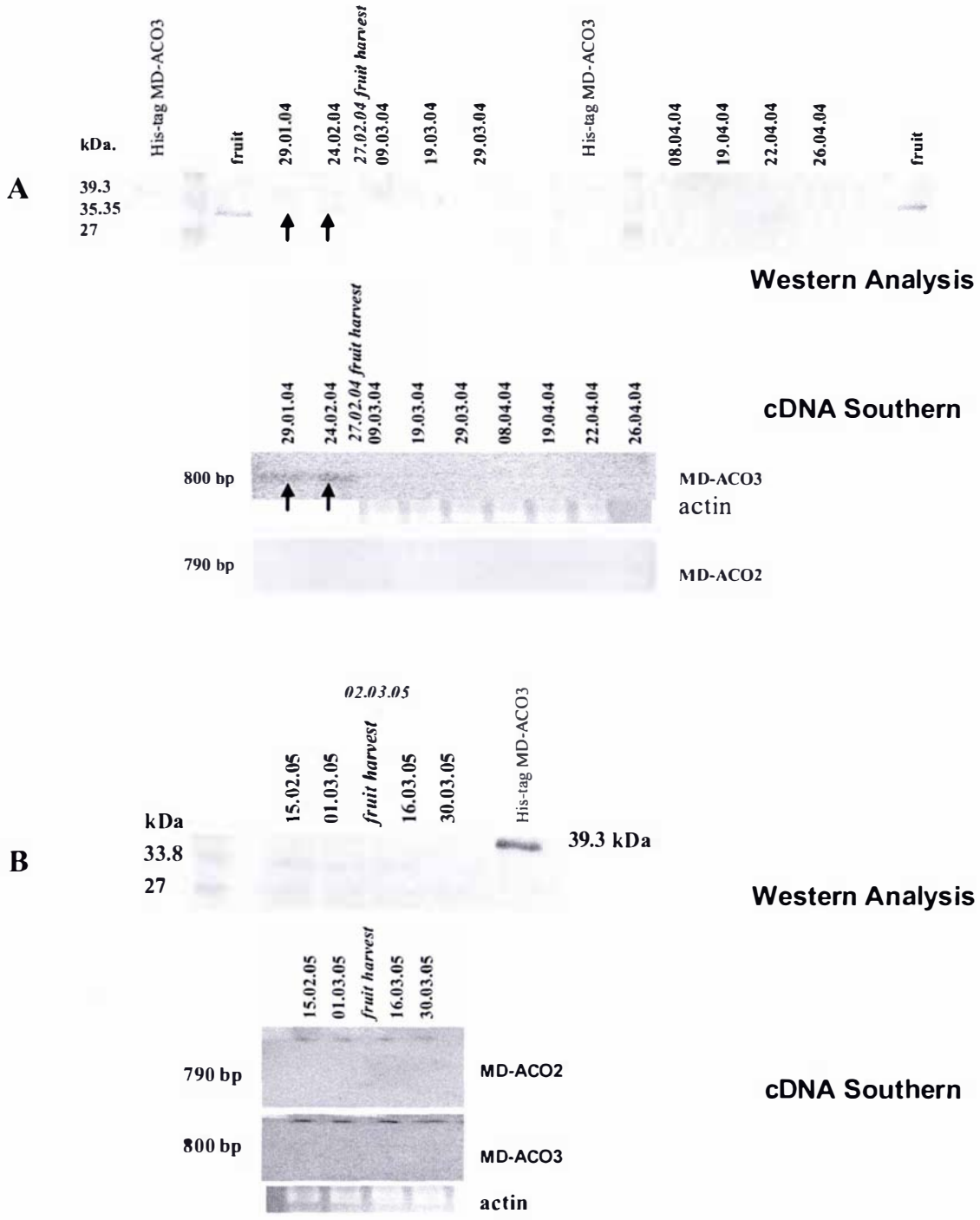


Figure 3.39: Gene Expression and Protein Accumulation of ACC Oxidase from Mid-Season Through to Senescence

Western blots analysis (40 µg protein per well) using antibody raised against recombinant MD-ACO3 for 2004 (A) and for 2005 (B). cDNA Southern blot analysis, using gene-specific primers and probes for both MD-ACO2 and MD-ACO3 for 2004 (A) and 2005 (B), (No bands were evident after a second round PCR either).

3.3.2 ACC Oxidase Gene Expression and Protein Accumulation in the Leaves of Apple over a 24 h Period

RT-PCR and cDNA Southern blot analysis were used in an attempt to establish whether ACO gene transcripts are expressed in a circadian rhythm. Patterns of ACO protein accumulation were also examined using western blot analysis with antibodies raised against MD-ACO3. Leaves were collected, from pre-tagged bourse shoots, every 3 h over a 24 h period, early in the season (collected from 20.11.03 to 21.11.03) and then late in the season (collected from 07.04.04 to 08.04.04, and 06.04.05 to 07.04.05).

In November (20.11.03 to 21.11.03), when the diameter of the abundant fruit measured approximately 2 cm, bourse shoots were chosen and tagged if they had 5 leaves and were then used to examine gene expression and protein accumulation patterns of ACO over a 24 h period. *MD-ACO2* probes hybridized to fragments at approximately six hourly intervals (noon, 6 pm, midnight, 6 am and noon) with a less intense band occurring at midnight (Figure 3.40A). *MD-ACO3* displayed a similar hybridization pattern to that of *MD-ACO2* at 6 hourly intervals (noon, 3 pm, 6 pm, midnight, 6 am and noon), although the midnight band is no less intense than the bands occurring during the daylight hours, and a further band occurs at 3 pm (Figure 3.40B). For *MD-ACO3*, the second round PCR reflects the cDNA Southern blot analysis, except that no band was visible at 3 pm (Figure 3.40C). Actin controls indicate that the RT reaction was successful in that cDNA actin was generated, in the absence of both hybridization and the generation of PCR products for the *MD*-ACOs. In contrast, the MD-ACO3 antibodies recognised protein at each of the sampling times, with no detectable difference in mass or intensity (Figure 3.40D). Further, the protein is of a higher mass than the ACO recognised from the fruit tissue (*ca.* 35.35 kDa).

In April (7.04.04 to 8.04.04), from pre-tagged bourse shoots (~50 cm), leaves (5, 6 or 7) were collected to investigate gene expression and protein accumulation patterns of ACO in the leaves of apple over a 24 h period. As the fruit had been harvested previously (27.02.04) both fruiting and non-fruiting bourse shoot leaves were used. *MD-ACO2* fragments hybridized at noon and 3 pm and then again at 9 pm during the hours of darkness (sunset 6 pm), after which some hybridization occurred at 6 am, before sunrise at 6.45 am, followed by stronger hybridization at 9 pm and at noon (Figure 3.41A). Second round PCR also reflects the cDNA Southern gene expression (data not shown). In contrast, *MD-ACO3* fragments hybridize at each of the sampling times over the entire 24 h period and, except for lower levels of transcript at sunset (6 pm) and at 3 am, gene expression appears to be constitutive (Figure 3.41B). Second round PCR also reflects the cDNA Southern gene expression (data not shown). Antibodies

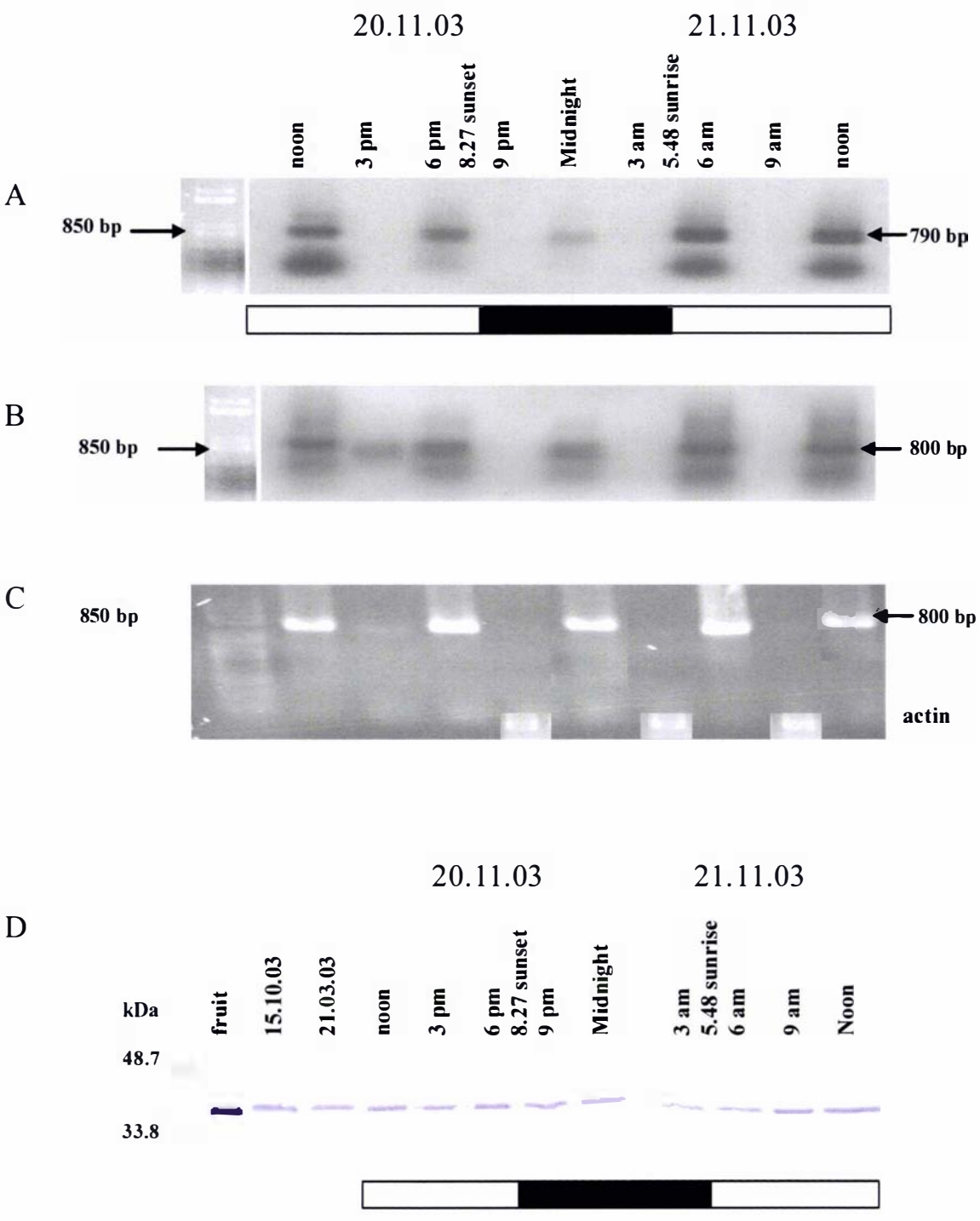


Figure 3.40: Circadian Rhythm of ACC Oxidase Gene Expression Over 24 h in the Leaves of M*alus domestica* (November, 2003).

The apple fruit were approximately 2 cm in diameter. Southern cDNA blot analysis using MD-ACO2 (A) and MD-ACO3 (B) fragments, Second round PCR using MD-ACO3 specific primers (C). Western blot analysis using antibodies raised against MD-ACO3 (D).

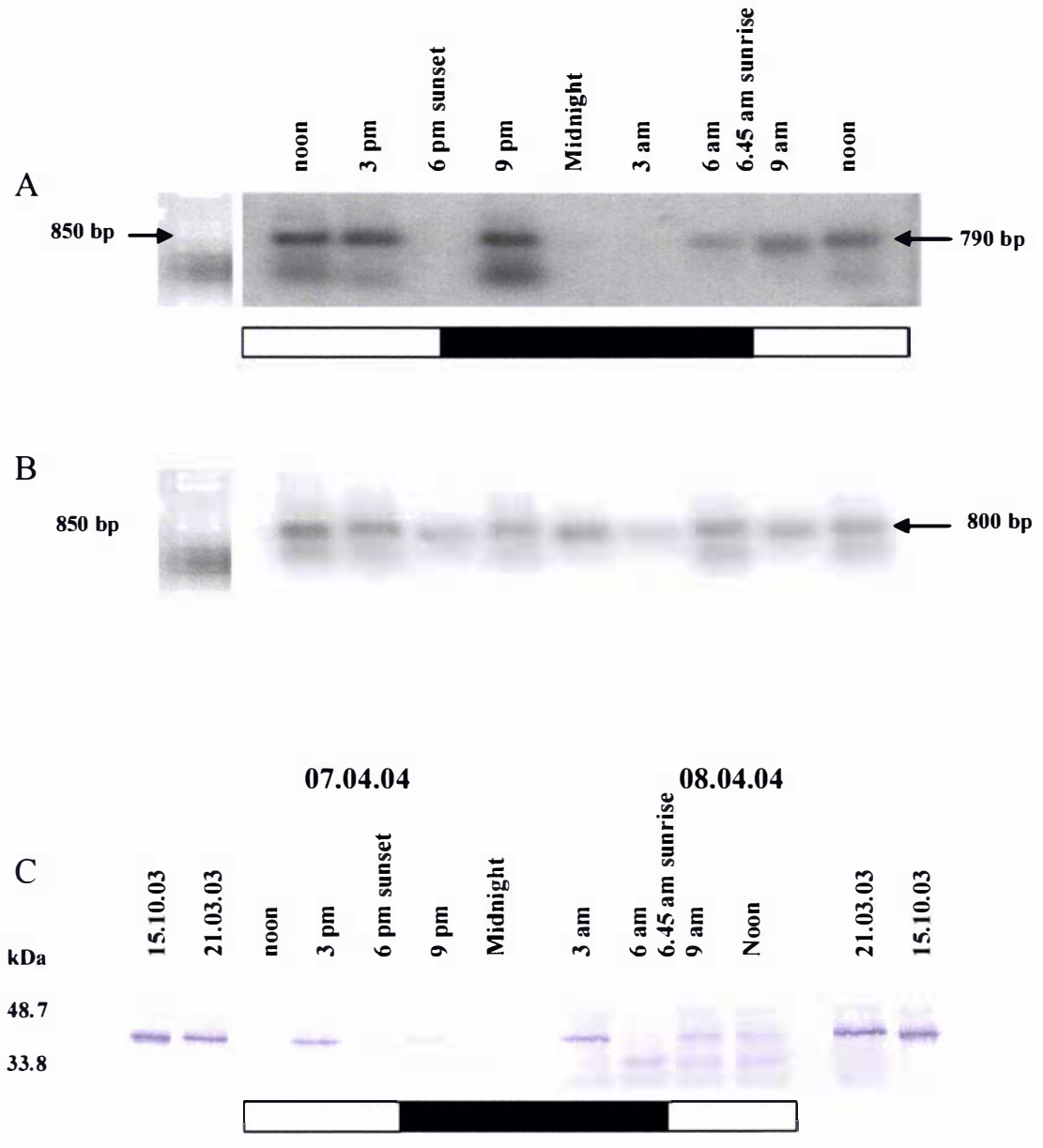


Figure 3.41: Circadian Rhythm of ACC Oxidase Gene Expression Over 24 h in the Leaves of *Malus domestica* (April, 2004).

Apple fruit had been harvested (27.02.04). Southern cDNA blot analysis using *MD-ACO2* (A) and *MD-ACO3* (B) fragments. Western blot analysis using antibodies raised against MD-ACO3 (C).

raised against MD-ACO3 recognise protein accumulation at 3 pm and 3 am in particular (Figure 3.41C), although lighter bands also appear over the whole period. The MD-ACO3 antibodies also recognise protein of a lower molecular mass (*ca.* 33.8 kDa) most notably at 6 am, which may be degraded MD-ACO3 or another MD-ACO isoform.

In April (06.04.05 to 07.04.05) pre-tagged bourse shoots on trees with fruit and on trees with the fruit removed (strip-picked 02.03.05) were used to examine whether gene transcript expression and protein accumulation patterns of ACO varied over 24 h as a direct consequence of the fruit status of the tree. Leaf tissue collected from the trees without fruit appeared not to express any ACO transcripts, as neither *MD-ACO2* nor *MD-ACO3* fragments hybridized (Figures 3.42A and 3.42B), which is also reflected in the second round PCR (Figure 3.42C), and MD-ACO3 antibody did not recognise any protein over the period (Figure 3.42D). In contrast, the trees with fruit appeared to express both *MD-ACO2* (Figure 3.43A) and *MD-ACO3* (Figure 3.43B) during the light period, and *MD-ACO3* fragments also hybridized at 3 am during the dark period (Figures 3.43B), which is also reflected in second round PCR (Figure 3.43C). Antibody raised against the MD-ACO3 antibody recognises some protein accumulation, of more than 35.35 kDa, over the entire 24 h period prior to fruit removal, perhaps slightly more at 3 am and 6 am of the dark period (Figure 3.43D). Taken as a whole it appears that MD-ACO2 or MD-ACO3 are not expressed in bourse shoot leaves once the fruit has been removed. Although the results of the 2004 season (Figure 3.41) indicate there are seasonal changes, and clearly something other than fruit removal must influence ACO expression and accumulation.

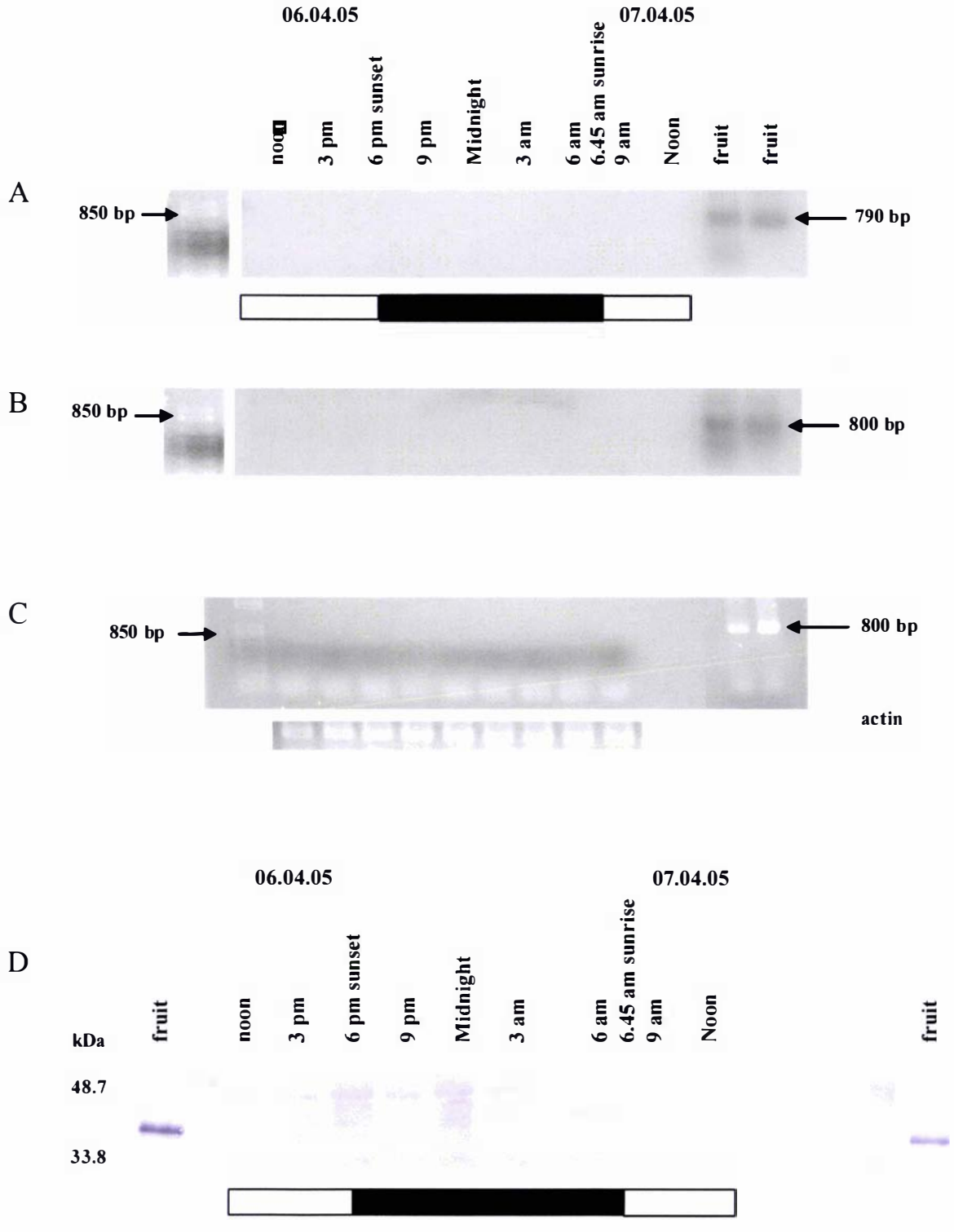


Figure 3.42: Circadian rhythm of ACC Oxidase Gene Expression Over 24 h in the Leaves of *Malus domestica* (Fruit Removed From the Trees; April, 2005).

The apple fruit were harvested 02.03.05. Southern cDNA blot analysis using *MD-ACO2* fragments (A), and *MD-ACO3* fragments (B). Second round PCR using gene specific primers to amplify fragments (C). Western blot analysis using antibodies raised against MD-ACO3 (D).

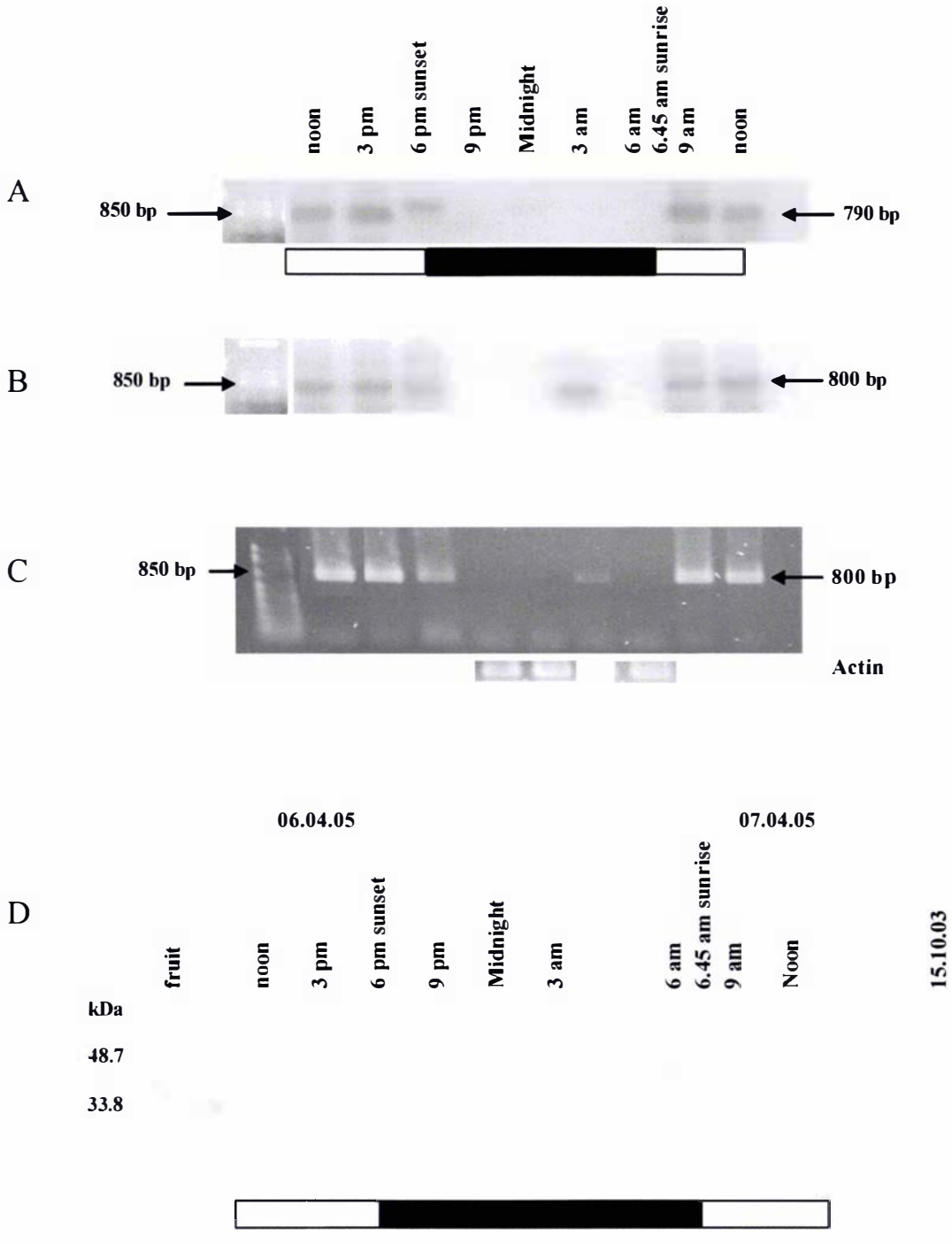


Figure 3.43: Circadian Rhythm of ACC Oxidase Gene Expression Over 24 h in the Leaves of *Malus domestica* (with Fruit; April, 2005).

The apple fruit remained on the trees. Southern cDNA blot analysis using *MD-ACO2* fragments (A), and *MD-ACO3* fragments (B). Second round PCR using gene specific primers to amplify fragments (C). Western blot analysis using antibodies raised against MD-ACO3 (D).

Chapter Four DISCUSSION

4.1 Overview

ACO gene expression, enzyme accumulation and kinetic properties have been well documented during apple fruit development (Atkinson *et al.*, 1998; Cin *et al.*, 2005; Ross *et al.*, 1992; Dong *et al.*, 1992b; Fernández-Maculet and Yang, 1992; Kuai and Dilley, 1992; Dilley *et al.*, 1993; Poneleit and Dilley, 1993; Fernández-Maculet *et al.*, 1993; Dupille *et al.*, 1993; Pirrung *et al.*, 1993), but not during apple leaf development. Therefore, this study seeks to investigate ACO in the bourse shoot leaves of apple, the leaves closely associated with fruit development, to enhance our understanding of the regulation of ACO during apple leaf maturation and senescence. The thesis is divided into three sections. The first section aims to establish the small multi-gene family of apple ACO and to confirm that each of the transcripts is encoded for by a distinct gene. The second section aims to establish that each of the three isoforms are different by analyses of the kinetic properties of each of the enzymes. The third section aims to establish the expression patterns of each of the genes during leaf ontogeny.

4.2 ACC Oxidase Genes in *Malus domestica*

4.2.1 Evidence of a Multi-Gene Family in Apple by Genomic Southern Analysis

Southern analysis of genomic apple DNA using sequences which spanned the ORF and the 3′-UTR as probes, confirmed that the *MD-ACO3* sequence is encoded by a gene distinct from both *MD-ACO1* and *MD-ACO2*, as the hybridization patterns following restriction digests with *Eco*RI, *Hind*III and *Xba*I, are clearly different (Figure 3.10B).

Interestingly, every one of the restriction digested fragments which have hybridised with *MD-ACO2* are of the same approximate size as fragments which have hybridized with *MD-ACO1*. A striking observation is that only one genomic fragment tends to hybridize with *MD-ACO2* whereas two fragments tend to hybridize with *MD-ACO1*. This is most evident with the *Hind*III digested fragments where fragments of 1.5 kb and 1.9 kb strongly hybridize with *MD-ACO1* compared with the one fragment of 1.9 kb which hybridized with *MD-ACO2* (Figure 3.10B). As in this study restriction sites for *Eco*RI, *Hind*III and *Xba*I are not present in the probe used for the genomic Southern hybridization, and therefore there are no internal restriction sites, when two fragments from the same digest hybridize with a specific probe this indicates that there maybe two copies of the gene in the genome, and similarly, when one fragment from the same digest hybridises with a specific probes this is indicative of a single gene present in the genome. In previous studies, the *pAP4* clone (cv. Golden Delicious; number X61390; Ross *et*

al., 1992; designated *MD-ACO1* in this thesis) was used as a RFLP marker (restriction fragment length polymorphisms) to construct linkage maps of the progeny of a cross between the apple cultivars Prima and Fiesta (in common with Royal Gala, these cultivars have 34 somatic chromosomes and a haploid number of 17), and was found at two loci, one on chromosome 5 (*pAP4*a) and one on chromosome 10 (*pAP4*b) (Maliepaard *et al.*, 1998). This indicates that *MD-ACO1* may be present at two different loci in the genome of the cv. Royal Gala. Also, Southern analysis using DNA extracted from cv. Golden Delicious, and digested with *Eco*RI, *Hind*III and *Bam*HI and then probed with ^{32}P-labelled *pAP4* (designated *MD-ACO1* in this thesis) (Ross *et al.*, 1992), revealed that two fragments hybridized with *pAP4* for each of the genomic digests. For example, for *Hind*III digested fragments, two fragments hybridized strongly with *pAP4* of *ca.* 1.5 kb and 1.9 kb, and these fragments are the same approximate size as the fragments which hybridised with *MD-ACO1* in the present study. Similarly, for the Golden Delicious genomic DNA digested with *Eco*RI a fragment hybridised strongly with *pAP4* of *ca.* 2.5 kb and less intensely with a fragment of *ca.* 5.0 kb. Again, the fragment sizes which hybridized with *MD-ACO1* in the present study are of the same approximate size and relative intensity, although there are also bands of a larger size present (of *ca.* 8, 10.5 and 12 kb). These larger fragments may represent partial digests as only a visual assessment of genome digestion is made. For the *Bam*HI digested fragments, *pAP4* also hybridized with two fragments of *ca.* 2 kb and 1 kb although the restriction enzyme *Bam*HI was not used in the present study. Hence, the evidence gathered to date strongly suggests that two copies of *MD-ACO1* are present in the cv. Royal Gala genome. By contrast one copy of *MD-ACO2* appears to be present in the cv. Royal Gala genome. For example, for the *Hind*III digest, one fragment of *ca.*1.9 hybridized with *MD-ACO2*, and for the *Xba*I digest, one fragment of *ca.* 15 kb hybridized with *MD-CO2,* (although there is another less intense larger fragment). For the *Eco*RI digest, the fragment which strongly hybridized with *MD-ACO2* of *ca.* 5 kb corresponds with the approximate fragment size which hybridized with *pAP4* (Ross *et al.*, 1992) and *MD-ACO1* in this study, and there is also a less intense band of *ca.* 8 kb.

The observation that the restriction digested fragments which have hybridized with *MD-ACO2* are the same approximate size as fragments which have hybridized with *MD-ACO1* suggests that *MD-ACO1* and *MD-ACO2* may be tightly clustered on the genome as the restriction digests are so similar (Dr Sue Gardiner, HortResearch, New Zealand, *pers. comm.*). However, the Southern blot analysis does not give enough information as to whether *MD-ACO1* and *MD-ACO2* are indeed clustered and encoded by distinct genes, or whether in fact they are alleles of the same gene. Gene mapping of the genomic or mRNA sequence of *MD-ACO2* would give the exact location(s) of the sequence on a specific chromosome(s) and may also determine whether

MD-ACO1 and *MD-ACO2* are clustered or allelic, but even so very fine grained mapping would be necessary.

MD-ACO3 is clearly a gene distinct from both *MD-ACO1* and *MD-ACO2*. However, while one fragment has strongly hybridised with *MD-ACO3* following an *Xba*I digest (of 5.1 kb), two fragments have strongly hybridised with *MD-ACO3* following a *Hind*III digest (3.3 kb and 5 kb), with a less intense band of *ca.* 6 kb. Therefore, *MD-ACO3* is probably present in the cv. Royal Gala genome as a single copy, but the two fragments which hybridize with the probe following the *Hind*III digest raise the possibility that two copies of *MD-ACO3* may be present. If *Xba*I were to be an infrequent cutter for example, and both copies were present on the same fragment, then perhaps the second copy could be missed using Southern analysis. Hybridisation with *MD-ACO3* following the *Eco*RI digest is unclear, but fragments have hybridized with *MD-ACO3* of *ca.* 2.9 kb and also with fragments of a larger size. Hence, it is unclear whether a single copy or two copies of MD-ACO3 are present in the Royal Gala genome.

Ross *et al.*, (1992) conclude that their Southern analysis confirms the presence of at least one *Hind*III restriction site in the gene, as predicted from the *pAP4* cDNA. A *Hind*III restriction site occurs in the third exon of both *MD-ACO1* and *MD-ACO2* (refer Figure 3.6). However, in this study neither the *MD-ACO1* nor the *MD-ACO2* sequences used as probes contain *Hind*III, *Eco*RI or *Xba*I restriction sites. As there are other less intense bands with all three restriction enzymes, even at high stringency, for all of the *MD-ACO* probes, they may represent the presence of sequences related but not totally identical to *MD-ACO1*, *MD-ACO2* and *MD-ACO3*, which may indicate a possible fourth MD-ACO gene.

4.2.2 Gene Structure of *MD-ACO1*, *MD-ACO2* and *MD-ACO3*; Comparison of Exons and Introns

MD-ACO1 and *MD-ACO2* genes share the same gene structure, in that each gene contains four exons interspersed with three intron sequences (Figure 3.6). As the genomic sequence of *MD-ACO3* is unavailable, the distribution of introns remains unknown.

All three *MD-ACO*s share the same nucleotide length for exon 1, exon 2 and exon 3, and while both *MD-ACO1* and *MD-ACO2* have a *Hind*III site at the same location on the third exon, they do not share the same location for the other restriction sites. For example, *MD-ACO1* has two *Hind*III sites and an *Eco*RI site in the second intron, which are not present in *MD-ACO2*, and *MD-ACO2* has a *Hind*III site in the first intron which is not present in *MD-ACO1*. This difference, again raises the question of whether *MD-ACO1* and *MD-ACO2* are encoded by

distinct genes or whether they are allelic forms of the same gene, as the restriction sites are so different. Exon 4 varies between *MD-ACO1* (276 bp) and *MD-ACO2* (324 bp) by 48 bp representing 16 extra amino acids (aa) at the carboxyl end of *MD-ACO2*. A comparison of average peptide number over the first 23 ACOs sequenced revealed a value of 314 residues (Kadyrzhanova *et al.*, 1997). Inspection of the of 85 ACO sequences available on the NCBI protein database, and gathered for the construction of the phylogenetic tree (Figure 3.8), reveal the majority of proteins are between 314 aa and 322 aa. However it is unclear whether all these are active enzymes. MD-ACO2 (330 aa) has the highest number of residues and is the only ACO with a peptide number more than 322 aa. Nevertheless, MD-ACO1 (314 aa), MD-ACO2 (330 aa) and MD-ACO3 (322 aa) structure is comparable with ACO from other species.

The conservation in gene structure is not only displayed in apple, but can also be observed in other species. In comparison with other published accounts of ACO gene structures, the occurrence of 4 exons interspersed with 3 introns has been observed in white clover (*TR-ACO1*, *TR-ACO2*, *TR-ACO3* and *TR-ACO4*) (Chen and McManus, 2006), melon (*CM-ACO1*) (Lasserre *et al.*, 1996), peach (*PP-ACO1*) (Ruperti *et al.*, 2001) and in petunia (*PH-ACO1*, *PH-ACO3* and *PH-ACO4*) (Tang *et al.*, 1993). It should be noted that other members of the melon family (*CM-ACO2*, *CM-ACO3*) and peach (*PP-ACO2*) comprise 2 introns interspersing 3 exons (Lasserre *et al.*, 1996; Ruperti *et al.*, 2001).

Identities calculated between the introns of *MD-ACO1* and *MD-ACO2* are lower than the identities between each of the the exons of *MD-ACO1* and *MD-ACO2* (Table 3.6). Sequence comparisons between the entire open reading frames (ORFs) of the *MD-ACO1* and *MD-ACO2* (93.9 %) transcripts (Table 3.7, A and B) reveals a higher identity than between the 3′-UTR sequences (69.5 %) which supports the hypothesis of these being two distinct *MD-ACO* genes. This is also consistent with white clover ACO studies (Hunter *et al.*, 1999) where greater identity was found over the reading frame (> 90 %) than the 3′-UTR (~70 %), and also with peach, where identity between the coding regions of *PP-ACO1* and *PP-ACO2* (77.7 %) is higher than for the 5′ and 3′-UTRs of 44 % and 50.4 % respectively (Ruperti *et al.*, 2001). The identities between the ORF transcripts of *MD-ACO3* and both *MD-ACO1* (78.5 %) and *MD-ACO2* (77.8 %) are almost as low as the identities between the *MD-ACO3* transcripts for the 3'-UTR of *MD-ACO1* (68.4 %) and *MD-ACO2* (69.5 %), indicating a greater divergence of *MD-ACO3* from both *MD-ACO1* and *MD-ACO2*.

Interestingly, the genome of Gala apple has been observed by Castiglione *et al.* (1999), to contain heterozygous alleles of different molecular weights and restriction patterns, following PCR-RFLP analysis of ACO using specific primers to the *pAP4* clone (designated *MD-ACO1* in

this thesis) and digested with *Hind*III. Such DNA polymorphism may suggest that *MD-ACO1* and *MD-ACO2* are two forms of the same gene (*MD-ACO1-1* and *MD-ACO1-2*), since polymorphism refers to the simultaneous occurrence in the population of genomes showing allelic variation (as seen either in alleles producing different phenotypes or, for example, in changes in DNA affecting the restriction pattern). For example, Sunako *et al.*, (1999) reported that the cv. Golden Delicious is either heterozygous for ACS (*ACS1-1* and *ACS1-2*) or homozygous for each type. Further, it was demonstrated that the level of transcript from *ACS1-2* during the ripening stage was very low and consequently has a longer storage life than *ACS1-1*. Such differences in alleles may lead to the possibility of one of the allelic forms being selected for breeding rather than another. Evidence from both the genomic Southern blot analysis and the comparison of the gene structure of *MD-ACO1*, *MD-ACO2* and *MD-ACO3* confirms that *MD-ACO3* is encoded by a gene distinct from *MD-ACO1* and *MD-ACO2*. However, it remains unclear whether *MD-ACO1* and *MD-ACO2* are two distinct genes or allelic forms of the same gene.

4.2.3 Translated Products of *MD-ACO* Genes

Amino acid sequence identity between MD-ACO1 and MD-ACO2 (92.04 %) is higher than either MD-ACO3 and MD-ACO1 (80.57 %) or MD-ACO3 and MD-ACO2 (75.16 %) and broadly reflects the nucleic acid sequence identities (Table 3.7C). It is of note that all three gene products of apple ACO have the conserved amino acids, found necessary to date (Zhang *et al.*, 2004; Dilley *et al.*, 2003; Kadyrzhanova *et al.*, 1999; 1997), for the appropriate structure and function of the protein (Figure 3.7).

Examination of the phylogenetic tree (Figure 3.8) indicates that MD-ACO1 and MD-ACO2 proteins would have diverged sometime ago (Dr Peter Lockhart, IMBS, Massey University, *pers. comm.*), as the length of the branches are indicative of the evolutionary time of divergence. Of note, PC-ACO1 of *Pyrus communis* (European pear) cloned from the cortical tissue of unripe mature fruit is located close to MD-ACO1, PP-AOX4 of *Pyrus pyrifolium* (Asian pear) cloned from the immature fruit is located close to MD-ACO2, whilst JP-AOX3 from ripe pear fruit (Japanese:Asian pear) is situated closest to MD-ACO3. This is in contrast to the virtual northern (Figure 3.11) where *MD-ACO1* and *MD-ACO2* are more closely associated with the fruit and *MD-ACO3* is associated with leaf tissue. Bootstrap analysis supports the evidence that MD-ACO1 and MD-ACO2 are encoded by two distinct genes. Overall, it seems *MD-ACO1* and *MD-ACO2* are distinct genes which diverged some time ago, but are closely related compared to *MD-ACO3*. It should be noted that the stop codon for *MD-ACO1* is **T**GA and when the *MD-ACO2* sequence is aligned with the *MD-ACO1* sequence, the codon at the same position for

MD-*ACO2* is **C**GA. Hence, a single base-pair mutation in either *MD-ACO1* or *MD-ACO2* perhaps underlies the divergence of the two genes. Phylogenetic analysis does not indicate in which order the three isoforms evolved. Taken together, the phylogenetic tree (Figure 3.8) constructed from an alignment of 85 ACO NCBI protein database sequences with the deduced amino acid sequences for *MD-ACO1*, *MD-ACO2* and *MD-ACO3* over the entire open reading frame, suggests that the gene products are derived from three different *MD-ACO* genes.

4.2.4 Confirmation of *MD-ACO* Differential Gene Expression *In Vivo*

In order to determine the gene expression patterns and relative abundance of *MD-ACO1*, *MD-ACO2* and *MD-ACO3* transcripts in apple, relative quantitative RT-PCR with ribosomal RNA controls was used (Figure 3.14). The debate about using a relative quantitative RT-PCR technique to successfully demonstrate levels of specific transcripts verses conventional northern blotting is ongoing (Hengen, 1995). Some supporters do find the RT-PCR method both more valid and reliable than northern analysis (Jaakola *et al.*, 2001). RNA extracted from young leaf, mature green leaf, young fruit (~ 2 cm diameter) and mature fruit tissue, after RT using random primers and PCR using gene specific primers, produced different expression patterns for each of the three genes as revealed by ethidium bromide staining.

Expression studies with *MD-ACO1* showed that the gene is expressed in mature fruit, with negligible amounts in young fruit, and no transcripts were visible at all in leaf tissue. This suggests that *MD-ACO1* is expressed in a tissue-specific manner, and is present only in fruit tissue and specifically in mature fruit tissue. This is consistent with the lack of *pAE12* mRNA transcript reported by Dong *et al.*, (1992b) in preclimacteric apple fruit untreated with ethylene, and also in agreement with the later western blot analysis in this study (Figure 3.24A) where an antibody raised against MD-ACO1 recognised a protein that accumulated in mature fruit. Both the virtual northern (Figure 3.11) and the cDNA Southern analysis (Figure 3.15) also support the RT-PCR findings that *MD-ACO1* is expressed (of the tissues examined) exclusively in apple fruit tissue *in vivo*. Further, fragments of the *MD-ACO1* (clone *pAP4*) promoter (-1966 bp upstream of ATG) fused to the β-glucuronidase (GUS) reporter gene and transformed as translational fusions expressed in tomato by Atkinson *et al.*, (1998) were found to be active only in the fruit in a ripening specific pattern.

In contrast, using relative quantitative RT-PCR, primers specific for *MD-ACO2* transcripts amplified products from apple tissue in a developmentally-regulated manner. A comparatively higher level of *MD-ACO2* was found in fruit tissue compared to a much smaller amount of transcript found in leaf tissue (Figure 3.14). However, in the virtual northern the EST sequence

most similar to *MD-ACO2* (EST 153710) was found in apple fruit and spur buds only (Figure 3.11). cDNA Southern analysis using semi-degenerate primers (Figure 3.15) supports the findings that *MD-ACO2* transcripts are expressed predominantly in apple fruit tissue and at lower levels in leaf tissue, although a non quantitative analysis using oligo $d(T)_{15}$ primers and 30 PCR amplification cycles (Figure 3.12) reveals bands of similar intensity in young leaf, mature leaf, young fruit and mature fruit. Although the relative quantitative RT-PCR must be seen as the more credible data, the question of the temporal expression of *MD-ACO2* in leaf tissue is raised. The EST sequence (EST 153710) that corresponds to *MD-ACO2* was extracted mainly from fruit but also from the spur buds (Figure 3.11), while the *MD-ACO2* identified in this study was cloned from the leaves of apple (initial, mature fully expanded and senescent) using degenerate universal primers (Figure 2.2), cloned into pGEM and sequenced. It must be concluded therefore that *MD-ACO2* is expressed in apple leaf tissue.

For *MD-ACO3*, gene-specific primers amplified products in all of the apple tissues examined in a developmentally regulated manner with less intense staining in mature fruit tissue and the most intense staining in young leaf tissue. In the virtual northern, the EST sequence most similar to *MD-ACO3* (EST 179706 and EST 192136) were identified in fruit, seedling leaves and senescing leaf tissue (Figure 3.11). In the cDNA Southern analysis (Figure 3.15), *MD-ACO3* transcripts occur predominantly in initial leaf tissue, less intensely in mature green tissue and even less intensely in young fruit tissue. Because the band is barely visible in mature fruit tissue in the cDNA Southern, it could be interpreted as an artefact of the high levels of *MD-ACO1* and *MD-ACO2* in mature apple fruit. However, using relative quantitative RT-PCR (Figure 3.14) *MD-ACO3* is clearly shown to be expressed in mature fruit tissue. Taken together, *MD-ACO3* in these studies is expressed most strongly in apple leaf and in particular young leaf tissue *in vivo*, but also young fruit, with a much lower level of expression in mature fruit tissue.

In summary, therefore, *MD-ACO1* transcripts are expressed predominantly in mature fruit with either very low levels (Figure 3.14) or lower levels (Figure 3.15) of expression in young fruit, while *MD-ACO2* transcripts are abundant in mature fruit, and either abundant (Figure 3.14) or expressed at a lower level (Figure 3.15) in young fruit, and then decline in mature green leaves and initial leaves. In contrast, *MD-ACO3* transcripts are highest in initial leaves and decline in mature green leaves, young fruit and then expression is very low in mature fruit.

The *pAP4* gene (designated as *MD-ACO1* in this thesis) from apple fruit, (designated the ripening-specific ACO by Ross *et al.*, 1992), was found to be up-regulated during the fruit ripening of Gala, Braeburn and Granny Smith. Expression in Gala was detected earlier than in

Braeburn and Granny Smith cultivars by Atkinson *et al.*, (1998), relative to the internal base-line levels of ethylene concentration for each of the cultivars. The *pAP4* clone (*MD-ACO1*) accumulated in the seeds of abscising apple fruitlets reaching a level nearly 1,000 times higher than in non abscising fruitlets (Cin *et al.*, 2005). In the cortex, the pattern of expression appeared to be quite similar to that observed in seed, although transcripts accumulated at a level 10 times lower (Cin *et al.*, 2005). In this study, the young fruit (~ 2 cm diameter) would have been non abscising since the levels of *MD-ACO1* transcript are not abundant. However, in a study by Lara and Vendrell (2000), no protein was detected using antibodies raised against the *pAE12* clone (also designated as MD-ACO1 in this thesis) during the preclimacteric stage of Granny Smith apples. Similarly, using antibodies raised against the *pAE12* clone (MD-ACO1), Dilley *et al.*, (1995) found that protein was not detectable in apples prior to the onset of the ethylene climacteric but increased markedly as the climacteric developed. Further, that mRNA (clone *pAE12*) encoding MD-ACO1 accumulated to high levels over the course of the ethylene climacteric. Ross *et al.*, (1992) found ACO (clone *pAP4*) probes not to hybridize to young immature apple fruit tissue extract. However, as ripening progressed the degree of hybridization increased. Such an increase in apple ACO mRNA transcript (Dilley *et al.*, 1995) would correspond with the climacteric rise in ethylene biosynthesis from the mature green stage (LeLievre *et al.*, 1997; Bleecker and Kende, 2000; Giovannoni, 2001) of apple fruit ripening. In this study, the *MD-ACO1* probes hybridized strongly with fragments from mature fruit tissue, less intensely with fragments from young immature fruit, and no hybridization was detectable with fragments from either young or mature leaf tissue.

MD-ACO1 in this study appears to have a similar expression pattern in fruit tissue to both the *pTOM13* (Hamilton *et al.*, 1990; 1991) also known as *LE-ACO1* (Barry *et al.*, 1996; Blume and Grierson, 1997) and to the *LE-ACO4*, both from tomato (Nakatsuka *et al.*, 1998), as well as *PP-ACO1* from peach (Ruperti *et al.*, 2001; Rasori *et al.*, 2003; Moon and Callahan, 2004) and *PA-ACO1* from apricot (Mbéguié-A-Mbéguié *et al.*, 1999). Both *LE-ACO1* and *LE-ACO4* are expressed in immature green and mature green fruit, with the abundance increasing greatly during the climacteric, particularly for *LE-ACO1* (Nakatsuka *et al.*, 1998) which appears ≥ two fold higher than *LE-ACO4*. In common with *MD-ACO1*, *LE-ACO4* is not detectable in leaf tissue (Nakatsuka *et al.*, 1998), whereas *LE-ACO1* transcripts have been observed to increase (up to 27-fold) at the onset of leaf senescence (Barry *et al.*, 1996). Given that both the tomato *LE-ACO1* and the peach *PP-ACO1* genes are expressed abundantly during the fruit climacteric and during leaf senescence, the prediction that either *MD-ACO1* or *MD-ACO2* are good candidates for the senescence associated gene (SAG) in apple leaf seems reasonable. However, from the results of this thesis neither *MD-ACO1* nor *MD-ACO2* have been observed to fulfil the role of a SAG in leaf tissue. Indeed, if either *MD-ACO1* or *MD-ACO2* were found to be SAG

genes in leaf tissue, any efforts to delay senescence through the manipulation of these genes would presumably also delay fruit ripening.

MD-ACO1, *MD-ACO2* and *MD-ACO3* most closely align with pear (*Pyrus pyrifolia* and *Pyrus communis*) ACO on the phylogenetic tree (Figure 3.8). *MD-ACO2* shares the closest alignment with an ACO (*PP-AOX4*) expressed in the immature fruit of pear, *MD-ACO1* is also associated with ACO expressed in pear fruit (*JP-AOX1* and *ACO1*) and unripe mature pear fruit (*PC-ACO1*). In contrast *MD-ACO3* shares the closest alignment with an ACO from ripe pear fruit (*JP-AOX3*, *PP-AOX2A* and *PP-AOX2B*). Unfortunately, the literature does not appear to contain data on pear ACO expression in leaf tissue, differential expression or even temporal expression in the fruit, but rather studies have focused on the role of ethylene, cold treatment and ACO accumulation postharvest in pear fruit ripening (Lelièvre *et al.*, 1997; Hiwasa *et al.*, 2003; Gao *et al.*, 2002; Foneseca *et al.*, 2004). For example, 21 days after harvest following cold treatment and ethylene treatment the ACO transcripts from the pear cv. Roche (*RP-ACO1*) double (Foneseca *et al.*, 2004). ACO from softening and wounded peach fruit (*PP-ACO1*) is also within the grouping of *MD-ACO3* (Figure 3.8). However, because a gene has been found to be expressed in a certain tissue, and entered into the Genbank it cannot be assumed that it is expressed predominantly in that tissue rather than another tissue, or that another member of the gene family is not present in a greater abundance. In other words, there is no indication of the relative quantity of expression compared to another member of the gene family. Broadly, the peach ACO (*PP-ACO1* and *PP-ACO2*) each fall into one of two groups, *PP-ACO1* in the *MD-ACO3* grouping, and *PP-ACO2* in the *MD-ACO1* and *MD-ACO2* grouping (Figure 3.8). Interestingly *PP-ACO1* resembles *MD-ACO3* as they are both expressed in young fully expanded green leaf tissue, but *PP-ACO1* also resembles *MD-ACO1* and *MD-ACO2* in that they are all expressed abundantly during the climacteric necessary for fruit ripening. However, unlike any of the *MD-ACO* genes, the *PP-ACO1* is a SAG gene as it is expressed abundantly in senescing leaf tissue. Interestingly, the observation that *pMEL1* from melon is expressed in climacteric fruit and wounded leaf tissue but was undetectable in both preclimacteric fruit and unwounded leaf tissue (Balague *et al.*, 1993), raises the possibility that *MD-ACO1* mRNA may also be detected in wounded leaf tissue. It has been shown that the *MD-ACO1* (clone *pAP4*) promoter lacks wound-response-elements (WUNs) and wound inducible (WIN) nucleotide sequences, and therefore may not be activated by wounding (Atkinson *et al.*, 1998). However, Ross *et al.*, (1992) observed a wound response in preclimacteric apple fruit, with a wounding response time of from 5 h to 24 h, which raises the question of whether either the *MD-ACO2* or the *MD-ACO3* promoter contains WIN and/or WUN boxes. As *MD-ACO1* (clone *pAP4*) has been reported to have two potential ethylene response elements (ERE)(Atkinson *et al.*, 1998),

an ethylene wound response could be augmented by *MD-ACO1* (but the gene expression may not be immediately induced by wounding).

The probability that *MD-ACO2* and *MD-ACO3* may also be tightly controlled by developmental and environmental stimuli is overwhelming, given the well established temporal and tissue specific expression of *ACO* genes from other plant species. In common with *MD-ACO2*, both *LE-ACO1* and *LE-ACO4* transcript expression is ripening specific in fruit, but unlike *MD-ACO2*, *LE-ACO4* has not been observed in leaf tissue. Therefore, *LE-ACO4* may correspond more closely with *MD-ACO1* as both are expressed in the fruit tissue but appear not to be expressed in leaf tissue. *MD-ACO2* and *LE-ACO1* transcripts are expressed in both leaf and fruit tissue, but the senescence specific accumulation of *LE-ACO1* mRNA has not been observed in *MD-ACO2* expression patterns. Neither *MD-ACO3* nor *LE-ACO3* exhibit classic fruit ripening expression patterns, and both are present in leaf and fruit tissue. However, unlike *MD-ACO3*, where transcripts predominate in young bourse shoot leaves, *LE-ACO3* has not been reported in young leaf tissue, but is rather associated with leaf senescence where transcript abundance is approximately 50 % that of *LE-ACO1* (Barry *et al.*, 1996). Further, the transient expression of *LE-ACO3* contrasts with the apparent developmentally regulated pattern observed in *MD-ACO3* transcript accumulation.

Neither *MD-ACO1*, *MD-ACO2* nor *MD-ACO3* appear to be expressed predominantly in senescing leaf tissue. Many studies have identified at least one member of the ACO gene family as a senescence associated gene (SAG), for example *TR-ACO3* and *TR-ACO4* in white clover (Hunter *et al.*, 1999; Chen and McManus, 2006), *LE-ACO1* in tomato (John *et al.*, 1995) and *CP-ACO2* in papaya (Chen *et al.*, 2003). Both *MD-ACO1* and *MD-ACO2* are expressed predominantly in mature fruit which may be associated with senescence, and *MD-ACO3* is more likely to be a photosynthetic associated gene (PAG), as it is expressed predominantly in initial bourse shoot leaf tissue. However, *MD-ACO3* is also expressed in mature green fully expanded leaf tissue, *MD-ACO2* is also expressed in initial bourse shoot leaf tissue and mature green fully expanded leaf tissue. Therefore *MD-ACO2* may also be a PAG.

Overall, these gene expression studies indicate that each of the three *MD-ACO* sequences are encoded by distinct genes as their expression patterns appear to be different. However, although *MD-ACO1* has not been identified in leaf tissue in this study, it can not be concluded that *MD-ACO1* is not present in apple leaf tissue. Further, the possibility can not be excluded that *MD-ACO1* and *MD-ACO2* are in fact heterozygous allelic forms of *MD-ACO1* (*MD-ACO1-1* and *MD-ACO1-2*). However, it may be unusual that one allele is expressed in leaf tissue and the other allele is not expressed at all in leaf tissue. For example, in the case of the *ACS1-1* and

ACS1-2 alleles reported by Sunako *et al.* (1999), one allele is expressed more frequently than the other allele in the same tissue, so that it is the level of expression which is different for each of the alleles in the fruit tissue. For *MD-ACO1* and *MD-ACO2* the difference is that they are expressed differentially in leaf tissue but exhibit very similar temporal expression in the fruit tissue. Therefore, the expression patterns of *MD-ACO1* and *MD-ACO2* may support the notion that they are encoded by two distinct genes.

4.3 Expression and Characterisation of MD-ACO1, MD-ACO2 and MD-ACO3 as recombinant proteins

ACO extracted from apple fruit tissue has been extensively characterized (Fernández-Maculet and Yang, 1992; Kuai and Dilley, 1992; Dong *et al.*, 1992b; Poneleit and Dilley, 1993; Pirrung *et al.*, 1993; Dilley *et al.*, 1993; Dupille *et al.*, 1993 and Mizutani *et al.*, 1995). In these studies genes that are most similar to MD-ACO1 have been expressed both in the *E. coli* strain BL-21 (clone *pAE12*) using the pET20b+ vector (Charng *et al.*, 1997; 2001), and in the yeast strain F808 (clone *pAP4*) using the pYES2 vector (Wilson *et al.*, 1993). While the investigation of MD-ACO1 (*pAE12*) inserted into the pET20b+ vector (designated *pAE20*) focussed on the degradation of α-aminoisobutyric acid and structure-function studies on the CO_2 binding site of ACO, both the K_m for ACC (K_m^{ACC}) and the K_{cat} are reported for the isoform purified to homogeneity from the *E. coli* background, together with the specific activity. Recently, MD-ACO1 (*pAE12*) inserted into the pET20b+ vector and expressed in *E. coli* (strain BL-21) was used for mutagenesis studies, and the K_m^{ACC}, K_{cat} and specific activity are documented (Yoo *et al.*, 2006). Activities are also reported by Charng *et al.* (1997) for a crude extract of the recombinant enzyme from the prokaryotic cells both in the presence of CO_2 (3.2 nmol mg^{-1} min^{-1}) and in the absence of CO_2 (0.06 nmol mg^{-1} min^{-1}). For MD-ACO1 (*pAP4*) expressed in yeast the enzyme was not extracted from the eukaryotic cells for characterization, so that the ACO assays were conducted by adding ACC (10 μL of 100 mM), ascorbic acid (6 μL of 0.5 mM) and $FeSO_4$ (4 μL of 1 mM) directly to 980 μL aliquots of yeast cell culture, containing the *pAP4* inserted into the pYES2 vector (designated *pAPY4*). The production of ethylene-forming ability of MD-ACO1 expressed in yeast is reported to have similar characteristics to those observed *in vitro* for partially purified (Dilley *et al.*,1993; Kuai and Dilley, 1992) and purified to near homogeneity (Dong *et al.*, 1992b) fruit tissue from the Golden Delicious cultivar, but was depended on the growth phase of the culture. In contrast to the above studies, the research in this thesis has investigated the kinetic properties of three MD-ACO isoforms expressed in *E. coli* (strain BL-21) using the pProEX-1 vector, (and it should be noted that both the *MD-ACO2* and *MD-ACO3* mRNA transcripts were extracted from the leaf tissue of the Gala cultivar prior to cloning, so both genes are expressed in the leaves of apple). This is the first study, therefore, that has compared multiple members of the apple gene family in this way.

4.3.1 Kinetic Properties of the MD-ACO Isoforms

Each of the three apple ACO cDNAs were expressed in *E. coli* and translated as fusion proteins containing a His-tag on the N-terminus, purified, and then the apparent kinetic properties of the enzymes were analyzed. Over expression of the recombinant MD-ACOs in *E. coli* resulted in

degradation of the protein as judged by fragmentation, which was particularly evident for the MD-ACO3 isoform (while degradation appeared to be much less for MD-ACO2 than for the other MD-ACO isoforms). Although all three of the MD-ACO isoforms have an autocleavage site between lysine at position 186 (L^{186}) and phenylalanine at position 187 (F^{187}) which would generate fragments of *ca.* 28.7 kDa, degradation products occur predominantly at *ca.* 35 kDa (Figure 3.19). Evenso anion exchange was used to separate the active enzyme from the inactive degraded forms of the protein (as well as from other *E. coli* chelating proteins), and it was this purified fraction that was used for further analysis.

A comparison of the kinetic parameters of MD-ACO1, MD-ACO2 and MD-ACO3 from this study with the MD-ACO1 *(pAE20)* isoform expressed in *E. coli* (Charng *et al.*, 2001), tomato LE-ACO1, LE-ACO2 and LE-ACO3 expressed in yeast (pBEJ15; Bidonde *et al.*, 1998), MD-ACOs purified from mature Golden Delicious fruit tissue (Dong *et al.*, 1992b; Dupille *et al.*, 1993; Pirrung *et al.*, 1993) and for white clover, an isoform purified from senescent leaf tissue (designated SE1) and an isoform purified from senescent leaf tissue (designated MGI) (Gong and McManus, 2000), are all shown as Table 4.1. Crude and partially purified ACO extracts have not been included in this comparison, as such extracts are more likely to contain more than one isoform, and these extracts may also affect the affinity of the ACOs for substrate. For example, the K_m^{ACC} of the partially purified enzyme from carnation flowers (Kosugi *et al.*, 1997) ranged from 111 μM to 125 μM compared with 425 μM determined for the crude enzyme (Nijenhuis De Vries *et al.*, 1994). The tomato and white clover ACOs have been included as they are the only studies where more than one isoform of a species has been characterized, and therefore comparisons of ACO can be made both within and between species. Also a comparison between ACO expressed in the eukaryotic background (Bidonde *et al.*, 1998) as opposed to ACO expressed in the prokaryotic background (Charng *et al.*, 1997; 2001; this thesis), together with ACOs purified from plant tissue (Dong *et al.*, 1992b; Dupille *et al.*, 1993; Pirrung *et al.*, 1993; Gong and McManus, 2000), may be meaningful.

For these studies shown as Table 4.1, the molecular masses are broadly similar (35 - 40 kDa), white clover has a neutral isoelectric point (pI) while the tomato isoforms are on the acidic side (6.1 to 6.8) and the theoretical pI of the recombinant apple isoforms are the most acidic ranging from 5 to 5.52. The tomato isoforms expressed in yeast share the same pH optimum, which is, incidentially, consistent with the pH of 7.2 used for LE-ACO1 expressed in *E. coli* (strain BL-21) using the pET-11a or pET-3c expression plasmid (Zhang *et al.*, 1995; Thrower *et al.*, 2001). As well, the same requirements for $FeSO_4$ and $NaHCO_3$ are determined, although the K_m^{ACC} of the senescence associated isoform (LE-ACO1) differs from the LE-ACO2 and LE-

Table 4.1: Comparison of the Kinetic Properties of Recombinant and Purified ACOs from Apple and Other Species

Kinetic Parametres	Apple							Tomato			White Clover	
	Recombinant in *E. coli*				Purified (mature fruit tissue)			Recombinant in Yeast			Purified	
	MD-ACO1 This thesis	**MD-ACO2** This thesis	**MD-ACO3** This thesis	**MD-ACO1** Charng/Yoo	**MD-ACO** Dong	**MD-ACO** Dupille	**MD-ACO** Pirrung	**LE-ACO1** Bidonde	**LE-ACO2** Bidonde	**LE-ACO3** Bidonde	**MG1** Gong	**SE1** Gong
kDa												
native	-	-	-	-	39	39	35.3amu	-	-	-	37.5	37.5
denatured	35.35 (aa.314)	37.50 (aa.330)	36.314 (aa.322)	35 (aa.314)	35	40	40	36 (aa.315)	36 (aa.316)	36 (aa.316)	37.0	35.0
pI	[1]5.24 5.15	[1]5.52	[1]5.28	[1]5.0/?	-	-	-	6.1	6.8	6.1	7.36	7.0
pH	7.2	7.8	7.5	[2]7.0/7.4	-	7.4	-	6.8 -7.2	6.8 -7.2	6.8 -7.2	7.5	8.5
$FeSO_4$ µM	20	15	20	[2]20/10	10	10	[2]100	10	10	10	16	24
Ascorbate mM	30	30	30	[2]20/10	1	3	[2]10	3	3	3	8	4
$NaHCO_3$ mM	30	30	30	[2]100/0	10	0	5	0 10	0 10	0 10	24	24
K_m µM	[3]89.39 [4]82.74	[3]401.03 [4]91.91	[3]244.5 -	230/105	-	20	12 ± 4	[5]30 [6]67	[5]12 [6]29	[5]13 [6]30	39.7 ± 7	110 ± 12
V_{max} nmol	[3]15.15 [4]17.73	[3]12.94 [4]18.38	[3]18.94	-	-	-	-	-	-	-	4.31	13.91
K_{cat} s^{-1}	0.066	0.0344	0.0914	0.07/0.054	-	-	0.0025	-	-	-	-	-

[1]theoretical pI; [2]used in assay, without direct evidence of optimization; [3]pProEx-1; [4]pGEX; [5]In the absence of $NaHCO_3/CO_2$; [6]In the presence of 10 mM of $NaHCO_3$

ACO3 isoforms. In contrast, the white clover isoforms (MGI and SE1) have different pH optima and require different concentrations of $FeSO_4$ and ascorbate, as well as having distinctly different K_m^{ACC}s. The senescence associated isoforms of tomato (LE-ACO1) and white clover (SEI) both have the highest K_m^{ACC} in their respective families. Interestingly, the K_m^{ACC} of the LE-ACO isoforms more than doubles in the presence of $NaHCO_3$ (10 mM), which suggests that were the white clover SEI isoform to have been assayed in the presence of less $NaHCO_3$ (10 mM rather than 24 mM) perhaps the K_m would be similar to that of its tomato counterpart (LE-ACO1). The K_m^{ACC} for recombinant MD-ACOs expressed in *E. coli* is high when compared with LE-ACOs expressed in yeast or from purified white clover leaf or apple fruit tissue, with the exception of the SEI isoform from white clover. However, MD-ACO1 (Charng *et al.*, 2001) was assayed in the presence of 100 mM of $NaHCO_3$ and the MD-ACOs in this study were assayed in the presence of 30 mM of $NaHCO_3$, which could have decreased the affinity of the enzymes expressed in *E. coli* for the ACC substrate (although in the absence of $NaHCO_3$ the K_m^{ACC}s for all three MD-ACOs was only slightly lower). Both LE-ACO3 expressed in mature green leaf tissue and LE-ACO2 expressed in flower tissue share identical kinetic properties (with the exception of the pIs), and both isoforms exhibit a very similar K_m^{ACC} to an ACO purified from mature apple fruit (Pirrung *et al.*, 1993). This may suggest that the kinetic variation in the enzyme is not tissue-specific, but could also be due to intra-species variation. The molecular mass of the TR-ACO (SE1) and the apple ACO (Dong *et al.*, 1992b) are both higher in the native state when compared with the denatured form, which suggests that these proteins may be posttranslationally modified.

The specific activities in this study for MD-ACO1 [14 ± 0.63 nmol mg^{-1} min^{-1} (pProEX-1) and 14.9 ±0.5 nmol mg^{-1} min^{-1} (pGEX)], for MD-ACO2 [11 ± 1.3 nmol mg^{-1} min^{-1} (pProEX-1) and 17.5 ± 0.8 nmol mg^{-1} min^{-1} (pGEX)], and for MD-ACO3 [17 ± 0.74 nmol mg^{-1} min^{-1} (pProEX-1)], are consistent with other MD-ACOs from purified mature fruit tissue (Dong *et al.*, 1992b; Pirrung *et al.*, 1993). However, the specific activity of MD-ACO1 expressed in *E. coli* (pET20b) is much higher at 122 ± 13 nmol mg^{-1} min^{-1} in the presence of 1 mM of ACC and 129 ± 1 nmol mg^{-1} min^{-1} in the presence of 10 mM of ACC (Charng *et al.*, 1997; 2001) than the values determined in the present study. In contrast, the specific activities of LE-ACO1 (25.1 ± 2.1 nmol mg^{-1} h^{-1}), LE-ACO2 (2.9 ± 0.6 nmol mg^{-1} h^{-1}) LE-ACO3 (11.5 ± 2.4 nmol mg^{-1} h^{-1}) expressed in yeast as well as the TR-ACO isoforms MG1 (2.59 ± 0.16 nmol mg^{-1} min^{-1}), SE1 (7.95 ± .87 nmol mg^{-1} min^{-1}) are very low when compared with the MD-ACOs in this study. However, in another study the specific activity of MD-ACO1 (1600 nL mg^{-1} h^{-1}) expressed in *E. coli* (pET20b) is also very low (Yoo *et al.*, 2006).

The specific activities for each of the MD-ACO, LE-ACO and TR-ACO isoforms are shown as Table 4.2, in which the values of the present study are consistent with the activities determined for the MD-ACOs purified from Golden Delicious fruit (as well as from the partially purified MD-ACO of 20 nmol mg^{-1} h^{-1}; Poneleit and Dilley, 1993). The specific activity is really a measurement of the purity of the enzyme, and hence is particularly useful during the extraction process. However, the true activity is higher because the activity is time-dependent, and the time resolution of current assays is too low. Of interest (as pear is closely associated phylogenetically with apple), an ACO purified to near homogeneity from pear fruit with an optimum pH of 6.7, an optimum requirement of 10 mM of ascorbate and where 16 % of CO_2 in the gas phase was used, exhibited a specific activity of 77.8 nmol mg^{-1} min^{-1} (Vioque and Castellino, 1994). Nevertheless the difference in specific activities may be indicative of the problems encountered when assessing the kinetic parameters of ACOs.

Table 4.2: Summary of the Specific Activities of ACOs

References	Isoforms	Specific Activities (nmol mg^{-1} min^{-1})
(This thesis) expressed in *E. coli*; pProEX-I	MD-ACO1	14 ± 0.63
pGEX		14.9 ±0.5
pProEX-I	MD-ACO2	11 ± 1.3
pGEX		17.5 ± 0.8
pProEX-I	MD-ACO3	17 ± 0.74
Charng *et al.*, 2001; (*pAE20*) expressed *E. coli*	MD-ACO1	
in the presence of 1mM ACC		122 ± 13
in the presence of 10 mM ACC		129 ± 1
Yoo *et al.*, 2006; (*pAE12/20*) expressed in *E. coli*	MD-ACO1	1.19
Dong *et al.*, 1992b; purified mature fruit tissue	MD-ACO	20
Dupille *et al.*, 1993; " " "	MD-ACO	-
Pirrung *et al.*, 1993; " " "	MD-ACO	18
Bidonde *et al.*, 1998; expressed in yeast	LE-ACO1	0.416 ± 0.035
	LE-ACO2	0.048 ± 0.01
	LE-ACO2	0.191 ± 0.04
Gong and McManus, 2000;		
purified mature green leaf tissue	MGI	2.59 ± 0.16
purified senescent leaf tissue	SEI	7.95 ± 0.87

MD-ACO1 in this thesis shares the same molecular mass as the recombinant MD-ACO1 expressed in *E. coli* (Charng *et al.*, 2001), as clones *pAE20* and *pAP4* have identical nucleotide sequences, as well as theoretical pI, pH, and their requirements for $FeSO_4$ and ascorbate. In contrast, the K_m^{ACC} is lower for the MD-ACO1 in this study when compared with the MD-ACO1 of Yoo *et al.* (2006) and Charng *et al.* (2001), probably due to the much higher amount of $NaHCO_3$ (100 mM) and CO_2 (4.2 % (v/v)) used in these assays compared to the lesser amount of $NaHCO_3$ (30 mM) used for MD-ACO1 in this study. Further, with the pET20B+ vector expression system a hexahistidine tag is fused to the C-terminus end of the recombinant proteins which may alter enzymatic activity. It is interesting that the catalytic rate (K_{cat}) is so similar. MD-ACO1 in this study was inhibited by high levels of $FeSO_4$ (>40 μM), but Pirrung *et al.* (1993) used 100 μM of $FeSO_4$ in the MD-ACO assay which may explain their lower K_{cat}. However, it is difficult to measure the initial velocity to obtain the true K_{cat} as the incubation time of the ACO assay is 20 min. Much more sensitive assays for the products of the enzyme need to be developed in order to overcome this problem. [In one study, initial velocities have been measured by the rate of oxygen consumption at 25 °C, pH 7.2, using an YSI model 5300 biological oxygen monitor for LE-ACOs expressed in *E. coli* (Thrower *et al.*, 2001)]. However, Fe^{2+} concentrations higher than 100 μM can be required. For example, an ACO activity from partially purified avocado fruit where neither $NaHCO_3$ nor CO_2 were included in the ACO assay, with an optimal requirement for ascorbate of 20 mM, in the presence of 5 mM DTT required 100 μM of Fe^{2+} with increased enzyme activity exhibited at 500 μM (McGarvey and Christoffersen, 1992). Also pear fruit ACO, purified to near homogeneity requires 200 μM of Fe^{2+} to maintain full enzyme activity (Vioque and Castellino, 1994). The K_m^{ACC} of MD-ACO from purified apple fruit has also been observed to increase in the presence of 4 % (v/v) CO_2 from 28 μM to 121 μM (Fernández-Maculet *et al.*, 1993). Using MD-ACO from partially purified apple tissue in the presence of 5 % and 20 % (v/v) CO_2, the K_m^{ACC} was observed to increase from 2 μM to 7 μM and 20 μM respectively (Poneleit and Dilley, 1993). The K_m^{ACC} values for the MD-ACO1 isoform expressed in *E. coli* are higher when compared with the purified MD-ACO from apple tissue, which again may be due to the different $NaHCO_3$ levels (Table 4.1), or to the expression of a eukaryotic protein in a prokaryotic background.

The molecular mass of the native MD-ACO determined by electrospray mass spectrometry is 35.3 amu/kDa (Pirrung *et al*, 1993), consistent with the molecular mass of the denatured MD-ACO1 in this study and for the recombinant MD-ACO1 of Charng *et al.* (2001), as well as for MD-ACO purified from apple tissue (Dong *et al.*, 1992b). However, a molecular mass of *ca.* 40 kDa for MD-ACO purified from apple has been observed following SDS-PAGE and coomassie staining (Pirrung *et al.*, 1993) and following SDS-PAGE and silver staining (Dupille *et al.*, 1993), which is similar to the molecular mass of the native protein determined by gel filtration

of 39 kDa (Dong *et al.*, 1992b; Dupille *et al.*, 1993). Even given the limitations of both SDS-PAGE (proteins can behave anomalously on SDS-PAGE) and gel filtration for the determination of protein size, these discrepancies in molecular mass may be explained by posttranslational processing, but it seems odd that the native protein has a lower mass than the denatured protein. It could however be that the proteins denatured by gel electrophoresis are the higher mass isoforms of MD-ACO3 (36.3 kDa), and particularly MD-ACO2 (37.5 kDa) described in this study.

For MD-ACO1, MD-ACO2 and MD-ACO3 in this study, the V_{max} decreased in the absence of $NaHCO_3$ by more than 50 % (Figure 3.27), which is in agreement with ACO from partially purified apple fruit (Poneleit and Dilley, 1993; Mizutani *et al.*, 1995), ACO from apple fruit purified to near homogeneity (Ferández-Maculet *et al.*, 1993) and from avocado fruit purified to near homogeneity (McGarvey and Christoffersen, 1992) where increased CO_2 concentrations increased the V_{max}, by as much as 10-fold. However, the non-enzymatic breakdown of ACC to give ethylene by iron and hydrogen peroxide (the Fenton Reaction) is also stimulated in the presence of HCO_3^-/CO_2, (McRae et al., 1983; Smith and John, 1993). The V_{max} values *in vitro* for the recombinant MD-ACOs determined in this study were proportional to the amount of enzyme in the MD-ACO assay mixture even though the Michaelis constant (K_m^{ACC}) remained unchanged (refer Figure 3.26). These findings are in agreement with Fernández-Maculet and Yang, (1992) using crude apple extracts with incubation times up to 2 h (at 30 °C), and McGarvey and Christoffersen (1992) using ACO activities from partially purified avocado.

ACO is an aerobic enzyme. In the present study, ambient dioxygen (O_2; 23 % by mass) levels would have been present in the atmosphere prior to the sealing of the vacutainer (*ca.* 0.0278 mL O_2 dissolves in 1 mL H_2O at 30 °C), and shaking would have helped aerate the medium. Neither CO_2 nor O_2 levels were measured in this study, although the concentration of HCO_3^- (substituting for CO_2) was known. However, ambient CO_2 (approximately 0.03 % (v/v)) and O_2 levels would have been present prior to sealing the vacutainer for the 20 min incubation period and so should not be limiting in the ACO reaction. Nevertheless, due to the variations in added CO_2 (both in the gas phase and as $NaHCO_3$) and O_2 used by researchers, direct comparisons between the activities of different ACOs (both within and between species) is often fraught with ambiguity.

MD-ACO1, MD-ACO2 and MD-ACO3 in this thesis display very similar kinetic properties overall and therefore the isoforms are unable to be distinguished. However, a number of factors may better unravel the kinetic properties of these enzymes. For example, although the criteria used in this study to determine the optimal concentration of $NaHCO_3$ required for MD-ACO

activation was based on the optimal V_{max}, given the observation, from many studies, that increased concentrations of $NaHCO_3$ increases both the V_{max} and the K_m^{ACC} (Poneleit and Dilley, 1993; Charng *et al.*, 1997; Bidonde *et al.*, 1998) it may be more relevant when optimizing $NaHCO_3$ to take both values into consideration. In this study all MD-ACOs were maximally activated with 30 mM of $NaHCO_3$, but were completely inhibited in the presence of 60 mM of $NaHCO_3$. For MD-ACOs purified from mature apple fruit, $NaHCO_3$ above 10 mM gave maximal activity (Dong *et al.*, 1992b) but another study found that $NaHCO_3$ followed saturating behaviour up to 5 mM and then became inhibitory, so that at 50 mM the enzyme activity had decreased by 50 % (Pirrung *et al.*, 1993). These values suggest that less $NaHCO_3$ is required for optimal enzymatic activity for MD-ACO purified from mature apple fruit when compared with the concentration required for recombinant MD-ACOs expressed in *E. coli.*

Similarly, although ACO exhibit an absolute requirement *in vitro* for ascorbate, the amount required for optimal activity of the MD-ACOs purified from mature apple fruit (1 to 10 mM), is lower when compared with the amount of ascorbate required for recombinant MD-ACOs (20 to 30 mM) activity. Further, the lower ascorbate requirements also give maximal activity for the tomato isoforms expressed in yeast and for TR-ACO purified from white clover leaf tissue. It is interesting that increased concentrations of ascorbate have been observed to decrease the MD-ACO activities (in this study), which is consistent with the LE-ACOs expressed in yeast (Bidonde *et al.*, 1998), the LE-ACO1 expressed in *E. coli* (Zhang *et al.*, 1995) and in the MGI and SE1 isoforms purified from white clover leaf tissue (Gong and McManus, 2000). Again these values suggest that the ACO requirement for substrates and co-factors is different for the enzyme expressed in yeast or purified from plant tissue when compared with MD-ACO expressed in *E. coli.*

Another factor is that the His-tag may affect MD-ACO activity differentially. For although the manufacturers of the plasmid vector (pProEX-1) (Gibco-BRL, Life Technologies) report the non-interference of the His-tag in terms of enzyme activity, the possibility can not be entirely ruled out. For example, in this study expression of MD-ACO2 in both the pProEX-1 vector and the pGEX vector resulted in the translation of proteins which exhibit very different kinetic properties even though they were both expressed in the *E. coli* strain BL-21. Such a disparity in the activity of MD-ACO2 expressed in pProEX-1, when compared with expression in the pGEX vector, suggests that the extra 24 amino acids making up the His-tag may be influencing enzymatic activity. However, a simple interference of the activity of MD-ACO1 following expression in either vector (pGEX or pProEX-1) is not evident in this study, as the enzyme exhibited similar kinetic properties in both vector systems (refer Table 3.13). Although MD-ACO3 expressed in the pGEX vector was of a lower molecular mass than expected and was

found not to be active, MD-ACO3 is active when expressed using the pProEX-1 vector and there is nothing to suggest His-tag interference, but there is also nothing to compare it with either. Although cleavage of the His-tag from the recombinant MD-ACO2 and MD-ACO3 isoforms was successful (data not shown) approximately 80 % of enzyme activity was lost during the procedure (data not shown), and so the removal of the His-tag was not pursued further.

A further possible factor which may explain the higher apparent affinity that MD-ACO, extracted from apple fruit tissue, exhibits for ACC, compared to the recombinant apple ACO expressed in *E. coli*, may reflect the eukaryotic (and specifically the natural plant background) as opposed to the accumulation of the enzyme in the fundamentally different background of the prokaryotic cell. For example, the apparent K_m^{ACC} of recombinant ACO from kiwi fruit expressed in *E. coli* (strain XL1-Blue) using the pGEX-4T-1 vector was 41 µM, and for the endogenous activity from partially purified fruit tissue 16 µM (Xu *et al.*, 1998). ACO extracted from avocado fruit and purified to near homogeneity had an apparent K_m^{ACC} of 32 µM (McGarvey and Christoffersen, 1992), whereas, an isoform expressed in fruit had an apparent K_m^{ACC} of 62 µM when expressed as a recombinant enzyme in *E. coli* (strain BL-21) using the pET-3c vector (Brunhuber *et al.*, 2000), with a specific activity of 16 nmol mg^{-1} min^{-1} (Brunhuber *et al.*, 2000) which is similar to the specific activities determined for the apple ACOs. However, although the tomato isoforms (LE-ACO1, LE-ACO2 and LE-ACO3) expressed in a eukaryotic background (Bidonde *et al.*, 1998) have lower apparent K_m^{ACC} when compared with the MD-ACOs in this study (Table 4.1), for LE-ACO1 expressed in *E. coli* (strain BL-21) using the pET-11a vector, an apparent K_m^{ACC} of 23.3 µM was determined in the presence of 10 mM of $NaHCO_3$ (Zhang *et al.*, 1995). This is lower than the K_m^{ACC} of 67 µM in the presence of 10 mM of $NaHCO_3$, and of 30 µM in the absence of $NaHCO_3$, for LE-ACO1 expressed in yeast (Bidonde *et al.*, 1998).

4.3.2 Thermostability of MD-ACO1, MD-ACO2 and MD-ACO3

No significant difference in thermostability was found in this study between the MD-ACO isoforms. However, the activities of the enzyme differed significantly between each of the temperatures over time (Table 3.14). ACO in apple is sensitive to high temperature. For example, in this study the half-life (t½) at 25 °C was determined to be ~ 29 min, at 35 °C the t½ is ~ 13 min and at an incubation temperature of 45 °C the t½ is ~ 5 min 30 s (Figure 3.30). A purified ACO from Golden Delicious fruit displayed a loss of activity during turnover when incubated at a temperature of 23 °C, with a t½ of ~ 2 h (Pirrung *et al.*, 1993). This is a considerably longer time than the t½ of 29 min found in this study for the recombinant Gala MD-ACOs incubated at a temperature of 25 °C (Table 3.14), indicating that the recombinant

MD-ACOs expressed in *E. coli* (strain BL-21) are less stable than the purified native MD-ACO extracted from apple fruit tissue. The increased lability of the recombinant MD-ACOs in comparison to the native MD-ACO may be due to the lack of acetylation on the N-terminus of the proteins in the prokaryotic background. Such acetylation is likely to occur if the residue following the initiator methionine is alanine (A) as is the case for both the MD-ACO1 and MD-ACO2 isoforms, whereas for the MD-ACO3 isoform, no removal of the initiator methionine or acetylation of the N-terminus would generally occur as the adjacent residue to the initiator methionine is glutamic acid (E). As the MD-ACOs in this study are fused to His-tags on the N-terminal it is almost certain that such processing could not occur. However, even with the His-tag removed, the mechanisms for processing proteins found in the eukaryotic cells maybe unavailable or unadaptable to the eukaryotic proteins in the prokaryotic background. If MD-ACO1 and MD-ACO2 are stabilized by N-terminus acetylation in the apple tissue, and are thus more resistant to degradation, both isoforms would be expected to have a longer half-life than the MD-ACO3 isoform in the plant, whereas in the prokaryotic background, all three recombinant isoforms appear equally unstable. For example, in this study following incubation at 25 °C for 60 min the loss of enzyme activity decreased ~ 75 % (Table 3.14). For an ACO purified to near homogeneity from pear fruit a t½ of 60 min was exhibited at an incubation temperature of 28 °C (Vioque and Castellano, 1998) which is more stable than the recombinant MD-ACOs expressed in *E. coli* in this study.

In contrast to this study, tomato recombinant ACO expressed in yeast (pBEJ15), showed a variation in thermostability between the three isoforms (Bidonde *et al.*, 1998). For example, following incubation at 45 °C, enzyme activity decreased for LE-ACO1 by 7 fold, for LE-ACO2 by 35 fold and for LE-ACO3 by 4 fold. However, at 29 °C, the t½ of both LE-ACO1 and LE-ACO3 (18 min) differed from LE-ACO2 (24 min). For LE-ACO1 expressed in *E. coli*, the activity decayed with a t½ of ~14 min (Smith *et al.*, 1994). All of these LE-ACO values are within the range determined in this study for recombinant MD-ACO expressed in *E. coli* using the pProEX-1 vector. The maximum activity for all of the recombinant LE-ACO isoforms was found to be at 28-30 °C, with an optima at 29 °C, and for the LE-ACO assays all isoforms were incubated at 29 °C for 15 min (Bidonde *et al.*, 1998).

A purified ACO from Golden Delicious fruit has an optimum activity at a temperature of 26 °C with a sharp inhibition at 35 °C (Dupille *et al.*, 1993), similar to the ethylene forming activity of fresh tissues *in vivo* (Apelbaum *et al.*, 1981). Temperatures of incubation for apple ACO assays vary. For example, for a recombinant apple ACO expressed in *E. coli*, a temperature of 30 °C for 10 to 15 min has been used (Charng *et al.*, 1997; 2001), while 23 °C for 1 h (Pirrung *et al.*, 1993) and 26 °C for 15 min (Dupille *et al.*, 1993) is used for an ACO purified from apple fruit

tissue. A temperature of 30 °C for 20 min has been used for both an enzyme purified to near homogeneity (Dong *et al.*, 1992b) and for a partially purified activity (Poneleit and Dilley, 1993). For activities using crude extracts of apple fruit conditions of 30 °C for 30 min have been used (Mizutani *et al.*, 1995). In the present study an incubation temperature of 30 °C for 20 min was used. Such a diversity of temperatures and times of incubation used for the apple ACO assay may make direct comparisons between enzyme activities difficult.

Even incubation at 4 °C for 16 h reduced enzyme activity by approximately 80 % in this study, which concurs with a purified ACO from apple fruit tissue incubated under aerobic conditions at 4 °C for 18 h, where approximately 80 % of ACO was lost (Dupille *et al.*, 1993). Incubation of a partially purified ACO from apple fruit stored at 2 °C for 5 h after extraction significantly reduced the activity of ACO (Fernández-Maculet and Yang, 1992). So that storage times may affect the specific activity value, if some of the enzyme is no longer active.

4.3.3 Physiological Significance of the Kinetic Properties of MD-ACOs,

The kinetic properties of the three MD-ACO isoforms are not markedly different, although the physiological environment in which each isoform is active may reflect the developmental status of the tissue. For example, ACC levels increase from approximately 1 nmol g^{-1} DW in the peel and the pulp of Golden Delicious prior to the climacteric to 57.32 nmol g^{-1} DW in the peel and 47.19 nmol g^{-1} DW in the pulp during the apple fruit climacteric (Tan and Bangerth, 2000; Lara and Vendrell, 2000). As the malate decarboxylating system is intimately related to the respiration climacteric (just prior to the malate effect, the fruit begins to produce ethylene) the pH increases as malic acid levels decrease during apple fruit ripening (Hulme and Rhodes, 1971). MD-ACO1 and MD-ACO2 are both abundant during the fruit climacteric. As fruit tissue becomes more alkaline during ripening an MD-ACO isoform with a higher pH may be expected to predominate. However, MD-ACO1 has the lower pH optimum of 7.2 (with the optimal range from pH 7.0 to 7.5) and the higher affinity for ACC (K_m^{ACC} of 89.39 μM), whereas, MD-ACO2 has a slightly higher pH optima of 7.8 (with the optimal range from pH 7.5 to 8.0), the same pH range as has been determined for ACO activities from partially purified avocado fruit (McGarvey and Christoffersen, 1992), and a low affinity for substrate (K_m^{ACC} 401 μM in the pProEX-1 vector) and the much slower turnover rate (K_{cat} 3.44 x 10^{-2}). It should be noted that MD-ACO2 expressed in the pGEX vector has an apparent K_m^{ACC} of 91.91 μM, which is very similar to that of the MD-ACO1 isoform. Given that the ACC levels are highest during the fruit climacteric, it could be expected that the affinity of the enzyme for its substrate would be less than if ACC were limiting. MD-ACO1 required saturating concentrations of ACC of 0.5 mM, and that of MD-ACO2 varied from 0.5 to 1.0 mM of ACC as a function of the expression vector system. However, there does seem to be more MD-ACO2 in preclimacteric fruit tissue

relative to the MD-ACO1 isoform, where ACC is limiting (Tan and Bangerth, 2000; Lara and Vendrell, 2000), and MD-ACO3 is also present in young fruit tissue.

The ACC content in white clover remained constant in developing and mature green tissues and then increased in senescent tissue concomitent with a significant increase in ethylene production (Hunter *et al.*, 1999). As a consequence of the increase in ammonia content as part of the proteolysis and aminotransferae activity (Smart, 1994), the cells may become more alkaline. MD-ACO2 and MD-ACO3 are expressed in all leaf tissue (including initial leaf tissue, mature green fully expanded leaf tissue and senescent leaf tissue). MD-ACO3 is expressed predominantly in young leaf tissue, and has a broader optimal pH range from 7.0 to 8.0, with maximal activity at pH 7.5, an affinity for ACC of K_m^{ACC} of 244.5 μM, and the faster turnover rate (K_{cat} 9.14 x 10^{-2}). These values suggest that in young apple leaf tissue ACC is not limiting and perhaps there is less need for MD-ACO3 to exhibit high affinity for its substrate. Both MD-ACO2 and MD-ACO3 require saturating concentrations of ACC of 1 mM, although MD-ACO2 requires half as much ACC (0.5 mM) when expressed from the pGEX expression vector system. The pH optimum of 7.5 determined for MD-ACO3 concurs exactly with the pH of the ACO purified from the mature green leaf tissue (MGI) of white clover (Gong and McManus, 2000). However, the affinity of the MGI isoform for its substrate is higher (K_m^{ACC} of 39.7 μM) when compared with the apparent K_m^{ACC} of MD-ACO3, but other studies have found that kiwi fruit and avocado ACOs expressed in *E. coli* exhibit approximately 50 % less affinity for ACC than ACO purified from fruit tissue (Xu *et al.*, 1998; McGarvey and Christoffersen, 1992; Brunhuber *et al.*, 2000). Also this apparent disparity may be a function of the expression vector system (pProEX-1), or it may be that the leaves of apple differ physiologically from the leaves of white clover (a legume).

The affects of $NaHCO_3$ on the activity of the MD-ACOs probably reflects the changing dynamics of the physiological environment of the enzymes in the plant. The observation that when CO_2/HCO_3^- concentrations are increased both the V_{max} and the K_m^{ACC} also increased has been made for ACO activities from partially purified mature apple fruit (Poneleit and Dilley, 1993), for recombinant MD-ACO1 (*pAE20*) expressed in *E. coli* (Charng *et al.*, 1997), for LE-ACOs expressed in yeast (Bidonde *et al.*, 1998) and for ACO from melon fruit (Smith and John, 1993). Conversely, an increase in the affinity of ACO for ACC in the absence of $NaHCO_3$ has been observed in crude carnation petal extracts (Nijenhuis-De Vries *et al.*, 1994). As CO_2 passes very rapidly through membranes, hydrates and dissociates into H^+ and HCO_3^- (and probably lowers the intracellular pH), the affinity of ACO for its substrate ACC would likely vary as a consequence of the HCO_3^-/CO_2 concentrations at or near the active site. If during photosynthesis HCO_3^-/CO_2 were to become limiting then it could be expected that the affinity of

the enzyme for ACC would increase, whereas it could be that the non-limiting higher HCO_3^-/CO_2 levels in non-photosynthetic tissue such as mature fruit may reduce the affinity of an ACO for substrate. Based on this hypothesis, it may also be that in very young and senescent leaves (with suboptimal photosynthetic capacity) the HCO_3^-/CO_2 levels are higher, when compared with mature green leaves, and as a consequence the affinity of ACO for ACC in these tissues is lower than in the leaves with full photosynthetic capacity. However, MD-ACO3 (expressed predominantly in the leaves) has a higher apparent K_m^{ACC} of 244.5 μM when compared to that of MD-ACO1 (expressed in apple fruit) of K_m^{ACC} 89.39 μM. Also for MD-ACO2, which is expressed in the leaves and also abundantly in climacteric apple fruit, an explanation of any kind is difficult to make, especially given the extremely high K_m^{ACC} of 401.03 μM of the isoform in the pProEX-1 vector when compared with the K_m^{ACC} of 91.91 μM in the pGEX vector. If, in this study, the $NaHCO_3$ concentration had been lower it may be that the K_m^{ACC} for all of the MD-ACOs would also have been lowered, which may also have resulted in greater differentiation between the K_m^{ACC} values determined for each of the isoforms, although Gong and McManus (2000) included a similar amount of $NaHCO_3$ (24 mM) in the TR-ACO assays and in mature green leaf tissue the K_m^{ACC} of 39.7 μM was lower than the K_m^{ACC} of 110 μM for ACO obtained from senescent leaf tissue.

Neither MD-ACO2 nor MD-ACO3 were observed to increase during leaf senescence (MD-ACO1 was not observed in leaf tissue in this study), although the more alkaline pH optimum of MD-ACO2 and the very low affinity of the enzyme for substrate (expressed from pProEX-1) would perhaps categorize this isoform as potentially senescence associated, when compared with the white clover senescence associated isoform (SEI) which exhibited a K_m^{ACC} of 110 μM and a pH optimum of 8.5 (Gong and McManus, 2000). However, the senescence associated tomato isoform (LE-ACO1) expressed in yeast (Bidonde *et al.*, 1998) has the same pH optimum as LE-ACO2 and LE-ACO3 (pH 6.8 to 7.2), and the K_m^{ACC} is lower at 30 μM (and in the presence of 10 mM of $NaHCO_3$ a K_m^{ACC} of 67 μM) when compared with the senescence associated isoform from white clover and the MD-ACOs in this study (Gong and McManus, 2000). The actual physiological concentrations of ACC, dioxygen, CO_2 and Fe^{2+} at the MD-ACO active site *in vivo*, the ionic strength or the pH, or indeed if ascorbate is the actual co-substrate which is oxidized during the conversion of ACC to ethylene, remain largely unknown in plant tissue, including the leaves of apple. Also, the variation in the physiological conditions under which MD-ACO is active no doubt depend on many variables, such as the developmental status of the tree, endogenous circadian clocks, environmental conditions and perhaps MD-ACO may require other, as yet unidentified, cofactors.

Alternatively, the fact that the C-terminus of each of the three MD-ACO isoforms are different lengths may be determining their kinetic properties rather than the physiological environment or

their expression patterns. For example, the C-terminus of ACO may play a role in effecting completion of catalytic cycles via assisting in the reduction of an oxidized form of the enzyme after oxidation of ACC (Rocklin *et al.*, 2004). As MD-ACO1 (314 aa), MD-ACO2 (330 aa) and MD-ACO3 (322 aa) have significantly different C termini, any discrepancies in the order of substrate binding arising from kinetic analysis may be due to the different C-termini (Thrower *et al.*, 2001; Brunhuber *et al.*, 2000). Interestingly, the penultimate residue on the C-terminus of MD-ACO2 is a glutamine (Q^{329})(Figure 3.7). This is of interest as in the solved crystal structure of isopenicillin N synthase (IPNS) obtained without substrate, the penultimate residue on the C terminus (a glutamine at position 330, Q^{330}) projects into the active site such that its side chain is close to the metal (Mn^{2+} substituting for Fe^{2+}) (Roach *et al.*, 1995). Upon substrate binding this residue is displaced from the immediate vicinity of the Fe^{2+} (Roach *et al.*, 1997). However, this was not observed in the solved crystal structure of *Petunia hybrida* ACO (Zhang *et al.*, 2004b), but this may be due to the presence of dimeric and tetrameric forms in the crystal lattice in the absence of the monomer form.

4.3.4 Some Possible Limitations of Expressing MD-ACOs in *E. coli*

As the apple ACO proteins were expressed in a prokaryotic cell, the mechanisms for processing such as posttranslational modification, chaperone proteins and other biological accessories may be unavailable to the eukaryotic protein in an *E. coli* background. Therefore, due to incorrect protein folding, and the fine tuning of the tertiary structure necessary for the correct orientation of the active site, the activity of the MD-ACO isoforms may be compromised. For example, the fragmentation of ACO expressed in *E. coli* may be a direct result of incorrectly folded protein (Zhang *et al.*, 1997), and another artefact of using *E. coli* has been observed to be the accumulation of the overexpressed proteins as insoluble, and inactive, membrane bound inclusion bodies inside the cell (Marston, 1986; Schein and Noteborn, 1988; Zhang *et al.*, 1995; Lay *et al.*, 1996; Xu *et al.*, 1998; Thrower *et al.*, 2001). The relative proportion of ACO expressed in the soluble form at 37 °C has been observed to be in the order of: kiwi fruit >> *Arabidopsis* > apple > petunia >> pea, with pea ACO expressed as insoluble inclusion bodies (Lay *et al.*, 1996). Hence, it may not be valid to compare the kinetic properties of apple ACO expressed in *E. coli* with purified and partially purified ACO from apple tissue.

Further, although proteins in the cytosol are not glycosylated, many secretory proteins and extracellular integral membrane proteins are glycosylated. All three MD-ACO isoforms have a site for a potential N-glycosidic linkage at residues N^{99} and S^{101}, and MD-ACO2 also has a site for a potential N-glycosidic linkage at residues N^{323} and T^{325}. Glycosylation of MD-ACO1 has been investigated by Dupille *et al.* (1993), but the lack of reactivity towards a mixture of seven different biotinylated lectins together with the absence of N-linked substitution at the potential

glycosylation site in a sequenced peptide found no evidence of glycosylation. However, the possibility of an O-glycosidic bond with the serine or threonine residues, and the possibility that the other isoforms (MD-ACO2 and MD-ACO3) are able to be glycosylated, can not be ruled out. As the MD-ACO isoforms are expressed in *E. coli,* the significance of this is that glycosylation which may have occurred in the eukaryotic cell may not be possible within the prokaryotic background.

Similarly, all MD-ACOs contain a RXS motif (R^{244} and S^{246}), a typical phosphorylation site. If, as proposed, residues R^{244} and S^{246} bind the carboxyl group of ACC (Kadyrzhanova *et al.*, 1999; Dilley *et al.*, 2003) or $NaHCO_3$ (Rocklin *et al.*, 1999), then phosphorylation at this site would probably inactivate or inhibit enzyme activity, hence the expression of MD-ACOs in *E. coli* may be an advantage. However, it is unknown whether ACO is phosphorylated *in vivo* or *in vitro.*

The observed similarity between the native and denatured molecular mass of the protein indicates that the apple ACO is active as a monomer (Dong *et al*, 1992b; Dupille *et al.*, 1993). However, the monomeric, and possible dimeric or tetrameric, form may be more active in eukaryotic cells than in the prokaryotic background. Although evidence gathered to date indicates ACO is active in the monomeric form, it is uncertain whether it is also active in dimeric or tetrameric forms. For example, the crystallographic study of Zhang *et al.*(2004b), of a recombinant isoform from *Petunia hybrida* expressed in *E. coli*, show dimeric and tetrameric interactions that form hydrophobically and electrostatically between the monomers. However, due to the restraints of the crystalline lattice such interactions between adjacent monomers may be artefactual, but the possibility remains that there may be co-operative interactions between adjacent monomers, that may not be possible when ACO is expressed in *E. coli.*

Also there may be a difference between the expression vectors in an *E. coli* background. For example, MD-ACO3 was truncated when expressed from the pGEX expression system, whereas from the pProEX-1 expression system the protein was successfully expressed and active. However, while both MD-ACO1 and MD-ACO2 were expressed intact and active in both the pGEX and pProEX-1 expression systems, the MD-ACO2 isoform was more active when expressed from the pGEX vector than when expressed from the pProEX-1 vector, whereas the activity of the MD-ACO1 isoform appeared unaffected by the expression system used. The variation could be random and as a result of less robust DNA repair mechanisms in *E. coli* compared with the eukaryotic system. Alternatively, the His-tag fusion may interfere with the correct tertiary orientation of the active site of the enzyme and may therefore be inhibitory to optimal enzymatic activity.

4.4 ACC Oxidase Accumulation and Gene Expression in the Bourse Shoot Leaves of *Malus domestica*

For the final section of this thesis, the accumulation of the MD-ACO proteins and the gene expression of the *MD-ACO*s, both during leaf and fruit development and in a circadian pattern, were examined. In this study, chlorophyll levels were used as an indicator of the developmental status of the leaf of apple, as the total chlorophyll concentration increased as the leaf matured from initial to a mature fully expanded status (chlorophyll *a* increased relative to chlorophyll *b*), and conversely, total chlorophyll levels decreased during senescence (chlorophyll *a* degraded more quickly than chlorophyll *b*) until necrosis (Figures 3.31 to 3.33). Although a report by Mae *et al.* (1984) suggests that chlorophyll levels are not a good indicator of the developmental status in primary wheat leaves, in this study the leaf carbon assimilation data collected (Figure 3.34) corresponded well with the decrease in chlorophyll levels as senescence progressed.

Polyclonal antibodies raised against either recombinant MD-ACO1 or recombinant MD-ACO3 were used in this study. As MD-ACO2 shares a close identity with MD-ACO1, the reasoning was that the antibody raised against MD-ACO1 would also recognise the MD-ACO2 native protein. Given the great abundance of ACO present in climacteric apple fruit (Dong *et al.*, 1992b; Dilley *et al.*, 1993) the probability is great that both polyclonal antibodies (MD-ACO1 and MD-ACO3) would recognise the protein in this tissue, as given the sequence and binding site data there would be epitopes in common. However, the antibody raised against MD-ACO1 recognizes protein accumulated in climacteric apple, but does not recognize ACO protein accumulated in young fruit, initial leaf tissue or senescent leaf tissue extract (Figure 3.24). These results are in agreement with Dilley *et al.* (1993) who report that antibodies raised against MD-ACO1 (clone *pAE12*) were unable to detect protein in preclimacteric apple (cv. Golden Delicious), nor was *in vivo* or *in vitro* ACO activity detected. Further, no MD-ACO proteins were detected during the preclimacteric stage in the Granny Smith cultivar (Lara and Vendrell, 2000) using antibodies raised against recombinant MD-ACO1 (clone *pAE12*; from Professor S.F. Yang) and also against ACO from apple (from Professor D. Dilley). These data suggest that either very low to undetectable levels of MD-ACO1 (and possibly MD-ACO2) are expressed and translated, or that MD-ACO1 (and possibly MD-ACO2) is absent in preclimacteric apple fruit and leaf tissue. However, MD-ACO2 mRNA was extracted from leaf tissue in this study, so it appears the antibody raised against recombinant MD-ACO1 is not recognizing native MD-ACO2 with the same specificity (Figure 3.24). In contrast, antibodies raised against recombinant MD-ACO3 recognize protein predominantly in young leaf tissue, and also in senescent leaf tissue, and notably in young fruit tissue.

A difference in the molecular masses between the isoforms is detectable using antibodies raised against MD-ACO1 and MD-ACO3 for western blot analysis (Figure 3.24). As the molecular mass predicted from the *MD-ACO1* and *MD-ACO3* nucleotide sequences in this study are 35.35 kDa and 36.3 kDa respectively it is consistent that MD-ACO1 antibody recognised protein of a lower mass (*ca.* 35.35 kDa) when compared to that of MD-ACO3 (*ca.* 36.3 kDa). As the MD-ACO2 isoform has a predicted molecular mass of 37.50 kDa it appears, therefore, as though the antibodies raised against the recombinant MD-ACO1 are not recognising a protein of the higher mass. Although the molecular mass of an ACO purified from apple as determined by gel filtration is 39 - 39.5 kDa (Dong *et al.*, 1992b; Dupille *et al.*, 1993), the vastly more accurate method (as far as protein size determination is concerned) of electrospray mass spectrometry (EMS) showed the mass to be 35.332 ± 5 atomic mass units (amu) (Pirrung *et al.*, 1993), similar to the predicted molecular mass of MD-ACO1 deduced by the nucleotide sequence in this thesis and in other studies (Ross *et al.*, 1992; Dong *et al.*, 1992a). The higher molecular masses (39 to 39.5 kDa) observed for ACO may not necessarily be the MD-ACO1 isoform. For example, an antibody raised against LE-ACO1 has been used to identify MD-ACO1 (Dupille *et al.*, 1993) and the denatured mass of MD-ACO observed by SDS-PAGE is approximately 40 kDa (Dupille *et al.*, 1993; Pirrung *et al.*,1993). Alternatively, MD-ACO1 could be posttranslationally modified, for example by phosphorylation, or associated in some way with a very small peptide which would increase the apparent molecular mass of MD-ACO1 on SDS-PAGE.

4.4.1 MD-ACO Accumulation and Gene Expression During Leaf Development

An investigation of the bourse shoot leaf ontogeny in the Gala cultivar was undertaken with respect to the accumulation of the MD-ACO isoforms and the differential gene expression of each of the transcripts throughout development, particularly with regard to mature and senescencing tissue. Bourse shoots were pre-tagged (refer section 2.1.1).

In young leaf tissue, from the initial leaf tissue through the young green fully expanded leaf tissue to the mature green fully expanded leaf tissue sampled in 2003 and 2004 (Figure 3.35), the MD-ACO1 isoform was not detected (using antibody raised against recombinant MD-ACO1). Although gene expression of the *MD-ACO1* transcript was not evident (Figure 3.38), gene expression of the *MD-ACO2* transcript was clearly evident in young and mature fully expanded leaf tissue, which indicates that the antibodies raised against recombinant MD-ACO1 are not recognising native MD-ACO2 in the leaf tissue. However, even though *MD-ACO2* is expressed in these tissues, it is possible that the MD-ACO2 isoform does not accumulate, perhaps because it is not translated or is degraded quickly, or the absence reflects the greater

difficulty in protein extraction from hardened mature leaves. *MD-ACO3* is expressed in these tissues, and although the translated product is strongly detectable in the young leaf tissue it declined to barely visible levels in the mature green fully expanded leaf tissue, prior to fruit harvest (Figure 3.37).

In this study MD-ACO1 (transcript and protein) was undetectable in the bourse shoot leaf tissue. Either MD-ACO1 is not expressed in the leaf tissue or the expression is below the level detectable using the techniques available in this study (Figures 3.35 and 3.38). In contrast both MD-ACO2 and MD-ACO3 (transcript and protein) are clearly present in the initial leaf tissue and also in the mature green leaf, middle and basal, tissue of the bourse shoot (Figures 3.36 and 3.38). As the senescence associated genes *LE-ACO1*, *PP-ACO1* and *CP-ACO2* are expressed both in mature fruit tissue and in senescing leaf tissue, it is unusual that the MD-ACO (transcript and protein) which increase in abundance during the climacteric (MD-ACO1 and MD-ACO2; Figures 3.14 and 3.15) do not also show a senescence associated increase at the onset of senescence in the leaves of apple. A likely conclusion, therefore, is that neither MD-ACO1, MD-ACO2 nor MD-ACO3 are senescence-associated in the leaf tissue. An as yet unidentified MD-ACO4 may be a candidate, or it may be that in apple leaves ACO is not senescence associated. However, as senescence associated genes have been identified in the leaves of tomato (Holdsworth *et al.*, 1988; Barry *et al.*, 1996; Blume and Grierson, 1997), of peach (Ruperti *et al.*, 2001; Rasori *et al.*, 2003), of melon (Lassere *et al.*, 1996), of papaya (Chen *et al.*, 2003), of sweet potato (Huang *et al.*, 2001) and also of white clover (Hunter *et al.*, 1999), it seems likely that an as yet unidentified MD-ACO will be found to be senescence associated.

In this study bourse shoot leaf tissue was collected over three years (2003, 2004 and 2005), with two or three collections prior to fruit harvest each year, when the leaves were green and fully expanded, and then leaf tissue was collected again two weeks after the fruit had been harvested, at intervals of approximately 10 days. When the colour of the leaves began to change rapidly (the visual onset of senescence) leaf tissue was collected more often, approximately every fifth day. It should be noted, that in this study the fruit was strip-picked rather than harvested over a number of pickings, and so there is an abrupt removal of the fruit. Over this time course neither the *MD-ACO1* transcript nor the translated product were detected in any of these tissues for 2003, 2004 or 2005. While some hybridisation with *MD-ACO2* is detectable prior to fruit harvest in 2003 (Figure 3.38), there is no detectable hybridisation with *MD-ACO2* for 2004 or 2005 post-harvest (Figure 3.39). Antibodies raised against recombinant MD-ACO3 recognise protein of the expected mass (36.3 kDa) in 2003 prior to fruit removal (Figure 3.37) although this is less strong in 2004, and with no protein recognition of the expected molecular mass in

2005 (Figure 3.39). However, in 2005 the MD-ACO3 antibody does faintly recognise some protein of *ca.* 27 kDa and 30 kDa predominantly prior to harvest but also post-harvest, which could be degraded or fragmented MD-ACO3, or alternatively another MD-ACO isoform. In leaf tissue collected prior to harvest in 2003 there is relatively strong hybridisation with *MD-ACO3*, less intensely for 2004 and not at all in 2005, which reflects the protein accumulation pattern. It is interesting that both *MD-ACO2* and *MD-ACO3* are expressed prior to fruit removal in 2003 (and also in 2004 for *MD-ACO3*), but expression is undetectable following the removal of the fruit, which suggests that the *MD-ACO2* and *MD-ACO3* genes are rapidly down regulated following fruit harvest. However, the lack of hybridisation with *MD-ACO3* in 2005 and the lack of hybridisation with *MD-ACO2* in both 2004 and 2005 prior to fruit removal suggests that the underlying regulation is not a simple one. Similarly, MD-ACO3 which accumulates prior to the removal of the fruit in 2003 and 2004 disappears following fruit harvest. The protein is probably rapidly degraded, rather than not translated as there is not very much protein prior to fruit removal anyway. A possibility may be that antibody raised against recombinant MD-ACO3 is recognising a fourth ACO as the protein recognition is so faint (Figures 3.37 and 3.39). Interestingly, the observation in melon, by Chen *et al.*, (2003) that *CP-ACO2* was induced at the very late stage of leaf senescence and fruit ripening, the fully yellowed stage in which the papaya leaf withers, is not consistent with undetectable amounts of *MD-ACO2* and of *MD-ACO3* post harvest. Apple ACO gene expression and protein accumulation may be affected by the physiological dynamics of fruit removal, or it may simply be coincidence. For example, as leaf tissue samples were always collected at the same time (11 am), it could be that the collection of tissue at another time would have produced quite different results, as the possible circadian and/or diurnal oscillations of MD-ACO may also be affected by environmental (light intensity, temperature) and developmental (hormones, sugars) cues. A more controlled study is probably necessary under controlled environmental conditions to examine the possible interplay between fruit and leaf tissue in the regulation of ACO. Nevertheless, this study indicates that the regulation of MD-ACO in the bourse shoot leaves of the Royal Gala cultivar may be changed following fruit removal.

From other studies it is well established that fruit removal does influence leaf physiology in apple trees (Tartachnyk and Blanke, 2004) and peach trees (Nii, 1997), particularly in regard to the accumulation of sugars and starch (Nii, 1997), although it is unclear or controversial as to the nature of the changes. For example, delayed apple fruit harvest has been observed to enhance autumn leaf photosynthesis, delay chlorophyll degradation and the nitrogen content declined less rapidly when compared with the leaves from the trees where the fruit had been harvested (Tartachnyk and Blanke, 2004). Such an apparent delaying of apple leaf senescence by delaying the fruit harvest, and conversely inducing the earlier onset of senescence by

removing the fruit, may underlie the regulation of MD-ACO2 and MD-ACO3, as both *MD-ACO2* and *MD-ACO3* were expressed (and MD-ACO3 accumulated) prior to fruit removal, but were undetectable following fruit harvest. Following fruit removal from peach trees, the sorbitol content increased in parallel with the accumulation of starch and remained high, but the sucrose content did not change markedly (Nii, 1997). As sorbitol is the major carbohydrate in mature Gala apple leaves (Zhou *et al.*, 2001), and high sugar levels have been reported to repress the transcription of photosynthetic genes (Sheen, 1990), and the over expression of hexokinase was reported to reduce photosynthesis and induce leaf senescence (Dai *et al.*, 1999), there may be a regulatory system whereby the accumulation of sorbitol in the leaves of apple (or peach or pear) could repress the gene expression the *MD-ACO2* and *MD-ACO3*.

Perhaps a more accurate measurement of the presence of MD-ACO in senescing apple leaves would be to collect leaves at different senescent stages on the same day (identified by colour similarity perhaps), rather than by pre-tagging. This is because the leaves of apple were observed, on any one day in autumn, to be at different senescence stages on the same tree and even on the same bourse shoot. The apple leaves were also observed to often become more progressively wounded (as by pathogens) as senescence progressed (the observation was made in this study that the bourse shoot leaves were often at a more advanced stage of senescence in comparison to the extension shoot leaves).

4.4.2 MD-ACO Accumulation and Gene Expression in Leaves over a 24 h Period

To complete the study on *MD-ACO* gene expression and MD-ACO protein accumulation in leaf tissue, expression/accumulation was examined in terms of a circadian rhythm. By definition, a circadian rhythm is one that persists for a period of approximately 24 h under constant conditions in the absence of an external timing cue (Barak *et al.*, 2000), and a diurnal rhythm is one that fluctuates between light and dark photoperiods.

In this study, bourse shoots of approximately 50 cm in length were tagged prior to sampling, and leaves were collected from positions 5, 6 and 7 on the bourse shoot for analysis (refer section 2.1). For the collection of leaf samples during the dark phase, (safe) green light was not used, and this may have affected the diurnal expression of ACO. Circadian analysis was not undertaken under controlled environmental conditions in this study. ACO gene expression has been observed to cycle in a diurnal and also in a circadian rhythmic pattern in *Stellaria longipes* (Kathiresan *et al.*, 1996) and in sorghum (Finlayson *et al.*, 1999), under controlled environmental conditions. Of the two ACO genes in sorghum (*Sb-ACO1* and *Sb-ACO2*), the

Sb-ACO2 was expressed in a diurnal rhythm in young 5 day old seedlings, whilst the expression of the *Sb-ACO1* transcript remained unchanged. In the present study, the expression of both *MD-ACO2* and *MD-ACO3* fluctuated in a similar way over a 24 h period (Figures 3.40 and 3.43).

Sb-ACO2 showed strong diurnal fluctuations under simulated high-shade conditions of low-irradiance, far-red-enriched light (with gene expression undetectable during the dark periods, over 3 days), but *Sb-ACO2* exhibited a weak circadian pattern under constant light and temperature (27 °C) over 48 h, and a damping of the rhythm with time. Whereas, under simulated light conditions (relatively bright, high red: far-red light) diurnal rhythmic expression could not be detected as the level of *Sb-ACO2* expression was extremely low, and there was no circadian rhythm. These data suggest that *ACO* gene expression is stimulated under high shade conditions in a strong diurnal pattern, in young sorghum seedlings under a 12 h/12 h photoperiod and a 31 °C/ 22 °C thermoperiod. A strong diurnal rhythm was also elicited in *Stellaria longipes* ACO (*Sl-ACO1*) over a 4 day period under a 16 h photoperiod (16 h at 22 °C and 8 h at 18 °C), with the maximum mRNA abundance occurring 5 h after the lights were switched on and the minimum abundance was in the middle of the dark phase (Kathiresan *et al.*, 1996). Further, as the *Sl-ACO1* diurnal fluctuation was maintained over 4 days of continuous illumination, and also over 4 days of continuous darkness this is a nice demonstration of the endogenous circadian regulation of *ACO* gene expression. However, the damping of the oscillations under constant light (Kathiresan *et al.*, 1996; Finlayson *et al.*, 1999) or constant dark conditions suggests that external cues are necessary for the initiation and perhaps the co-ordination of the rhythmic expression of ACO, which may not occur spontaneously.

Both *MD-ACO2* and *MD-ACO3* were expressed in strong diurnal fluctuations over 24 h (from noon 06.04.05), in the bourse shoot leaves, when the fruit was left on the tree after the commercial harvest date (02.03.05). Except for *MD-ACO3* expression at 3 am, expression for both genes is undetectable during the dark period from 6 pm until 6.45 am (Figure 3.43). As in this study, Finlayson *et al.* (1999) collected samples at three hourly intervals, and interestingly at the first data point of each of the light periods *Sb-ACO2* expression is undetectable, which seems to suggest that *Sb-ACO2* is induced by light (and/or temperature), and that time (within three hours; sampling times are not given) is needed for gene expression to occur. In the present study, no such lag period is apparent, as *MD-ACO* gene expression is observed in the first sampling following sunrise (with the except of 2005 without fruit), perhaps due to the gradual change which occurs at sunset and sunrise when compared with the abrupt change of the controlled environment (light and temperature). Further, any lag-time may have been picked up if the sampling times had been shorter (less than 3 h). Interestingly, *MD-ACO2* and

MD-ACO3 expression is observed approximately 3 h after sunset in November 2003, and also in April 2004 when *MD-ACO2* expression occurred approximately 3 h after sunset. However, this phenomenon is not observed in April 2005 for either *MD-ACO2* or *MD-ACO3*. There are many variables which could come into play when comparing *ACO* expression in young sorghum seedlings (5 days), *Stellaria longipes* from the wild of an unknown age, and 10 year old fruiting apple trees. In the present study over the same 24 h (from noon 06.04.05) in the absence of fruit (harvested on 02.03.05) neither *MD-ACO2* nor *MD-ACO3* expression was detectable (Figure 3.42), which suggests that in the bourse shoot leaves the fruit status of the tree may also alter the regulation of ACO. The plant hormones cytokinin, auxin and abscisic acid are known to display diurnal rhythms (Nováková *et al*., 2005) and to affect gene expression. For example, in tobacco under a 16 h photoperiod cytokinin activity peaked after 9 h of light to *ca*. 6 pmol g^{-1} FW and coincided with the major auxin peak of *ca*. 250 pmol g^{-1} FW, and abscisic acid peaked on entering the dark-phase to *ca*. 800 pmol g^{-1} FW. Interestingly, the concentration of sorbitol, the major photosynthate in the mature leaves of apple and the major transport form of carbohydrate, increases gradually after dawn and reaches its highest level of 18.0 mg g^{-1} fresh weight at 4 pm, and then declines to its lowest level of 9.6 mg g^{-1} at the end of the dark period (Zhou *et al*., 2001). This may affect the regulation of *ACO* gene expression in the leaves of apple.

However, the diurnal rhythmicity of *MD-ACO* in this study was inconsistent. For example, in bourse shoot leaves collected over 24 h, and after the commercial harvest date (27.02.04; Figure 3.41), *MD-ACO2* was expressed during the daylight hours (at noon and 3 pm on the 07.04.04, and at 9 am and noon on the 08.04.04), and hence exhibits diurnal oscillations but for an abundance of transcript at 9 pm following sunset (6 pm), and extremely low levels of transcript at 6 am prior to sunrise (at 6.45 am). In contrast *MD-ACO3* was expressed over the entire 24 h period with less transcript observed at 6 pm (sunset) and 3 am (Figure 3.41). The *MD-ACO3* expression is puzzling as the 2004 and 2005 are clearly different, but may reflect differences in environmental cues. For example, it was windy, raining and cold (temperature from 14 °C in the light period to 4 °C in the dark period) during the collection of leaf tissue in 2004, and still, fine and mild (temperature from 16 °C in the light period to 12 °C in the dark period) when the leaf samples were collected in 2005. Perhaps the temperature variation between the light and dark periods may inhibit or induce the expression of MD-ACO in the bourse shoot leaves of apple. However, in 2004, *MD-ACO2* and *MD-ACO3* exhibit different expression patterns from each other, whereas in 2005 they exhibit very similar expression patterns (Figures 3.41 and 3.43 respectively). Thus an explanation may be that one of the *MD-ACO* genes is more sensitive to exogenous and/or endogenous cues than the other *MD-ACO* gene.

Almost irrespective of the photoperiod, both *MD-ACO2* and *MD-ACO3* were expressed at six hourly intervals (noon, 6 pm, midnight, 6 am and noon) over a 24 h from 20.11.03 (Figure 3.40), when the young fruit was approximately 2 cm in diameter. These oscillations suggest an endogenous (developmental cues perhaps) rhythmic regulation of both *MD-ACO2* and *MD-ACO3*, rather than a pattern of expression entrained by red light. For example, perhaps CO_2 levels may affect gene expression in plants.

For sorghum lacking expression of a functional phytochrome B protein (Finlayson *et al.*, 1999), the mutant (*phyB-1*) expressed *Sb-ACO2* more abundantly and constitutively when compared with the wild type, but nevertheless exhibited weak diurnal and circadian rhythmic patterns under all conditions, with a particularly weak circadian rhythm observed under the simulated high-shade condition. Such reduced *Sb-ACO2* photoperiod sensitivity in the absence of phytochrome B, demonstrates the importance of red light in regulating the gene expression of ACO. For example, a 15 min red light pulse (660 nm; but not a blue light pulse) was observed to reset the circadian rhythm of *Stellaria longipes* ACO (*Sl-ACO1*) under the condition of continuous darkness (Kathiresan *et al*, 1996), suggesting that a red-light signal transduction pathway may be involved in the rhythmic regulation of ACO expression.

This study shows that *MD-ACO2* elicited strong diurnal rhythms in bourse shoot leaves in April (2004 and 2005), while MD-ACO3 was expressed over all sampling times in April 2004, but exhibited a diurnal rhythm in April 2005 when the fruit remained unharvested. Both *MD-ACO2* and *MD-ACO3* oscillate in approximately 6 h cycles early in the season (November, 2003).

MD-ACO3 protein accumulated abundantly and constitutively over the 24 h period from 20.11.03, and clearly lacks a diurnal oscillation pattern (Figure 3.40). This result suggests that MD-ACO3 may undergo post translational modification to prevent degradation, as the gene is only expressed at approximately six hourly intervals and ACO from apple has a half life (t½) of approximately 2 h at 23 °C (Pirrung *et al.*, 1993) while the recombinant MD-ACOs in this study have t½s of approximately 29 min at 25 °C and 13.5 min at 35 °C (Figure 3.30). MD-ACO3 is unlikely to be stabilized by acetylation at the N-terminus as the adjacent amino acid is charged (glutamic acid), but the protein could be phosphorylated, perhaps glycosylated or associated with another protein. Also or alternatively, mRNA (*MD-ACO3*) may be stabilized and thus allow more protein to accumulate. MD-ACO3 protein also accumulated constitutively, at very low levels, when the fruit was left on the tree after the harvest date (02.03.05) over the 24 h from 06.04.05, when a strong diurnal expression of *MD-ACO3* occurs (except for expression at 3 am; Figure 3.43). In the absence of fruit there is no evidence of MD-ACO3 accumulation (Figure 3.42), except at 6 am (prior to sunrise of 6.45 am). Protein accumulated at 3 pm and 3

am in an apparent circadian rhythm over a 24 h period from 07.04.04 (harvest date 27.02.04), in contrast the gene is expressed constitutively with lower levels observed at 6 pm and 3 am (Figure 3.41). The observation of MD-ACO3 accumulation over a 24 h period at 3 h intervals in this study is that, from 20.11.03 protein accumulates abundantly and constitutively, whilst over a 24 h period from 07.04.04 and from 06.04.05 protein accumulates at very low levels, often spasmodically.

In a similar study, a diurnal type accumulation pattern was observed in the mature green leaves of *Trifolium repen* ACO (TR-ACO2) over a 24 h period at 3 h intervals, for 9 h and 15 h photoperiods (Du and McManus, 2006). The highest accumulation for the short day was between 6 am and noon, and also between midnight and 3 am, whilst the lowest accumulation was between 3 pm and 9 pm. Similarly, for the long day the highest accumulation was between 9 pm and 3 am and also at 9 am, whilst the lowest accumulation was from noon to 6 pm and also at 6 am. This protein accumulation data shows that TR-ACO2 in the leaves of white clover displays a 24 h rhythm across light and dark periods, which may be due to post translational regulation. Such rhythmicity of ACO protein accumulation (MD-ACO2 and MD-ACO3) is not evident in the bourse shoot leaves of apple, which is in contrast to the strong oscillating gene expression patterns shown for *MD-ACO2* and *MD-ACO3*.

4.5 Summary

In conclusion, this study has established that in the Royal Gala cultivar there is a small multigene family of ACO which comprises at least two and possibly three members. Although the kinetic properties of each of the isoforms are not particularly divergent, they do display differential gene expression patterns *in vivo*. MD-ACO2 and MD-ACO3 do display diurnal patterns of gene expression but not protein accumulation, which may be conditional upon endogenous or environmental factors as the patterns were not consistent from season to season. As a leaf senescence associated ACO was not identified in this study, this indicates either that the leaves of apple do not have an *ACO* gene which is up-regulated at the onset of senescence, or it has yet to be found.

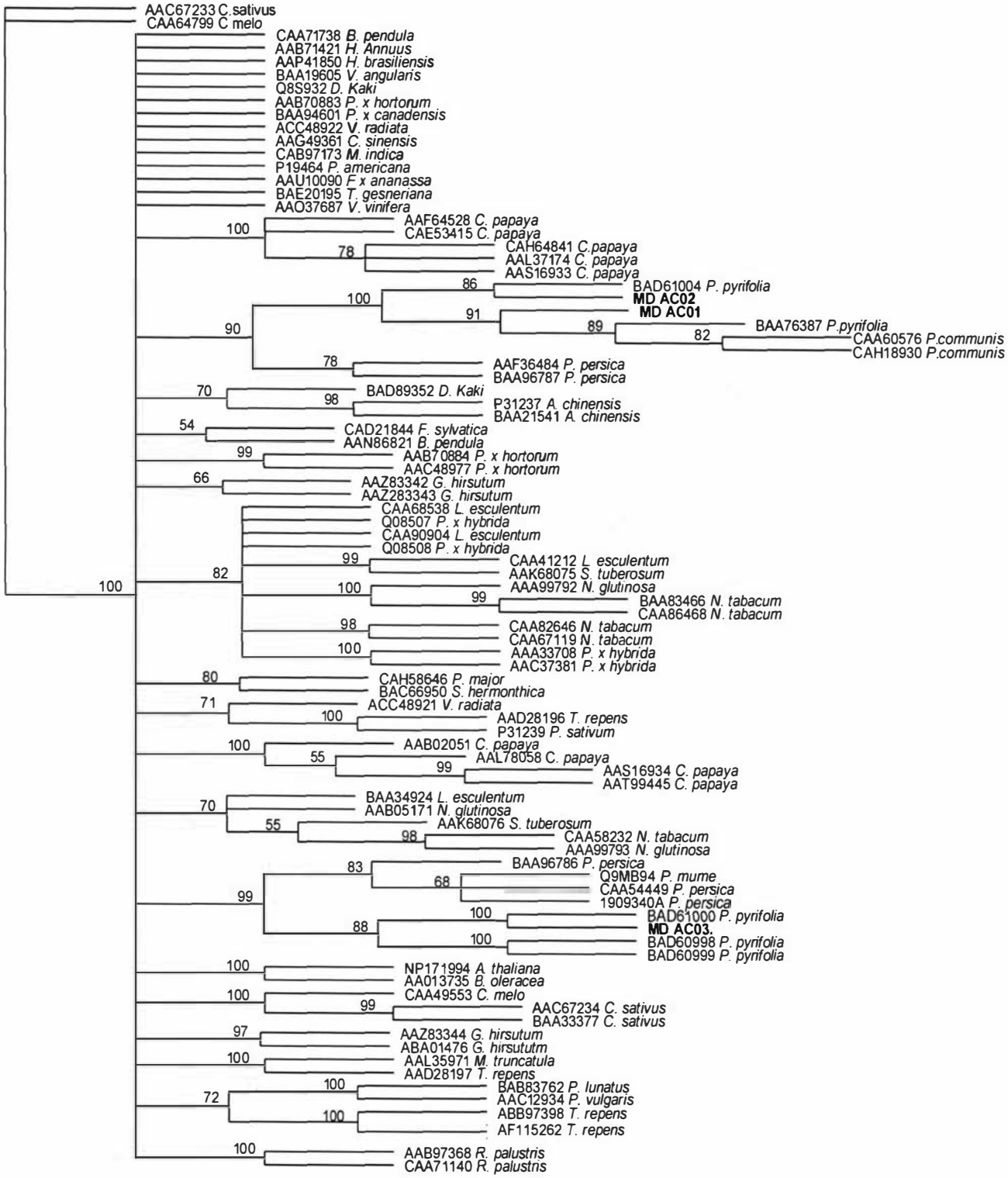
4.6 Future directions

- An assay needs to be developed which can measure ACO activity over a short period of time, i.e. less than one minute. Such an assay would be able to accurately and reliably measure the rate of ACO activity, thus enabling valid comparisons between the ACO isoforms. Ideally, a colourmetric assay which is able to measure either an increase or decrease in products as the reaction progresses. Such as the decrease in ACC or the increase of cyanide over a short period of time that is analysed using an instrument such as the varian spectrophotometer (Cary1E/Cary 3E UV-Vis) which follows the reaction over time.
- The 5′-UTR promoter sequence of each of the apple ACO genes needs to be cloned, and then *MD-ACO* promoter-GUS fusion sequences constructed and expressed in apple (although the juvenile phase of apple is usually 6 to 8 years, and so the expresson of *MD-ACO* in tomato may be more appropriate). Such an experiment may reveal in which tissue *MD-ACO1*, *MD-ACO2* and *MD-ACO3* are expressed, and may also give some indication of the relative abundance of each of the translated products, at various developmental stages, particularly in the leaf and fruit tissue.
- Use Real-Time PCR to determine differential expression of *MD-ACO1*, *MD-ACO2* and *MD-ACO3*
- Map of the MD-ACO2 nucleotide sequence to assess the distinction between the two isoforms (MD-ACO1 and MD-ACO2).
- Raise a polyclonal antibody against the 16 amino acids on the carboxyl terminal of *MD-ACO2*, to determine the pattern of MD-ACO2 protein accumulation.
- To overcome any artefactual problems due to the expression of enzymes in *E. coli*, a more meaningful investigation may be to express the MD-ACOs from this study in yeast (*pBEJ15*), and/or to purify the MD-ACOs from apple (leaves and fruit), and then repeat the kinetic comparisons.
- Compare gene expression patterns of ACO in spur leaves and extension shoot leaves as well as bourse shoot leaves (particularly prior to and following fruit harvest). Use temperature controlled rooms to study leaf development, particularly senescence and fruit ripening
- Further determination of the reaction rates and kinetic analysis of Malonyl ACC transferase and Glutamyl ACC transferase in conjunction with ACO to establish the significance of the ACC conjugations. Also examine the reaction rates and kinetic analysis of SAM decarboxylase in conjunction with ACS to establish the regulation of these important biochemical pathways for the biosynthesis of polyamines and ethylene in plant biology.

APPENDIX 1A: The Full Phylogenetic Analysis of the ACO Amino Acid Sequences from *Malus domestica* with Other ACO Genes in the Genbank Database.

Neighbour Joining Tree (p-distances) made from 235 homologous positions of ACO.

Non parametric bootstrap values are shown.



APPENDIX 1B: The Full Name for Each Entry of the Eighty Five ACOs in the Phylogenetic Analysis

Short name	Amino acids	Full name	Accession number
PP-AOX4	314	*Pyrus pyrifolia*	BAD61004
Cs-ACO2	318	*Cucumis sativus*	ACC67233
pGEFE1	318	*Pelargonium x hortorum*	AAC48977
ACO	319	*Actinidia chinensis*	P31237
ACO	318	*Betula pendula*	CAA71738
ACO	318	*Carica papaya*	AAF64528
ACO2	318	*Carica papaya*	AAL37174
CP-ACO1	318	*Carica papaya*	AAS16933
ACO	318	*Carica papaya*	CAE53415
ACO2	318	*Carica papaya*	CAH64841
CM-ACO3	320	*Cucumis melo*	CAA64799
ACO1	319	*Fagus sylvatica*	CAD21844
G-ACO3	320	*Pelargonium x hortorum*	AAB70884
ACO1	319	*Gossypium hirsutum*	AAZ83342
ACO	307	*Helianthus annuus*	AAB71421
ACO	318	*Hevea brasiliensis*	AAP41850
LE-ACO1	315	*Lycopersicon esculentum*	CAA41212
LE-ACO2	316	*Lycopersicon esculentum*	CAA68538
ACO3	320	*Petunia x hybrida*	QO8507
ACO1	318	*Plantago major*	CAH58646
ACO2	318	*Prunus persica*	AAF36484
PC-ACO1	313	*Pyrus communis*	CAA60576
ACO1	314	*Pyrus communis*	CAH18930
JP-AOX1	314	*Pyrus pyrifolia*	BAA76387
ACO1	315	*Solanum tuberosum*	AAK68075
SH-ACO1	318	*Striga hermonthica*	BAC66950
TR-ACO1	318	*Trifolium repens*	AAD28196
pVR-ACO1	317	*Vigna radiata*	ACC48921
ACO	317	*Actinidia deliciosa*	BAA21541
EFE	323	*Arabidopsis thaliana*	NP171994
AB-ACO1	310	*Vigna angularis*	BAA19605
ACO2	315	*Betula pendula*	AAN86821
EFE	310	*Carica papaya*	AAL78058
DK-ACO2	320	*Diospyros kaki*	BAD89352
DK-ACO1	318	*Diospyros kaki*	Q8S932
gEFE2	323	*Pelargonium x hortorum*	AAB70883
LE-ACO4	320	*Lycopersicon esculentum*	BAA34924
LE-ACO3	316	*Lycopersicon esculentum*	CAA90904
NG-ACO1	320	*Nicotiana glutinosa*	AAA99792
ACO	319	*Nicotiana tabacum*	BAA83466
EFE	308	*Nicotiana tabacum*	CAA58232
cEFE-26	319	*Nicotiana tabacum*	CAA82646
cEFE-27	319	*Nicotiana tabacum*	CAA86468
EFE	320	*Petunia x hybrida*	AAA33708
ACO1	319	*Petunia x hybrida*	AAC37381

contd.

Short name	Amino acids	Full name	Accession number
ACO4	319	*Petunia x hybrida*	Q08508
ACO	317	*Pisum sativum*	P31239
PE-ACO1	319	*Populus x canadensis*	BAA94601
ACO1	319	*Prunus mume*	Q9MB94
ACO	319	*Prunus persica*	1909340A
PP-ACO2	270	*Prunus persica* (partial)	BAA96787
PAO1-ACO	319	*Prunus persica*	CAA54449
JP-AOX3	322	*Pyrus pyrifolia*	BAD61000
pVR-ACO2	308	*Vigna radiate*	ACC48922
ACO2	319	*Solanum tuberosum*	AAK68076
ACO3	321	*Brassica oleracea*	AAO13735
ACO	310	*Carica papaya*	AAB02051
CP-ACO2	310	*Carica papaya*	AAS16934
ACO2	310	*Carica papaya*	AAT99445
ACO	319	*Citrus sinensis*	AAG49361
EFE	318	*Cucumis melo*	CAA49553
ACO3	317	*Cucumis sativus*	AAC67234
Cs-ACO1	317	*Cucumis sativus*	BAA33377
ACO2	319	*Gossypium hirsutum*	AAZ83343
ACO3	317	*Gossypium hirsutum*	AAZ83344
ACO4	310	*Gossypium hirsutum*	ABA01476
ACO1	322	*Mangifera indica*	CAB97173
ACO	323	*Medicago truncatula*	AAL35971
NG-ACO2	313	*Nicotiana glutinosa*	AAA99793
NG-ACO3	316	*Nicotiana glutinosa*	AAB05171
ACO	299	*Nicotiana tabacum*	CAA67119
ACO	320	*Persea Americana*	P19464
ACO	315	*Phaseolus lunatus*	BAB83762
ACO1	315	*Phaseolus vulgaris*	AAC12934
PP-ACO1	268	*Prunus persica* (partial)	BAA96786
PP-AOX2A	322	*Pyrus pyrifolia*	BAD60998
PP-AOX2B	322	*Pyrus pyrifolia*	BAD60999
ACO	314	*Rumex palustris*	CAA71140
ACO2	314	*Rumex palustris*	AAB97368
ACO	320	*Fragaria x ananassa*	AAU10090
TR-ACO2	314	*Trifolium repens*	AAD28197
TR-ACO3	306	*Trifolium repens*	ABB97398
TR-ACO4	306	*Trifolium repens*	AF115262
ACO	316	*Tulipa gesneriana*	BAE20195
ACO1	293	*Vitis vinifera* (partial)	AA037687

(Searched 27.01.06)

BIBLIOGRAPHY

Abeles FB. (1973) Ethylene in Plant Biology, ed. Abeles FB, Academic Press, New York and London.

Abeles FB, Morgan PW and Saltveit ME. (1992) Ethylene in Plant Biology, 2nd ed. Abeles FB, Morgan PW, Saltveit ME. Academic Press, San Diego, California.

Adams DO and Yang SF (1977) Methionine metabolism in apple tissue: implication of S-adenosylmethionine as an intermediate in the conversion of methionine to ethylene. *Plant Physiology*, **60:** 892-896.

Adams DO and Yang SF (1979) Ethylene biosynthesis: identification of 1-aminocyclopropane-1-carboxylic acid as an intermediate in the conversion of methionine to ethylene. *Proceedings of the National Academy of Sciences, USA,* **76:** 170-174.

Alabadi D, Oyama T, Yanovsky MJ, Harmon FG, Mas P and Kay SA. (2001) Reciprocal regulation between TOC1 and LHY / CCA1. *Science*, **293:** 880-883.

Alexander L and Grierson D. (2002) Ethylene biosynthesis and action in tomato: a model for climacteric fruit ripening. *Journal of Experimental Botany*, **53:** 2039-2055.

Allada R, Emery P, Takahashi JS and Rosbash M. (2001) Stopping time: the genetics of fly and mouse circadian clocks. *Annual Review of Neuroscience*, **24:** 1091-1119.

Alonso JM, Hirayama T, Roman G, Nourizadeh S and Ecker JR. (1999) EIN2, a bifunctional transducer of ethylene and stress responses in *Arabidopsis*. *Science*, **284:** 2148-2152.

Altschul SF, Madden TL, Schäffer AA, Zhang J, Zhang Z, Miller W and Lipman DJ. (1997) "Gapped BLAST and PSI-BLAST: a new generation of protein database search programs". *Nucleic Acids Research*, **25:** 3389-3402.

Amrhein NH, Schneebeck H, Skorupka H and Tophof S. (1981) Identification of a major metabolite of the ethylene precursor 1-aminocycloproprane-1-carboxylic acid in higher plants. *Naturwissenschaft*, **68:** 619-620.

Amrhein NH, Breuning F, Eberle J, Skorupka H and Tophof S. (1982) The metabolism of 1-aminocyclopropane-1-carboxylic acid. In: Plant Growth Substances, ed. Wareing P, Academic Press, 249-258.

Andrew JRP, Borlakoglu JT and John P. (1986) Activity of ethylene-forming enzyme in relation to plant cell structure and organization. *Plant Physiology*, **125:** 207-216.

Apelbaum A, Burgoon AC, Anderson JD, Solomos T and Lieberman M. (1981) Some characteristics of the system converting 1-aminocyclopropane-1-carboxylic acid to ethylene. *Plant Physiology*, **67:** 80-84.

Arumuganathan K and Earle ED. (1991) Nuclear DNA content of some important plant species. *Plant Molecular Biology Reporter*, **9:** 208-218.

Arimura G, Ozawa R, Nishioka T, Boland WL, Koch T, Kuhnemann F and Takabayashi J. (2002) Herbivore-induced volatiles induce the emission of ethylene in neighbouring lima bean plants. *Plant Journal*, **29:** 87-98.

Atkinson RG, Bolitho KM, Wright MA, Iturriagagoitia-Bueno T, Reid SJ and Ross GS. (1998) Apple ACC-oxidase and polygalacturonase: ripening-specific gene expression and promoter analysis in transgenic tomato. *Plant Molecular Biology*, **38:** 449-460.

Balagué C, Watson CF, Turner AJ, Rouge P, Picton S, Pech JC and Grierson D. (1993) Isolation of a ripening and wound-induced cDNA from *Cucumis melo* L. encoding a protein with homology to the ethylene forming enzyme. *European Journal of Biochemistry*, **212:** 27-34.

Barak S, Tobin EM, Andronis C, Sugano S and Green RM. (2000) All in good time: the Arabidopsis circadian clock. *Trends in Plant Sciences*, **5:** 517-522.

Barlow JN, Zhang Z, John P, Baldwin JE and Schofield CJ. (1997) Inactivation of 1-aminocyclopropane-1-carboxylate oxidase involves oxidative modifications. *Biochemistry*, **36:** 3563-3569.

Barry CS, Blume B, Bouzayen M, Cooper W, Hamilton AJ and Grierson D. (1996) Differential expression of the 1-aminocyclopropane-1-carboxylate oxidase gene family of tomato. *The Plant Journal*, **9:** 525-535.

Barry CS, McQuinn RP, Thompson AJ, Seymour GB, Grierson D and Giovannoni JJ. (2005) Ethylene insensitivity conferred by the *Green-ripe* and *Never-ripe* 2 ripening mutants of tomato. *Plant Physiology*, **138:** 267-275.

Barry CS and Giovannoni JJ. (2006) Ripening in the tomato *Green-ripe* mutant is inhibited by ectopic expression of a protein that disrupts ethylene signaling. *The Proceedings of the National Academy of Sciences*, USA, **103:** 7923-7928.

Bassett CL, Artlip TS and Callahan AM. (2002) Characterization of the peach homologue of the ethylene receptor, PpETR1, reveals some unusual features regarding transcript processing. *Planta*, **215:** 679-688.

Baur AH and Yang SF. (1972) Methionine metabolism in apple tissue in relation to ethylene biosynthesis. *Phytochemistry*, **11:** 3207-3214.

Bekman EP, Saibo NJM, Cataldo AD, Regalado AP, Ricardo CP and Rodrigues-Pousada C. (2000) Differential expression of four genes encoding 1-aminocyclopropane-1-carboxylate synthase in *Lupinus albus* during germination, and in response to indole-3-acetic acid and wounding. *Planta*, **211:** 663-672.

Benchou M, Martinezreina G, Romojaro F, Pech JC and Latché A. (1995) Partial-purification and properties of a 36-kDa. 1-aminocyclopropane-1-carboxylate *N*-malonyltransferase from mung bean. *Physiologia Plantarum*, **94:** 629-634.

Bidonde S, Ferrer MA, Zegzouti H, Ramassamy S, Latché A, Pech JC, Hamilton AJ, Grierson D and Bouzayen M. (1998) Expression and characterization of three tomato 1-aminocyclopropane-1-carboxylate oxidase cDNAs in yeast. *European Journal of Biochemistry*, **253:** 20-26.

Binder BM, O'Malley RC, Wang W, Moore JM, Parks BM, Spalding EP and Bleecker AB. (2004a) *Arabidopsis* seedling growth response and recovery to ethylene. A kinetic analysis. *Plant Physiology*, **136:** 2913-2920.

Binder BM, Mortimore LA, Stepanova AN, Ecker JR and Bleecker AB. (2004b) Short-term growth responses to ethylene in *Arabidopsis* seedlings are EIN3/EIL1 independent. *Plant Physiology*, **136:** 2921-2927.

Bleecker AB, Kenyon H, Somerville SC and Kende H. (1986) Use of monoclonal antibodies in the purification and characterization of 1-aminocyclopropane-1-carboxylate synthase, an enzyme in ethylene Biosynthesis. *Proceedings of the National Academy of Sciences, USA*, **83:** 7755-7759.

Bleecker AB, Robinson G and Kende H. (1988) Studies on the regulation of 1-aminocyclopropane-1-carboxylate synthase in tomato using monoclonal antibodies. *Planta*, **173:** 385-390.

Bleecker AB, Estelle MA, Somerville C and Kende H. (1988) Insensitivity to ethylene conferred by a dominant mutation in *Arabidopsis thaliana. Science*, **214:** 1086-1089.

Bleecker AB. (1999) Ethylene perception and signaling: an evolutionary perspective. *Trends in Plant Science*, **4:** 269-274.

Bleecker AB and Kende H. (2000) Ethylene: A Gaseous signal molecule in plants. *Annual Review of Cell and Developmental Biology*, **16:** 1-18.

Blume B and Grierson D. (1997) Expression of ACC oxidase promoter-GUS fusions in tomato and *Nicotiana plumbaginifolia* regulated by developmental stimuli. *The Plant Journal*, **12:** 731-746.

Boerjan W, Bauw G, Vanmontagu M and Inze D. (1994) Distinct phenotypes generated by overexpression and suppression of S-adenosyl-L-methionine synthetase reveal developmental patterns of gene silencing in tobacco. *Plant Cell*, **6:** 1401-1414.

Boissel JP, Kasper TJ, Shah SC, Malone JI and Bunn HF. (1985) Amino-terminal processing of proteins: hemoglobin south florida, a variant with retention of initiator methionine and N^{α}-acetylation. *Proceedings of the National Academy of Sciences, USA*, **82:** 8448-8452.

Bolitho KM, Lay-Yee M, Knighton ML and Ross GS. (1997) Antisense apple ACC-oxidase RNA reduces ethylene production in transgenic tomato fruit. *Plant Science*, **122:** 91-99.

Boller T, Herner RC and Kende H. (1979) Assay for and enzymatic formation of an ethylene precursor, 1-aminocyclopropane-1-carboxylic acid. *Planta*, **145:** 293-303.

Boller T. (1985) Time-dependent inactivation of 1-aminocyclopropane-1-carboxylate synthase by its substrate S-adenosyl methionine. In: The International Conference on Plant Substances, Abstract. Heidelberg, Germany, p.36.

Bonghi C, Tonutti P and Ramina A. (2000) Biochemical and molecular aspects of fruitlet abscission. *Plant Growth Regulation*, **31:** 35-42.

Bouzayen M, Latché A, Albert G and Pech JC. (1988) Intercellular sites of synthesis and storage of 1-(malonylamino) cyclopropane-1-carboxylic acid in *Acer pseudoplatanus* cells. *Plant Physiology*, **88:** 613-617.

Bouzayen M, Felix G, Latché A, Pech JC and Boller T. (1991) Iron: an essential cofactor for the conversion of 1-aminocyclopropane-1-carboxylic acid to ethylene. *Planta (Heidelberg),* **184:** 244-247.

Bouzayen M, Cooper W, Barry C Zegzouti H, Hamilton AJ and Grierson D. (1993) EFE multigene family in tomato plants; expression and characterization. In: Cellular and Molecular Aspects of the Plant Hormone Ethylene, eds. Pech JC, Latché A, Balagué C., Kluwer Academic Publishers, Dordrecht, The Netherlands, pp 76-81.

Bradford MM. (1979) A rapid and sensitive method for the quantitation of microgram quantities of protein utilizing the principle of protein-dye binding. *Analytical Biochemistry*, **72:** 248-254

Brenna O, Perrella M, Pace M and Pietta PG. (1975) Affinity chromatography purification of alkaline phosphatase from calf intestine. *Biochemical Journal*, **151:** 291-296.

Britsch L and Grisebach H. (1986) Purification and characterization of (2S)-flavanone 3-hydroxylase from *Petunia hybrida*. *European Journal of Biochemistry*, **156:** 569-577.

Brunhuber NM, Mort JL, Christoffersen RE and Reich NO. (2000) Steady-state kinetic mechanism of recombinant avocado ACC oxidase: initial velocity and inhibitor studies. *Biochemistry*, **39:** 10730-10738.

Buchanan-Wollaston V. (1997) The molecular biology of leaf senescence. *Journal of Experimental Botany*, **48:** 181-199.

Buchanan-Wollaston V, Earl S, Harrison E, Mathas E, Navabpour S, Page T and Pink D. (2003) The molecular analysis of leaf senescence – a genomics approach. *Plant Biotechnology Journal*, **1:** 3-22.

Bufler G. (1984) Ethylene-enhanced 1-aminocyclopropane-1-carboxylic acid synthase activity in ripening apples. *Plant Physiology*, **75:** 192-195.

Burg SP and Stolwijk JAJ. (1959) A highly sensitive katharometer and its application to the measurement of ethylene and other gases of biological importance. *Journal of Biochemical and Microbiological Technology and Engineering*, **1:** 245-259.

Burg SP. (1973) Ethylene in plant growth. *Proceedings of the National Academy of Sciences, USA*, **70:** 591-597.

Bjerrum OJ and Schafer-Nielsen C. (1986) Analytical Electrophoresis, ed. Dunn MJ., Verlag Chemie, Weinheim: 315-327.

Cameron AC, Fenton CAL, Yu Y, Adams DO and Yang SF. (1979) Increased production of ethylene from plant tissues treated with 1-aminocyclopropane-1-carboxylic acid. *HortScience*, **14:** 178-180.

Capitani G, Hohenester E, Feng L, Storici P, Kirsch JF and Jansonius JN. (1999) Structure of 1-aminocyclopropane-1-carboxylate synthase, a key enzyme in the biosynthesis of the plant hormone ethylene. *Journal of Molecular Biology*, **294:** 745-756.

Carpenter CD, Kreps JA and Simon AE. (1994) Genes encoding glycine-rich *Arabidopsis thaliana* proteins with RNA-binding motifs are influenced by cold treatment and an endogenous circadian rhythm. *Plant Physiology*, **104:** 1015-1025.

Carré IA and Kim JY. (2002) MYB transcription factors in the *Arabidopsis* circadian clock. *Journal of Experimental Botany*, **53:** 1551-1557.

Casal JJ. (2000) Phytochromes, cryptochromes, phototropin: photoreceptor interactions in plants. *Photochemistry and Photobiology*, **71:** 1-11.

Cashmore AR, Jarillo JA, Wu YJ and Liu D. (1999) Cryptochromes: blue light receptors for plants and animals. *Science*, **284:** 760-765.

Castiglione S, Malerba M, Pirola B, Bianchetti R, Sala F, Venura M, Pancaldi M and Sansavini S. (1997a) Allelic forms of ripening-related ACC oxidase in apple. Genbank Accession number AJ001646 (unpublished in Journal).

Castiglione S, Pirola B, Sala F, Venura M, Pancaldi M and Sansavini S. (1997b) Allelic forms of ripening-related ACC oxidase and ACC synthase genes in Malus clones and cultivars. Genbank Accession number X98627 (unpublished in Journal).

Castiglione S, Malerba M, Pirola B, Bianchetti R, Sala F, Venura M, Pancaldi M and Sansavini S. (1998) Allelic forms of ripening-related ACC oxidase in apple. Genbank Accession number Y14005 (unpublished in Journal).

Castiglione S, Pirola B, Sala F, Venura M, Pancaldi M and Sansavini S. (1999) Molecular studies of ACC synthase and ACC oxidase genes in apple. *Acta Horticulturae*, **484**: 305-309.

Chae HS, Faure F and Kieber JJ. (2003) The *eto1*, *eto2*, and *eto3* mutations and cytokinin treatment increase ethylene biosynthesis in *Arabidopsis* by increasing the stability of ACS protein. *Plant Cell*, **15:** 545-559.

Chae HS, Xu S, Hansen M and Kieber JJ. (2006) The regulation of ethylene biosynthesis in *Arabidopsis*. In: Book of Abstracts, 7th International Symposium of the Plant Hormone Ethylene, Sant'Anna School of Advanced Studies, Pisa, Italy, 17.

Challice JS. (1974) Rosaceae chemotaxonomy and the origin of the Pomidae. *Botanical Journal of the Linnaean Society*, **69:** 239-259.

Challice JS and Westwood MN. (1973) Numerical taxonomic studies of the genus *Pyrus* using both chemical and botanical characters. *Botanical Journal of the Linnaean Society*, **67:** 121-148.

Chang C, Kwok SF, Bleecker AB and Meyerowitz EM. (1993) *Arabidopsis* ethylene-response gene ETR1: similarity of product to two-component regulators. *Science*, **262:** 539-544.

Chang C and Shockey JA. (1999) The ethylene-response pathway: signal perception to gene regulation. *Current Opinion in Plant Biology*, **2:** 352-358.

Chang C and Stadler R. (2003) Ethylene hormone receptor action in *Arabidopsis*. *BioEssays*, **23:** 619-627.

Chang C and Bleecker AB. (2004) Ethylene Biology: more than a gas. *Plant Physiology*, **136:** 2895-2899.

Chao Q, Rothenberg M, Solano R, Roman G, Terzaghi W and Ecker JR. (1997) Activation of the ethylene gas response pathway in *Arabidopsis* by the nuclear protein ETHYLENE-INSENSITIVE3 and related proteins. *Cell*, **89:** 1133-1144.

Charng Y, Liu Y, Dong JG and Yang SF. (1997) On 1-aminocyclopropane-1-carboxylic acid (ACC) oxidase: degradation of α-aminoisobutyric acid and structure-function studies on the CO_2 binding site. In: Biology and Biotechnology of the Plant Hormone Ethylene, eds. Kanellis AK, Chang C, Kende H and Grierson D., Kluwer Academic Publishers, Dordrecht, The Netherlands: 23-29.

Charng Y, Chou SJ, Jiaang WT, Chen ST and Yang SF. (2001) The catalytic mechanism of 1-aminocyclopropane-1-carboxylic acid oxidase. *Archives of Biochemistry and Biophysics*, **385:** 179-185.

Chen QG and Bleecker AB. (1995) Analysis of ethylene signal-transduction kinetics associated with seedling-growth response and chitinase induction in wild-type and mutant *Arabidopsis*. *Plant Physiology*, **108:** 597-607.

Chen YF, Randlett MD, Findell JL and Schaller GE. (2002) Localization of the ethylene receptor ETR1 to the endoplasmic reticulum of *Arabidopsis*. *Journal of Biological Chemistry*, **277:** 19861-19866.

Chen YT, Lee YR, Yang CY, Wang YT, Yang SF and Shaw JF. (2003) A novel papaya ACC oxidase gene (*CP-ACO2*) associated with late stage fruit ripening and leaf senescence. *Plant Science*, **164:** 531-540.

Chen CM and McManus MT. (2006) Expression of 1-aminocyclopropane-1-carboxylate (ACC) oxidase genes during the development of vegetative tissues in white clover (*Trifolium repens* L.) is regulated by ontological cues. *Plant Molecular Biology*, **60:** 451-467.

Chervin C, El-Kereamy A, Roustan JP, Latché A, Lamon J and Bouzayen M. (2004) Ethylene seems required for the berry development and ripening in grape, a non-climacteric fruit. *Plant Science*, **167:** 1301-1305.

Choi SJ, Bufler G and Bangerth F. (1994) Ethylene sensitivity of apple and tomato fruit during their development. *Gartenbauwissenschaft*, **59:** 154-158.

Chomczynski P and Sacchi N. (1987) Single-step method of RNA isolation by acid guanidinium thiocyanate-phenol-chloroform extraction. *Analytical Biochemistry*, **162**: 156-159.

Chomczynski P. (1992a) One-hour downward alkaline capillary transfer for blotting of DNA and RNA. *Analytical Biochemistry*, **201**: 134-139.

Chomczynski P. (1992b) Solubilization in formamide protects RNA from degradation. *Nucleic Acids Research*, **20:** 3791.

Chomczynski P and Mackey K. (1994) One-hour downward capillary blotting of RNA at neutral pH. *Analytical Biochemistry*, **221:** 303-305.

Christie JM and Briggs WR. (2001) Blue light sensing in higher plants. *Journal of Biological Chemistry*, **276:** 11457-11460.

Chung MC, Chou SJ, Kuang LY, Charng YY and Yang SF. (2002) Subcellular localization of 1-aminocyclopropane-1-carboxylic acid oxidase in apple fruit. *Plant Cell Physiology*, **43:** 549-554.

Church GM and Gilbert W. (1984) Genomic sequencing. *Proceedings of the National Academy of Sciences,* USA, **81:** 1991-1995.

Ciardi JA and Klee H. (2001) Regulation of ethylene mediated responses at the level of the receptor. *Annals of Botany*, **88:** 813-822.

Cin VD, Danesin M, Boschetti A, Dorigoni A and Ramina A. (2005) Ethylene biosynthesis and perception in apple fruitlet abscission (*Malus domestica* L.Borck). *Journal of Experimental Botany*, **56:** 2995-3005.

Clark KL, Larsen PB, Wang XX and Chang C. (1998) Association of the *Arabidopsis* CTR1 Raf-like kinase with the ETR1 and ERS ethylene receptors. *Proceedings of the National Academy of Sciences, USA*, **95:** 5401-5406.

Costas M, Mehn MP, Jensen MP and Que L Jr. (2004) Dioxygen activation at mononuclear nonheme iron active site: enzymes, models and intermediates. *Chemical Review*, **104:** 939-986.

Costa F, Stella S, van de Weg WE, Guerra W, Cecchinel M, Dallavia J, Koller B and Sansavini S. (2005) Role of the genes *Md-ACO1* and *Md-ACS1* in ethylene production and shelf life of apple (*Malus domestica* Borkh). *Euphytica*, **141:** 181-190.

Dai N, Schaffer A, Petreikov M, Shahak Y, Giller Y, Ratner K, Levine A and Granot D. (1999) Overexpression of *Arabidopsis* hexokinase in tomato plants inhibits growth, reduces photosynthesis, and induces rapid senescence. *The Plant Cell*, **11:** 1253-1266.

Darlington CD and Moffett AA. (1930) Primary and secondary balance in *Pyrus*. *Journal of Genetics*, **22:** 129-159.

Defilippi BG, Kader AA and Dandekar AM (2005) Apple aroma: alcohol acyltransferase, a rate limiting step for ester biosynthesis, is regulated by ethylene. *Plant Science*, **168:** 1199-1210.

De Laat AMM, Brandenburg DCC and van Loon LC. (1981) The modulation of the conversion of 1-aminocyclopropane-1-carboxylic acid to ethylene by light. *Planta*, **153:** 193-200.

Devlin PF. (2002) Signs of the time: environmental input to the circadian clock. *Journal of Experimental Botany*, **53:** 1535-1550.

Dilley DR, Kuai J, Poneleit L, Zhu Y, Pekker Y, Wilson ID, Burmeister DM, Gran C and Bowers A. (1993) Purification and characterization of ACC oxidase and its expression during ripening in apple fruit. In: Cellular and Molecular Aspects of the Plant Hormone Ethylene. eds. Pech JC, Latché A and Balagué C., Kluwer Academic Publishers, Dordreecht, The Netherlands, 46-52.

Dilley DR, Kuai J, Wilson ID, Pekker Y, Zhu Y, Burmeister DM and Beaudry RM. (1995) Molecular biology investigation of ACC oxidase and its expression attending apple fruit ripening. *Acta Horticulturae*, **379:** 25-39.

Dilley DR, Wang Z and Kadyrzhanova DK. (2003) Structure-function analysis of ACC oxidase by site-directed mutagenesis. In: Biology and Biotechnology of the Plant Hormone Ethylene III, eds. Vendrell M, Klee H, Pech JC and Romojaro F, IOA Press, The Netherlands: 9-14.

Dolan L. (1997) The role of ethylene in the development of plant form. *Journal of Experimental Botany*, **48:** 201-210.

Dong JG, Yip WK and Yang SF. (1991) Monoclonal antibodies against apple 1-aminocyclopropane-1-carboxylate synthase. *Plant Cell Physiology*, **32:** 25-31.

Dong JG, Olson D, Silverstone A and Yang SF. (1992a) Sequence of a cDNA coding for a 1-aminocyclopropane-1-carboxylate oxidase homolog from apple fruit. *Plant Physiology*, **98:** 1530-1531.

Dong JG, Fernandez-Maculet JC and Yang SF. (1992b) Purification and characterization of 1-aminocyclopropane-1-carboxylate oxidase from apple fruit. *Proceedings of the National Academy of Sciences, USA*, **89:** 9789-9793.

Dong Z and Dunstan D. (1996) A reliable method for extraction of RNA from various conifer tissues. *Plant Cell Reports*, **15**: 516-521.

Du ZN and McManus MT. (2006) Post-translational regulation of ACC oxidase activity in the pasture legume white clover (*Trifolium repens* L.) In: Book of Abstracts, 7th International Symposium of the Plant Hormone Ethylene, Sant' Anna School of Advanced Studies, Pisa, Italy, pp 31.

Dupille E, Rombaldi C, Lelièvre JM, Cleyet-Marcel JC, Pech JC and Latché A. (1993) Purification, properties and partial amino-acid sequence of 1-aminocyclopropane-1-carboxylic acid oxidase from apple fruits. *Planta*, **190:** 65-70.

Dupille E and Zacarias L. (1996) Effect of 2-oxoglutarate and other structural analogs on ACC oxidase activity from apple fruits. In: Abstract of Papers, Symposium on Metabolism and Mode of Action of Phytohormones, Barcelona, Spanish Society of Plant Physiology, Barcelona.

Ecker JR. (2004) Reentry of the ethylene MPK6 module. *Plant Cell*, **16:** 3169-3173.

Edery I. (1999) Role of posttranscriptional regulation in circadian clocks: lessons from *Drosophila*. *Chronobiology International*, **16:** 377-414.

Emery RJN, Kathiresan A, Reid DM and Chinnappa CC. (1997) Ecotypic differences in rhythmicity of ethylene production in *Stellaria longipes*: the possible roles of ACC, MACC, and ACC oxidase. *Canadian Journal of Botany*, **75:** 1027-1033.

Eriksson ME and Millar AJ. (2003) The circadian clock. A plant's best friend in a spinning world. *Plant Physiology*, **132:** 732-738.

Espartero J, Pintortoro JA and Pardo JM. (1994) Differential accumulation of S-adenosylmethionine synthetase transcripts in response to salt stress. *Plant Molecular Biology*, **25:** 217-227.

Fankhauser C, Yeh KC, Lagarias JC, Zhang H, Elich TD and Chory J. (1999) PKS1, a substrate phosphorylated by phytochrome that modulates light signaling in *Arabidopsis*. *Science*, **284:** 1539-1541.

Fankhauser C and Staiger D. (2002) Photoreceptors in *Arabidopsis thaliana*: light perception, signal transduction and entrainment of the endogenous clock. *Planta*, **216:** 1-16.

Felsenstein J. (1985) Confidence limits on phylogenies: an approach using the bootstrap. *Evolution*, **39:** 783-791.

Ferree DC and Carlson RF. (1987) Apple rootstocks. In: Rootstocks for Fruit Crops. Rom RC, Carlson RF, eds, John Wiley & Sons, New York, pp 107-144.

Fernández-Maculet JC and Yang SF. (1992) Extraction and partial characterization of the ethylene-forming enzyme from apple fruit. *Plant Physiology*, **99:** 751-754.

Fernández-Maculet JC, Dong JG and Yang SF (1993) Activation of 1-aminocyclopropane-1-carboxylate oxidase by carbon dioxide. *Biochemical and Biophysical Research Communications*, **193:** 1168-1173.

Finlayson SA, Liu JH and Reid DM. (1996) Localization of ethylene biosynthesis in roots of sunflower (*Helianthus annuus*) seedlings. *Physiologia Plantarum*, **96:** 36-42.

Finlayson SA, Lee IJ, Mullet JE and Morgan PW. (1999) The mechanism of rhythmic ethylene production in sorghum. The role of phytochrome B and simulated shading. *Plant Physiology*, **119:** 1083-1089.

Fluhr R and Mattoo AK (1996) Ethylene-biosynthesis and perception. *CRC Critical Reviews in Plant Science,* **15:** 479-523.

Fonseca S, Barreiro MG, Monteira L and Pais M. (2004) Cold storage induces pear fruit ACC oxidase: enzyme activity, gene expression, promoter isolation and analysis. In: Maturacão e Pós-Colheita, Futos e Horticolas, M. Graca Barreiro/EAN-INIAP (ed.), Oeiras, Portugal: 151-156.

Fujimoto SY, Ohta M, Usui A, Shinshi H and Ohme-Takagi M. (2000) *Arabidopsis* ethylene-response element binding factors act as transcriptional activators or repressors of GCC box-mediated gene expression. *Plant Cell*, **12:** 393-404.

Frohman MA, Dush MK and Martin GR. (1988) Rapid production of full-length cDNAs from rare transcripts: amplification using a single gene-specific oligonucleotide primer. *Proceedings of the National Academy of Sciences*, USA, **85:** 8998-9002.

Gamble RL, Coonfield ML and Schaller GE. (1998) Histidine kinase activity of the ETR1 ethylene receptor from *Arabidopsis*. *Proceedings of the National Academy of Sciences, USA*, **95:** 7825-7829.

Gan S and Amasino RM.l (1995) Inhibition of leaf senescence by autoregulated production of cytokinin. *Science*, **270:** 1986-1988.

Gane R. (1934) Production of ethylene by some fruits. *Nature*, **134:** 1008.

Gao M, Matsuta N, Nishimura K, Tao R, Murayama H, Toyomasu T, Mitsuhashi W, Dandekar AM, Hammerschlag FA, Saxena P, Hicklenton P, Bowen P, Pritchard M and Chong C. (2002) Transformation of pear (*Pyrus communis* cv. `La France') with genes involved in ethylene biosynthesis. *Acta Horticulturae*, **625:** 387-393.

Gao ZY, Chen YF, Randlett MD, Zhjao XC, Findell JL, Kieber JJ and Schaller GE. (2003) Localization of the Raf-like kinase CTR1 to the endoplasmic reticulum of *Arabidopsis* through participation in ethylene receptor signaling complexes. *Journal of Biological Chemistry*, **278:** 34725-34732.

Gardiner SE, Bus VGM, Rusholme RL, Chagné D and Rikkerink EHA. (2007) Apple. In: Genome Mapping and Molecular Breeding in Plants: Fruits and Nuts, ed. Chittaranjan Kole, Springer-Verlag Berlin Heidelberg, **4:** 1-62.

Gepstein S and Thimann KV. (1981) The role of ethylene in the senescence of oat leaves. *Plant Physiology*, **68;** 349-354.

Gepstein S, Sabehi G, Carp MJ, Hajouj T, Nesher MFO, Yariv I, Dor C and Bassani M. (2003) Large-scale identification of leaf senescence-associated genes. *Plant Journal*, **36:** 629-642.

Giovannoni J. (2001) Molecular biology of fruit maturation and ripening. *Annual Review of Plant Physiology and Plant Molecular Biology*, **52:** 725-749.

Gomez-Gomez L and Carrasco L. (1998) Hormonal regulation of S-adenosyl-L-methionine synthetase transcripts in pea ovaries. *Plant Molecular Biology*, **30:** 821-832.

Gong D and McManus MT. (2000) Purification and characterization of two ACC oxidases expressed differentially during leaf ontogeny in white clover. *Physiologia Plantarum*, **110:** 13-21.

Grbić V and Bleecker AB. (1995) Ethylene regulates the timing of leaf senescence in Arabidopsis. *The Plant Journal*, **8:** 595-602.

Grbić V. (2003) SAG2 and SAG12 protein expression in senescing *Arabidopsis* plants. *Physiologia Plantarum*, **119:** 263-269.

Greer DH, Wünsche JN and Palmer JW. (1997) Effects of fruiting on seasonal apple leaf chlorophyll fluorescence. *Acta Horticulturae*, **451:** 345-350.

Greer DH, Wünsche JN and Halligan EA. (2002) Influence of postharvest temperatures on leaf gas exchange, carbohydrate reserves and allocations, subsequent budbreak, and fruit yield of 'braeburn' apple (*Malus domestica*) trees. *New Zealand Journal of Crop and Horticultural Science,* **30:** 175-185.

Grichko VP and Glick BR (2001) Ethylene and flooding stress in plants. *Plant Physiology and Biochemistry*, **39:** 1-9.

Grodzinski B, Boesel I and Horton RF. (1982) The effect of light intensity on the release of ethylene from leaves. *Journal of Experimental Botany*, **33:** 1185-1193.

Grodzinski B, Boesel I and Horton RF. (1983) Light stimulation of ethylene release from leaves of *Gomphrena globosa* L., *Plant Physiology*, **71:** 932-935.

Guo L, Arteca RN, Phillips AT and Liu Y. (1992) Purification and characterization of 1-aminocyclopropane-1-carboxylate *N*-malonyltransferase from etiolated mung bean hypocotyls. *Plant Physiology*, **100:** 2041-2045.

Guo H and Ecker JR. (2004) The ethylene signaling pathway: new insights. *Current Opinion in Plant Biology*, **7:** 40-49.

Guy M and Kende H. (1984) Conversion of 1-aminocyclopropane-1-carboxylic acid to ethylene by isolated vacuoles of *Pisum sativum* L. *Planta*, **160:** 281-287.

Guzman P and Ecker JR. (1999) Exploiting the triple response of *Arabidopsis* to identify ethylene-related mutants. *Plant Cell*, **2:** 513-523.

Hadfield C, Jordan B, Mount RC, Pretorius GHJ and Burak E. (1990) G418-resistance as a dominant marker and reporter gene for gene expression in Saccharomyces cerevisiae. *Current Genetics*, **18:** 303-313.

Hall TC, Ma Y, Buchbinder BU, Pyne JW, Sun SM and Bliss FA. (1978) Messenger RNA for G1 protein of french bean seeds: cell-free translation and product characterization. *Proceedings of the National Academy of Sciences,* USA, **75**: 3196-3200.

Hall AE, Finell JL, Schaller GE, Sisler EC and Bleecker AB. (2000) Ethylene perception by the ERS1 protein in *Arabidopsis. Plant Physiology*, **123:** 1449-1457.

Hamilton AJ, Lycett GW and Grierson D. (1990) Antisense gene that inhibits synthesis of the hormone ethylene in transgenic plants. *Nature*, **346:** 284-287.

Hamilton AJ, Bouzayen M and Grierson D. (1991) Identification of a tomato gene for the ethylene-forming enzyme by expression in yeast. *Proceedings of the National Academy of Sciences, USA*, **88:** 7434-7437.

Harpham N, Berry a, Knee E, Rovedahoyos G, Raskin I, Sanders I, Smith A, Wood C and Hall M. (1991) The effect of ethylene on the growth and development of wild-type and mutants *Arabidopsis thaliana* (L.) Heynh. *Annals of Botany*, **68:** 55-61.

Harris SA, Robinson JP and Juniper BE. (2002) Genetic clues to the origin of the apple. *Trends in Genetics*, **18:** 426-430.

Hatsuyama Y, Sawada R, Igarashi M, Ogasawara H, Wakasa Y, Suzuki M and Harada T. (2002) Md-ACO2: 1-aminocyclopropane-1-carboxylate oxidase of apple. Genbank Accession number AB086888, (unpublished in Journal).

Henderson J, Lyne L and Osborne DJ (2001) Failed expression of an endo-beta-1,4-glucanhydrolase (cellulose) in a non-abscinding mutant of *Lupinus angustifolius* cv Danja. *Phytochemistry*, **58:** 1025-1034.

Hengen PN. (2001) Quantitative PCR: an accurate measure of mRNA? *Trends in Biochemical Sciences (TIBS)*, **20:** 476-477.

Hiwasa K, Kinugasa Y, Amano S, Hashimoto A, Nakano R, Inaba A and Kubo Y. (2003) Ethylene is required for both the initiation and progression of softening in pear (*Pyrus communis* L.) fruit. *Journal of Experimental Botany*, **54:** 771-779.

Hock B, Liebmann S, Beyrle H and Dressel K. (1992) Phytohormone analysis by enzyme immunoassays. *Methods in Microbiology*, **24:** 249-273.

Hoffman NE, Yang SF and McKeon T. (1982) Identification of 1-(Malonylamino) cyclopropane-1-carboxylic acid as a major conjugate of 1-aminocyclopropane-1-carboxylic acid, an ethylene precursor in higher plants. *Biochemical and Biophysical Research Communications*, **104:** 765-770.

Hoffman NE, Yang SF, Ichihara A and Sakamura S. (1982) Stereospecific conversion of 1-aminocyclopropane-1-carboxylic acid to ethylene by plant tissues. Conversion of stereoisomers of 1-amino-2-ethylcyclopropanecarboxylic acid to 1-butene. *Plant Physiology*, **70:** 195-199.

Hoffman NE, Fu JR and Yang SF. (1983) Identification and metabolism of 1-(malonylamino) cyclopropane-1-carboxylic acid in germinating peanut seeds. *Plant Physiology*, **71:** 197-199.

Hohenester E, White MF, Kirsch JF and Jansonius JN. (1994) Crystallization and preliminary x-ray analysis of recombinant 1-aminocyclopropane-1-carboxylate synthase from apple. *Journal of Molecular Biology*, **243:** 947-949.

Holdsworth MJ, Bird CR, Ray J, Schuch W and Grierson D. (1987) Structure and expression of an ethylene-related mRNA from tomato. *Nucleic Acids Research*, **15:** 731-739.

Holmes DS and Quigley M. (1981) A rapid boiling method for the preparation of bacterial plasmids. *Analytical Biochemistry*, **114**: 193-197.

Honma M and Shimomura T. (1978) Metabolism of 1-aminocyclopropane-1-carboxylic acid. *Agricultural Biological Chemistry*, **42:** 1825-1831.

Hua J, Chang C, Sun Q and Meyerowitz EM. (1995) Ethylene insensitivity conferred by *Arabidopsis* ERS gene. *Science*, **269:** 1712-1714.

Hua J and Meyerowitz EM. (1998) Ethylene responses are negatively regulated by a receptor gene family in *Arabidopsis thaliana. Cell*, **94:** 261-271.

Hua J, Sakai H, Nourizadeh S, Chen QG, Bleecker AB, Ecker JR and Meyerowitz EM. (1998) EIN4 and ERS2 are members of the putative ethylene-receptor gene family in *Arabidopsis. Plant Cell*, **10:** 1321-1332.

Huai Q, Xia YH, Chen YQ, Callahan B, Li N and Ke HM. (2001) Crystal structures of 1-aminocyclopropane-1-carboxylate (ACC) synthase in complex with aminoethoxyvinytlglycine and pyridoxal-5'-phosphate provide new insights into catalytic mechanisms. *Journal of Biological Chemistry*, **276:** 38210-38216.

Huang PL, Do YY, Huang FC, Thay TS and Chang TW. (1997) Characterization and expression analysis of a banana encoding 1-aminocyclopropane-1-carboxylate oxidase. *Biochemistry and Molecular Biology International*, **41:** 941-950.

Huang PL and Do YY. (1998) Cloning and characterization of genes encoding 1-aminocyclopropane-1-carboxylate oxidase specific for fruit ripening in banana. In: Biology and Biotechnology of the Plant Hormone Ethylene II, eds. Kanellis AK, Chang C, Grierson D, Klee H and Pech JC., European Union Tmr-Euroconference programme, pp 67.

Huang YJ, To KY, Yap MN, Chiang WJ, Suen DF and Chen SCG. (2001) Cloning and characterization of leaf senescence up-regulated genes in sweet potato. *Physiologia Plantarum*, **113:** 384-39

Huang Y, Li H, Hutchison CE, Laskey J and Kieber JJ. (2003) Biochemical and functional analysis of CTR1, a protein kinase that negatively regulates ethylene signaling in *Arabidopsis. The Plant Journal*, **33:** 221-233.

Huelin FE and Kennett BH. (1959) Nature of the olefins produced by apples. *Nature*, **184:** 996.

Hulme AC and Rhodes (1971) Pome fruits. In: The Biochemistry of Fruits and their Products, ed. Hulme AC., Academic Press London and New York, **2:** 333-373.

Hunter DA, Yoo SD, Butcher SM and McManus MT. (1999) Expression of 1-aminocyclopropane-1-carboxylate oxidase during leaf ontogeny in white clover. *Plant Physiology*, **120:** 131-142.

Hunter DA and Reid MS. (2001) A simple and rapid method for isolating high quality RNA from flower petals. *Acta Horticulturae.* 33-37.

Hunter DA, Steele BC and Reid MS. (2002) Identification of genes associated with perianth senescence in Daffodil (*Narcissus pseudonarcissus* L. 'Dutch Master'). *Plant Science*, **163:** 13-21.

Huson DH nd Bryant D. (2006) Application of phylogenetic networks in evolutionary studies. *Molecular Biology and Evolution*, **23:** 254-267.

Imaizumi T, Tran HG, Swartz TE, Briggs WR and Kay SA. (2003) FKF1 is essential for photoperiodic-specific light signaling in *Arabidopsis*. *Nature*, **426:** 302-306.

Imaseki H and Watanabe A. (1978) Inhibition of ethylene production by osmotic shock. Further evidence for membrane control of ethylene production. *Plant Cell Physiology*, **19:** 345-348.

Imaseki H. (1999) Control of ethylene biosynthesis and metabolism. In: Biochemistry and Molecular Biology of Plant Hormones, eds Hooykaas PJJ, Hall M A and Libbenga KR., Elsevier Science B.V: 209-245.

Inskeep WP and Bloom PR. (1985) Extinction coefficients of chlorophyll *a* and *b* in N,N-dimethylformamide and 80% acetone. *Plant Physiology*, **77**: 483-485.

Iturriagagoitia-Bueno T, Gibson EJ Schofield CJ and John P. (1996) Inhibition of 1-aminocyclopropane-1-carboxylate oxidase by 2-oxoacids. *Phytochemistry*, **43:** 343-349.

Jaakola L, Pirttilä AM and Hohtola A. (2001) cDNA blotting offers an alternative method for gene expression studies. *Plant Molecular Biology Reporter*, **19:** 125-128.

Jasoni RL, Cothren JT, Morgan PW and Sohan DE. (2002) Circadian ethylene production in cotton. *Plant Growth Regulation*, **36:** 127-133.

Jensen PJ, Rytter J, Detwiler EA, Travis JW and McNellis TW. (2003) Rootstock effects on gene expression patterns in apple tree scions. *Plant Molecular Biology*, **493:** 493-511.

Jiang YM and Fu J. (2000) Ethylene regulation of fruit ripening: molecular aspects. *Plant Growth Regulation*, **30:** 193-200.

Jiao XZ, Philosoph-Hada S, Su LY and Yang SF (1986) The conversion of 1-(malonyl) cyclopropane-1-carboxylic acid to 1-aminocyclopropane-1-carboxylic acid in plant tissue. *Plant Physiology*, **81:** 637-641.

Jing HC, Schippers JHM, Hille J and Dijkwel PP. (2005) Ethylene-induced leaf senescence depends on age-related changes and OLD genes in *Arabidopsis*. *Journal of Experimental Botany*, **56:** 2915-2923.

John I, Drake R, Farrell A, Cooper W, Lee P, Horton P and Grierson D. (1995) Delayed leaf senescence in ethylene-deficient ACC-oxidase antisense tomato plants: molecular and physiological analysis. *The Plant Journal*, **7:** 483-490.

John P. (1983) The coupling of ethylene biosynthesis to a transmembrane electrogenic proton flux. *FEBS Letters*, **152:** 141-143.

John P. (1997) Ethylene biosynthesis: the role of 1-aminocyclopropane-1-carboxylate (ACC) oxidase, and its possible evolutionary origin. *Physiologia Plantarum*, **100:** 583-592.

Johnson PR and Ecker JR. (1998) The ethylene signal transduction pathway: a molecular perspective. *Annual Review of Genetics*, **32:** 227-254.

Jun SH, Han MJ, Lee S, Seo YS, Kim WT and An G. (2004) OsEIN2 is a positive component in ethylene signaling in rice. *Plant Cell Physiology*, **45:** 281-289.

Junghans H and Metziaff M. (1990) A simple and rapid method for the preparation of total plant DNA. *BioTechniques*, **8**: 176.

Kadyrzhanova DK, McCully TJ, Jaworski SA, Ververidis P, Vlachonasios KE, Murakami KG and Dilley DR. (1997) Structure-function analysis of ACC oxidase by site-directed mutagenesis. In: Biology and Biotechnology of the Plant Hormone Ethylene, eds. Kanellis AK, Chang C, Kende H and Grierson D., Kluwer Academic Publishers, Dordrecht, The Netherlands: 5-13.

Kadyrzhanova DK, McCully TJ, Warner T, Vlachonasios KE, Wang Z and Dilley DR. (1999) Analysis of ACC oxidase activity by site-directed mutagenesis of conserved amino acid residues. In: Biology and Biotechnology of the Plant Hormone Ethylene II, eds. Kanellis AK, Chang C, Klee H, Bleecker AB, Pech JC and Grierson D., Kluwer Academic Publishers, Dordrecht, The Netherlands: 7-12.

Kao CH and Yang SF. (1982) Light inhibition of the conversion of 1-aminocyclopropane-1-carboxylic acid to ethylene in leaves is mediated through carbon dioxide. *Planta*, **155:** 261-266.

Kapust RB, Tözsér J, Fox JD, Anderson DE, Cherry S, Copeland TD and Waugh DS. (2001) Tobacco etch virus protease: Mechanism of autolysis and rational design of stable mutants with wild-type catalytic proficiency. *Protein Engineering*, **14**: 993-1000.

Kapust RB, Tözsér J, Copeland TD and Waugh DS. (2002a) The P1' specificity of tobacco etch virus protease. *Biochemical and Biophysical Research Communications*, **294:** 949-955.

Kathiresan A, Reid DM and Chinnappa CC. (1996) Light and temperature-entrained circadian regulation of activity and mRNA accumulation of 1-aminocyclopropane-1-carboxylic acid oxidase in *Stellaria longipes*. *Planta*, **199:** 329-335.

Kathiresan A, Nagarathna KC, Moloney MM, Reid DM and Chinnappa CC. (1998) Differential regulation of 1-aminocyclopropane-1-carboxylate synthase gene family and its role in phenotypic plasticity in *Stellaria longipes*. *Plant Molecular Biology*, **36:** 265-274.

Kawalleck P, Plesch G, Hahlbrock K and Somssich IE. (1992) Induction by fungal elicitor of S-adenosyl-L-methionine synthetase and S-adenosyl-L-homocysteine hydrolase messenger-RNAs in cultured-cells and leaves of *Petroselinum-crispum*. *Proceedings of the National Academy of Sciences, USA*, **89:** 4713-4717.

Keb-Llanes M, Gonzaliz G, Chi-Manzanero B, and Infante D. (2002) A rapid and simple method for small-scale DNA extraction in *Agavaceae* and other tropical plants. *Plant Molecular Biology Reporter*, **20**: 299a-299e.

Kendall RL and Bradshaw RA. (1992) Isolation and characterization of the methionine aminopeptidase from porcine liver responsible for the co-translational processing of proteins. *Journal of Biological Chemistry*, **267:** 20667-20673.

Kende H. (1993) Ethylene biosynthesis. *Annual Review of Plant Physiology and Plant Molecular Biology*, **44:** 283-307.

Kende H and Zeevaart JAD. (1997) The five "classical" plant hormones. *The Plant Cell*, **9:** 1197-1210.

Kepczynski J and Kepczynska E. (1997) Ethylene in seed dormancy and germination. *Physiologia Plantarum*, **101:** 720-726.

Kieber JJ, Rothenberg M, Roman G, Feldman KA and Ecker JR. (1993) CTR1, a negative regulator of the ethylene response pathway in Arabidopsis, encodes a member of the Raf family of protein kinases. *Cell*, **72:** 427-441.

Kim CS, Kwak JM, Nam HG, Kim KC and Cho BH. (1994) Isolation and characterization of 2 cDNA clones that are rapidly induced during the wound response of *Arabidopsis-thaliana*. *Plant Cell Reports*, **13:** 340-343.

Kim WT and Yang SF. (1992) Turnover of 1-aminocyclopropane-1-carboxylic acid synthase protein in wounded tomato fruit tissue. *Plant Physiology*, **100:** 1126-1131.

Kim WT and Yang SF. (1994) Structure and expression of cDNA encoding 1-aminocyclopropane-1-carboxylate oxidase homologs isolated from excised mung bean hypocotyls. *Planta*, **194:** 223-229.

Kim YS, Choi D, Lee MM, Lee SH and Kim WT. (1998) Biotic and abiotic stress-related expression of 1-aminocyclopropane-1-carboxylate oxidase gene family in *Nicotiana glutinosa* L. *Plant and Cell Physiology*, **39:** 565-573.

Klee H. (2003) Hormones in the air. *Proceedings of the National Academy of Sciences, USA*, **100:** 10144-10145.

Klee H. (2006) Highly conserved proteins that modify plant ethylene responses. *Proceedings of the National Academy of Sciences, USA*, **103:** 7537-7538.

Knee M. (1985) Metabolism of 1-aminocyclopropane-1-carboxylic acid during apple fruit development. *Journal of Experimental Botany*, **36:** 670-678.

Korban SS, Vodkin LO, Liu L, Aldwinckle HS and Carroll N. (2004) Towards apple functional genomics: the EST project (abstract no. 39). In: International Plant and Animal Genomes XII Conference, Genome Sequencing and ESTs Section, January 10-14, San Diego.

Kosugi Y, Oyamada N, Satoh S, Yoshioka T, Onodera EI and Yamada Y. (1997) Inhibition by 1-aminocyclobutane-1-carboxylate of the activity of 1-aminocyclopropane-1-carboxylate oxidase obtained from senescing petals of carnation (*Dianthus caryophyllus* L.) flowers. *Plant and Cell Physiology*, **38:** 312-318.

Kuai J, and Dilley DR. (1992) Extraction, partial purification and characterization of 1-aminocyclopropane-1-carboxylic acid oxidase from apple fruit. *Postharvest Biology and Technology*, **1:** 203-211.

Laemmli UK. (1970) Cleavage of structural proteins during the assembly of the head of bacteriophage T4. *Nature*, **227:** 680-685.

Lanahan MB, Yen HC, Giovannoni JJ and Klee HJ. (1994) The never ripe mutation blocks ethylene perception in tomato. *Plant Cell*, **6:** 521-530.

Lang A, and Volz RK. (1998) Spur leaves increase calcium in young apples by promoting xylem inflow and outflow. *Journal of the American Society for Horticultural Science*, **123:** 956-960.

Lara I and Vendrell (2000) Changes in abscisic acid levels, ethylene biosynthesis, and protein patterns during fruit maturation of 'Granny Smith' apples. *Journal of the American Society of Horticultural Science*, **125:** 183-189.

Lashbrook CC, Tieman DM and Klee HJ. (1998) Differential regulation of the tomato ETR gene family throughout plant development. *The Plant Journal*, **15:** 243-252.

Lasserre E, Bouquin T, Hernandez JA, Bull J, Pech JC, and Balague C. (1996) Structure and expression of three genes encoding ACC oxidase homologs from melon (*Cucumis melo* L.). *Molecular and General Genetics*, **251**: 81-90.

Lasserre E, Godard F, Bouquin T, Hernandez JA, Pech JC, Roby D and Balagué (1997) Differential activation of two ACC oxidase gene promoters from melon during plant development and in response to pathogen attack. *Molecular and General Genetics*, **256:** 211-222.

Lay-Yee M, Dellapenna D and Ross GS. (1990) Changes in mRNA and protein during ripening in apple fruit (*Malus domestica* Borkh. cv. Golden Delicious). *Plant Physiology*, **94:** 850-853.

Lay VJ, Prescott AG, Thomas PG and John P. (1996) Heterologous expression and site-directed mutagenesis of the 1-aminocyclopropane-1-carboxylate oxidase from kiwifruit. *European Journal of Biochemistry*, **242:** 228-234.

Lee MM, Lee SH and Park KY. (1997) Effects of spermine on ethylene biosynthesis in cut carnation (*Dianthus caryophyllus* L.) flowers during senescence. *Plant Physiology*, **151:** 68-73.

Legge RL, Thompson JE and Baker JE. (1982) Free radical-mediated formation of ethylene from 1-aminocyclopropane-1-carboxylic acid: a spin-trap study. *Plant Cell Physiology*, **23:** 171-177.

Lelievre JM, Latché A, Jones B, Bouzayen M and Pech JC. (1997) Ethylene and fruit ripening. *Physiologia Plantarum*, **101:** 727-739.

Leclercq J, Adams-Philips LC, Zegzouti H, Jones B, Latché A, Giovannoni JJ, Pech JC and Bouzayen M. (2002) LeCTR1, a tomato CTR1-like gene, demonstrates ethylene signaling ability in *Arabidopsis* and novel expression patterns in tomato. *Plant Physiology*, **130:** 1132-1142.

Lespinasse D, Givet L, Troispoux V, Rodiez-Goud M, Pinard F, and Seguin M (2000). Identification of QTLs involved in the resistance in South American leaf blight (*Microcyclus ulei*) in the rubber tree. *Theoretical and Applied Genetics*, **100:** 975-984.

Lespinasse Y, Bouvier L, Djulbic M, and Chevreau E. (1999) Haploidy in apple and pear. Proceedings of the Eucarpia Symposium on Fruit Breeding and Genetics, Eds. Tobutt KR, Alston FH. *Acta Horticulturae*, **484:** 49-54.

Liang XW, Abel S, Keller JA, Shen NF and Theologis A. (1992) The 1-aminocyclopropane-1-carboxylate synthase gene family of *Arabidopsis-thaliana*. *Proceedings of the National Academy of Sciences, USA*, **89:** 11046-11050.

Lieberman M, Kunishi A, Mapson LW and Wardale DA. (1966) Stimulation of ethylene production in apple tissue slices by methionine. *Plant Physiology*, **41:** 376-382.

Lieberman M. (1979) Biosynthesis and action of ethylene. *Annual Review of Plant Physiology*, **30:** 533-591.

Li S, Taylor KB, Kelley SK and Jedrzejas MJ. (2001) Vitamin C inhibits the enzymatic activity of streptococcus pneumoniae hyaluronate lyase. *Journal of Biological Chemistry*, **276:** 15125-15130.

Lin Z, Hackett R, Payton S and Grierson D. (1998) A tomato sequence (AJ005077) encoding an *Arabidopsis* CTR1 homolog. *Plant Physiology*, **117:** 1125.

Lineweaver H and Burk D. (1934) The determination of enzyme dissociation constants. *Journal of the American Chemical Society*, **56:** 658-666.

Liu Y, Hoffman NE and Yang SF. (1985a) Promotion by ethylene of the capability to convert 1-aminocyclopropane-1-carboxylic acid to ethylene in preclimacteric tomato and cantaloupe fruits. *Plant Physiology*, **77:** 407-411.

Liu Y, Su LY and Yang SF (1985b) Ethylene promotes the capability to malonate 1-aminocyclopropane-1-carboxylic acid and D-amino acids in preclimacteric tomato fruits. *Plant Physiology*, **77:** 891-895.

Liu JH, Lee-Tamon SH and Reid DM. (1997) Differential and wound-inducible expression of 1-aminocyclopropane-1-carboxylate oxidase genes in sunflower seedlings. *Plant Molecular Biology*, **34:** 923-933.

Liu YD and Zhang SQ. (2004) Phosphorylation of 1-aminocyclopropane-1-carboxylic acid synthase by MPK6, a stress-responsive mitogen-activated protein kinase, induces ethylene biosynthesis in *Arabidopsis*. *Plant Cell*, **16:** 3386-3399.

Lizada MCC and Yang SF. (1979) A simple and sensitive assay for 1-aminocyclopropane-1-carboxylic acid. *Analytical Biochemistry*, **100:** 140-145.

Ma B, Cui ML, Sun HJ, Takada K, Mori H, Kamada H and Ezura H. (2006) Subcellular localization and membrane topology of the melon ethylene receptor CmERS1. *Plant Physiology*, **141:** 587-597.

Mae T, Kai N, Makino A and Ohira K. (1984) Relation between ribulose bisphosphate carboxylase content and chloroplast number in naturally senescing primary leaves of wheat. *Plant and Cell Physiology*, **25:** 333-336.

Maliepaard G, Alston FH, van Arkel G, Brown LM, Chevreau E, Dunemann F, Evans KM, Gardiner S, Guilford P, van Heusden AW, Janse J, Laurens F, Lynn JR, Manganaris AG, den Nijs APM, Periam N, Rikkerink E, Roche P, Ryder C, Sansavini S, Schmidt H, Taretarini S, Verhaegh JJ, Vrielink-van Ginkel M and King GJ. (1998) Aligning male and female linkage maps of apple (*Malus pumila* Mill.) using multi-allelic markers. *Theoretical and Applied Genetics*, **97:** 60-73.

Marston FAO. (1986) The purification of eukaryotic polypeptides synthetases in *Escherichia coli*. *Biochemical Journal*, **240:** 1-12.

Marton MN, Cohen JD and Saftner RA. (1995) A new 1-aminocyclopropane-1-carboxylic acid conjugating activity in tomato fruit. *Plant Physiology*, **109:** 917-926.

Marton MN and Saftner RA. (1995) Purification and characterization of 1-aminocyclopropane-1-carboxylic acid *N*-malonyltransferase from tomato fruit. *Plant Physiology*, **108:** 1241-1249.

Matilla AJ. (2000) Ethylene in seed formation and germination. *Seed Science Research*, **10:** 111-126.

Maunders MJ, Holdsworth MJ, Slater A, Knapp JE, Bird CR, Schuch W and Grierson D. (1987) Ethylene stimulates the accumulation of ripening-related messenger-RNAs in tomatoes. *Plant Cell and Environment*, **10:** 159-165.

Mayne MB, Coleman JR and Blumwald E. (1996) Differential expression during drought conditioning of a root-specific S-adenosylmethionine synthetase from jack pine (**Pinus banksiana** Lamb) seedlings. *Plant Cell and Environment*, **19:** 958-966.

Mbéguié-A-Mbéguié D, Chahine H, Gomez RM, Gouble B, Reich M, Audergon JM, Souty M, Albagnac G and Fils Lycaon B. (1999) Molecular cloning and expression of cDNA encoding 1-aminocyclopropane-1-carboxylate (ACC) oxidase from apricot fruit (*Prunus armeniaca*). *Physiologia Plantarum*, **105:** 294-303.

McGarvey DJ, Yu H and Christoffersen RE. (1990) Nucleotide sequence of a ripening-related cDNA from avocado fruit. *Plant Molecular Biology*, **15:** 165-167.

McGarvey DJ, and Christoffersen RE. (1992) Characterization and kinetic parameters of ethylene-forming enzyme from avocado fruit. *The Journal of Biological Chemistry*, **267:** 5964-5967.

McKeon TA and Yang SF. (1984) A comparison of the conversion of 1-amino-2-ethylcyclopropane-1-carboxylic acid stereoisomers to 1-butene by pea epicotyls and by a cell-free system. *Planta*, **160:** 84-87.

McRae DG, Coker JA, Legge RL and Thompson JE. (1983) Bicarbonate / CO_2 facilitated conversion of 1-aminocyclopropane-1-carboxylic acid to ethylene in model systems and intact tissues. *Plant Physiology*, **73:** 784-790.

Memelink J, Swords KM, Staehelin LA and Hoge JH. (1994) Southern, northern and western blot analysis. In: Plant Molecular Biology Manual, 2nd ed. Gelvin SB & Schilperoot RA. eds., Kluwer Academic, London, UK: F-10.

Miller JD, Arteca RN and Pell EJ (1999) Senescence-associated gene expression during ozone-induced leaf senescence in *Arabidopsis*. *Plant Physiology*, **120:** 1015-1023.

Miyazaki JH and Yang SF. (1987) The methionine salvage pathway in relation to ethylene and polyamine biosynthesis. *Physiologia Plantarum*, **69:** 366-370.

Mizutani F, Dong JG and Yang SF. (1995) Effect of pH on CO_2-activated 1-aminocyclopropane-1-carboxylate oxidase activity from apple fruit. *Phytochemistry*, **39:** 751-755.

Moeder W, Barry CS, Tauriainen AA, Betz C, Tuomainen J, Utriainen M, Grierson D, Sandermann H, Langebartels C and Kangasjärvi J. (2002). Ethylene synthesis regulated by biphasic induction of 1-aminocyclopropane-1-carboxylic acid synthase and 1-aminocyclopropane-1-carboxylic acid oxidase genes is required for hydrogen peroxide accumulation and cell death in ozone-exposed tomato. *Plant Physiology*, **130:** 1918-1926.

Moon H and Callahan AM. (2004) Developmental regulation of peach ACC oxidase promoter-GUS fusions in transgenic tomato fruits. *Journal of Experimental Botany*, **55:** 1519-1528.

Moran R and Porath D. (1980) Chlorophyll determination in intact tissues using N,N dimethylformamide. *Plant Physiology*, **65:** 478-479.

Moran R. (1982) Formulae for determination of chlorophyllous pigments extracted with N,N-dimethylformamide. *Plant Physiology*, **69:** 1376-1381.

Morgan PW, Finlayson SA, Lee IJ, Childs KL, He CJ, Creelmand RA, Drew MC and Mullet JE. (1997) Regulation of circadianly rhythmic ethylene production by phytochrome B in sorghum. In: Biology and Biotechnology of the Plant Hormone Ethylene, eds. Kanellis AK, Chang C, Kende H and Grierson D., Kluwer Academic Publishers, Dordrecht, The Netherlands: 105-110.

Morgan DR, Soltis DE and Robertson KR. (1994) Systematic and evolutionary implications of rbcL sequence variation in Rosaceae. *American Journal of Botany*, **81:** 890-903.

Mori H, Kamiyoshihare Y, Iwata M, Fukaya T and Tatsuki M. (2006) The regulatory mechanism of the turnover of LeACS2 by phosphorylation. In: Book of Abstracts, 7th International Symposium of the Plant Hormone Ethylene, Sant'Anna School of Advanced Studies, Pisa, Italy, 18.

Morris PC. (2001) Tansley review no. 126: MAP kinase signal transduction pathways in plants. *New Phytologist*, **151:** 67-89.

Moser C, Gatto P, Moser M, Pindo M and Velasco R. (2004) Isolation of functional RNA from small amounts of different grape and apple tissues. *Molecular Biotechnology*, **26:** 95-100.

Moussatche P and Klee HJ. (2004) Autophosphorylation activity of the *Arabidopsis* ethylene receptor multigene family. *Journal of Biological Chemistry*, **279:** 48734-48741.

Moya-Leon MA and John P. (1995) Purification and biochemical characterization of 1-aminocyclopropane-1-carboxylate oxidase from banana fruit. *Phytochemistry*, **39:** 15-20.

Muller-Dieckmann HJ, Grantz AA and Kim SH. (1999) The structure of the signal receiver domain of the *Arabidopsis thaliana* ethylene receptor ETR1. *Structure with Folding and Design*, **7:** 1547-1556.

Nagy F and Schaefer E. (2000) Nuclear and cytosolic events of light-induced, phytochrome-regulated signaling in higher plants. *The European Molecular Biology Organisation (EMBO) Journal*, **19:** 157-163.

Nagy F and Schaefer E. (2002) Phytochromes control photomorphogenesis by differentially regulated, interacting signaling pathways in higher plants. *Annual Review of Plant Physiology and Molecular Biology*, **53:** 329-355.

Nakajima N and Imaseki H. (1986) Purification and properties of 1-aminocyclopropane-1-carboxylate synthase of mesocarp of *Cucurbita maxima* Duch. fruits. *Plant and Cell Physiology*, **27:** 969-980.

Nakajima N, Nakagawa N and Imaseki H. (1998) Molecular size of wound-induced 1-aminocyclopropane-1-carboxylate synthase from *Cucurbita maxima* Duch. and change of translatable mRNA of the enzyme after wounding. *Plant Cell Physiology*, **29:** 989-998.

Nakajima N, Matsuyama T, Tamaoki M, Saji H, Aono M, Kubo A and Kondo N. (2001) Effects of ozone exposure on the gene expression of ethylene biosynthetic enzymes in tomato leaves. *Plant Physiology and Biochemistry*, **39:** 993-998.

Nakano T, Suzuki K, Fujimura T and Shinshi H. (2006) Genome-wide analysis of the ERF gene family in *Arabidopsis* and rice. *Plant Physiology*, **140:** 411-432.

Nakatsuka A, Murachi S, Okunishi H, Shiomi S, Nakano R, Kubo Y and Inaba A. (1998) Differential expression and internal feedback regulation of 1-aminocyclopropane-1-carboxylate synthase, 1-aminocyclopropane-1-carboxylate oxidase, and ethylene receptor genes in tomato fruit during development and ripening. *Plant Physiology*, **118:** 1295-1305.

Nallamsetty S, Kapust RB, Tözsér J, Cherry S, Tropea JE, Copeland TD and Waugh DS. (2004) Efficient site-specific processing of fusion proteins by tobacco vein mottling virus protease in *vivo* and in *vitro*. *Protein Expression and Purification*, **38:** 108-115.

Nam KH and Kim WT (1998) ACC oxidase from apple fruit. Genbank Accession number AF015787 (unpublished in Journal).

Neal MW and Florini JR. (1973) A rapid method for desalting small volumes of solution. *Analytical Biochemistry*, **55:** 328-330.

Newcomb RD, Crowhurst RN, Gleave AP, Rikkerink EHA, Allan AC, Beuning LL, Bowen JH, Gera E, Jamieson KR, Janssen BJ, Laing WA, McArtney S, Nain B, Ross GS, Snowden KC, Souleyre EJF, Walton EF and Yauk YK. (2006) Analysis of expressed sequence tags from apple. *Plant Physiology*, **141:** 147-166.

Nie XZ, Singh RP and Tai GCC. (2002) Molecular characterization and expression analysis of 1-aminocyclopropane-1-carboxylate oxidase homologs from potato under abiotic and biotic stresses. *Genome*, **45:** 905-913.

Nii N. (1997) Changes of starch and sorbitol in leaves before and after removal of fruits from peach trees. *Annals of Botany*, **79:** 139-144.

Nijenhuis-De Vries MA, Woltering EJ and Vrije T. (1994) Partial characterization of carnation petal 1-aminocyclopropane-1-carboxylate oxidase. *Plant Physiology*, **144:** 549-554.

Nimmo HG. (1998) Circadian regulation of a plant protein kinase. *Chronobiology International*, **15:** 109-118.

Noodén LD and Guiamét JJ. (1989) Regulation of the assimilation and senescence by the fruit in monocarpic plants. *Physiologia Plantarum*, **77:** 267-274.

Novakova GV, Moshkov IE, Smith AR and Hall MA. (2000) The effect of ethylene on MAPKinase-like activity in *Arabidopsis thaliana*. *FEBS Letters*, **474:** 29-32.

Novákova M, Motyka V, Dobrev PI, Malbeck J, Gaudinová A and Vanková R. (2005) Diurnal variation of cytokinin, auxin and abscisic acid levels in tobacco leaves. *Journal of Experimental Botany*, **56:** 2877-2883.

Odawara S, Watanabe A and Imaseki H. (1977) Involvement of cellular membrane in regulation of ethylene production. *Plant Cell Physiology*, **18:** 569-575.

Oeller PW, Wong LM, Taylor LP, Pike DA and Theologis A. (1991) Reversible inhibition of tomato fruit senescence by antisense RNA. *Science* **254:** 437-439.

Oh SA, Lee SY, Chung IK, Lee CH and Nam HG. (1996) A senescence-associated gene of *Arabidopsis thaliana* is distinctively regulated during natural and artificially induced leaf senescence. *Plant Molecular Biology,* **30:** 739-754.

Osborne DJ. (1989a) The control role of ethylene in plant growth and development. In: Biochemical and Physiological Aspects of Ethylene Production in Lower and Higher Plants, eds. Clijsters H, De Proft M, Marcelle R and van Poucke M., Kluwer Academic Publishers.

Osborne DJ. (1989b) Abscission. *Critical Reviews in Plant Sciences*, **8:** 103-129.

Osborne DJ (1991) Ethylene in leaf ontogeny and abscission. In: The Plant Hormone Ethylene, Mattoo AK and Suttle JC eds., CRC Press, Boca Raton, Florida, USA, 193-214.

Ouaked F, Rozhon W, Lecourieux D and Hirt H. (2003) A MAPK pathway mediates ethylene signaling in plants. *The EMBO Journal*, **22:** 1282-1288.

Pandey S, Ranade SA, Narar PK and Kumar N. (2000) Role of polyamines and ethylene as modulators of plant senescence. *Journal of Bioscience*, **25:** 291-299.

Park S, Sugimoto N, Larson MD, Beaudry R and Nocker van S. (2006) Identification of genes with potential roles in apple fruit development and biochemistry through large-scale statistical analysis of expressed sequence tags. *Plant Physiology*, **141:** 811-824.

Payton S, Fray RG, Brown S and Grierson D. (1996) Ethylene receptor expression is regulated during fruit ripening, flower senescence and abscission. *Plant Molecular Biology*, **31:** 1227-1231.

Peiser GD, Wang TT, Hoffman NE, Yang SF, Liu HW and Walsh CT. (1984) Formation of cyanide from carbon 1 of 1-aminocyclopropane-1-carboxylic acid during its conversion to ethylene. *Proceedings of the National Academy of Sciences, USA*, **81:** 3059-3063.

Peiser G and Yang SF. (1998) Evidence for 1-(malonylamino) cyclopropane-1-carboxylic acid being the major conjugate of aminocyclopropane-1-carboxylic acid in tomato fruit. *Plant Physiology*, **116:** 1527-1532.

Peleman J, Saito K, Cottyn B, Engler G, Seurinck J, Van Montagu M and Inze E. (1989) Structure and expression analysis of the S-adenosylmethionine synthetase gene family in *Arabidopsis thaliana. Gene*, **84:** 359-369.

Petruzzelli L. Harren F and Reuss J. (1994) Patterns of C_2H_4 production during germination and seedling growth of pea and wheat as indicated by a laser-driven photoacoustic system. *Environmental and Experimental Botany*, **34:** 55-61.

Petruzzelli L, Coraggio I and Leubner-Metzger G. (2000) Ethylene promotes ethylene biosynthesis during pea seed germination by positive feedback regulation of 1-aminocyclopropane-1-carboxylic acid oxidase. *Planta*, **211:** 144-149.

Phan J, Zdanov A, Evdokimov AG, Tropea JE, Peters HPK III, Kaput RB, Li M, Wlodawer A and Waugh DS. (2002) Structural basis for the substrate specificity of tobacco etch virus protease. *Journal of Biological Chemistry*, **277**: 50564-50572.

Picton W, Barton SL, Bouzayen M, Hamilton AJ and Grierson D. (1993) Altered fruit ripening and leaf senescence in tomatoes expressing an antisense ethylene-forming enzyme transgene. *The Plant Journal*, **3:** 469-481.

Pirrung MC. (1985) Ethylene biosynthesis 3. Evidence concerning the fate of C1 and N1 of 1-aminocyclopropane-1-carboxylic acid. *Bioorganic Chemistry*, **13:** 219-226.

Pirrung MC, Kaiser LM and Chen J. (1993) Purification and properties of the apple fruit ethylene-forming enzyme. *Biochemistry*, **32:** 7445-7450.

Pirrung MC, Cao J and Chen C. (1995) Ethylene biosynthesis 12. Analog approach to the active site topography of the ethylene-forming enzyme. Novel hydroxymate inhibitors. *Journal of Organic Chemistry*, **60:** 5790-5794.

Pirrung MC, Cao J and Chen J. (1998) Ethylene biosynthesis: Processing of a substrate analog supports a radical mechanism for the ethylene-forming enzyme. *Chemistry and Biology*, **5:** 49-57.

Pirrung MC. (1999) Histidine kinases and two-component signal transduction systems. *Chemistry and Biology*, **6:** R167-R175.

Pogson BJ, Downs CG and Davies KM. (1995) Differential expression of two 1-aminocyclopropane-1-carboxylic acid oxidase genes in broccoli after harvest. *Plant Physiology*, **108:** 651-657.

Poneleit LS and Dilley DR. (1993) Carbon dioxide activation of 1-aminocyclopropane-1-carboxylate (ACC) oxidase in ethylene synthesis. *Postharvest and Biology and Technology*, **3:** 191-199.

Prescott AG. (1993) A dilemma of dioxygenases (or where biochemistry and molecular biology fail to meet). *Journal of Experimental Botany*, **44:** 849-851.

Prescott AG and John P. (1996) Dioxygenases: molecular structure and role in plant metabolism. *Annual Review of Plant Physiology and Plant Molecular Biology*, **47:** 245-271.

Quail PH. (2002a) Photosensory perception and signaling in plant cells: new paradigms? *Current Opinions in Cell Biology*, **14:** 180-188.

Quail PH (2002b) Phytochrome photosensory signaling networks. *Nature Reviews: Molecular Cell Biology*, **3:** 85-93.

Ramassamy S. Olmos E, Bouzayen M, Pech JC and Latché A. (1998) 1-aminocyclopropane-1-carboxylate oxidase in apple fruit is periplasmic. *Journal of Experimental Botany*, **49:** 1909-1915.

Rasori A, Ruperti B, Bonghi C, Tonutti P and Ramina A. (2002) Characterization of two putative ethylene receptor genes expressed during peach fruit development and abscission. *Journal of Experimental Botany*, **53:** 2333-2339.

Rasori A, Bertolasi B, Furini A, Bonghi C, Tonutti P and Ramina A. (2003) Functional analysis of peach ACC oxidase promoters in transgenic tomato and in ripening peach fruit. *Plant Science*, **165:** 523-530.

Raz V and Fluhr R. (1992) Calcium requirements for ethylene dependent responses. *The Plant Cell*, **4:** 1123-1130.

Raz V and Fluhr R. (1993) Ethylene signal is transduced via protein phosphorylation events in plants. *The Plant Cell*, **5:** 523-530.

Resnick JS, Wen CK, Shockey JA and Chang C. (2006) REVERSION-TO-ETHYLENE SENSITIVITY1, a conserved gene that regulates ethylene receptor function in *Arabidopsis*. *The Proceedings of the National Academy of Sciences, USA*, **103:** 7917-7922.

Roach PL, Clifton IJ, Fülop V, Harlos K, Barton GJ, Hajdu J, Andersson I, Schofield CJ and Baldwin JE. (1995) Crystal structure of isopenicillin N synthase is the first from a new structural family of enzymes. *Nature*, **375:** 700-704.

Roach PL, Clifton IJ, Hensgens CM, Shibata N, Schofield CJ, Hajdu CJ, Hajdu J and Baldwin JE. (1997) Structure of isopenicillin N synthase complexed with substrate and the mechanism of penicillin formation. *Nature*, **387:** 827-830.

Rocklin AM, Tierney DL, Kofman V, Brunhuber NM, Hoffman BM, Christoffersen RE, Reich NO, Lipscomb JD and Que L Jr. (1999) Role of the nonheme Fe(II) center in the biosynthesis of the plant hormone ethylene. *Proceedings of the National Academy of Sciences, USA*, **96:** 7905-7909.

Rocklin AM, Kato K, Liu HW, Que L Jr. and Lipscomb JD. (2004) Mechanistic studies of 1-aminocyclopropane-1-carboxylic acid oxidase: single turnover reaction. *Journal of Biological Inorganic Chemistry*, **9:** 171-182.

Rodriguez FI, Esch JJ, Hall AE, Binder BM, Schaller GE and Bleecker AB. (1999) A copper cofactor for the ethylene receptor ETR1 from *Arabidopsis*. *Science*, **283:** 996-998.

Roe S. (1989) Separation based on structure. In: Protein Purification Method: A Practical Approach, eds. Harris EL, Angal S. IRL Press, Oxford, UK: 175-244.

Roman G, Lubarsky B, Kieber JJ, Rothenberg M and Ecker JR. (1995) Genetic analysis of ethylene signal transduction in *Arabidopsis thaliana*: five novel mutant loci integrated into a stress response pathway. *Genetics*, **139:** 1393-1409.

Rombaldi C, Lelièvre JM, Latché A, Pepitprea M, Bouzayen M and Pech JC. (1994) Immunocytolocalization of 1-aminocyclopropane-1-carboxylic acid oxidase in tomato and apple fruit. *Planta*, **192**: 453-460.

Ross GS, Knighton ML and Lay-Yee M. (1992) An ethylene-related cDNA from ripening apples. *Plant Molecular Biology*, **19:** 231-238.

Rottmann WH, Peter GF, Oeller PW, Keller JA, Shen NF, Nagy BP, Taylor LP, Campbell AD and Theologis A. (1991) 1-aminocyclopropane-1-carboxylate synthase in tomato is encoded by a multigene family whose transcription is induced during fruit and floral senescence. *Journal of Molecular Biology*, **222:** 937-961.

Rubinstein PA and Martin DJ (1983) NH_2-terminal processing of *Drosophila melanogaster* actin: sequential removal of two amino acids. *Journal of Biological Chemistry*, **258**: 3931-3966.

Rudolph R and Lilie H. (1996) *In vitro* folding of inclusion body proteins. *The Federation of the American Society of Experimental Biology Journal*, **10:** 49-56.

Ruperti B, Bonghi C, Rasori A, Ramina A. and Tonutti P. (2001) Characterization and expression of two members of the peach 1-aminocyclopropane-1-carboxylate oxidase gene family. *Physiologia Plantarum*, **111:** 336-344.

Ryle MJ and Hausinger RP. (2002) Non-heme iron oxygenases. *Current Opinion in Chemical Biology*, **6:** 193-201.

Sakai H, Hua J, Chen QG, Chang CR, Medrano LJ, Bleecker AB and Meyerowitz EM. (1998) ETR2 is an ETR1-like gene involved in ethylene signaling in *Arabidopsis*. *Proceedings of the National Academy of Sciences, USA*, **95:** 5812-5817.

Sambrook J, Fritsch EF, Maniatis T. (1989) Molecular Cloning: A Laboratory Manual, 2nd Ed. Cold Spring Harbor Laboratory Press, Cold Spring Harbor, NY., USA.

Sanders IO, Ishizawa K, Smith AR and Hall MA. (1990) Ethylene binding and action in rice seedlings. *Plant and Cell Physiology*, **31:** 1091-1099.

Sandmann G and Boger P. (1980) Copper-mediated lipid peroxidation processes in photosynthetic membranes. *Plant Physiology*, **66:** 797-800.

Sarquis JI, Morgan PW and Jordan WR (1992) Metabolism of 1-aminocyclopropane-1-carboxylic acid in etiolated maize seedlings grown under mechanical impedance. *Plant Physiology*, **98:** 1342-1348.

Sato T. and Theologis A. (1989) Cloning the mRNA encoding 1-aminocyclopropane-1-carboxylate synthase, the key enzyme for ethylene biosynthesis in plants. *Proceedings of the National Academy of Sciences, USA*, **86:** 6621-6625.

Sato T, Oeller PW and Theologis A. (1991) The 1-aminocyclopropane-1-carboxylate synthase of *Cucurbita*. *The Journal of Biological Chemistry*, **266:** 3752-3759.

Satoh S and Esashi Y. (1984) Changes in ethylene production and in 1-aminocyclopropane-1-carboxylic acid (ACC) and malonyl-ACC contents of cocklebur seeds during their development. *Plant and Cell Physiology*, **25:** 1277-1283.

Satoh S and Esashi Y. (1986) Inactivation of 1-aminocyclopropane-1-carboxylic acid synthase of etiolated mung bean hypocotyl segments by its substrate, S-adenosyl-$_L$-methionine. *Plant Cell Physiology*, **27:** 285-291.

Satoh S and Yang SF. (1988) S-Adenosylmethionine-dependent inactivation and radiolabeling of 1-aminocyclopropane-1-carboxylate synthase isolated from tomato fruits. *Plant Physiology*, **88:** 109-114.

Satoh S and Yang SF. (1989a) Specificity of S-adenosyl-$_L$-methionine in the inactivation and the labeling of 1-aminocyclopropane-1-carboxylate synthase isolated from tomato fruits. *Archives of Biochemistry and Biophysics*, **271:** 107-112.

Satoh S and Yang SF. (1989b) Inactivation of 1-aminocyclopropane-1-carboxylate synthase by L-vinylglycine as related to the mechanism-based inactivation of the enzyme by S-adenosyl-$_L$-methionine. *Plant Physiology*, **91:** 1036-1039.

Schaller GE, Ladd AN, Lanahan MB, Spanbauer JM and Bleecker AB. (1995) The ethylene response mediator ETR1 from *Arabidopsis* forms a disulfide-linked dimer. *Journal of Biological Chemistry*, **270:** 12526-12530.

Schaller GE and Bleecker AB. (1995) Ethylene-binding sites generated in yeast expressing the *Arabidopsis* ETR1 gene. *Science*, **270:** 1809-1811.

Schaller GE. (2000) Histidine kinases and the role of two-component systems in plants. *Advances in Botanical Research*, **32:** 109-148.

Schaller GE and Kieber JJ. (2002) Ethylene. In: The *Arabidopsis* Book, American Society of Plant Biologists, eds. Somerville CR and Meyerowitz EM, **130:** 1983-1991.

Schein CH and Noteborn MHM. (1988) Formation of soluble recombinant proteins in *E. coli* is favored by lower growth temperature. *Biotechnology*, **6:** 291-294.

Schroder G, Eichel J, Breinig S and Schroder J. (1997) Three differentially expressed S-adenosyl methionine synthetases from *Catharanthus roseus*: molecular and functional characterization. *Plant Molecular Biology*, **33:** 211-222.

Scopes RK. (1994) Protein Purification: Principles and Practice. 3rd Ed. Springer-Verlag, NY., USA.

Sell S and Hehl R. (2005) A fifth member of the tomato 1-aminocyclopropane-1-carboxylic acid (ACC) oxidase gene family harbours a leucine zipper and is anaerobically induced. *DNA Sequence*, **16:** 80-82.

Seo YS, Yoo A, Jung J, Sung SK, Yang DR, Kim WT and Fee W. (2004) The active site and substrate-binding model of 1-aminocyclopropane-1-carboxylate oxidase determined by site-directed mutagenesis and comparative modeling studies. *Biochemical Journal*, **380:** 339-346.

Sharp KH, Mewies M, Moody PCE and Raven ML (2003) Crystal structure of the ascorbate peroxidase-ascorbate complex. *Nature Structural Biology*, **10:** 303-307.

Shaw JF, Chou YS, Chang RC and Yang SY. (1996) Characterisation of the ferrous iron binding sites of apple 1-aminocyclopropane-1-carboxylate oxidase by site-directed mutagenesis. *Biochemical and Biophysical Research Communications*, **225:** 697-700.

Sheen J. (1990) Metabolic repression of transcription in higher plants. *Plant Cell*, **2:** 1027-1038.

Shibuya K, Barry KG, Ciardi JA, Loucas HM, Underwood BA, Nourizadeh S, Ecker JR, Klee HJ and Clark DG. (2004) The central role of PhEIN2 in ethylene responses throughout plant development in petunia. *Plant Physiology*, **136:** 2900-2912.

Shih YP, Wu CW, Hu SM, Wang TF and Wang AHJ. (2005) Self-cleavage of fusion protein *in vivo* using TEV protease to yield native protein. *Protein Science*, **14:** 936-941.

Sisler EC. (1991) Ethylene-binding components in plants. In: The Plant Hormone Ethylene, eds Mattoo AK and Suttle JC, Boca Raton, CRC Press, 81-99.

Sisler EC, Dupille E and Serek M. (1996) Effect of 1-methylcyclopropene and methylenecyclopropane on ethylene binding and ethylene action on cut carnations. *Plant Growth Regulation*, **18:** 79-86.

Sisler EC and Serek M. (1997) Inhibitors of ethylene responses in plants at the receptor level: Recent developments. *Physiologia Plantarum*, **100:** 577-582.

Slater A, Mauders MJ, Edwards K, Schuch W and Grierson D. (1985) Isolation and characterization of cDNA clones for tomato polygalacturonase and other ripening-related proteins. *Plant Molecular Biology*, **5:** 137-147.

Smalle J, Haegman M, Mertens J, Vangronsvild J, Van Montagu M and Van Der Straeten D. (1999) The expression pattern of the *Arabidopsis* ACC synthase gene 1 during rosette leaf development. *Journal of Experimental Botany*, **50:** 1561-1566.

Smart CM. (1994) Tansley review no. 64: gene expression during leaf senescence. *New Phytologist*, **126:** 419-448.

Smith CJS, Slater A and Grierson D. (1986) Rapid appearance of an mRNA correlated with ethylene synthesis encoding a protein of molecular weight 35000. *Planta*, **168:** 94-100.

Smith JJ, Ververidis P and John P. (1992) Characterization of the ethylene forming enzyme partially purified from melon. *Phytochemistry*, **31:** 1485-1494.

Smith JJ and John P. (1993) Activation of 1-aminocyclopropane-1-carboxylate oxidase by bicarbonate/carbon dioxide. *Phytochemistry*, **32:** 1381-1386.

Smith JJ, Zhang ZH, Schofield CJ John P and Baldwin JE. (1994) Inactivation of 1-aminocyclopropane-1carboxylate (ACC) oxidase. *Journal of Experimental Botany*, **45:** 521-527.

Solano R, Stepanova A, Chao QM and Ecker JR. (1998) Nuclear events in ethylene signaling: a transcriptional cascade mediated by ETHYLENE-INSENSITIVE3 and ETHYLENE-RESPONSE FACTOR1. *Genes and Development*, **12:** 3703-3714.

Southern EM. (1975) Detection of specific sequences among DNA fragments separated by gel electrophoresis. *Journal of Molecular Biology*, **98:** 503-517.

Spanu P, Felix G and Boller T. (1990) Inactivation of stress induced 1-aminocyclopropane carboxylate synthase *in vivo* differs from substrate-dependent inactivation *in vitro*. *Plant Physiology*, **93:** 1482-1485.

Spanu P, Grosskopf DG, Felix G and Boller T. (1994) The apparent turnover of 1-aminocyclopropane-1-carboxylate synthase in tomato cells is regulated by protein-phosphorylation and dephosphorylation. *Plant Physiology*, **106**: 529-535.

Staiger D. (2002) Circadian rhythms in *Arabidopsis*: time for nuclear proteins. *Planta*, **214:** 334-344.

Staiger D, Zecca L, Kirk DAW, Apel K and Eckstein L. (2003) The circadian clock regulated RNA-binding protein AtGRP7 autoregulates its expression by influencing alternative splicing of its own pre-mRNA. *The Plant Journal*, **33:** 361-371.

Stepanova AN and Ecker JR. (2000) Ethylene signaling: from mutants to molecules. *Current Opinion in Plant Biology*, **3:** 353-360.

Stock AM, Robinson VL and Goudreau PN. (2000) Two-component signal transduction. *Annual Review of Biochemistry*, **69:** 183-215.

Strommer J, Gregerson R, Vayda M. (1993) Isolation and characterization of plant mRNA. In: Methods in plant molecular biology and biotechnology. Glick B.R., Thompson J.E. eds., CRC Press, Boca Raton, USA: 49-65.

Stryer L. (1988) Biochemistry 3rd Ed. W.H.Freeman and Company New York, USA.

Summers JE, Voesenek LACJ, Blom CWPM, Lewis MJ and Jackson MB. (1996) Potamogeton pectinatus is constitutively incapable of synthesizing ethylene and lacks 1-aminocyclopropane-1-carboxylic acid oxidase. *Plant Physiology*, **111:** 901-908.

Sunako T, Sakuraba W, Senda M, Akada S, Ishikawa R, Niizeki M and Harada T. (1999) An allele of the ripening-specific 1-aminocyclopropane-1-carboxylic acid synthase gene (ACS1) in apple fruit with a long storage life. *Plant Physiology*, **119:** 1297-1303.

Tabor CW and Tabor H. (1984) Methionineadenosyltransferase (S-adenosylmethionine synthetase) and S-adenosylmethionine decarboxylase. *Advanced Enzymology*, **56:** 251-282.

Tan T and Bangerth F. (2000) Regulation of ethylene, ACC, MACC production, and ACC-oxidase activity at various stages of maturity of apple fruit and the effect of exogenous ethylene treatment. *Gartenbauwissenschaft*, **65:** S.121-128.

Tang XY, Wang H, Brandt AS and Woodson WR. (1993) Organization and structure of the 1-aminocyclopropane-1-carboxylate oxidase gene family from *Petunia-hybrida. Plant Molecular Biology*, **23:** 1151-1164.

Tartachnyk I and Blanke M. (2004) Key processes in leaf senescence of fruiting apple trees. *Acta Horticulturae*, **636:** 59-67.

Tarun AS and Theologis A. (1998) Complementation analysis of mutants of 1-aminocyclopropane-1-carboxylate synthase reveals the enzyme is a dimer with shared active sites. *Journal of Biological Chemistry*, **273:** 12509-12514.

Tarun AS, Lee JS, Theologis A. (1998) Random mutagenesis of 1-aminocyclopropane-1-carboxylate synthase: a key enzyme in ethylene biosynthesis. *Proceedings of the National Academy of Sciences, USA*, **95:** 9796-9801.

Tatsuki M and Mori H. (1999) Rapid and transient expression of 1-aminocyclopropane-1-carboxylate synthase isogenes by touch and wound stimuli in tomato. *Plant Cell Physiology*, **40:** 709-715.

Tatsuki M and Mori H. (2001) Phosphorylation of tomato 1-aminocyclopropane-1-carboxylic acid synthase, LE-ACS2, at the C-terminal region. *Journal of Biological Chemistry*, **276:** 28051-28057.

Tayeh MA, Howe DL, Salleh HM, Sheflyan GY, Son JK and Woodard JW. (1999) Kinetic and mutagenic evidence for the role of histidine residues in the *Lycopersicon esculentum* 1-amincocyclopropane-1-carboxylate oxidase. *Journal of Protein Chemistry*, **18:** 55-68.

Tenorio G, Orea A, Romero JM and Mérida A. (2003) Oscillation of mRNA level and activity of granule-bound starch synthase I in *Arabidopsis* leaves during the day/night cycle. *Plant Molecular Biology*, **51:** 949-958.

Terhoeven-Urselmans A and Blanke MM. (1999) Post-harvest photosynthesis of apple leaves. *Gartenbauwissenschaft*, **64:** 233-238.

Thain SC, Vandenbussche F, Laarhoven JJ, Dowson-Day MJ, Wang ZY, Tobin EM, Harren FJM, Millar AJ and Straeten DVD. (2004) Circadian rhythms of ethylene emission in *Arabidopsis. Plant Physiology*, **136:** 3751-3761.

Theologis A. (1992) One rotten apple spoils the whole bushel; The role of ethylene in fruit ripening. *Cell*, **70:** 181-184.

Theologis A, Oeller PW, Wong LM, Rottmann WH and Gantz DM. (1993) Use of a tomato mutant constructed with reverse genetics to study fruit ripening, a complex developmental process. *Developmental Genetics*, **14:** 282-295.

Thomas H. (1997) Chlorophyll: a symptom and a regulator of plastid development. *New Phytologist*, **136;** 163-181.

Thomas D and Surdin-Kerjan Y. (1991) The synthesis of the two S-adenosylmethionine synthetases is differentially regulated in *Saccharomyces cerevisiae. Molecular and General Genetics*, **226:** 224-232.

Thomine W, Wang R, Ward JM, Crawford NM and Schroeder JI. (2000) Cadmium and iron transport by membranes of a plant metal transporter family in *Arabidopsis* with homology to Nramp genes. *Proceedings of the National Academy of Sciences, USA*, **97:** 4991-4996.

Thrower JS, Blalock R III, and Klinman JP. (2001) Steady-state kinetics of substrate binding and iron release in tomato ACC oxidase. *Biochemistry*, **40:** 9717-9724.

Tieman DM and Klee HJ. (1999) Differential expression of two novel members of the tomato ethylene-receptor family. *Plant Physiology*, **120:** 165-172.

Tieman DM, Taylor MG, Ciardi JA and Klee HJ. (2000) The tomato ethylene receptors NR and LeETR4 are negative regulators of ethylene response and exhibit functional compensation within a multigene family. *Proceedings of the National Academy of Sciences, USA*, **97:** 5663-5668.

Tierney DL, Rocklin AM, Lipscomb JD, Que L Jr. and Hoffman BM. (2005) ENDOR studies of the ligation and structure of the non-heme iron site in ACC oxidase. *Journal of the American Chemical Society*, **127:** 7005-7013.

Towbin H, Staehelin T and Gordon J. (1979) Electrophoretic transfer of proteins from polyacrylamide gels to nitrocellulose sheets: procedure and some applications. *Proceedings of the National Academy of Sciences, USA* , **97:** 4350-4354.

Tsai DS, Arteca RN, Bachman JM and Phillips AT. (1988) Purification and characterization of 1-aminocyclopropane-1-carboxylate synthase from etiolated mungbean hypocotyls. *Archives of Biochemistry and Biophysics*, **264:** 632-640.

Tsai DS, Arteca RN, Arteca JM and Phillips AT. (1991) Characterization of 1-aminocyclopropane-1-carboxylate synthase from etiolated mungbean hypocotyls. *Journal of Plant Physiology*, **137:** 301-306.

Tsuchisaka A and Theologis A. (2004a) Heterodimeric interactions among the 1-aminocyclopropane-1-carboxylate synthase polypeptides encoded by the *Arabidopsis* gene family. *Proceedings of the National Academy of Sciences, USA*, **101:** 2275-2280.

Tsuchisaka A and Theologis A. (2004b) Unique and overlapping expression patterns among the *Arabidopsis* 1-amino-cyclopropane-1-carboxylate synthase gene family members. *Plant Physiology*, **136:** 2982-3000.

Tuomainen J, Betz C, Kangasjarvi J, Ernst D, Yin ZH, Langebartels C and Sandermann H. (1997) Ozone induction of ethylene emission in tomato plants: regulation by differential accumulation of transcripts for the biosynthetic enzymes. *Plant Journal*, **12:** 1151-1162.

Tustin DS, Stanley CJ and Adams HH. (1997) Physiological and phenological responses of apple trees to artificial reduction of the growth period from harvest to leaf fall. *Acta Horticulturae*, **451:** 383-392.

Urao T, Yamaguchi-Shinozaki K and Shinozaki K. (2000) Two-component systems in plant signal transduction. *Trends in Plant Science*, **5:** 67-73.

Valegård K, Vanscheltinga ACT, Lloyd MD, Hara T, Ramaswamy S, Perrakis A, Thompson A, Lee HJ, Baldwin JE, Schofield CJ, Hajdu J and Andersson I. (1998) Structure of a cephalosporin synthase. *Nature*, **394:** 805-809.

Van Der Straeten D, Van Wiemeersch L, Goodman HM and Van Montagu M. (1990) Cloning and sequencing of two different cDNAs encoding 1-aminocyclopropane-1-carboxylate synthase in tomato. *Proceedings of the National Academy of Sciences, USA*, **87:** 4859-4863.

Ververidis P and John P. (1991) Complete recovery *in vitro* of ethylene-forming enzyme activity. *Phytochemistry*, **30:** 725-727.

Vioque B and Castellano JM. (1994) Extraction and biochemical characterization of 1-aminocyclopropane-1-carboxylic acid oxidase from pear. *Physiologia Plantarum*, **90:** 334-338.

Vioque B and Castellano JM. (1998) *In vivo* and *in vitro* 1-aminocyclopropane-1-carboxylic acid oxidase activity in pear fruit: role of ascorbate and inactivation during catalysis. *Journal of Agriculture and Food Science*, **46:** 1706-1711.

Vogel JP, Woeste KE, Theologis A and Kieber JJ. (1998) Recessive and dominant mutations in the ethylene biosynthetic gene ACS5 of *Arabidopsis* confer cytokinin insensitivity and ethylene overproduction, respectively. *Proceedings of the National Academy of Sciences, USA*, **95:** 4766-4771.

Volz RK, Tustin DS, and Ferguson IB. (1996) Mineral accumulation in apple fruit as affected by spur leaves. *Scientia horticulturae*, **65:** 151-161.

Walker JRL. (1997) Software review, *NZ BioScience*, **5:** 8-9.

Wan CY and Wilkins TA. (1994) A modified hot borate method significantly enhances the yield of high-quality RNA from cotton (*Gossypium hirsutum* L.). *Analytical Biochemistry.*, **223:** 7-12.

Wang KLC, Li H and Ecker JR. (2002) Ethylene biosynthesis and signaling networks. *Plant Cell*, **14:** S131-S151.

Wang KLC, Yoshida H, Lurin C and Ecker JR. (2004) Regulation of ethylene gas biosynthesis by the *Arabidopsis* ETO1 protein. *Nature*, **428:** 945-950.

Watillon B, Kettmann R, Boxus P and Burny A. (1993) Developmental and circadian pattern of rubisco activase mRNA accumulation in apple plants. *Plant Molecular Biology*, **23:** 501-502.
Westwood MN. (1993) Temperate Zone Pomology: Physiology and Culture. Westwood MN 3rd ed., Timber Press, Portland, Oregon.

White MF, Vasquez J, Yang SF, Kirsch Jf. (1994) Expression of apple 1-aminocycloprpane-1-carboxylate synthase in *Escherichia coli*: kinetic characterization of wild-type and active-site mutant forms. *Proceedings of the National Academy of Sciences, USA*, **91:** 12428-12423.

Whittaker DJ, Smith GS and Gardner RC. (1997) Expression of ethylene biosynthetic genes in *Actinidia chinensis* fruit. *Plant Molecular Biology*, **34:** 45-55.

Wilkins TA and Smart LB. (1996) Isolation of RNA from plant tissue. In: A Laboratory Guide to RNA: Isolation, Analysis and Synthesis. Krieg PA ed., Wiley-Liss, New York, USA: 21-41.

Wilkinson JQ, Lanahan MB, Yen HC, Giovannoni JJ and Klee HJ. (1995) An ethylene inducible component of signal transduction encoded by *Never-ripe*, *Science*, **257:** 967-971.

Williams OJ and Golden KD. (2002) Purification and characterization of ACC oxidase from *Artocarpus altilis*. *Plant Physiology and Biochemistry*, **40:** 273-279.

Wilmouth R, Turnbull JJ, Welford RWD, Clifton IJ, Prescott AG and Schofield CJ. (2002) Structure and mechanism of anthocyanidin synthase from *Arabidopsis thaliana*. *Structure*, **10:** 93-103.

Wilson ID, Zhu Y, Burmeister DM and Dilley DR. (1993) Apple ripening related cDNA pAP4 confers ethylene-forming ability in transformed *Saccharomyces cerevisiae*. *Plant Physiology*, **102:** 783-788.

Woeste KE, Ye C and Kieber JJ. (1999) Two Arabidopsis mutants that overproduce ethylene are affected in the posttranscriptional regulation of 1-aminocyclopropane-1-carboxylic acid synthase. *Plant Physiology*, **119:** 521-529.

Wong SC, Grimley C, Padua A, Bourell JH and Henzel WJ. (1993) Peptide mapping of 2-D gel proteins by capillary HPLC. In: Techniques in Protein Chemistry IV, ed. Angeletti RH, Academic Press Inc., NY, USA; p 371-378.

Woodson WR, Park KY, Drory A, Larsen PB and Wang H. (1992) Expression of ethylene biosynthetic pathway transcripts in senescing carnation flowers. *Plant Physiology*, **99:** 526-532.

Wright STC. (1981) The effect of light and dark periods on the production of ethylene from water-stressed wheat leaves. *Planta*, **153:** 172-180.

Wu J, Rossomando AJ, Her JH, Del Vecchio R, Weber MJ and Sturgill TW. (1991) Autophosphorylation *in vitro* of recombinant 42-kilodalton mitogen-activated protein kinase on tyrosine. *Proceedings of the National Academy of Sciences, USA*, **88:** 9508-9512.

Wünsche JN and Palmer JW (1997) Effects of fruiting on seasonal leaf and whole-canopy carbon dioxide exchange of apple. *Acta Horticulturae*, **451:** 295-301.

Wünsche JN, Palmer JW and Greer DH. (2000) Effects of crop load on fruiting and gas-exchange characteristics of `braeburn'/M.26 apple trees at full canopy. *Journal of the American Society for Horticultural Science*, **125:** 93-99.

Wurgler-Murphy SM and Saito H. (1997) Two-component signal transducers and MAPK cascades. *Trends in Biochemical Science*, **22:** 172-176.

Xu ZC, Hyodo H, Ikoma Y, Yano M and Ogawa K. (1998) Biochemical characterization and expression of recombinant ACC oxidase in *Escherichia coli* and endogenous ACC oxidase from kiwifruit. *Postharvest Biology and Technology*, **14:** 41-50.

Yamagami T, Tsuchisaka A, Yamada K, Haddon WF, Harden LA and Theologis A. (2003) Biochemical diversity among the 1-amino-cyclopropane-1carboxylate synthase isozymes encoded by the *Arabidopsis* gene family. *Journal of Biological Chemistry*, **278:** 49102-49112.

Yang SF and Hoffman NE. (1984) Ethylene biosynthesis and its regulation in higher plants. *Annual Review in Plant Physiology*, **35:** 155-189.

Yang SF. (1985) Biosynthesis and action of ethylene. *HortScience*, **20:** 41-45.

Yang SF and Dong JG (1993) Recent progress in research of ethylene biosynthesis. *Botanical Bulletin of Academia Sinica*, **34:** 89-101.

Yi HC, Joo S, Nam KH, Lee JS, Kang BG and Kim WT. (1999) Auxin and brassinosteroid differentially regulate the expression of three members of the 1-aminocyclopropane-1-carboxylate synthase family in mung bean (*Vigna radiata* L.) *Plant Molecular Biology*, **41:** 443-454.

Yip WK, Jiao XZ and Yang SF. (1988) Dependence of *in vivo* ethylene production rate on 1-aminocycloproprane-1-carboxylic acid content and oxygen concentration. *Plant Physiology*, **88:** 553-558.

Yip WK, Dong JG, Kenny JW, Thompson GA and Yang SF. (1990) Characterization and sequencing of the active site of 1-aminocyclopropane-1-carboxylate synthase. *Proceedings of the National Academy of Sciences, USA*, **87:** 7930-7934.

Yip WK, Dong JG and Yang SF. (1991) Purification and characterization of 1-aminocyclopropane-1-carboxylate synthase from apple fruits. *Plant Physiology*, **95:** 251-257.

Yoo A, Seo YS, Jung JW, Sung SK, Kim WT, Lee W and Yang DR. (2006) Lys296 and Arg299 residues in the C-terminus of MD-ACO1 are essential for a 1-aminocyclopropane-1-carboxylate oxidase enzyme activity. *Journal of Structural Biology*, **156:** 407-420.

Yoshii H and Imaseki H. (1982) Regulation of auxin-induced ethylene biosynthesis. Repression of inductive formation of 1-aminocyclopropane-1-carboxylate synthase by ethylene. *Plant Cell Physiology*, **23:** 639-649.

Young MW and Kay SA. (2001) Time zones: a comparative genetics of circadian clocks. *Nature Review: Genetics*, **2:** 702-715.

Yu YB and Yang SF. (1979) Auxin-induced ethylene production and its inhibition by aminoethoxy vinylglycine and cobalt ion. *Plant Physiology*, **64:** 1074-1077.

Yu YB, Adams DO and Yang SF. (1979) 1-aminocyclopropanecarboxylate synthase, a key enzyme in ethylene biosyntheis. *Archives of Biochemistry and Biophysics*, **198:** 280-286.

Yung KH, Yang SF and Schlenk F. (1982) Methionine synthesis from 5-methylthioribose in apple tissue. *Biochemical and Biophysical Research Communications*, **104:** 771-777.

Zacarias L and Reid MS (1992) Inhibition of ethylene action prevents root penetration through compressed media in tomato (*Lycopersicon esculentum*) seedlings. *Physiologia Plantarum*, **86:** 301-307.

Zanetti ME, Terrile MC, Arce D, Godoy AV, Segundo BS and Casalongué C. (2002) Isolation and characterization of a potato cDNA corresponding to a 1-aminocyclopropane-1-carboxylate (ACC) oxidase gene differentially activated by stress. *Journal of Experimental Botany*, **53:** 2455-2457.

Zegzouti H, Jones B, Frasse P, Marty C, Maitre B, Latché A, Pech JC and Bouzayen M. (1999) Ethylene-regulated gene expression in tomato fruit: characterization of novel ethylene-responsive and ripening-related genes isolated by differential display. *The Plant Journal*, **18:** 589-600.

Zhang L Buchet R and Azzar G. (2004) Phosphate binding in the active site of alkaline phosphatase and the interactions of 2-nitrosacetophenone with alkaline phosphatase-induced small structural changes. *Biophysical Journal*, **86:** 3873-3881.

Zhang ZH, Schofield CJ, Baldwin JE, Thomas P and John P. (1995) Expression, purification and characterization of 1-aminocyclopropane-1-carboxylate oxidase from tomato in *Escherichia coli*. *Biochemical Journal*, **307:** 77-85.

Zhang ZH, Barlow JN, Baldwin JE and Schofield CJ. (1997) Metal-catalyzed oxidation and mutagenesis studies on the iron (II) binding site of 1-aminocyclopropane-1-carboxylate oxidase. *Biochemistry*, **36:** 15999-16007.

Zhang ZG, Zhou HL, Chen T, Gong Y, Cao WH, Wang YJ, Zhang JS and Chen S. (2004a) Evidence for serine/threonine and histidine kinase activity in the tobacco ethylene receptor protein NTHK2. *Plant Physiology*, **136:** 2971-2981.

Zhang Z, Ren JS, Clifton IJ and Schofield CJ. (2004b) Crystal structure and mechanistic implications of 1-aminocyclopropane-1-carboxylic acid oxidase – the ethylene forming enzyme. *Chemistry and Biology*, **11:** 1383-1394.

Zhou DB, Mattoo AK and Tucker ML. (1996) Molecular cloning of a tomato cDNA encoding an ethylene receptor. *Plant Physiology*, **110:** 1435-1436.

Zhou R, Sicher R and Quebedeaux B. (2001) Diurnal changes in carbohydrate metabolism in mature apple leaves. *Australian Journal of Plant Physiology*, **28:** 1143-1150.

Zhou J, Rocklin AM, Lipscomb JD, Que L Jr. and Solomon EI. (2002) Spectroscopic studies of 1-aminocyclopropane-1-carboxylic acid oxidase: molecular mechanism and CO_2 activation in the biosynthesis of ethylene. *Journal of the American Chemical Society*, **124:** 4602-4609.

Zhu J, Gardiner SE and Lay-Yee M. (1995) Physical mapping of three fruit ripening genes: endopolygalacturonase, ACC oxidase and ACC synthase from apple (*Malus* x *domestica*) in an apple rootstock A106 (*Malus sieboldii*). *Cell Research*, **5:** 243-253.

Zor T, Selinger Z. (1996) Linearization of the Bradford protein assay increases its sensitivity: theoretical and experimental studies. *Analytical Biochemistry*, **236:** 302-308.